Ocean Engineering Studies

Compiled 1991

Volume VI:
Acrylic Windows—

Typical Applications
in Pressure Housings

J. D. Stachiw

NAVAL OCEAN SYSTEMS CENTER

Ocean Engineering Studies

Compiled 1991

Volume VI: Acrylic Windows—
Typical Applications
in Pressure Housings

J. D. Stachiw

NAVAL OCEAN SYSTEMS CENTER

92-04070

Ocean Engineering
Studies

Compiled 1991

Volume VI: Acrylic Windows—
Typical Applications
in Pressure Housings

J. D. Stachiw

Foreword

For successful operation, all manned diving systems, submersibles, and hyperbaric chambers require pressure-resistant viewports. These viewports allow the personnel inside the diving bells and submersibles to observe the environment outside the pressure-resistant hulls. In addition, on land, operators of hyperbaric chambers can observe the behavior of patients or divers undergoing hyperbaric treatment inside the chambers.

Since the viewports form a part of the pressure-resistant envelope, they must meet or surpass the safety criteria used for designing either the metallic or plastic composite pressure envelope. The ASME Boiler and Pressure Vessel Code Section 8 provides such design criteria, and the chambers/pressure hulls designed on their basis have generated an unexcelled safety record.

The viewports, because of the unique structural properties of the acrylic plastic used in constructing the windows, could not be designed according to the same criteria as for the pressure envelopes fabricated of metallic or plastic composite materials. To preclude potential catastrophic failures of windows designed on the basis of inadequate data, in 1965, the U.S. Navy initiated a window testing program at the Naval Civil Engineering Laboratory and the Naval Ocean Systems Center. Under this program, window testing was conducted until 1975.

The objective of the window testing program was to generate test data concerning the structural performance of acrylic-plastic windows fabricated in different shapes, sizes, and thicknesses. Candidates for investigation included the effect of major design parameters, like the thickness to diameter ratio, bevel angle of bearing surfaces, and the ratio of window diameter to seat-opening diameter on the structural performance of the windows; and empirical relationships were to be formulated between these variables and the critical pressures at which windows fail. To make the test results realistic, the test conditions were varied to simulate the in-service environment that the windows were to be subjected. Thus, during testing, the windows were subjected not only to short-term pressurization at room temperature, but also to long-term sustained and repeated pressurization at different ambient temperatures.

On the basis of these data, empirical relationships were formulated between design parameters and test conditions. Committees in the Pressure Technology Codes of the American Society of Mechanical Engineers subsequently incorporated these relationships into the Safety Standard for Pressure Vessels for Human Occupancy (ASME PVHO-1 Safety Standard). Since that time, this ASME Safety Standard has formed the basis — worldwide — for designing acrylic windows in pressure chambers for human occupancy. Their performance record is excellent; since the publication of the Safety Standard in 1977, no catastrophic failures have been recorded that resulted in personal injury.

The data generated by the Navy's window testing program were originally disseminated in technical reports of the Naval Civil Engineering Laboratory and the Naval Ocean Systems Center, and were made available to the general public through the Defense Technical Information Center. To facilitate distribution of these data to users inside and outside of the Department of Defense, the technical reports have been collected and are being reissued as volumes of the U.S. Navy Ocean Engineering Studies.

These volumes, containing the collected technical reports on pressure-resistant plastic windows, will be deposited in technical libraries of Naval Laboratories and universities with ocean engineering programs. This dissemination of collected data should significantly reduce the effort currently being expended by students, engineers, and scientists in their search for data dispersed among the many reports published over a 10-year period by several Naval activities.

Volume VI of the Ocean Engineering series is a compilation of several technical reports describing typical applications of acrylic plastic windows to man-rated chambers with different operational features. Four of the reports cover typical window installations, while the fifth summarizes recommended practices for designing, fabricating, prooftesting, and inspecting windows in man-rated hyperbaric chambers.

One of the reports describes in detail the design, fabrication, and qualification of spherical sector windows for the hulls of a deep-diving submersible. A other report describes the application of free-formed hemispherical shells to the construction of an inexpensive pressure hull for a shallow-depth elevator. In addition, another report describes the design, fabrication, and mounting of a large transparent dome in the bow of a surface ship's small-waterplane-area twin hull (SWATH). A report is also included that enumerates the process employed for selecting the appropriate window design and the subsequent qualification of this design for windows used in a hyperbaric chamber for a 450-psi service pressure.

The report on recommended practices for designing, fabricating, prooftesting, and performing in-service inspection of windows in hyperbaric chambers concisely summarizes structural parameters that must be considered in the procurement and operation of safe pressure-resistant windows. The recommended practices should be considered as guidelines, rather than rules, since each statutory authority may impose stricter requirements that differ substantially from these recommended practices. One of such sets of requirements that is accepted by most statutory authorities (i.e., the U.S. Navy, U.S. Coast Guard, American Bureau of Shipping, etc.) is the American Society of Mechanical Engineers Safety Standard for Pressure Vessels for Human Occupancy (ASME PVHO-1). The designer should become familiar with the requirements of the statutory authority in whose jurisdiction the chamber will be located and thus include in his window design the additional requirements imposed by the statutory authority.

The pressure and duration of loading data summarized in the reports apply directly to windows of any size with an identical t/Di ratio, while the displacements shown must be multiplied by a scale factor based on the ratio of minor diameters on the test and operational windows. To date, these test data have been used successfully in designing windows in sizes up to 96 inches for tourist submarines.

J. D. Stachiw
Marine Materials Office
Ocean Engineering Division

TABLE OF CONTENTS: VOLUME VI

SPHERICAL-SHELL SECTOR WINDOWS OF ACRYLIC PLASTIC WITH 12,000-FOOT OPERATIONAL DEPTH CAPABILITY FOR SUBMERSIBLE ALVIN

J. D. Stachiw
Ocean Technology Department

R. Sletten
Det Norske Veritas

May 1975

nuc

NAVAL UNDERSEA CENTER. SAN DIEGO. CA 92132

AN ACTIVITY OF THE NAVAL MATERIAL COMMAND

ROBERT H. GAUTIER, CAPT, USN
Commander

HOWARD L. BLOOD, PhD
Technical Director

ii

REPORT DOCUMENTATION PAGE		READ INSTRUCTIONS BEFORE COMPLETING FORM
1. REPORT NUMBER NUC TP 453	2. GOVT ACCESSION NO.	3. RECIPIENT'S CATALOG NUMBER
4. TITLE (and Subtitle) SPHERICAL-SHELL SECTOR WINDOWS OF ACRYLIC PLASTIC WITH 12,000-FOOT OPERATIONAL DEPTH CAPABILITY FOR SUBMERSIBLE ALVIN		5. TYPE OF REPORT & PERIOD COVERED Research and Development March-December, 1974
		6. PERFORMING ORG. REPORT NUMBER
7. AUTHOR(s) J. D. Stachiw and R. Sletten		8. CONTRACT OR GRANT NUMBER(s)
9. PERFORMING ORGANIZATION NAME AND ADDRESS Naval Undersea Center San Diego, CA 92132		10. PROGRAM ELEMENT, PROJECT, TASK AREA & WORK UNIT NUMBERS
11. CONTROLLING OFFICE NAME AND ADDRESS Naval Undersea Center San Diego, CA 92132		12. REPORT DATE May 1975
		13. NUMBER OF PAGES 94
14. MONITORING AGENCY NAME & ADDRESS(if different from Controlling Office)		15. SECURITY CLASS (of this report) UNCLASSIFIED
		15a. DECLASSIFICATION DOWNGRADING SCHEDULE

16. DISTRIBUTION STATEMENT (of this Report)

Approved for public release; distribution unlimited.

17. DISTRIBUTION STATEMENT (of the abstract entered in Block 20, if different from Report)

18. SUPPLEMENTARY NOTES

19. KEY WORDS (Continue on reverse side if necessary and identify by block number)

ALVIN	Acrylic plastic
Submersibles	Windows
Viewports	

20. ABSTRACT (Continue on reverse side if necessary and identify by block number)

    The purpose of the work in this report was to develop spherical-shell sector windows of acrylic plastic for the deep-diving submersible ALVIN, which has a 12,000-foot depth capability. Results show that the spherical windows can be used in ALVIN without modification of the window seat flanges. The following characteristics were also observed during tests:

DD FORM 1473   1 JAN 73   EDITION OF 1 NOV 65 IS OBSOLETE

20. (Continued)

    1. They have a higher short-term critical pressure and develop more uniform stress distribution during a typical dive to 12,000 feet than do the conical frustum windows now in ALVIN

    2. They can withstand, without catastrophic failure, 100 hours of sustained pressure to 20,000 psi and 33 pressure cycles of 7-hour duration to 13,500 feet without any signs of fatigue.

    3. They experience less than 15,000 microinches of strain during a simulated, typical, prooftest dive to 13,500 feet.

    4. They present a 50 percent larger view in water than the windows to be replaced; this permits the observer to visually cover more ocean bottom during a single pass along the bottom and thus decrease the cost of a typical, bottom-search mission.

SUMMARY

PROBLEM

Spherical-shell sector windows of acrylic plastic are better suited, both structurally and optically, for high-pressure service than are flat disc or conical frustum windows. However, the typical application of the former has been as large single bow windows in submersibles of continental depth capability.

The remaining deep-submergence submersibles continue to use almost exclusively the conical frustum windows with which they were originally equipped. The primary reason for the reluctance to replace these with the spherical-shell sector windows has been lack of data on the performance of thick 90° spherical-shell sectors in massive metallic flanges under long-term and cyclic pressurizations.

To make these sectors attractive as replacements for existing windows in submersibles, an experimental study was conducted at the Naval Undersea Center (NUC). The particular objective was to develop spherical-shell sector windows for the deep-diving submersible ALVIN, which has a 12,000-foot depth capability.

RESULTS

1. The 90° conical frustum windows with a ratio of $t/D_i = 0.7$ in the ALVIN submersible can be replaced with 90° spherical-shell sector windows with a ratio of $t/D_i = 1.0$ without modification of the window seat flanges.

2. The spherical-shell sector windows exhibited the following characteristics.

   - They have a higher short-term critical pressure and develop more uniform stress distribution during a typical dive to 12,000 feet than do the plane conical windows.

   - They can withstand, without catastrophic failure, 100 hours of sustained loading under 20,000 pounds-per-square-inch hydrostatic pressure.

   - They can withstand 33 pressure cycles of 7 hours duration to 13,500 feet without any signs of fatigue.

   - They experience less than 15,000 microinches of strain during a simulated typical prooftest dive to 13,500 feet.

   - They present a 50 percent larger view in water than the windows to be replaced: this permits the observer to visually cover more ocean bottom during a single pass along the bottom and thus decrease the cost of a typical bottom-search mission.

3. The spherical-shell windows ($t/D_i = 1.0$) are structurally adequate for service to 12,000 feet in submersibles with 90° flanges sized for conical frustum windows ($t/D_i = 0.7$).

RECOMMENDATION

Operators of other submersibles should carefully consider the optical and structural advantages associated with replacement of existing 90° conical frustum windows with thicker 90° spherical-shell sector windows.

CONTENTS

GLOSSARY

CL – center line

D_f – minor diameter of flange seat

D_i – minor diameter of window's low-pressure face

D_o – major diameter of window's high-pressure face

E – modulus of elasticity under uniaxial compression

P_{ci} – implosion pressure

P_{op} – operational pressure

R – radius

R_i – spherical radius of concave low-pressure face on spherical window

R_o – spherical radius of convex high-pressure face on spherical window

Short-term pressure – pressurization at 650 psi per minute rate

STCP – short-term critical pressure; hydrostatic pressure at which catastrophic failure of the window occurs, psi
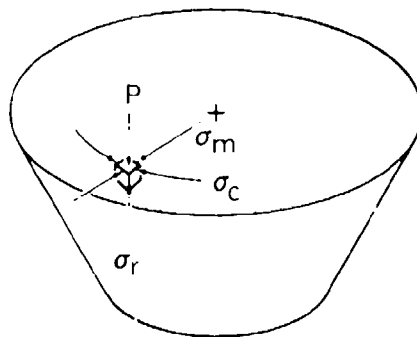
t – thickness of window

α – included conical angle of window's seating surface

σ_c – tangential stress with circumferential orientation

σ_m – tangential stress with meridional orientation

σ_t – radial stress; perpendicular to high-pressure face of window

σ_{ti} – tangential stresses – stresses tangent to high- or low-pressure face of window

4

INTRODUCTION

Since their introduction in 1969 (reference 1), acrylic plastic spherical-shell sectors have found extended application as panoramic windows in work and research submersibles. Because of their importance, economical ways of fabricating large and small windows for shallow- and deep-submergence applications have been investigated (references 2, 3, 4, and 5) and the performance of such windows under different kinds of static and dynamic loadings studied (references 6 and 7). This report describes the study on the replacement of conical frustum windows in existing submersibles, operating to 12,000 feet, with the spherical-shell sector windows; the replacement does not require modification of window flanges on the submersible.

BACKGROUND

The research submersible ALVIN (figure 1) was designed in 1963 by General Mills Corporation under contract to the Office of Naval Research (reference 8). The 79.3-inch inside diameter, spherical, pressure hull was built of 1.33-inch thick HY-100 steel, giving the submersible an operational depth of 6000 feet with a calculated safety factor of at least 2. Because of the four viewports located in the hull, the crew had reasonable visibility of the surrounding hydrospace.

The submersible was outfitted in 1973 (reference 9) with a new titanium alloy hull, which (1) allowed operations to 12,000 feet with a proven safety factor of 1.9 and (2) increased the vessel's buoyancy. Because the new hull was patterned after the old steel hull, the number, diameter, and thickness of the window flanges remained the same. This created a problem since the plane conical frustum acrylic windows chosen for service to 6000 feet now had to withstand operational dives to 12,000 feet and prooftesting to 13,200 feet.

The original windows chosen for ALVIN were conical $90°$ included angle plane frustums of $t/D_i = 0.7$ and $D_i = 5.0$ inches (figure 2), which were mounted in appropriate window flanges on the spherical pressure hull. The $t/D_i = 0.7$ gave the windows a short-term critical pressure of approximately 30,000 psi (reference 10). The 10:1 relationship between the short-term implosion pressure and the operational pressure made these windows extremely safe for operation to 6000 feet and prooftesting to 7500 feet. Tests conducted on the original ALVIN windows confirmed these findings.

The situation changed drastically when the same windows were incorporated in the new titanium hull. The increased diving depth (to 12,000 feet) reduced the previously comfortable P_{ci}/P_{op} ratio of 10 to 5. Although the ratio of 5 is acceptable for man-rated use of conical frustum acrylic windows, it is marginal when prooftesting in excess of the operational pressure is performed on the windows or when dynamic impulse loading is superimposed on static loading at the maximum operational depth. Thus, there existed a requirement for redesign of the windows with the objective of increasing their critical pressure without changing the configuration of the existing window flanges in the hull.
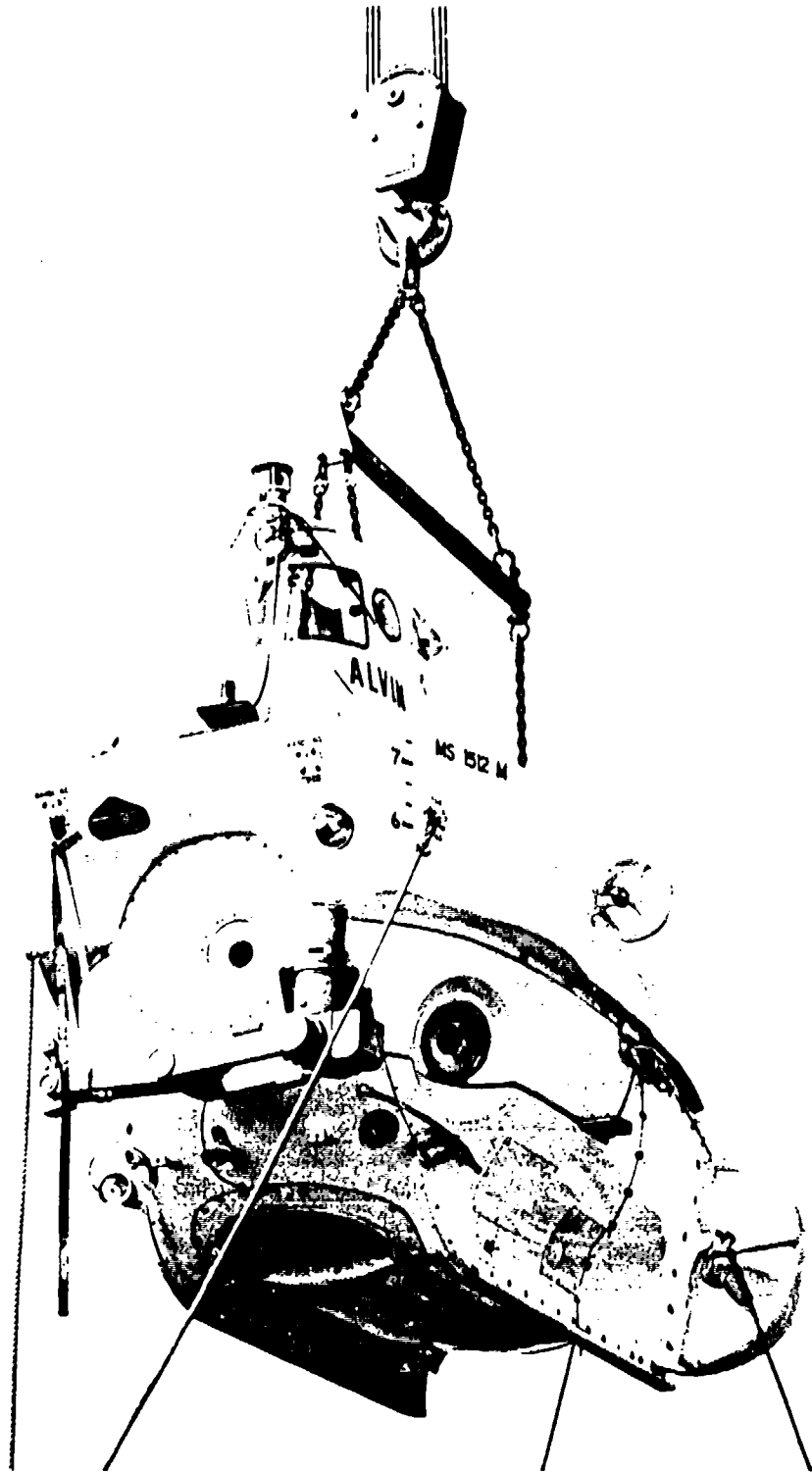
Figure 1. ALVIN submersible with 12,000-foot operational depth capability.

MATERIAL: PLEXIGLAS G ACRYLIC PLASTIC OR EQUIVALENT
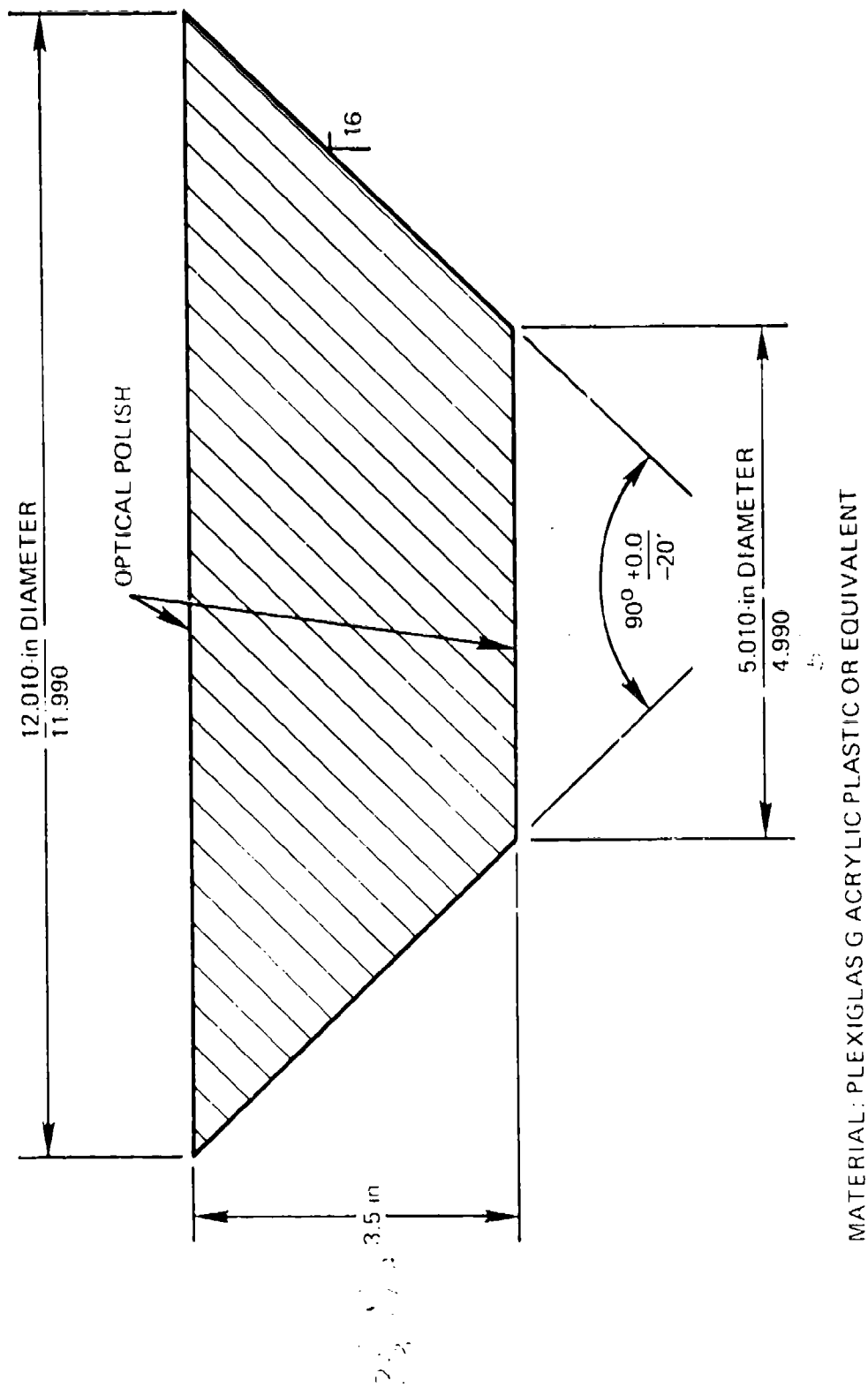
Figure 2. Conical frustum windows used as original equipment in both the steel and titanium hulls.

7

PROGRAM DESCRIPTION

OBJECTIVE

The objective of the study was to replace the existing 90° conical frustum windows in ALVIN with 90° spherical sector windows without modifying the existing window flanges. The benefits of the change were to be improved structural and optical performance of acrylic windows.

SCOPE

The extent of the study was limited to the existing 90° window flanges in ALVIN (figure 3) with D_i = 4.440 inches and D_o = 12.000 inches. Modifications to the window flange assembly were to be limited only to redesign of the window's retention ring and sealing system.

APPROACH

The approach was to be empirical. The dimensions of the spherical sector window were to be chosen on the basis of the existing window flanges, while the evaluation of the structural performance was to be on the basis of displacements and strains measured on the window during hydrostatic loading. The evaluation of the optical performance was to be empirical also.

PLAN OF ACTION

It was planned to conduct the study in four consecutive phases:

1. Selection of appropriate dimensions for the spherical sector window.

2. Fabrication of the spherical sector window to meet Navy material and dimensional specifications.

3. Evaluation of the spherical sector window under simulated operational conditions.

4. Prooftesting of individual windows prior to mounting in the ALVIN.

Figure 3. Flange detail in ALVIN hull.

9

ENGINEERING CRITERIA SELECTION

SPHERICAL SECTORS

The criteria for choosing the dimensions of the spherical sector window were that the outside (D_o) and inside (D_i) diameters be identical to those of the conical frustum window in ALVIN. Using these criteria, the window was chosen to have out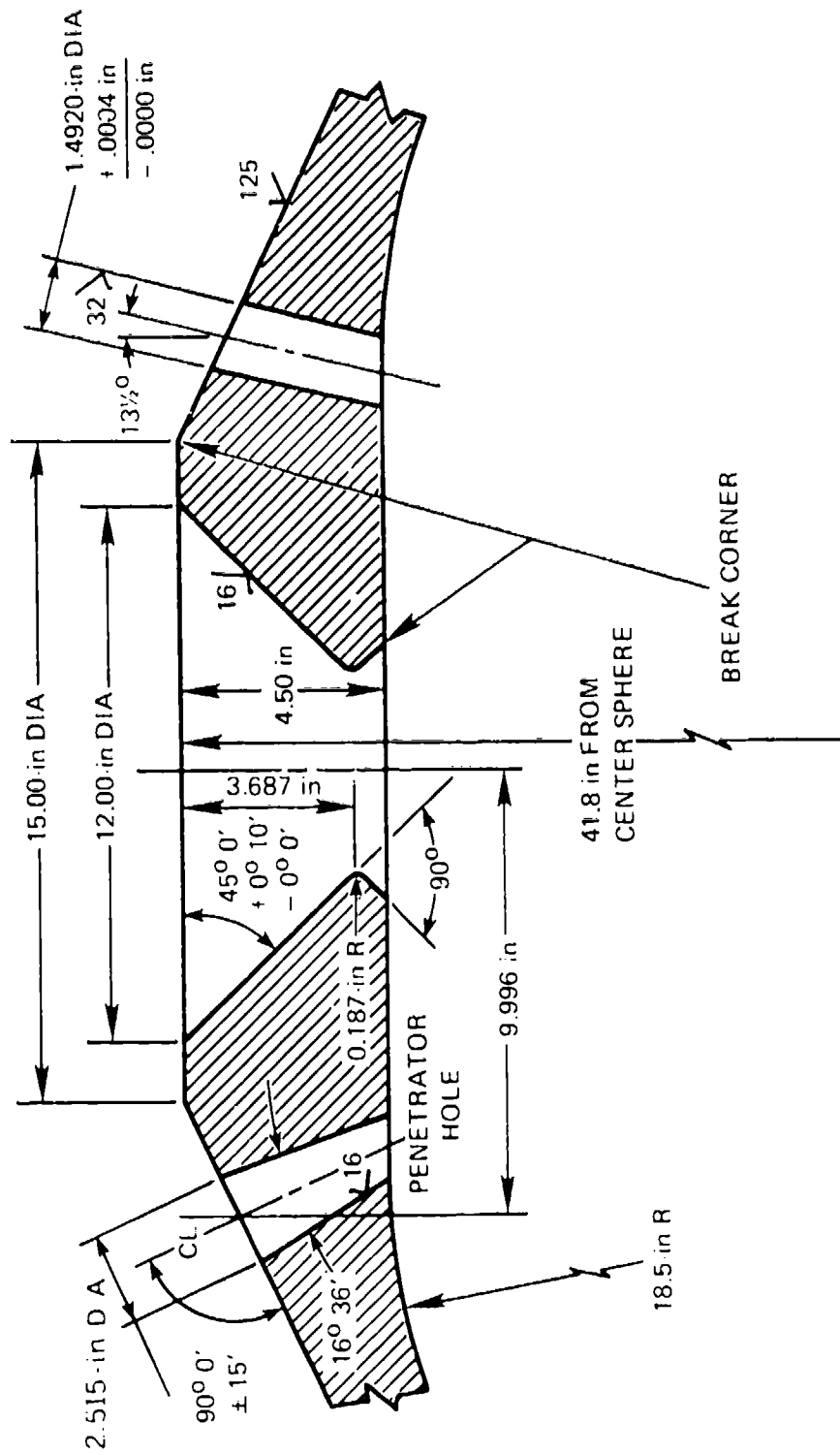side (R_o) and inside (R_i) spherical radii of 8.520 and 3.520 inches, respectively, and a shell thickness (t) of 5 inches. Thus, by matching the D_o and D_i of the spherical sector window to the D_o and D_i of the conical frustum window, a 42 percent increase in window thickness was realized (increasing t from 3.5 to 5 inches, figures 2 and 4).

FABRICATION OF SPHERICAL SECTORS

The criteria used in selection of the fabrication technique were (1) the window had to be monolithic and (2) the plastic material had to meet the mechanical and physical properties specified by the Navy for pressure-resistant acrylic windows (reference 12).

Acrylic windows are usually machined from Plexiglas G plate, which is limited in thickness to 4 inches. Since the spherical sectors for ALVIN required machining stock of over 6-inch thickness, the sectors either had to be machined from blocks of acrylic prepared by laminating several plates of Plexiglas G or from custom-cast blocks of acrylic plastic. The latter approach proved to be the more economical. After determination of their mechanical properties, the custom-cast blocks were used as machining stock for the windows.

EVALUATION TESTS FOR SPHERICAL SECTORS

The criteria chosen for selection of the evaluation tests were (1) the test parameters had to simulate operational conditions, (2) the test parameters had to be more severe than those found under typical operational conditions, and (3) the tests had to be conducted only on windows (chosen at random) not slated for service in the submersible.

PROOFTEST PARAMETERS

The criteria used were (1) the prooftest was not to decrease significantly the potential service life of the window, (2) it had to be structurally meaningful, and (3) it had to serve as a benchmark for future prooftests applied to the same window because of repairs or statutory safety inspection requirements (reference 12).

12.010-in DIAMETER
11.990

POLISH

POLISH

$\frac{8.538}{8.520}$ in R_o

$\frac{3.530}{3.520}$ in R_i

$\frac{90°5'}{90°0'}$

BREAK SHARP POLISH
EDGES

NOTES:

1. ANNEAL THE WINDOW ONCE AFTER ROUGH MACHINING AND ONCE AFTER FINAL MACHINING AND POLISHING.

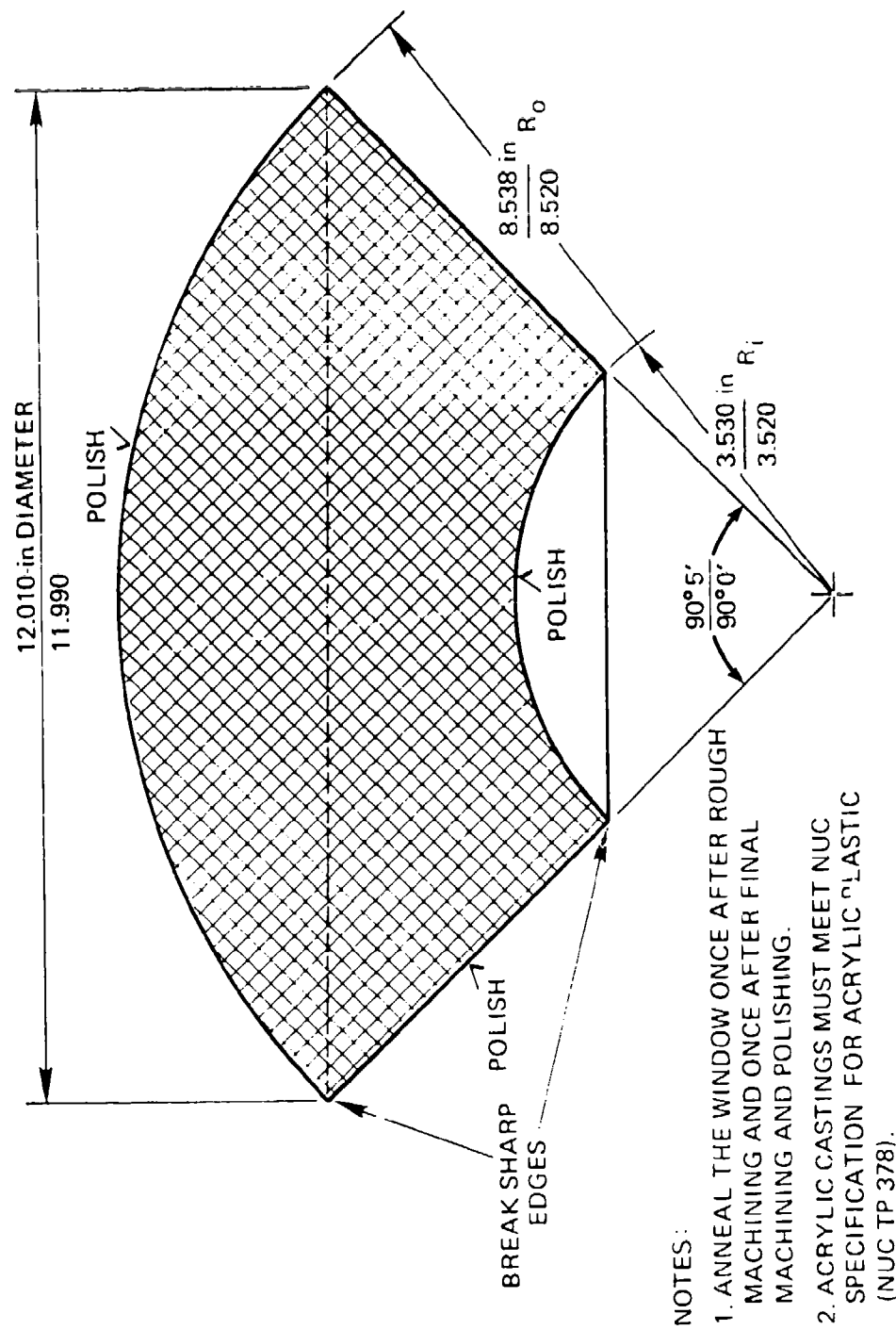2. ACRYLIC CASTINGS MUST MEET NUC SPECIFICATION FOR ACRYLIC PLASTIC (NUC TP 378).

Figure 4A. Spherical sector window to replace conical frustum windows in ALVIN.

11

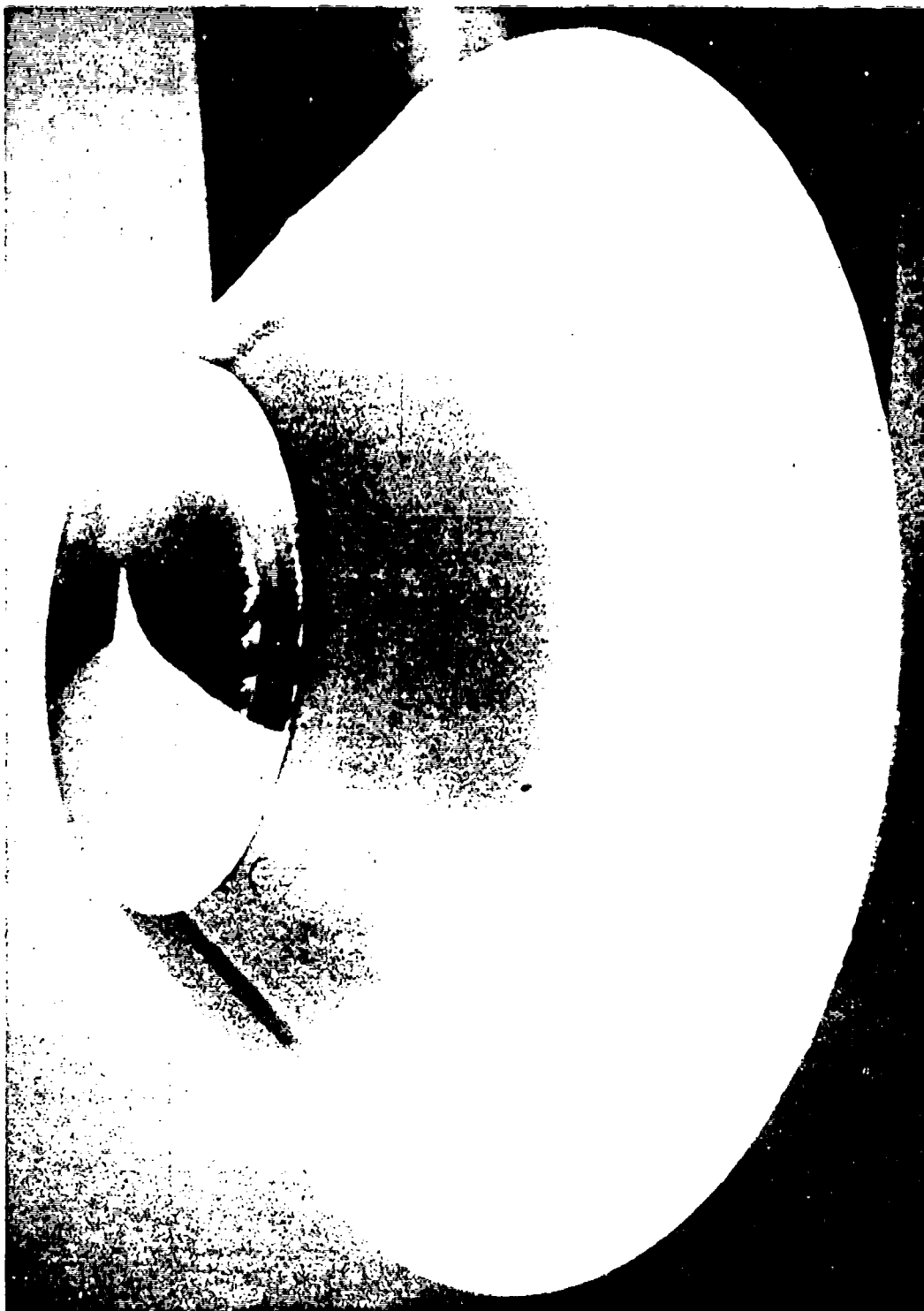Figure 48. High-pressure face of spherical sector window.

Figure 4C. Low-pressure face of spherical sector window.

13

FABRICATION

The spherical sector windows (figure 4) for ALVIN were machined by Reynolds and Taylor of Santa Ana, California, from custom-cast acrylic plastic, prepared by Polymer Products, Inc., of Oakland, California. The latter firm was selected because of its ability to produce massive, acrylic plastic castings whose mechanical properties meet the Navy's material property specifications for man-rated pressure-resistant windows (reference 12).

Seven massive acrylic plastic blocks were cast simultaneously from the same batch of acrylic monomer resin and polymer powder mix. One massive casting was sent to Delsen Laboratories of Burbank, California, for break-down into material test specimens and performance of material quality-control tests. Results show (table 1) that the massive castings met not only all mandatory material requirements, but also most elective requirements (reference 12).

The remaining six castings were machined into finished spherical sector windows for ALVIN (figure 4). Two (numbers 3 and 4) were chosen for testing and evaluation, and the other four (numbers 1, 2, 5, and 6) were earmarked for prooftesting and mounting into ALVIN.

Table 1. Physical Properties of Acrylic Castings
for ALVIN Spherical Windows.

Property	Specified	Actual
ASTM D638		
Room temperature, 0.05-inch/minute rate of test*		
Tensile strength, ultimate, psi	9000	9460
Tensile modulus, psi	4×10^5	4.5×10^5
Elongation, percent	2	2.9
ASTM D790		
Room temperature, 0.2-inch/minute rate of test, span of 7.246 inches		
Flexural strength, ultimate, psi	14,000	14,500
Flexural modulus, psi	4×10^5	5.1×10^5
ASTM D695		
Room temperature, 0.05-inch/minute rate of test		
Compressive yield, psi	15,000	15,700
Compressive modulus, psi	4×10^5	5.6×10^5
ASTM D621 Method A		
122°F, 4000-psi applied stress, 24-hour duration		
Deformation under compressive load, percent	<1.0	0.53
ASTM D792		
Specific gravity	1.18 to 1.20	1.18

Table 1. (Continued).

Property	Specified	Actual
ASTM D570 24-hour duration Water absorption, percent	<0.25	0.11
ASTM D542 23°C Index of refraction	1.48 to 1.50	1.462
ASTM D696 Air environment, 5°C/minute rate, 75°–240°F range Thermal expansion, inch/inch/°F	**	4.6×10^{-5}
ASTM D648 4.0-inch span Deflection temperature under load, °F	200	213
ASTM D732 Room temperature, 0.999-inch punch diameter, 0.05-inch/minute rate Shear strength, ultimate, psi	8000	9530

ASTM D256
Room temperature
    Notch Izod impact strength, foot-pound/inch
    of notch
	0.30	0.33

ASTM D785 Room temperature Rockwell "M" hardness	90	102

*Room temperature was in the 21.1 to 23.9°C range.

**Value not specified.

EXPERIMENTAL EVALUATION

TEST SETUP AND INSTRUMENTATION

The test setup used for the experimental evaluation and prooftesting is shown in figure 5. The window was secured to the test flange with a retainer ring similar to those used on the submersible. Between the retainer ring and window was inserted a 0.125-inch thick gasket to provide initial seal. Silicone grease was applied to the seating surfaces of the window and flange before assembly to serve as the secondary seal.
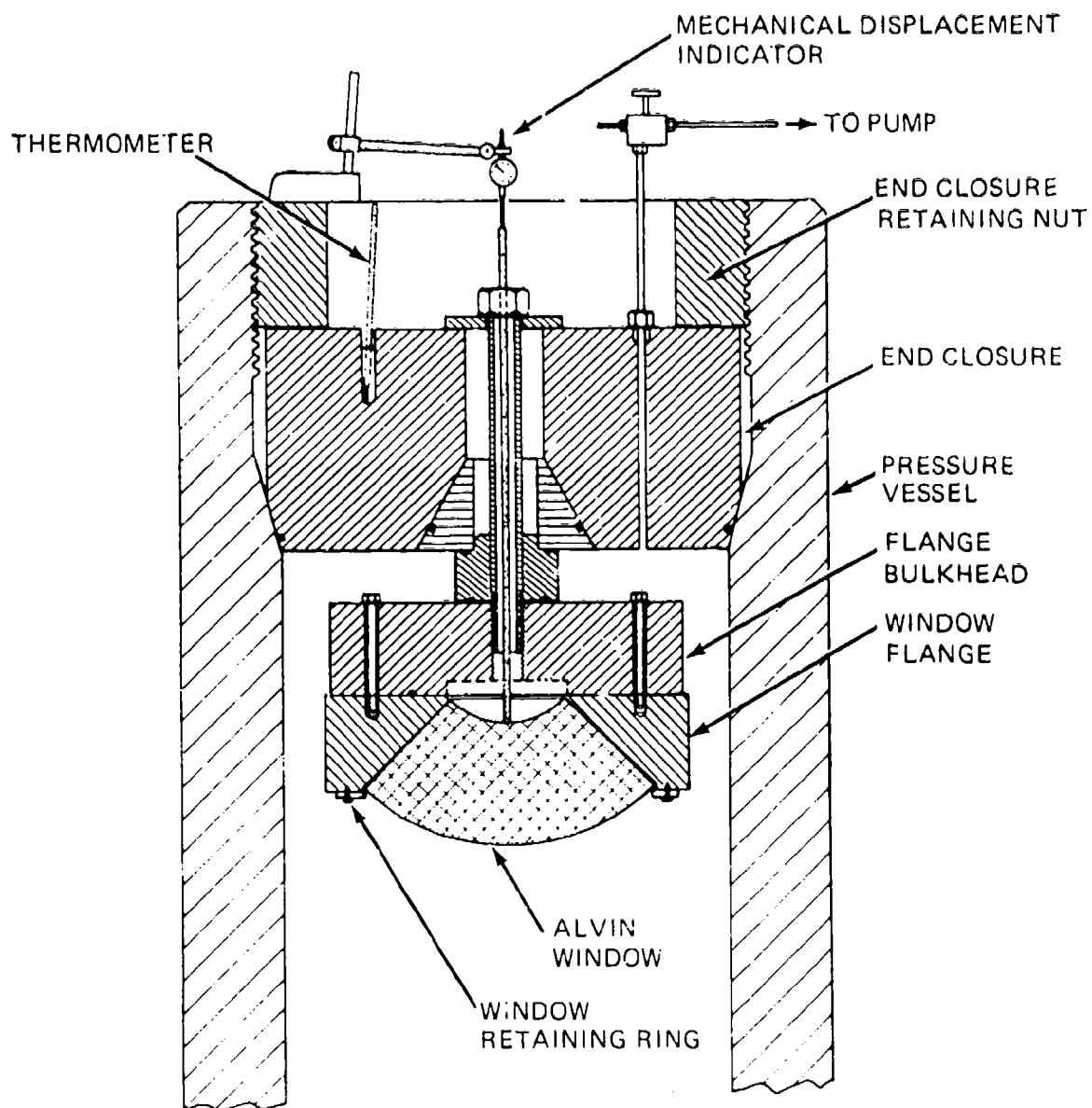
Figure 5. Testing arrangement for ALVIN windows in CEL's Deep Ocean Simulation Facility.

The test flange had a smaller included conical angle than the window (figure 6); the difference was measured to be about 50'. The window, therefore, seated only along the exterior face. However, there was no leakage of water at any time during the tests because of adequate compression in the gasket seal. In addition, it was found that the D_f of the test flange was 4.99 inches, while the D_f of the window flanges on the submersible's pressure hull was 4.40 inches. The differences between the test flange and the window seats in the submersible were not a conscious effort on the part of the authors, but was the result of circumstances. The test flange was leftover from the previous test program, conducted on conical frustum windows for ALVIN in 1966. The only advantage associated with using the undersized old test flange was that it allowed direct comparison between strains measured on spherical sector window 4 and the old conical frustum window 3 (reference 11).

Hydrostatic loading of the window was performed in the 18-inch diameter pressure vessel of the Deep Ocean Laboratory of CEL, Port Hueneme, California. Most strain measurements were made using a manual-type Budd strain indicator with a switch box. Only for test cycles 31 and 33 was an automatic data logger available; this was a 100-channel B&F digital unit with both magnetic- and paper-tape outputs. Scanning speed was 10 channels per second. The strain gages were connected in a 1/4-bridge using a standard three-wire connection. Throughout the test, a check gage was monitored to confirm proper operation of the equipment. A summary of the strain measuring instrumentation is in table 2. Subsequent to the tests, the accuracy of the Budd strain indicator and B&F data logger was checked using standard resistors. It was found that the B&F equipment was accurate within 0.5 percent and the Budd indicator within 1.5 percent in the range of strains measured in the tests.

TEST PROGRAM

The evaluation program chosen for windows 3 and 4 met all criteria postulated for a minimal experimental evaluation program.

Pressure Cycling

Spherical sector window 4, instrumented with nine electric strain gages on the concave face (figures 7 and 8) and mounted in an ALVIN-type window test flange (figure 6), was subjected to repeated pressure cycles. The typical cycle consisted of

1. Pressurizing the window with tap water at 75°F to 6000 psi at a 650-psi/minute rate.

2. Holding the pressure for 7 hours.

3. Depressurizing to 0 psi at a 650-psi/minute rate.

4. Relaxing at 0 pressure for 17 hours.

Strains were recorded during pressurization, sustained pressure loading, depressurization, and relaxation.

The objective was to prove conclusively that no permanent deformation or cracking occurred during a typical pressure cycle. The reason for selecting 6000 psi as the maximum pressure was that it was sufficiently greater than the 5357 psi encountered at the actual

RETAINING RING

NEOPRENE GASKET

FLANGE WITH 89° 10' INCLUDED ANGLE

ACRYLIC WINDOW WITH 90° INCLUDED ANGLE

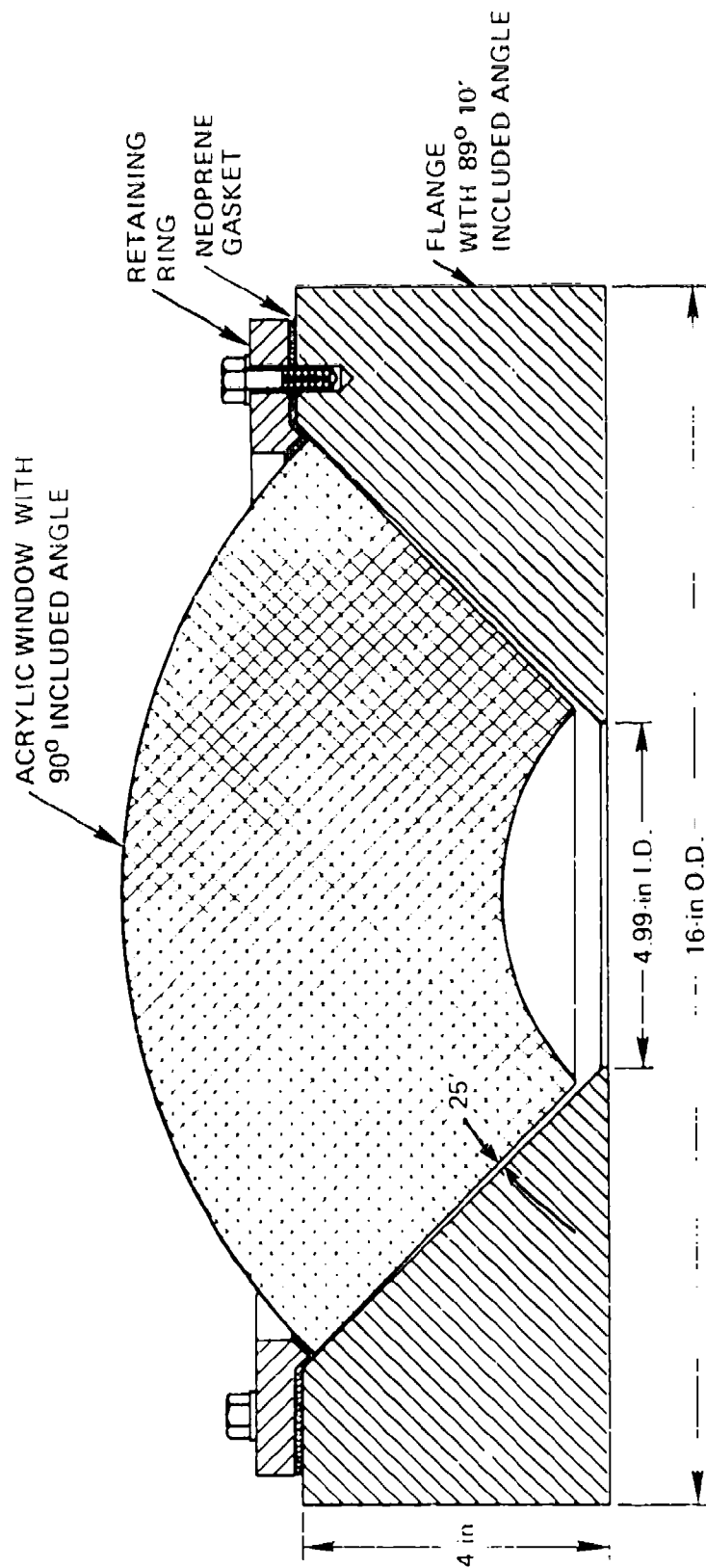4.99-in I.D.

16-in O.D.

25°

4 in

Figure 6. Window flange used in hydrostatic testing of conical frustum window and spherical sector window for ALVIN.

18

Table 2. Strain Gage Instrumentation on ALVIN Window Number 4.

| | | Description | | | | Placement | |
| | | | | | | Location of Gage Center | |
Gage No.	Make	Type	Gage Length, in.	Gage Factor	Orientation	Planned Cord Distance, in.	Actual Cord Distance, in.
1	BLH	FAE-25-12S6ET	1/4	2.04 ± 1%	Circumferential	0.20	0.21
2	BLH	FAE-25-12S6	1/4	2.03 ± 1%	Meridional	0.20	0.19
3	BLH	FAE-25-12S6ET	1/4	2.04 ± 1%	Circumferential	0.20	0.20
4	BUDD	C12-142B	1/4	2.08 ± 1/2%	Meridional	0.20	0.17
5	BLH	FAE-25-12S6ET	1/4	2.04 ± 1%	Circumferential	1.50	1.56
6	BLH	FAE-25-12S6	1/4	2.03 ± 1%	Meridional	1.50	1.56
7	BLH	FAE-25-12S6ET	1/4	2.04 ± 1%	Circumferential	1.50	1.50
8	BLH	FAE-25-12S6	1/4	2.03 ± 1%	Meridional	1.50	1.50
9	BLH	FAE-25-12S6	1/4	2.03 ± 1%	Meridional	2.70*	2.66*
10	BUDD	C12-142B	1/4	2.08 ± 1/2%	check gages on separate disc of acrylic material		
11	BUDD	C12-142B	1/4	2.08 ± 1/2%			

*Cord measurements from edge of window at gages 2 and 4.

SPILLED RTV
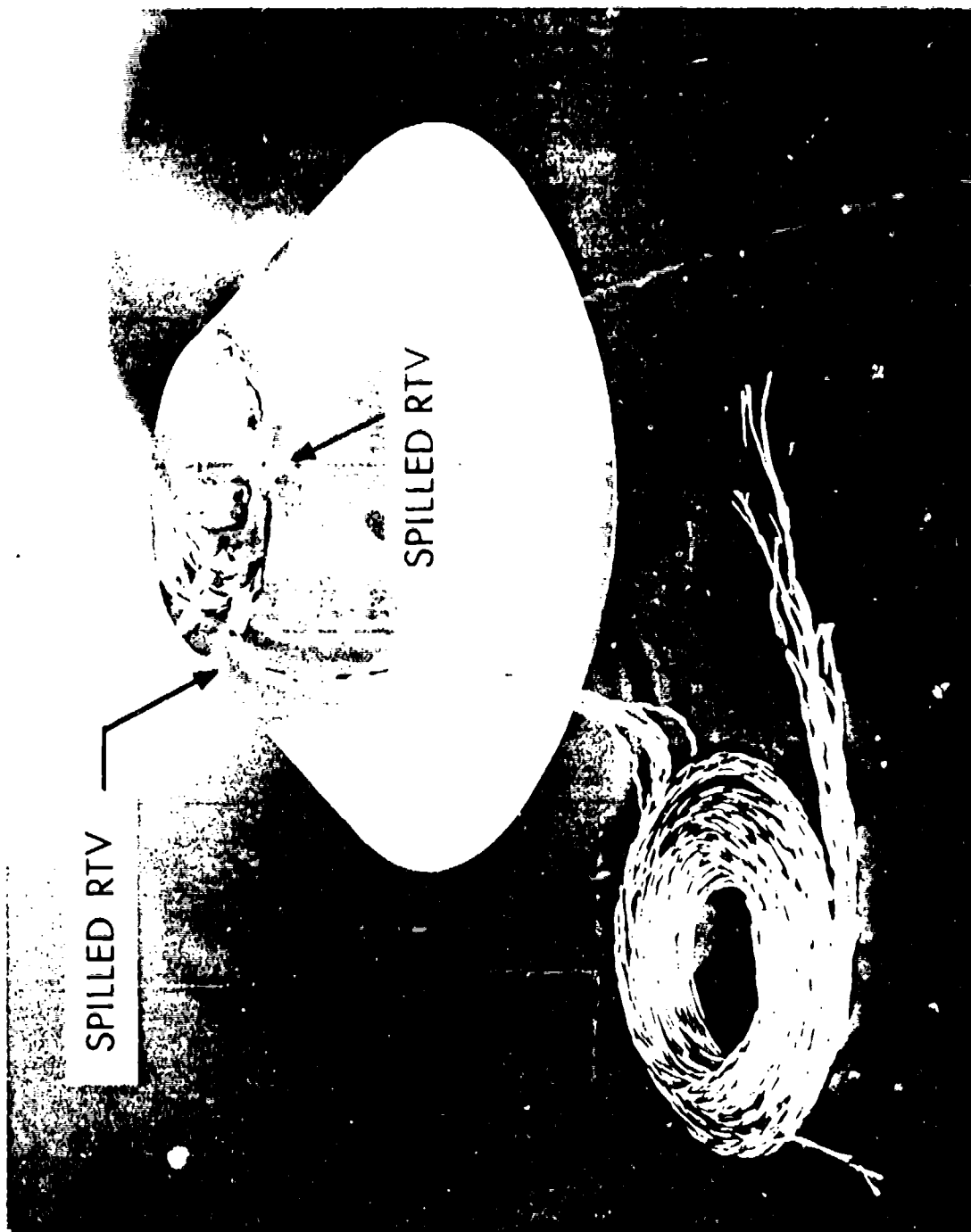
SPILLED RTV

Figure 7A. Spherical sector window 4 instrumented with electrical-resistance strain gages. Overall view.
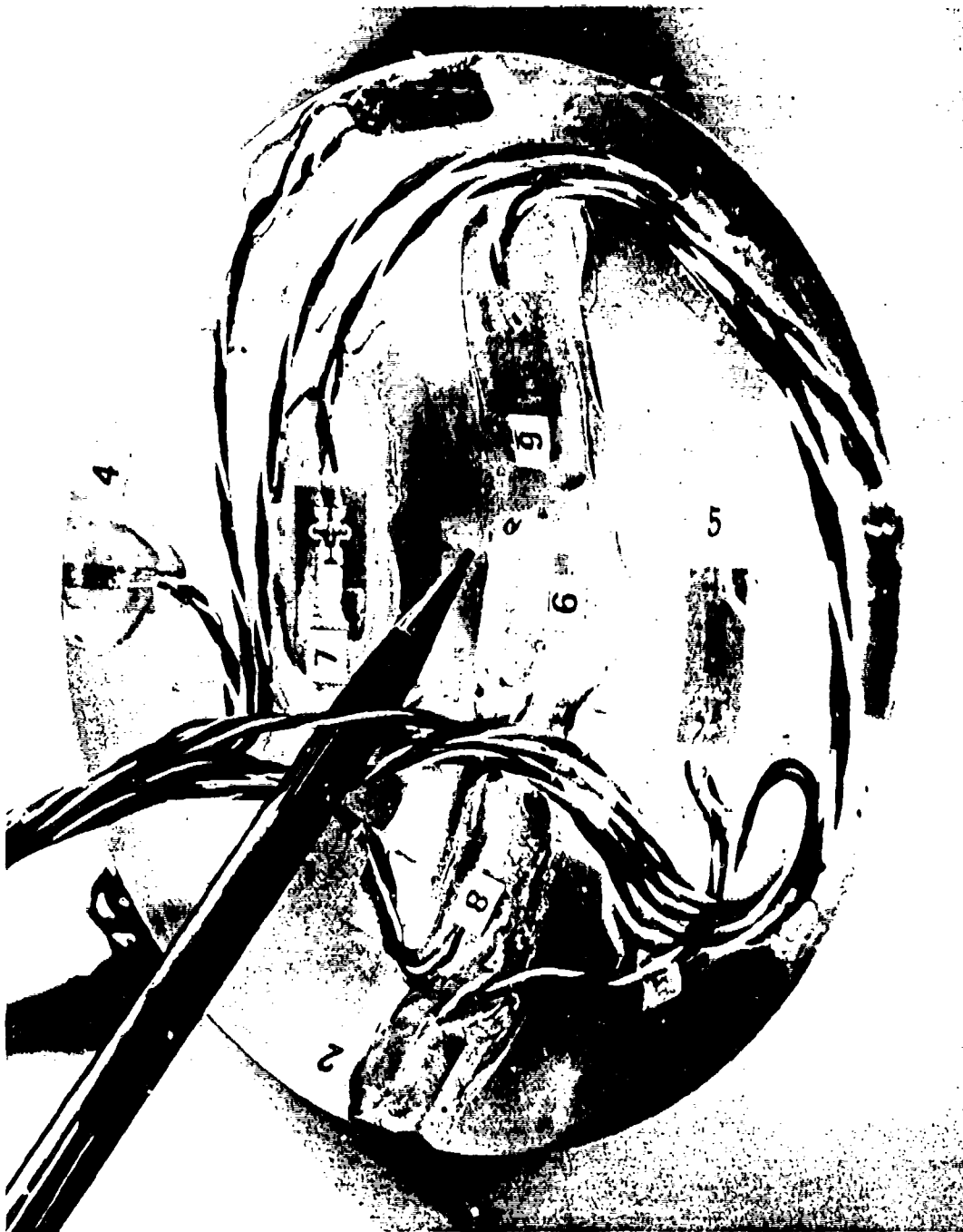
Figure 7B. San... window as in figure 7A. Close-up view.

21

Figure 7C. Typical test arrangement for window in figure 7A. Shown after long-term sustained pressure loading at 20,000 psi.
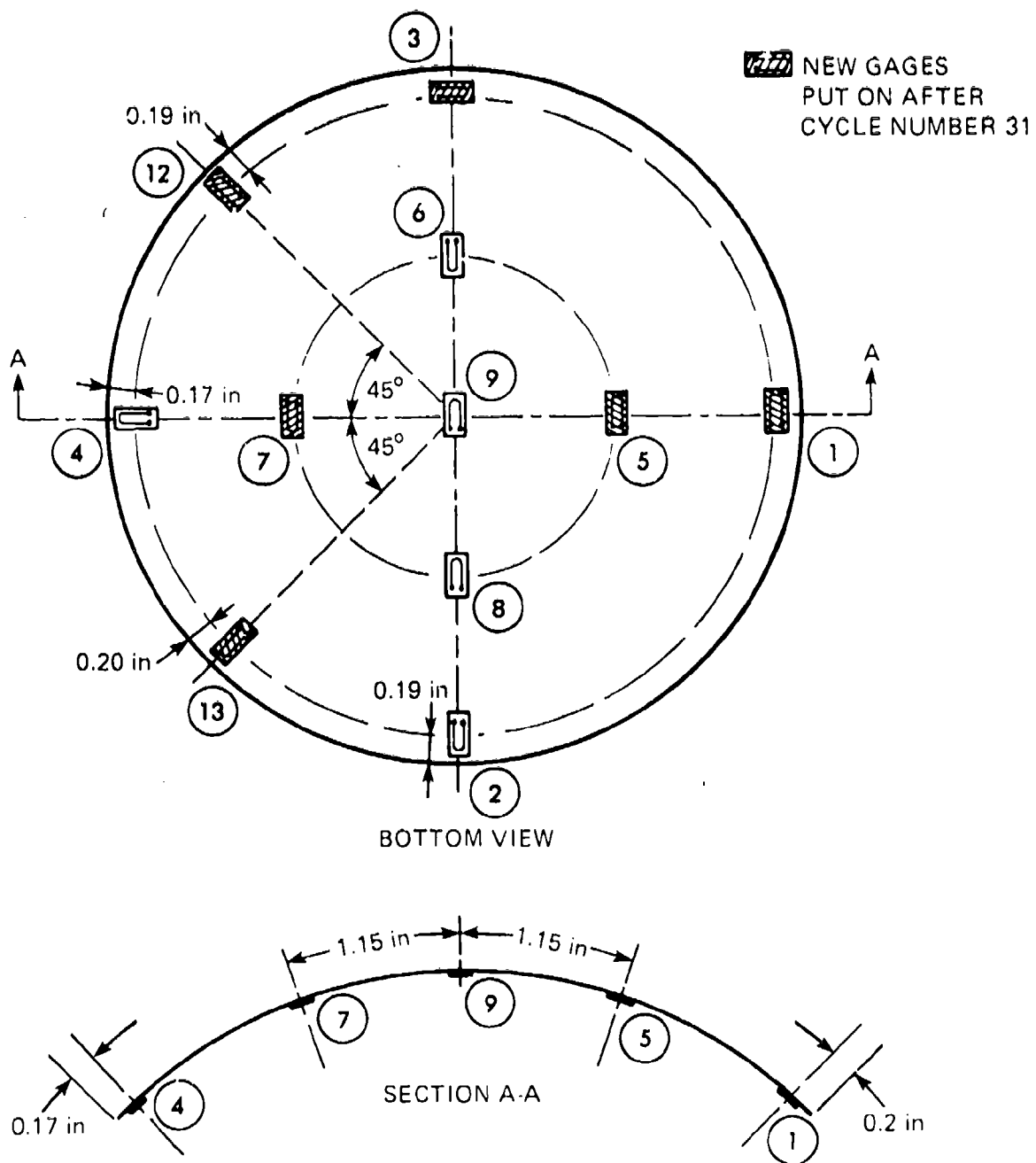
22

Figure 8. Location of strain gages on low-pressure face of spherical sector window.

operating depth. This compensated for a possible, small variation in material strength between test window 4 and operational windows 1, 2, 5, and 6. The 7 hours of sustained loading represented the maximum duration of a typical dive at maximum depth, while 17 hours of relaxation represented the typical time interval between successive dives at sea. The temperature of 75°F was used, as it was a severe test condition for pressure cycling (acrylic creeps more at 75°F than at the 35°F typical temperature at 12,000 feet).

Long-Term Loading

Spherical window 3, instrumented with a mechanical displacement gage and mounted in an ALVIN-type window test flange (figure 5), was pressurized with 75°F tap water at a 650-psi/minute rate to 20,000 psi; held at pressure for 100 hours; and depressurized to 0 psi. Axial displacements were recorded during pressurization, sustained pressure loading, and depressurization.

The objective was to prove conclusively that, despite the great depth at which a submersible comes to rest after a disabling accident and its remaining trapped for a maximum of 100 hours (extent of life-support functions), the windows would not be a source of catastrophic failure. Since 20,000 psi represents pressure in excess of any found in the deepest ocean and 100 hours are in excess of the life-support functions, they were chosen as the pressure and loading parameters.

Prooftesting

This consisted of subjecting each operational spherical acrylic window (numbers 1, 2, 5, and 6) to a single 7-hour pressure loading with 6000 psi as the maximum pressure, followed by 17 hours of relaxation at 0 pressure. Axial displacement was measured during the pressurization and relaxation phases of the prooftest. Pressurization was accomplished with tap water at 75°F and at a 650-psi/minute rate.

A pressure of 6000 psi was chosen because it was sufficiently higher than that encountered at the 12,000-foot maximum operational depth. This provided a margin of safety, but it was also not so high as to decrease significantly the potential fatigue life of the window.

TEST OBSERVATIONS

CYCLIC PRESSURE LOADING

Tests in Flanges with 89°10' Included Angle

Pressure Cycles 1 through 30. Because the included angle of the window seat was smaller than that of the window, the contact between them was very localized when mounted in the flange (figure 6). Because the contact between the acrylic and metal occurred only at the large diameter of the window, accurate positioning of the window in the seat was hard to attain. It was assumed, however, that the retainer ring would cause

the window to seat evenly around the circumference when it was bolted in place. After seating the window in the flange, the clearance between the corner of the window's low-pressure face and the steel seat was about 0.040 inch.

Because of this mismatch, the entire bearing surface of the window would not contact the flange until the external hydrostatic pressure had deformed the sector angle by approximately 50' or about 1 percent of the included angle. This is verified by strains measured at nine locations on the low-pressure face during pressurization from 0 to 6000 psi (figures 8 and 9). As soon as the external pressure began to rise so did the strains, but not at a uniform rate, and, in some cases, in unexpected directions. Instead of being compressive, the circumferential strains were tensile, which indicated that the spherical sector was under flexure and that the low-pressure face was in tension.

When the external hydrostatic pressure reached about 1500 psi, the contact between the window and flange was completely extended to the diameter of the low-pressure face. Additional increases in hydrostatic pressure did not generate any bending forces in the window, but wedged it like a plug into the steel flange. This is substantiated by the fact that at pressures above approximately 1500 psi the tensile strains began to decrease until they became compressive at about 3000 psi. From 3000 to 6000 psi, the compressive strains increased linearly with pressure.

Because the fit between the window and flange changed with external pressure, the distribution of strains across the window face also became a function of pressure. The circumferential strains varied with pressure in the following manner.

1. At 1000 psi of external pressure, the strains were all positive and fairly uniform across the entire width of the low-pressure face (figure 10).

2. At 3000 psi, the strains in the center of the face were negative, while those at the edge were still positive.

3. At 6000 psi, the strains across the low-pressure face were negative and those at the edge were the lowest.

The distribution of the meridional strains varied in a different manner with pressure:

1. At 1000 psi, the meridional strains at the edge were negative, while in the center they were still positive.

2. At 3000 psi, the strains were negative and those at the edge were the highest.

3. At 6000 psi, the strains were not only negative, but also fairly uniform across the face.

During the period of sustained loading at 6000 psi, the compressive strain increased by about 17 percent, indicating that only moderate creep had occurred (figure 9). The residual strain in the window at the end of the 17-hour relaxation period increased to about -400 microinches during the first four to five load cycles (figure 11). Further cycling of the window did not lead to any further increase of the residual strain. In fact, during the latter third of the cycling period, the residual strain was observed to drop back towards the -300-microinch level.
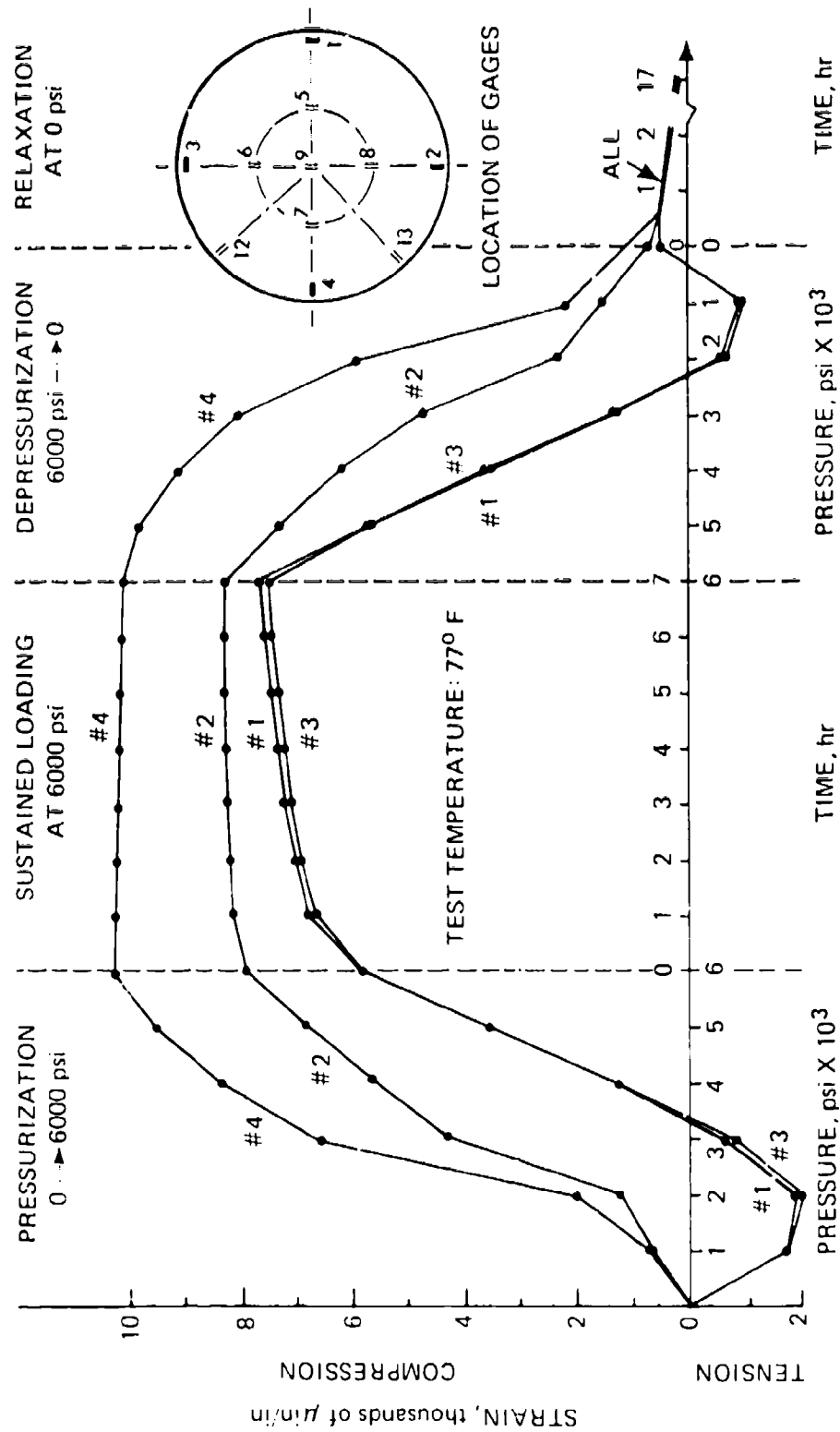
Figure 9A. Strains around edge of low-pressure face on spherical sector window 4. Tests conducted in flange seat with 89°10' included angle. Pressure cycle 1.
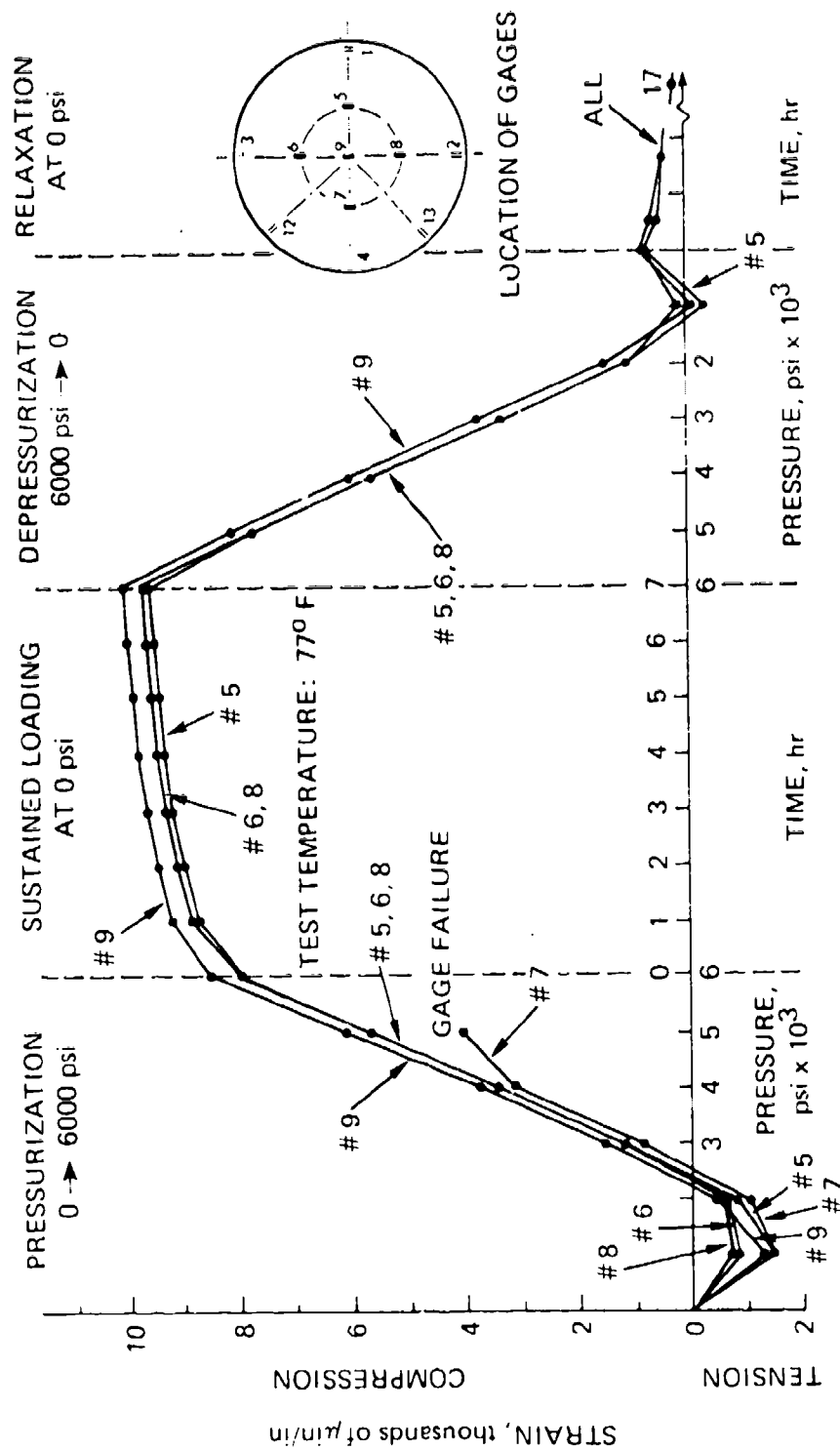
Figure 9B. Strains in central area of low-pressure face of spherical sector window 4.
Tests conducted in flange seat with 89°10' included angle. Pressure cycle 1.

27
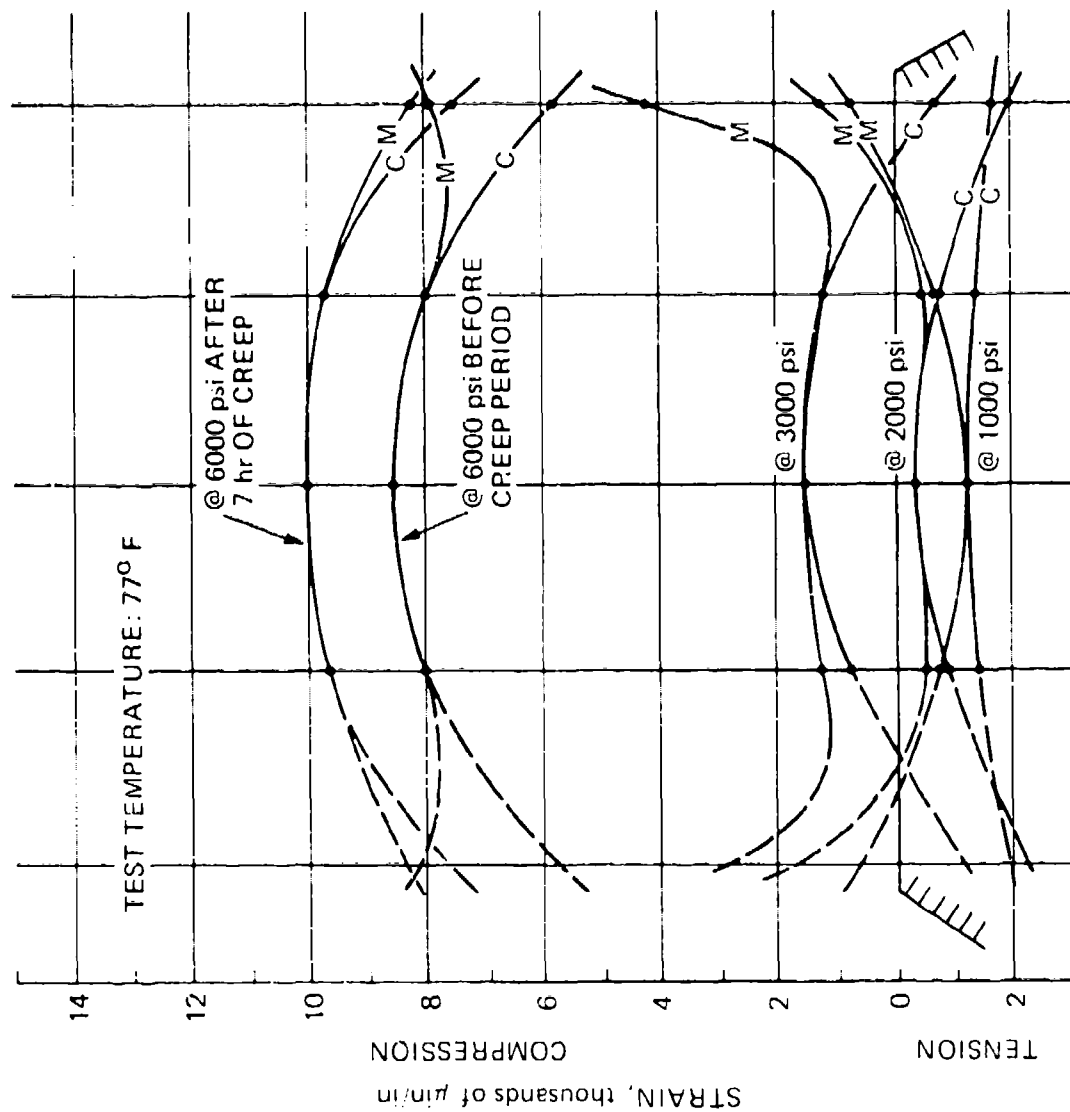
Figure 10. Distribution of strains on low-pressure face of spherical sector window 4. Tests conducted in flange seat with 89° 10' included angle. Pressure cycle 1. (M, meridional; C, circumferential orientation.)

28
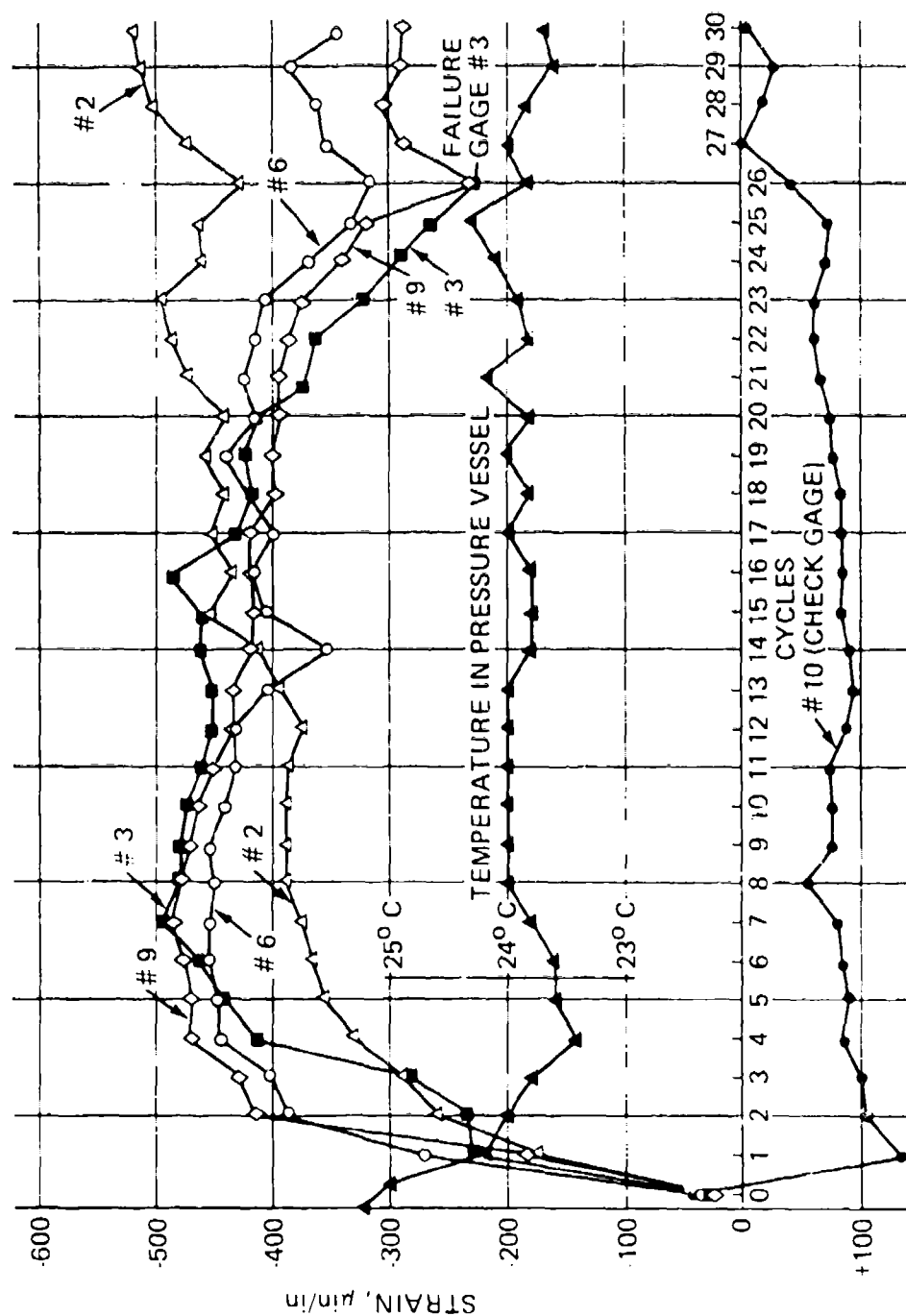
Figure 11. Strain readings on low-pressure face of spherical sector window 4 just prior to beginning of each pressure cycle to 6000 psi. Note the large change in temperature and strain during the first two pressure cycles. All tests were conducted in flange seat with 89° 10' included angle.

The maximum strain produced during each load cycle was always measured at the end of the creep period, except for gage 4 which usually indicated little or no creep at that location. For other gages, as the cycling progressed, a gradual reduction of the maximum strain was recorded on all gages. The reduction was about 8 to 10 percent at the edge and about 5 to 7 percent away from the edge, most of it occurring during the first few load cycles (figure 12). Some reduction in the strains' magnitude was caused by a decrease in ambient temperature from 77.36 to 75.7°F.

These two observations regarding the change in the residual and total strains seem to indicate that the window seated itself during the first two cycles and that the support of the window in the flange did not later change. It is of interest to note that, although residual compressive strains were generated in the window during the first few pressure cycles, this did not result in a changed window shape that better fitted the flange. This postulate is substantiated in all 31 pressure cycles to which the window was subjected and in the 89°10' test flange by the reversal of strain direction during pressurization from 0 to 3000 psi. The reversal of strain direction indicated the presence of flexure during pressurization in that pressure range.

Inspection of Window after Load Cycle 30. Visual inspection did not reveal cracks, crazing, or permanent deformation after the 30 load cycles to 6000 psi. (The latter is also verified by the strain measurements in figure 12.)

Scuff marks on the seating surface, similar to those seen on the four prooftested windows, were observed. Because of their axial orientation and length (approximately 0.063 inch), they had to be the result of sliding in the flange (figure 13).

Pressure Cycle 31. It was decided to continue the test to determine what the strains would be if the window were removed and reseated in the same 89°10' flange. To obtain good data for comparison, new gages were mounted to replace those that had failed and two additional gages were mounted in the meridional direction near the edge. The window was then remounted in the 89°10' included angle and subjected to another pressure cycle to 6000 psi. An automatic high-speed data logger was used for recording the data.

Figure 14 shows that the same flexure was observed. The strains recorded by the gages away from the edge corresponded well with those previously measured, considering the difference in temperature and instrumentation (figures 9B and 14B). This was also true for the two gages in the circumferential direction at the edge of the window.

The gages measuring meridional strains close to the edge, however, provided results quite different from those recorded before the window was removed (figures 9A and 14A). Also, except during the first 2000 psi of pressurization, the gages recorded different amounts of strain. During all load cycles, prior to removal and remounting of the window, the meridional strain had always been higher than the circumferential strain (figure 10); but the opposite occurred during this cycle (figure 15).

The only explanation offered for this and for the apparent nonuniform circumferential distribution of meridional strains near the edge is that during installation in a flange whose seat angle did not match that of the window it became cocked. During the first mounting it was probably cocked on one direction, and after remounting for load cycle 31 it was cocked a little differently. Since during cycle 31 the meridional strains close to the
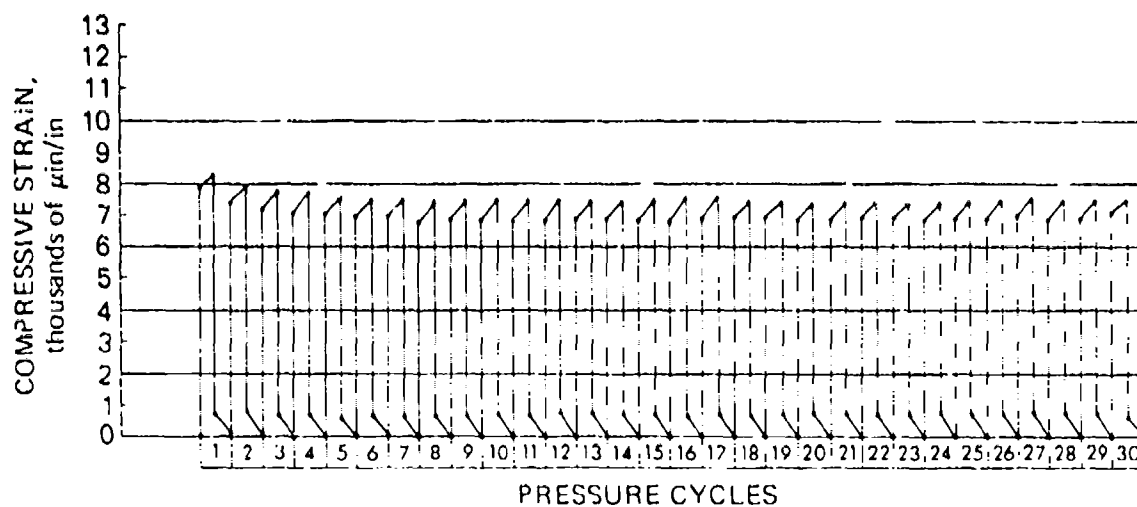
Figure 12A. Meridional strains at edge of low-pressure face on spherical sector window 4. Strains occurred during repeated pressure cycling to 6000 psi in a flange seat with 89°10' included angle. During each pressure cycle of 24 hours the pressure was applied for 7 hours. Gage 2.
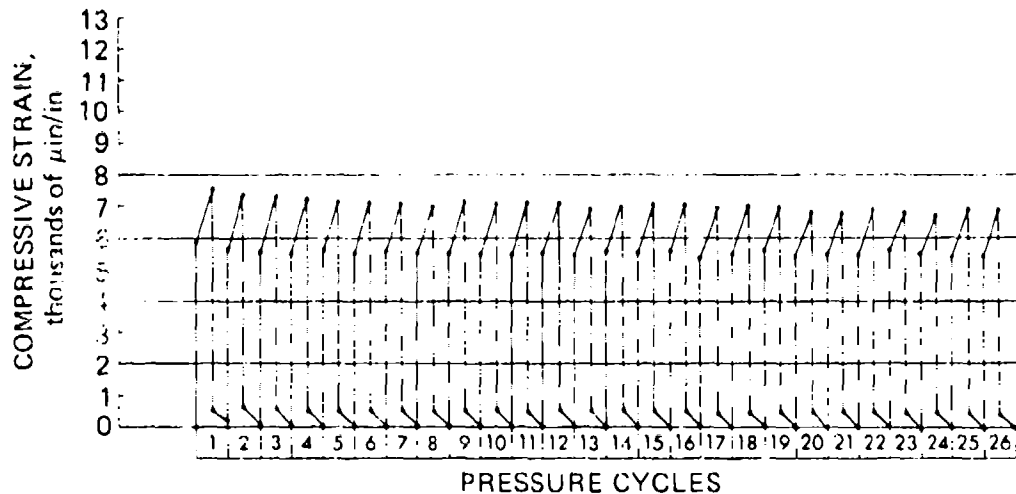

Figure 12B. Circumferential strains at edge of low-pressure face on spherical sector window 4. Strains occurred during repeated pressure cycling to 6000 psi in a flange seat of 89°10' included angle. Gage 3.
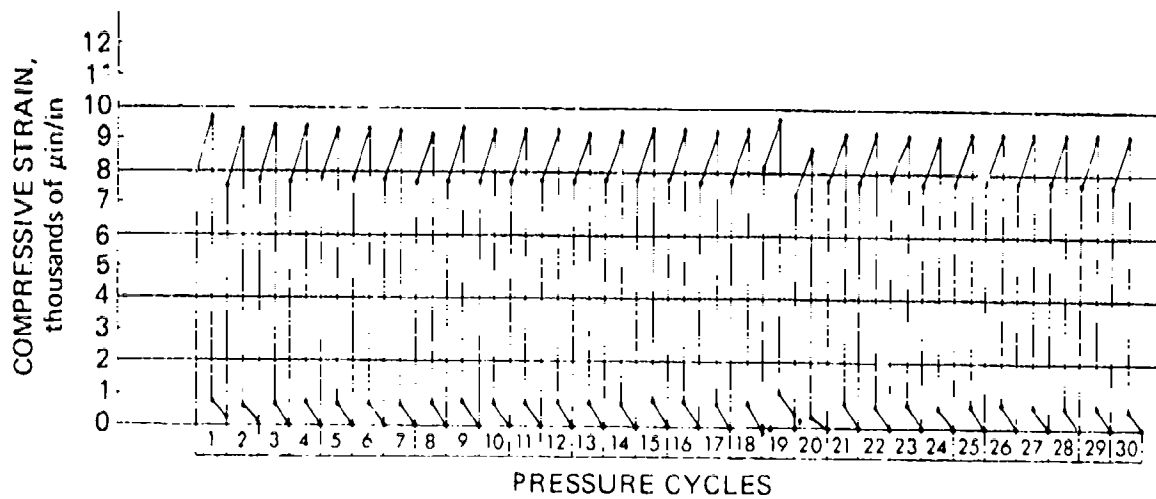
Figure 12C. Meridional strains on low-pressure face of spherical sector window 4 midway between the edge and center of the face. Strains occurred during repeated pressure cycling to 6000 psi in a flange seat with 89°10′ included angle. Gage 6.
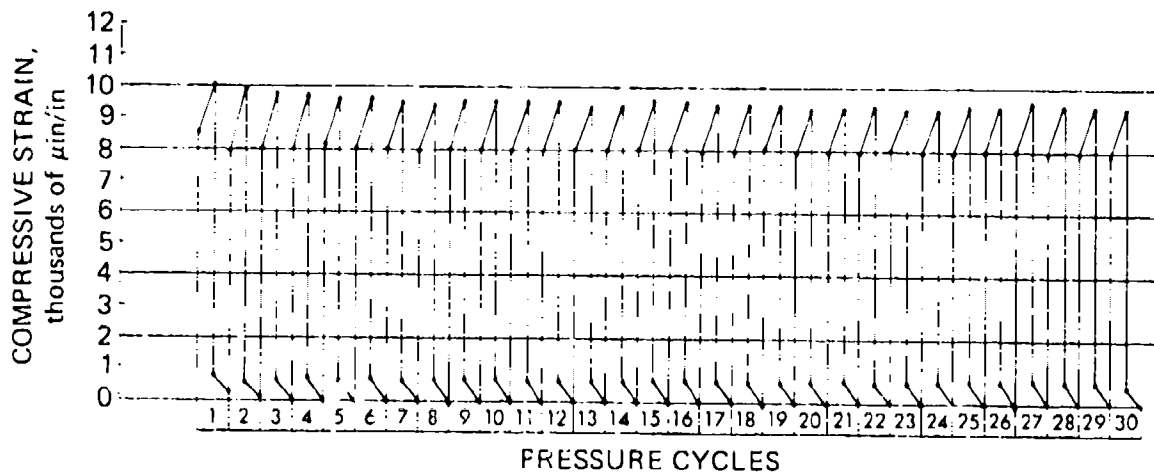
Figure 12D. Strains at the center of low-pressure on spherical sector window 4. Strains occurred during repeated pressure cycling to 6000 psi in a flange seat with an 89°10′ included angle. Gage 9.
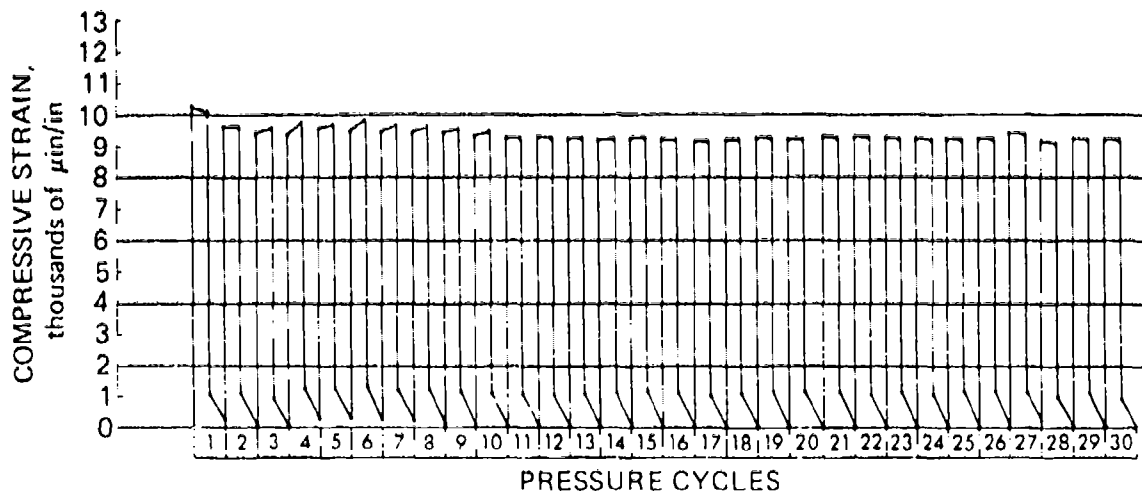
Figure 12E. Meridional strains at edge of low-pressure face of spherical sector window 4. Strains occurred during repeated pressure cycling to 6000 psi in a flange seat with 89°10' included angle. Gage 4.
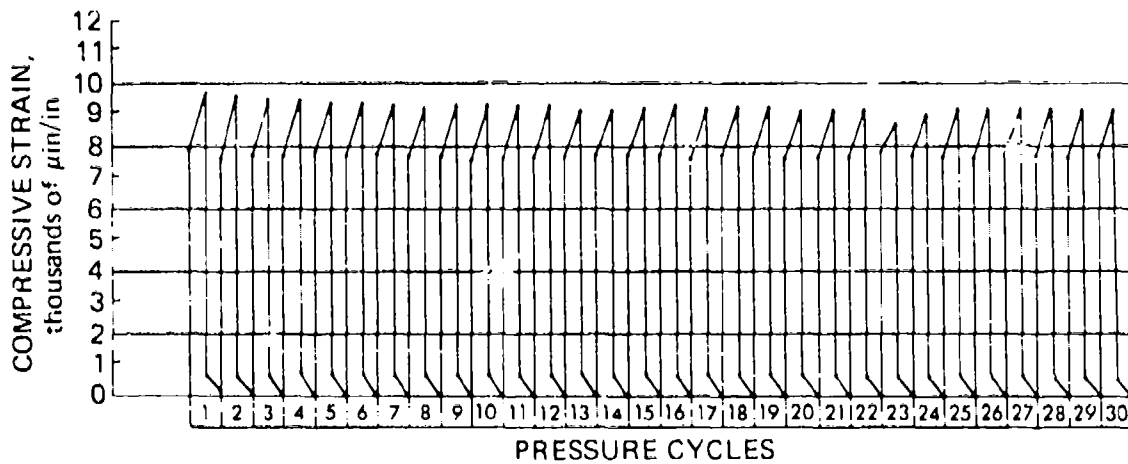
Figure 12F. Meridional strains at edge of low-pressure face of spherical sector window 4 midway between edge and center of face. Strains occurred during repeated pressure cycling to 6000 psi in a flange seat with 89°10' included angle. Gage 8.

33
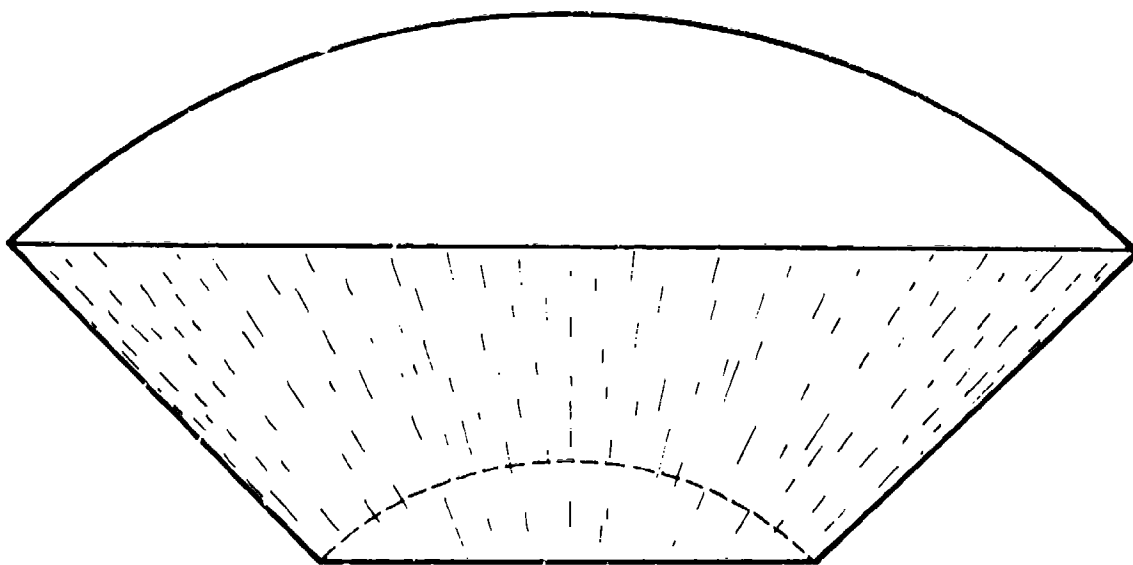
Figure 13A. Location and direction of scuff marks on spherical sector window 4 af . undergoing 30 pressure cycles to 6000 psi.
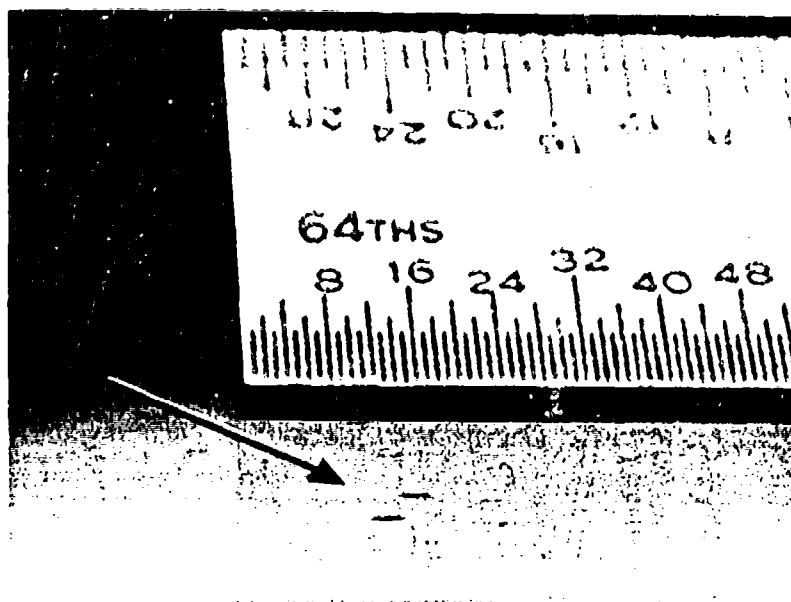
Figure 13B. Scuff marks shown in figure 13A.

Figure 14A. Strains around edge of low-pressure face on spherical sector window 4. Strains occurred during pressure cycle 31 in flange seat with 89°10' included angle.

Figure 14B. Strains in central area of low-pressure of spherical sector window 4. Strains occurred during pressure cycle 31 in flange seat with 89°10' included angle.

Figure 15. Distribution of strains on low-pressure face of spherical sector window 4.
Strains occurred during pressure cycle 31 in flange seat with 89°10' included angle.

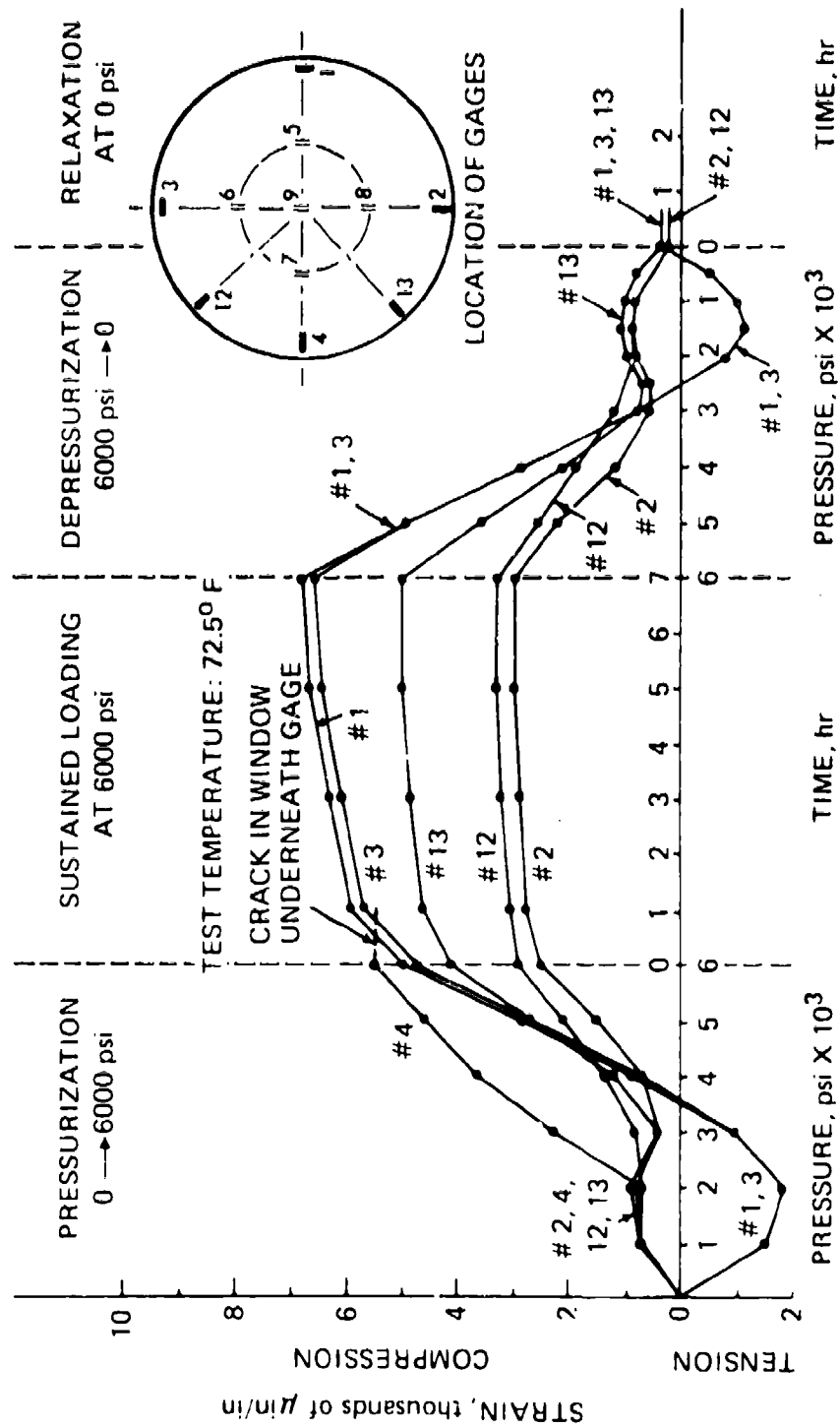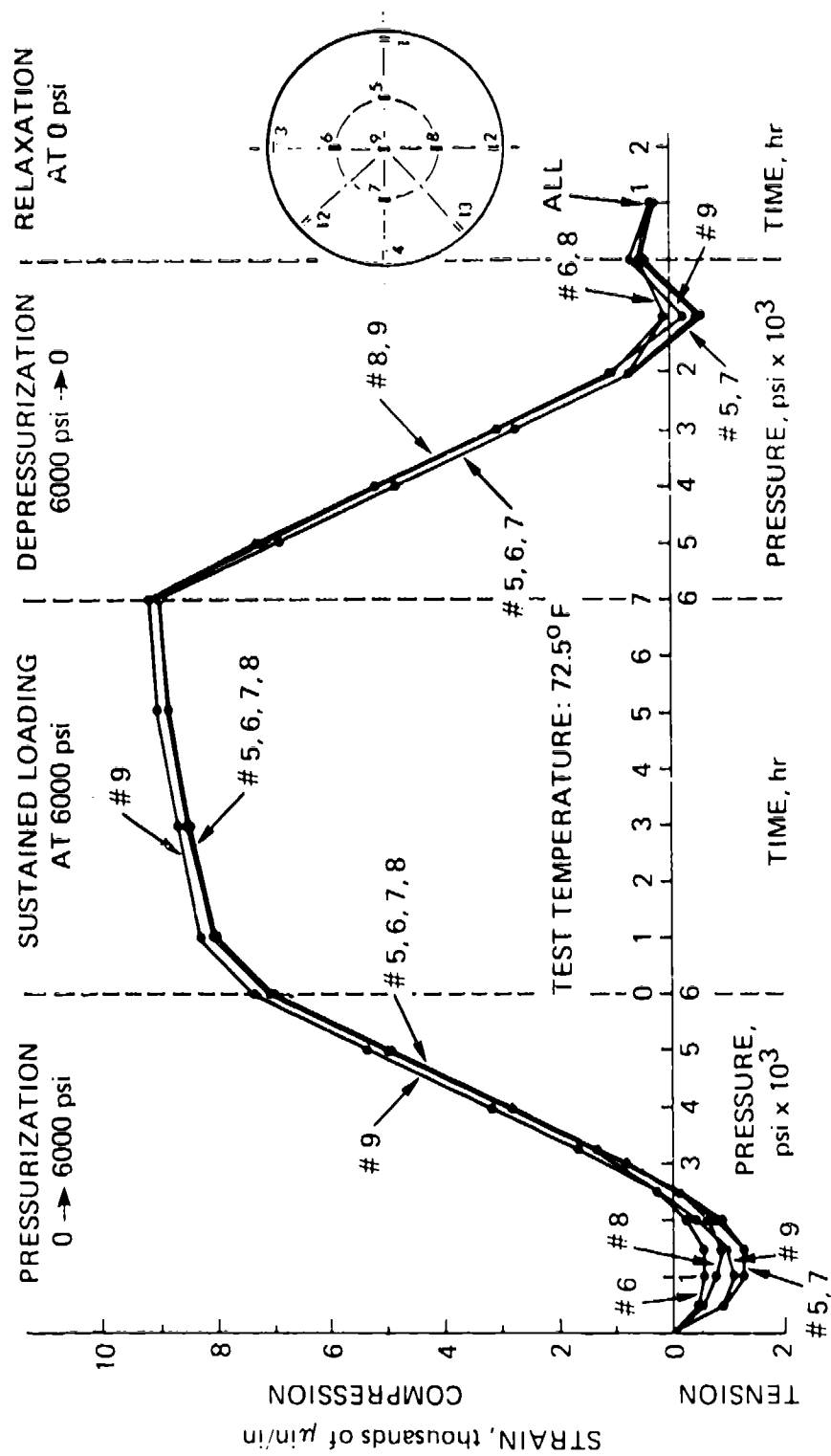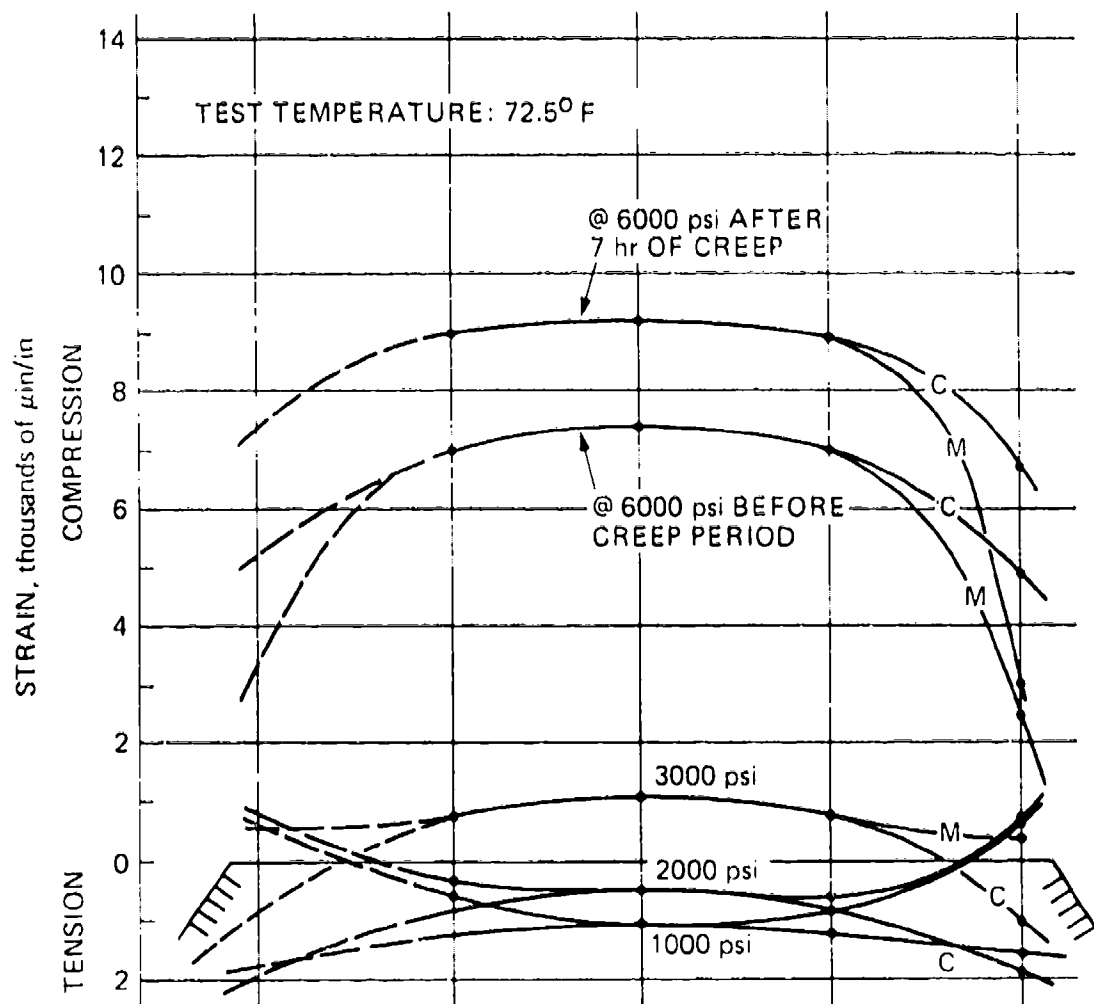edge were substantially lower than those away from the edge, a steep strain gradient did probably exist close to the edge. This made the distance of the gages from the edge of critical importance, and, with this in mind, it was measured as accurately as possible. It was found that gage 4 was the closest to the edge, but that gages 2 and 12 when compared with gage 13 were also close to the edge (table 2). It was also noticed (figure 14A) that not only did the magnitude of meridional strains vary along the edge of the window but that the strains recorded by the different gages started to increase at different times during pressurization and their rates of increase also varied.

Inspection after Load Cycle 31. It was found that the window was in excellent shape but that a small halfmoon crack had developed on the window seat below gage 4 (figure 16). This crack explained the erratic strains generated by this gage during pressurization to 6000 psi. Some surface crazing was also discovered on the window seat below gage 2. These surface discontinuities were caused by the RTV* used to waterproof the gages. Some RTV was accidentally spilled on the window seat, and the acetic acid contained in the RTV sensitized the surface to tensile and shear stresses. When shear stresses were generated on the window seat during pressurization, the sensitized surface crazed while the bulk of the unsensitized window seat withstood the shear stresses without damage. Similar cracking of sensitized acrylic bearing surfaces was observed previously in another study, where RTV was accidentally applied to the hatch seat in a spherical acrylic pressure hull.

Test in Flange with 90° Included Angle

Flange Modification. The flange was machined to provide an accurate fit for the 90° spherical sector window. During machining, no other significant deviation from its ideal shape was found. The new finish was, at best, as good as the finish of the original machining.

Test Cycles 32 and 33. With the window remounted in the remachined flange, two additional pressure cycles were performed. No initial tensile strains were recorded in the central part of the window (figure 17). Almost from the beginning of pressurization, the strain increased approximately linearly with pressure, without the characteristic dip in the curve that was recorded during all previous load cycles. There was no significant difference in the strains produced during the two load cycles. The average strain rate in the 3000- to 5000-psi range (which was very close to being a true linear range) was 2.1 microinches per inch per psi of pressure. This is the same rate observed during the 3000- to 5000-psi pressure range for cycle 31, prior to machining the flange (figure 14B).

The magnitude of the strains was observed to be substantially higher than before. The strain in the center of the low-pressure face reached about 15,000 microinches per inch as compared to about 9000 during load cycle 31. Also, the distribution of the strains in the central area had changed, with the highest strains in the circumferential direction halfway between the center and the edge (figure 17). During the previous load cycles, the highest strain was always at the center. Along the edge of the window, the two circumferential strain gages (1 and 3) recorded the same approximately linear relationship with pressure as

*RTV, room temperature vulcanizing silicon rubber. The acetic acid in RTV slightly dissolves acrylic plastic insuring an excellent bond with the plastic.

39
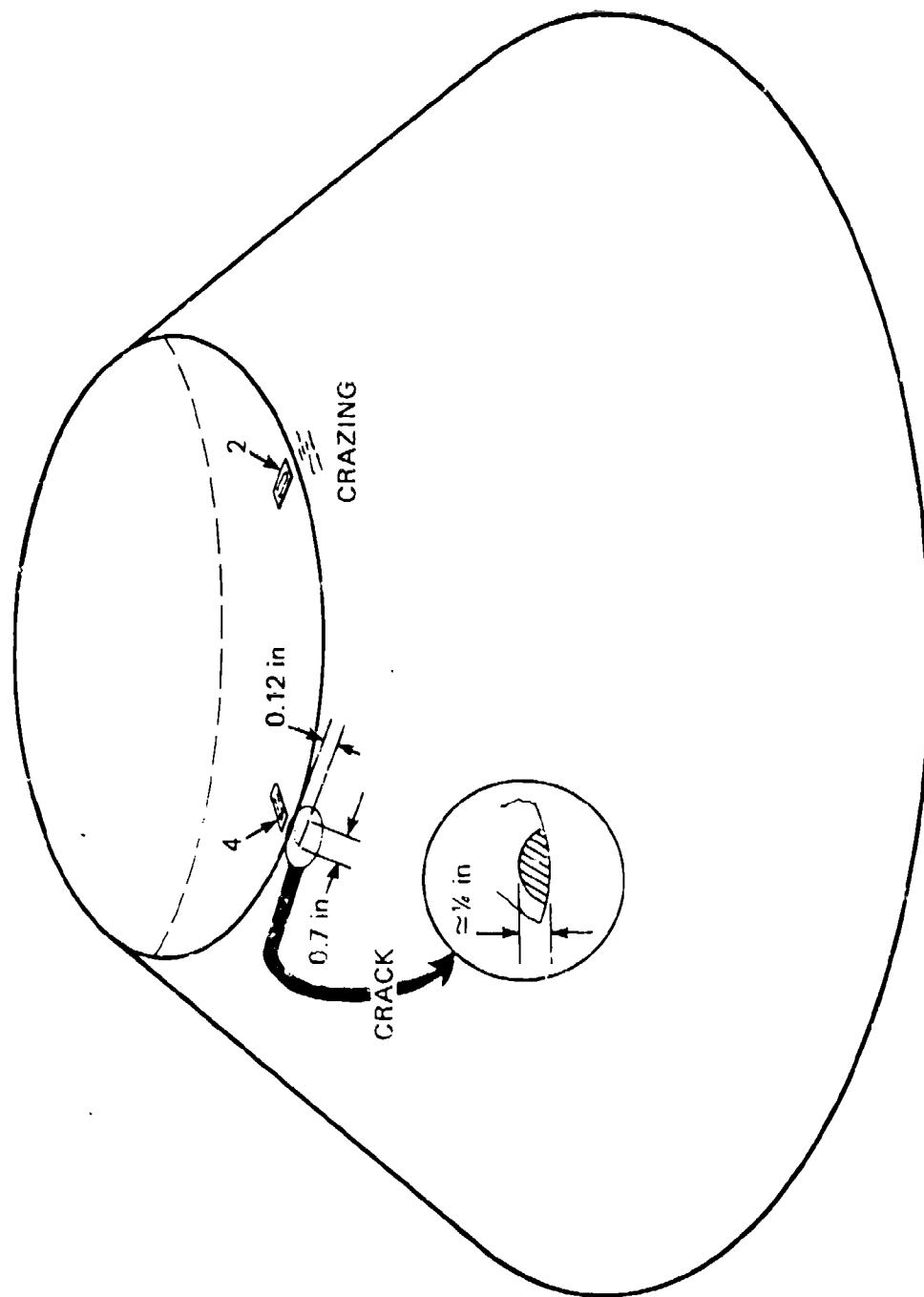
Figure 16A. Location of crack and crazing observed after 31 pressure cycles to 6000 psi.
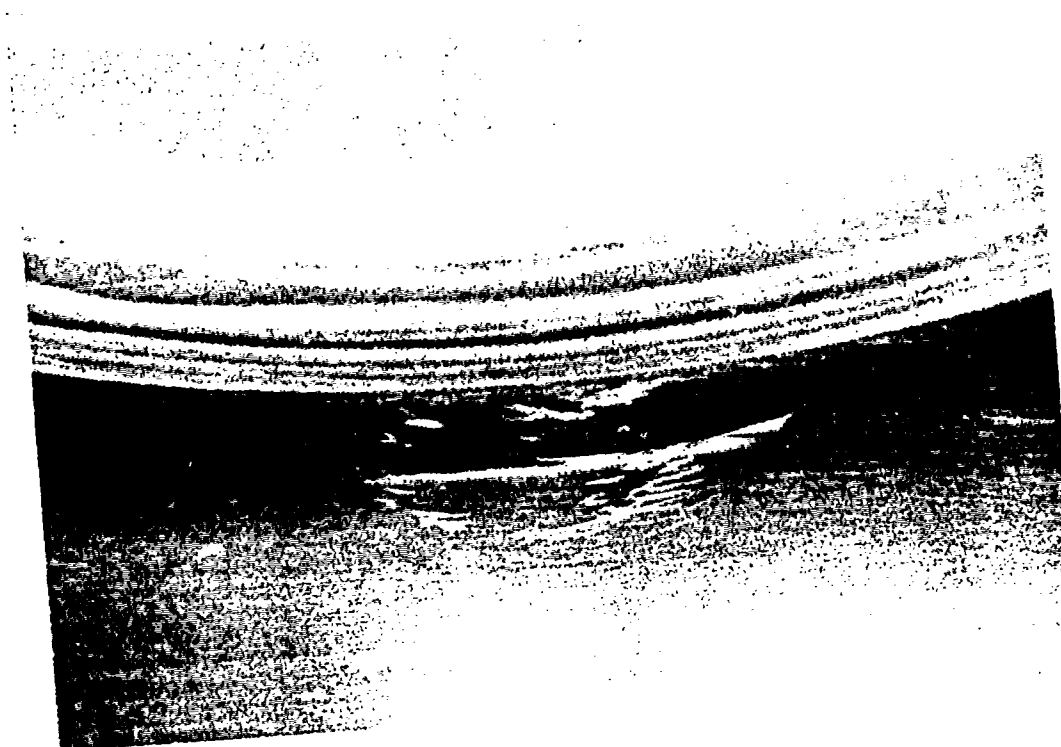
Figure 16B. Close-up view of crack observed on bearing surface below gage 4 after 31 pressure cycles to 6000 psi. Location of crack shown in figure 16A.

Figure 16C. Close-up view of crazing observed on the bearing surface of window 4 below gage 2 after 31 pressure cycles to 6000 psi. Location of crazing shown in figure 16A.
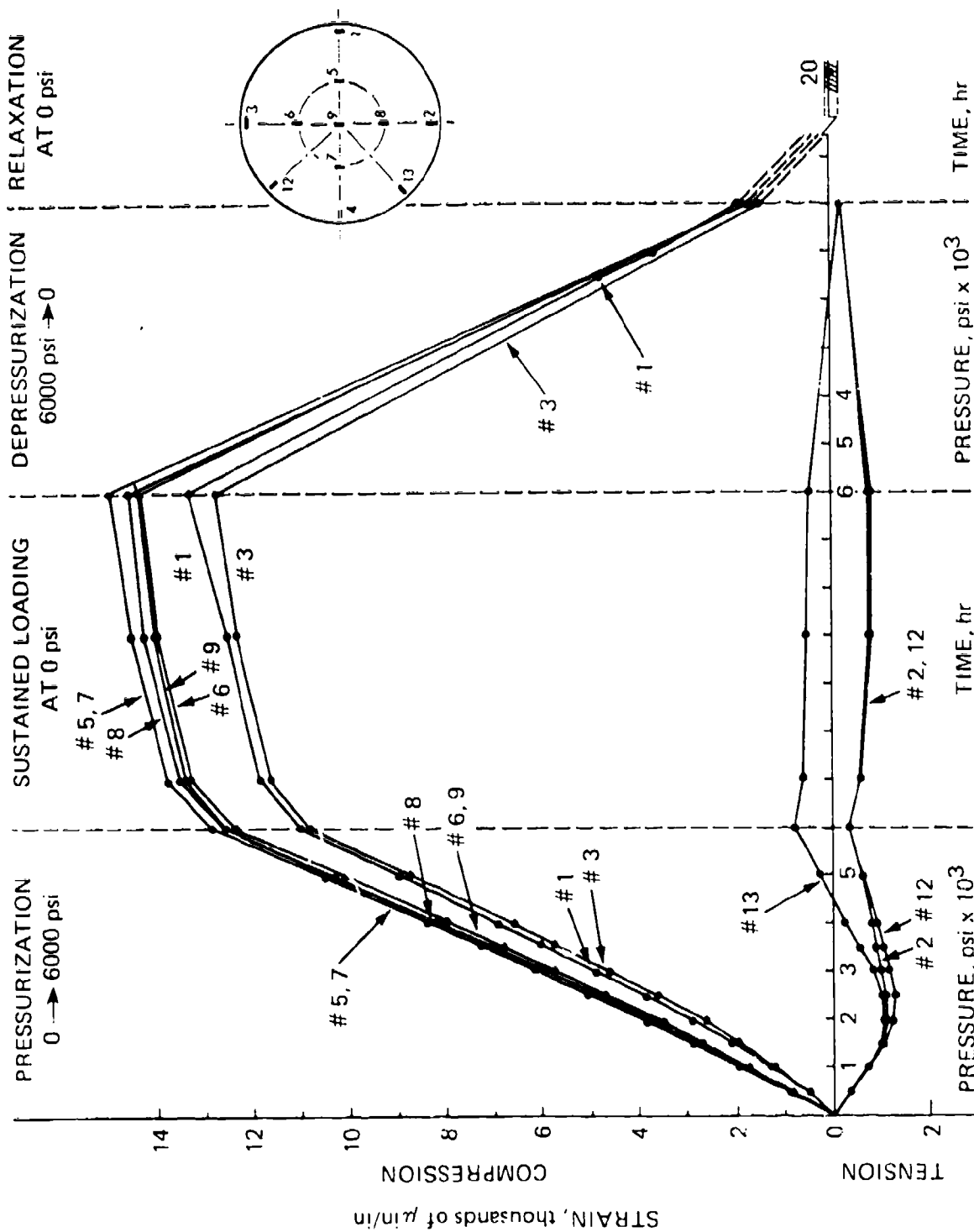
Figure 17A. Strains on low-pressure face of spherical sector window 4. Strains occurred during pressure cycle 32 in flange seat with 90° included angle.

43

Figure 17B. Strains on low-pressure face of spherical sector window 4. Strains occurred during pressure cycle 33 in flange seat with 90° included angle.

44

the gages in the central part. The strain reached about 13,000 microinches per inch com-
pared to about 6700 microinches per inch during load cycle 31. The strain rate was close
to 2 microinches per psi or about 5 percent less than in the central part. This is close to the
same strain observed during the linear portion of the previous load cycles for the same gages.
These results support the conclusion that, when there is no angular mismatch between the
flange seat and the window, the window does not flex.

The meridional strains at the edge of the window, as measured by gages 2, 12, and
13, show puzzling results (figure 17). During the first third of the pressurization, the gages
recorded an almost uniform tension over the half of the window edge covered by the gages.
At 2000 psi, the tensile strain was about 1000 microinches per inch. This behavior is almost
exactly the reverse of that exhibited during cycle 31. During the latter two thirds of pres-
surization, the strain decreased and actually became negative at one strain gage location.
Thus, instead of recording the general compression, which had to occur in all directions in
the low-pressure face when the window was pushed into the gradually decreasing cross-
section of the conical seat, the gages showed that close to the edge the compression was
nearly cancelled by some other effect (figure 18). This behavior is difficult to explain, but
it might be caused by the acrylic material in contact with the seat being retarded in its
motion under load, relative to the rest of the material in the window. There is also another
factor complicating the picture: It appears that the edge of the low-pressure face almost
reached the edge of the seat when the window was seated in the remachined flange. In this
way, it lost contact with the seat when the window was pushed into the flange by the
external pressure.

Long-Term Loading in Flange with 89°10' Included Angle

Spherical sector window 3 successfully withstood the 100 hours of sustained loading
at 20,000-psi hydrostatic pressure. Although no cracking noise was observed, cracks originat-
ing on the conical bearing surface and propagating at right angles into the interior of the
window developed (figure 19). The origin, character, and pattern of propagation were simi-
lar to those previously observed in conical frustum windows with a 90° included angle. As
typical for 90° conical windows, all cracks, when measured from the low-pressure face, were
located in the first half of the bearing surface's length (references 13 through 16).

A permanent deformation in the body of the window was also observed. Located on
the conical bearing surface adjacent to the window's low-pressure face (figure 19F), it was
shaped like a cylindrical protuberance and was caused by a plastic extrusion of the window
past the lower lip of the flange. During relaxation of the window after pressure release, the
cylindrical extrusion expanded and was gripped tightly by the lip of the flange. Since the
rest of the window body created a tremendous axial force caused by elastic expansion of the
previously compressed plastic, a separation had to occur between the wedged cylindrical
extrusion and the rest of the window. This separation took place approximately 1 inch from
the edge of the conical surface of the window.

The axial displacement of window 3 was quite linear during pressurization in the
2000- to 10,000-psi pressure range; above that level the magnitude of displacement began to
increase faster than the magnitude of pressure (figure 20A). The large initial displacement
observed during pressurization from 0 to 1000 psi was caused by: (1) extrusion of grease
from between the mating bearing surfaces and (2) angular mismatch between the window
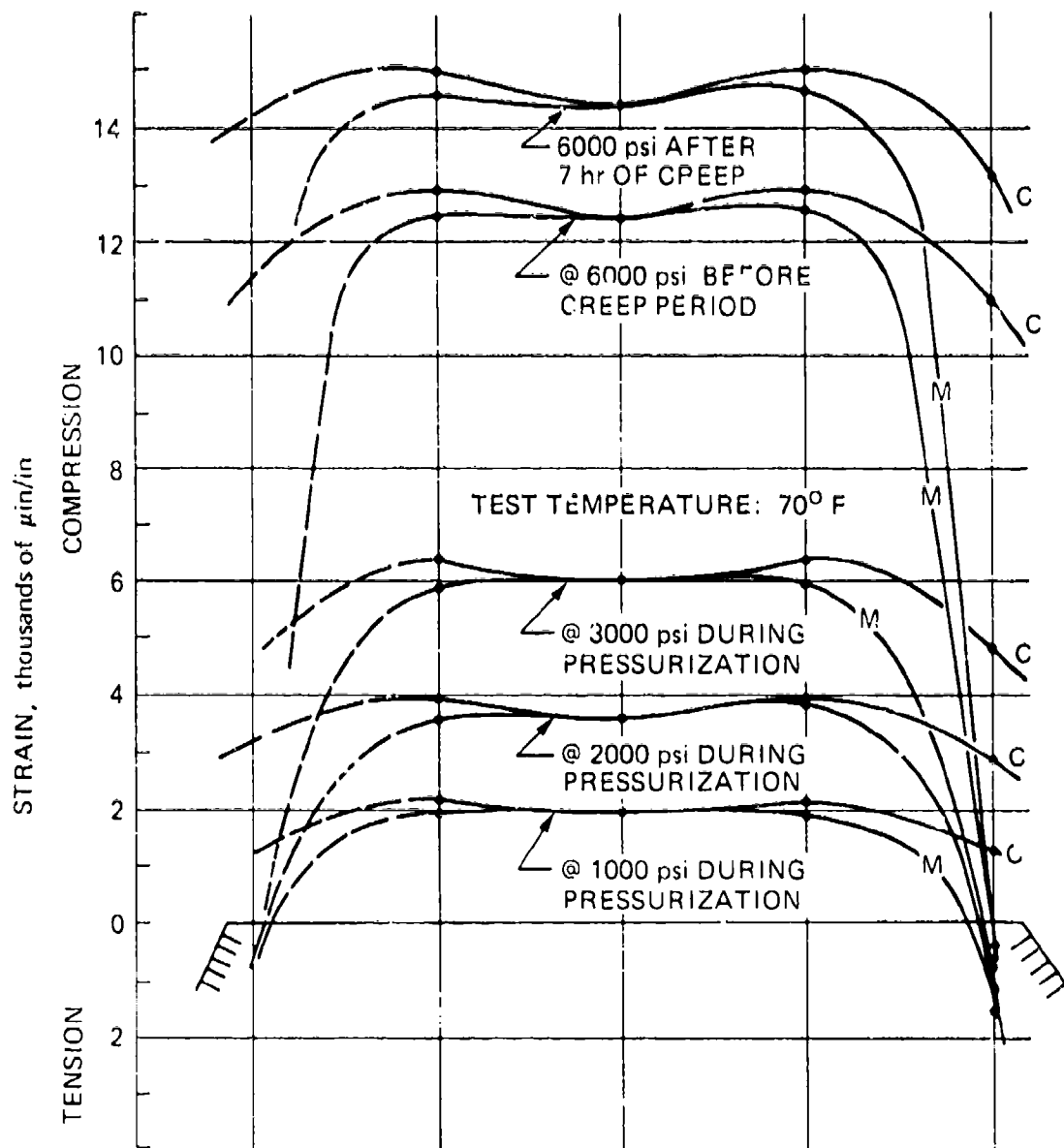
Figure 18. Typical distribution of strains on low-pressure face of spherical sector window 4. Pressure cycles 32 and 33 in flange seat with 90° included angle.
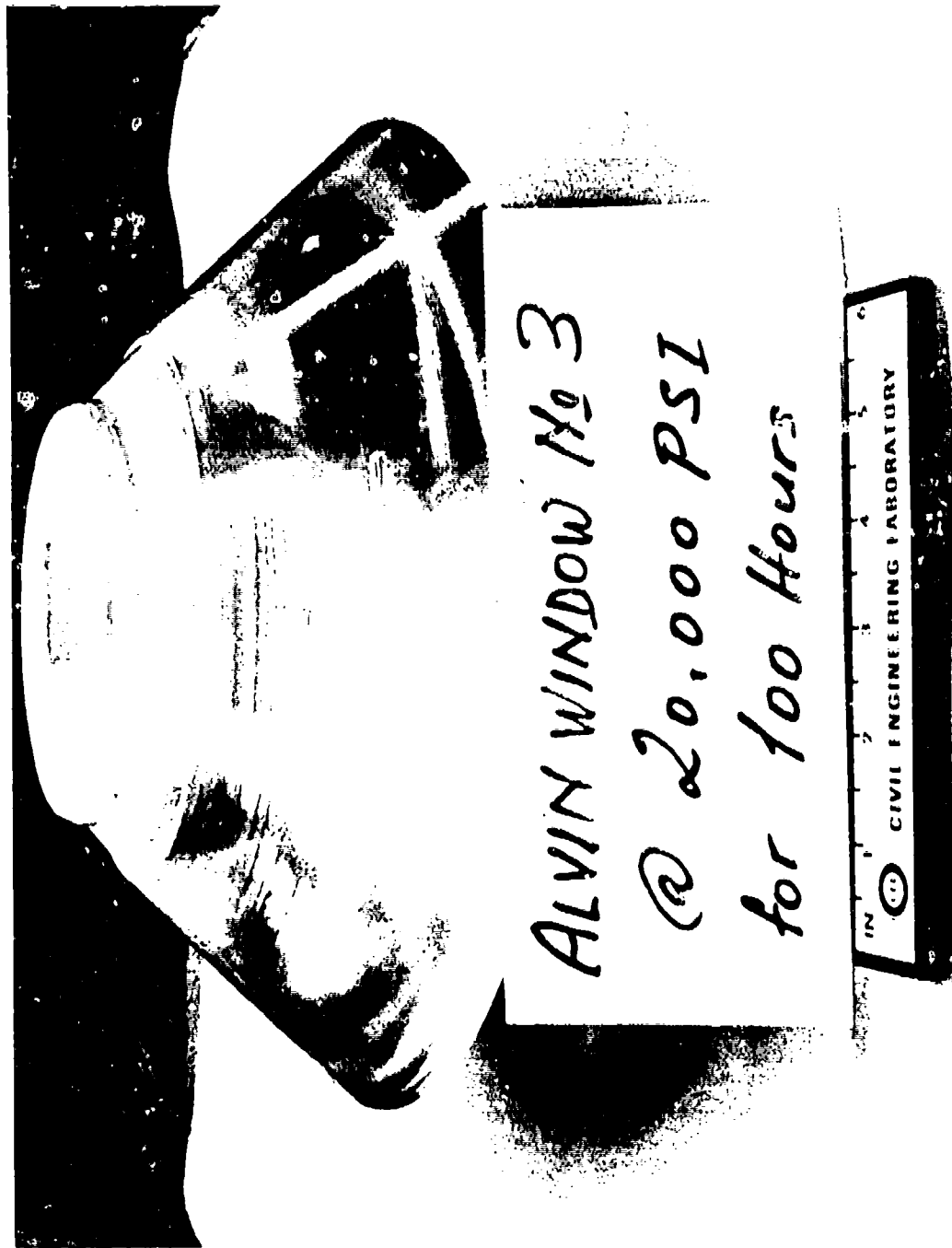
Figure 19A. Overall view of spherical sector window 3 after 100-hour sustained pressurization under 20,000-psi hydrostatic loading.

Figure 19B. Close up of the circular fracture plane originating on the bearing surface of window 3 in figure 19A.

48
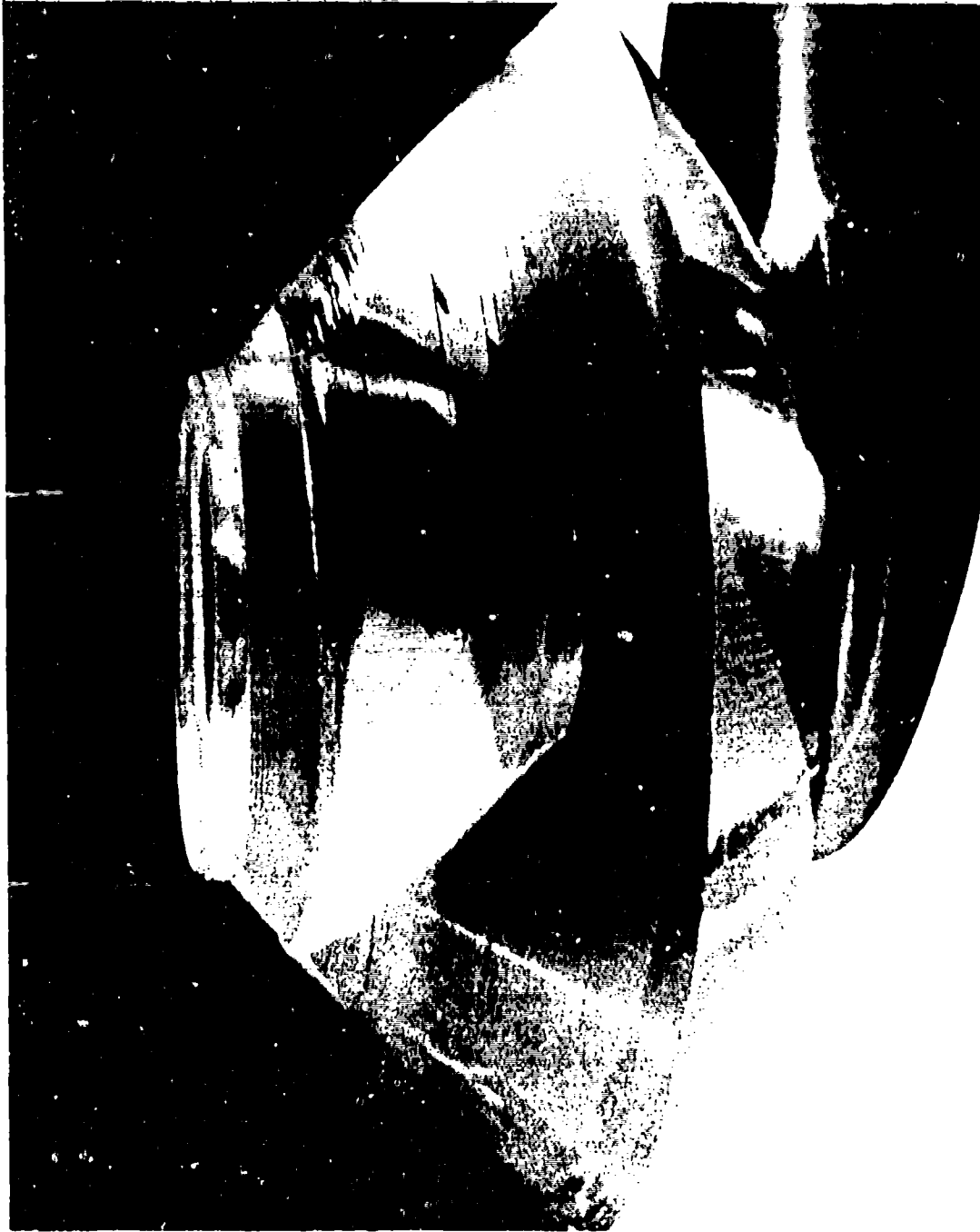
Figure 19C. Side view of circular fracture plane originating on the bearing surface of window 3 in figure 19A.

Figure 19D. View of circular fracture cone through the high-pressure face of window 3 in figure 19A.

Figure 19E. Close up of circular cracks originating on bearing surface of window 3 in figure 19A. Note the total absence of cracks on the bearing surface close to the high-pressure face.

Figure 19F. Close up of permanently extruded low-pressure face of window 3 in figure 19A.
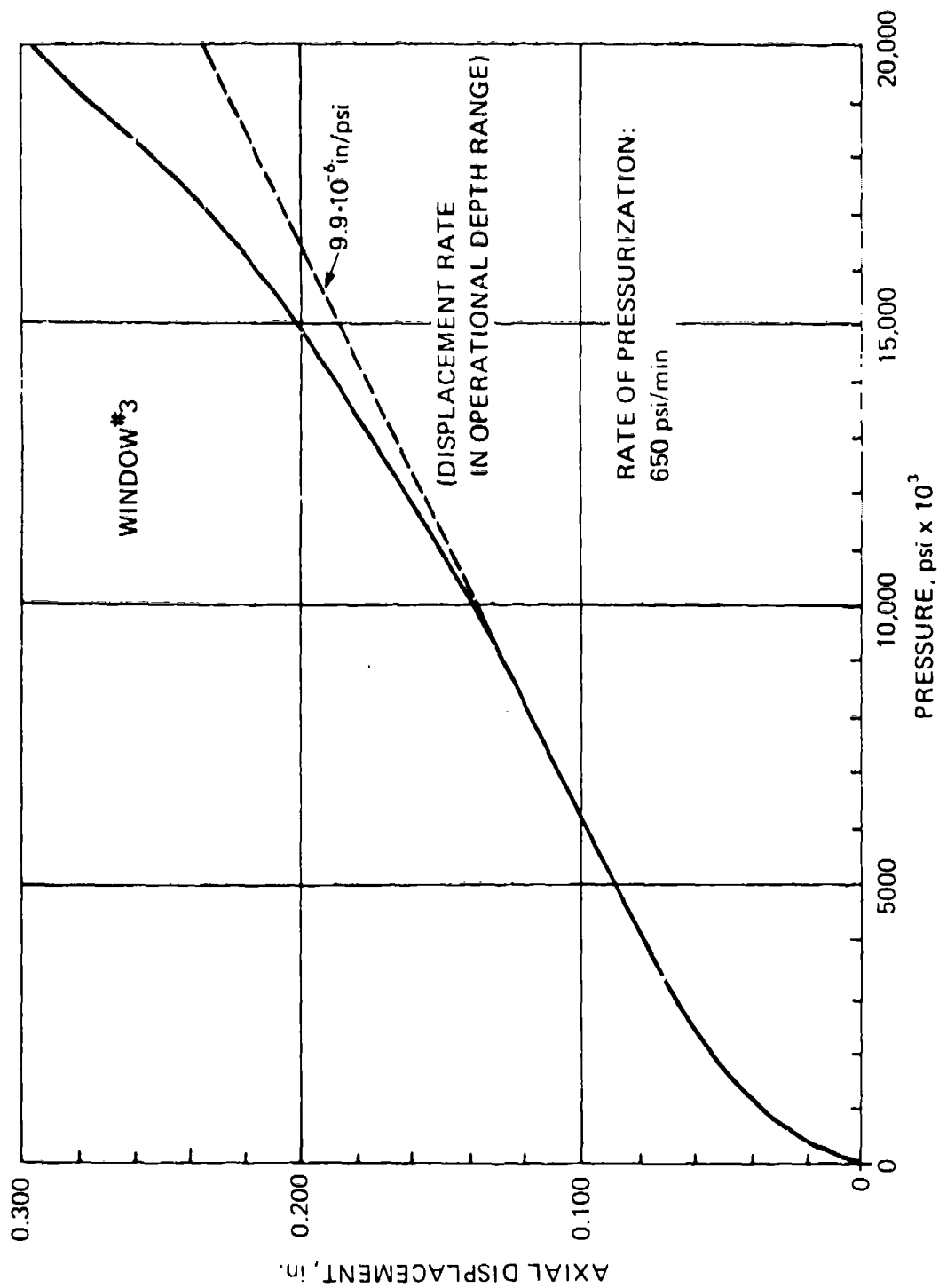
Figure 20A. Axial displacement of spherical sector window 3 measured during pressurization to 20,000-psi hydrostatic pressure.

WINDOW #3

9.9·10⁻⁶ in/psi

(DISPLACEMENT RATE IN OPERATIONAL DEPTH RANGE)

RATE OF PRESSURIZATION: 650 psi/min

PRESSURE, psi x 10³

AXIAL DISPLACEMENT, in.
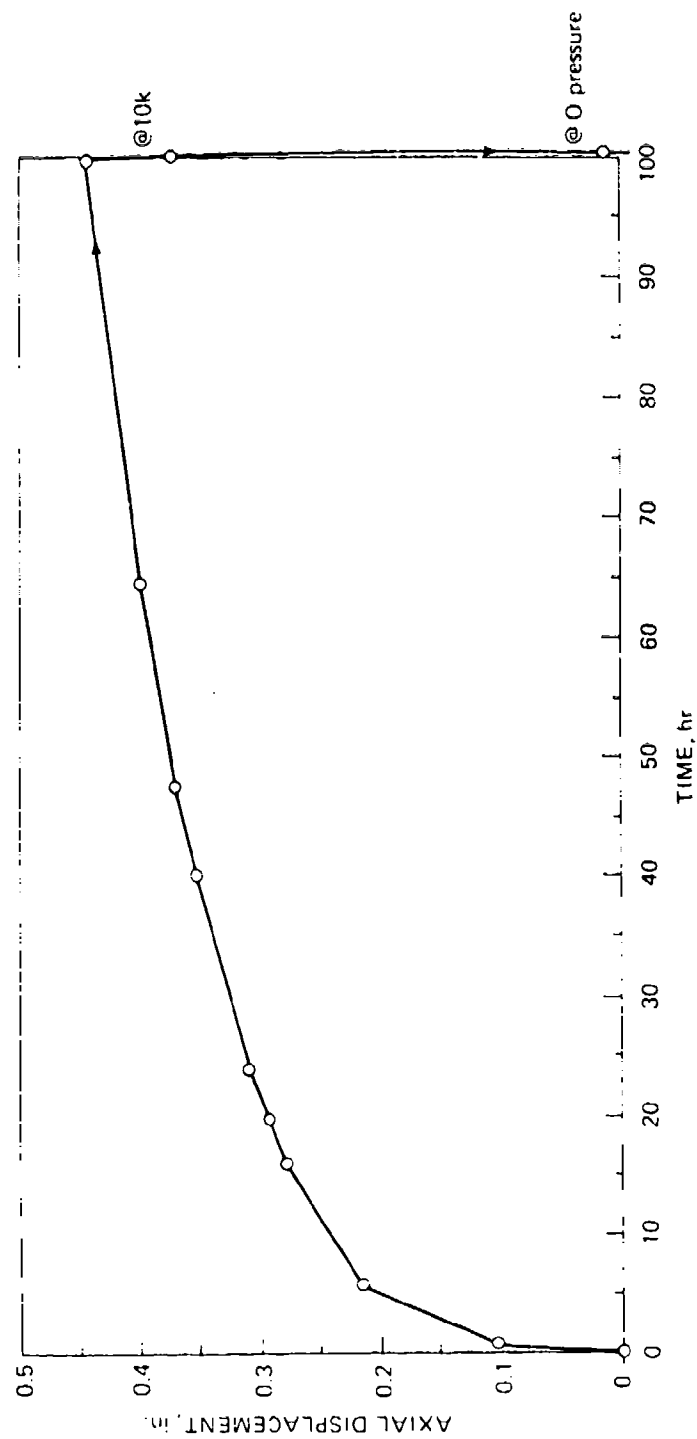
Figure 20B. Axial displacement creep of spherical sector window 3 measured during sustained pressure loading at 20,000 psi.

54

and flange (the included flange angle was 50' smaller than the window). During sustained pressure loading at 20,000 psi, the displacement doubled in magnitude during the first 20 hours of sustained loading (figure 20B). Following the 0.295-inch rise of displacement during the first 20 hours the rate of displacement decreased significantly, and during the following 80 hours the displacement increased only another 0.150 inch.

Prooftesting in Flange with 89°10' Included Angle

The axial displacements of the low-pressure face's apexes on windows 1, 2, 5, and 6, measured during 7-hour sustained loading at 6000 psi, were of the same magnitude (figure 21). This substantiates the postulate made during the fabrication process that all castings from which the spherical sector windows for ALVIN were machined had identical mechanical properties.

Very little creep was observed during the 7-hour sustained loading (figure 21). The small magnitude of creep at 6000 psi and the return to 0 after 17 hours of relaxation at 0 psi indicate that prooftesting to 6000 psi did not damage the spherical sector windows for ALVIN. (Average creep for the four windows during the 7-hour period was 6.9 percent, compared to maximum and minimum values of 8.6 and 5.3 percent, respectively.) The test temperature was close to 76°F for all tests.

Visual observation of all surfaces on windows 1, 2, 5, and 6, conducted at conclusion of the prooftests, failed to discover any signs of crazing or cracking. Scuff or drag scratches of approximately 1/16-inch length were observed on the conical bearing surfaces (figure 13), indicating the probable magnitude of window seat movement along the steel flange seat.

55
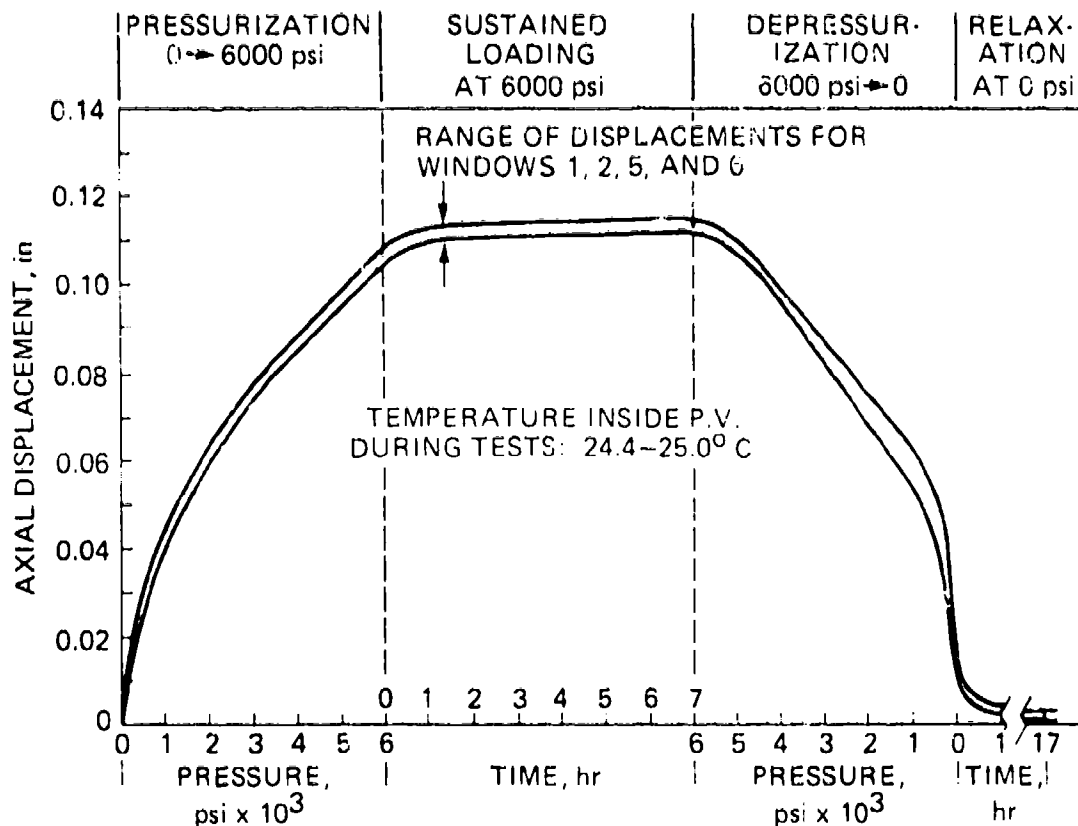
Figure 21. Axial displacement of spherical sector windows 1, 2, 5, and 6 during prooftesting to 6000-psi hydrostatic pressure.

DISCUSSION OF TEST RESULTS

EFFECT OF WINDOW FIT

As expected, the flange seat with an included angle approximately 1° smaller than that of the window generated strains in the window's low-pressure face that were lower (figure 14B) than those generated by a flange seat (figure 17A) whose included angle matched that of the window. The reduction was from 30 to 50 percent based on the strains measured when the window was seated in the flange with no mismatch. The strains on the high-pressure face were not measured, but only calculated, in this study. However, these strains must have been larger during angular mismatch, compared to strains measured when the window's angle matched that of the flange.

Calculations using Lamé's equation show that, under 6000-psi hydrostatic loading, stresses on the low-pressure face (9683 psi) are about 50 percent higher than the tangential stresses on the high-pressure face (6682 psi). Also, the high-pressure face is subjected to a triaxial state of compression which is likely to enhance the strength of the material in this

56

area (compared to the material on the low-pressure face). This shows that it would be favorable to transfer some 15 to 20 percent of the tangential stresses from the low-pressure face to the high-pressure face.

The 50' included angle mismatch caused a transfer of about twice this amount, based on the 30 to 50 percent reduction of stresses in the low-pressure face (figures 22 and 23). In the properly supported window the maximum measured tangential stress on the low-pressure face was 8500 to 9000 psi, while in the partially supported window it varied only from 5000 to 6000 psi. On this basis, it seems appropriate to conclude that an angular mismatch from $0°$ to $1°$, which causes the window to seat only around its high-pressure face, does not adversely affect the cyclic or long-term life of the window. In fact, it might be expected that a mismatch of about $1/2°$ slightly increases its fatigue life because it transfers stresses from high to low stress areas.

This conclusion is verified by the many observations of cracks in the bearing surface of conical frustum windows with $90°$ included angles (references 13 through 16). These shear cracks are always found on the part of the seating surface closest to the low-pressure face. This must, therefore, be the highest strained area of the window, and any relief given to this area by angular mismatch between the window and flange would affect the structure beneficially.

DEFORMATION OF WINDOW UNDER HYDROSTATIC LOADING

From the measurements of tangential strain in the low-pressure face, it was seen that the window deformed uniformly under hydrostatic loading. Only close to the seating surface was deformation somewhat retarded. Also, for the completely seated window, the tangential strain and radial displacement of the low-pressure face changed linearly with pressure down to the maximum working depth. It makes no difference whether complete seating results from a good initial fit or from deformation of an angularly mismatched window during the first part of pressurization. In both cases, a constant strain rate of approximately 2.1×10^{-6} inches per inch per psi of pressure and an equally constant displacement rate of approximately 10.4×10^{-6} inches per psi of pressure were measured (figures 9B, 14B, 17A, 17B, and 20A).

The significance of this straight-line relationship can be shown by plotting the strain rate and the displacement rate divided by the initial radius of the low-pressure face as a function of the t/D_i ratio (figure 24). The experimental data points for the ALVIN window fall relatively close to the curve representing Lamé's theoretical thick-wall equation for complete spherical shells (reference 17).

For purposes of comparison, some earlier experimental values in the smaller t/R_i range are included in figure 24 (references 1 and 18). Again, a reasonable correlation with Lamé's curve is observed. This confirms that the $90°$ spherical sector window for ALVIN acts like a very thick spherical shell, which means that increasing further the thickness of an already thick spherical window decreases only minutely the displacement of the low-pressure face under hydrostatic loading.

Hence, if minimization of window displacement were the only criterion, the increase in wall thickness from 3.5 to 5.0 inches would hardly be worth the expense. The reduction in displacement for a 5-inch thick spherical window for the same change in pressure is only about 6 percent when compared to a 3.5-inch thick spherical window.
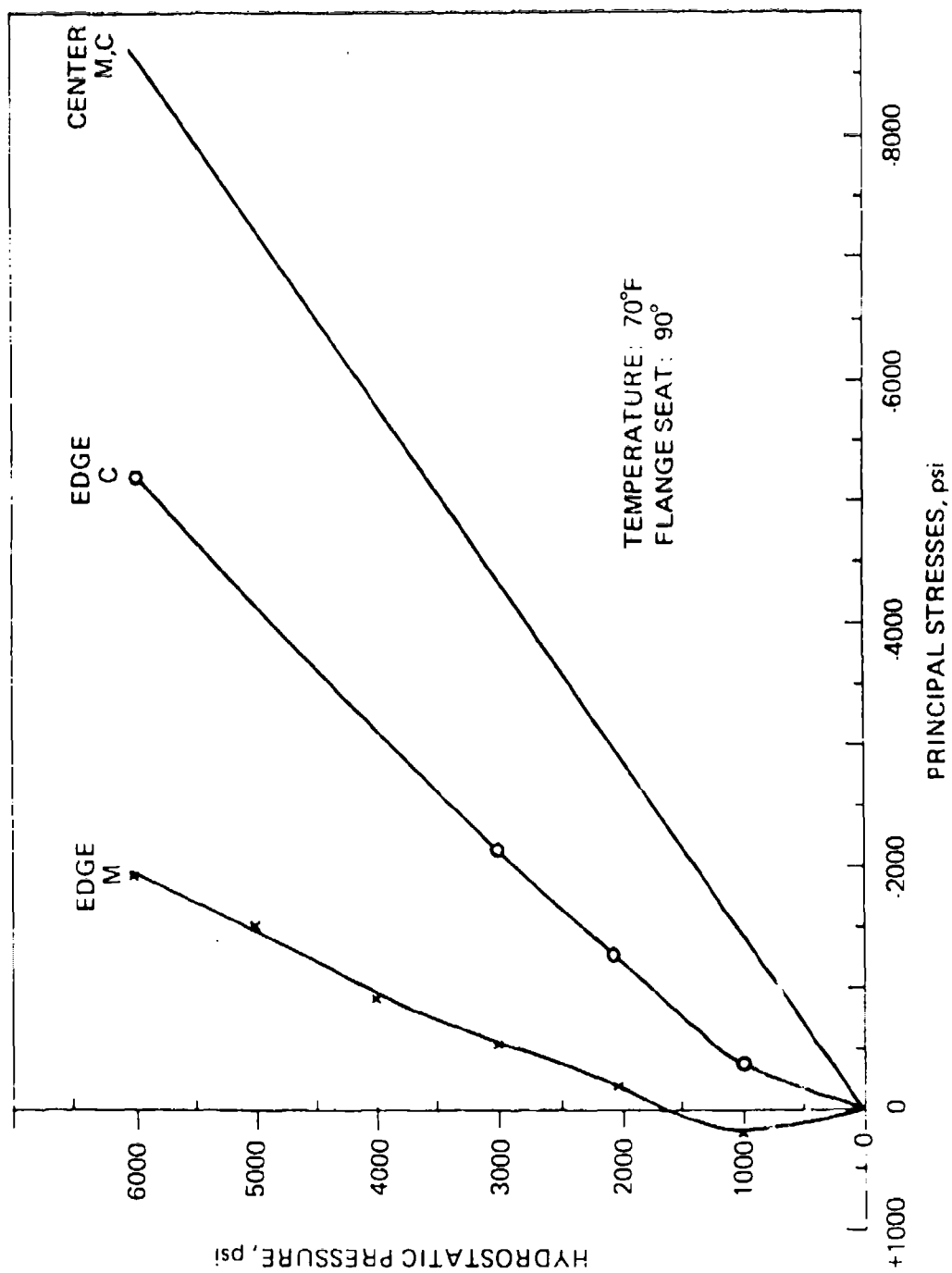
Figure 22A. Principal stresses on low-pressure face of spherical sector window 4 during short-term pressurization to 6000 psi in the flange seat with 90° included angle. (C, circumferential; M, meridional.)

58
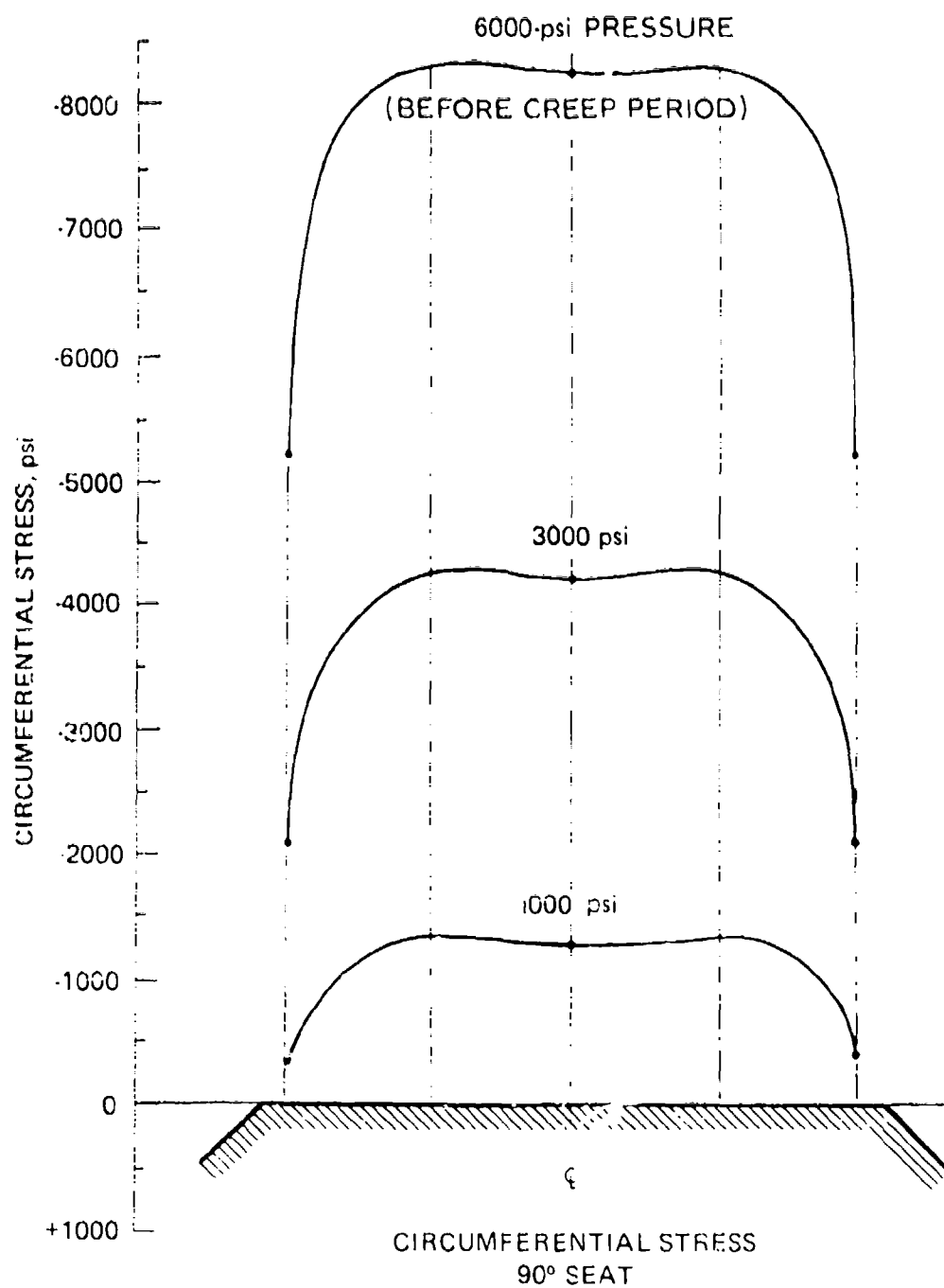
Figure 22B. Distribution of circumferential stresses on window in figure 22A.
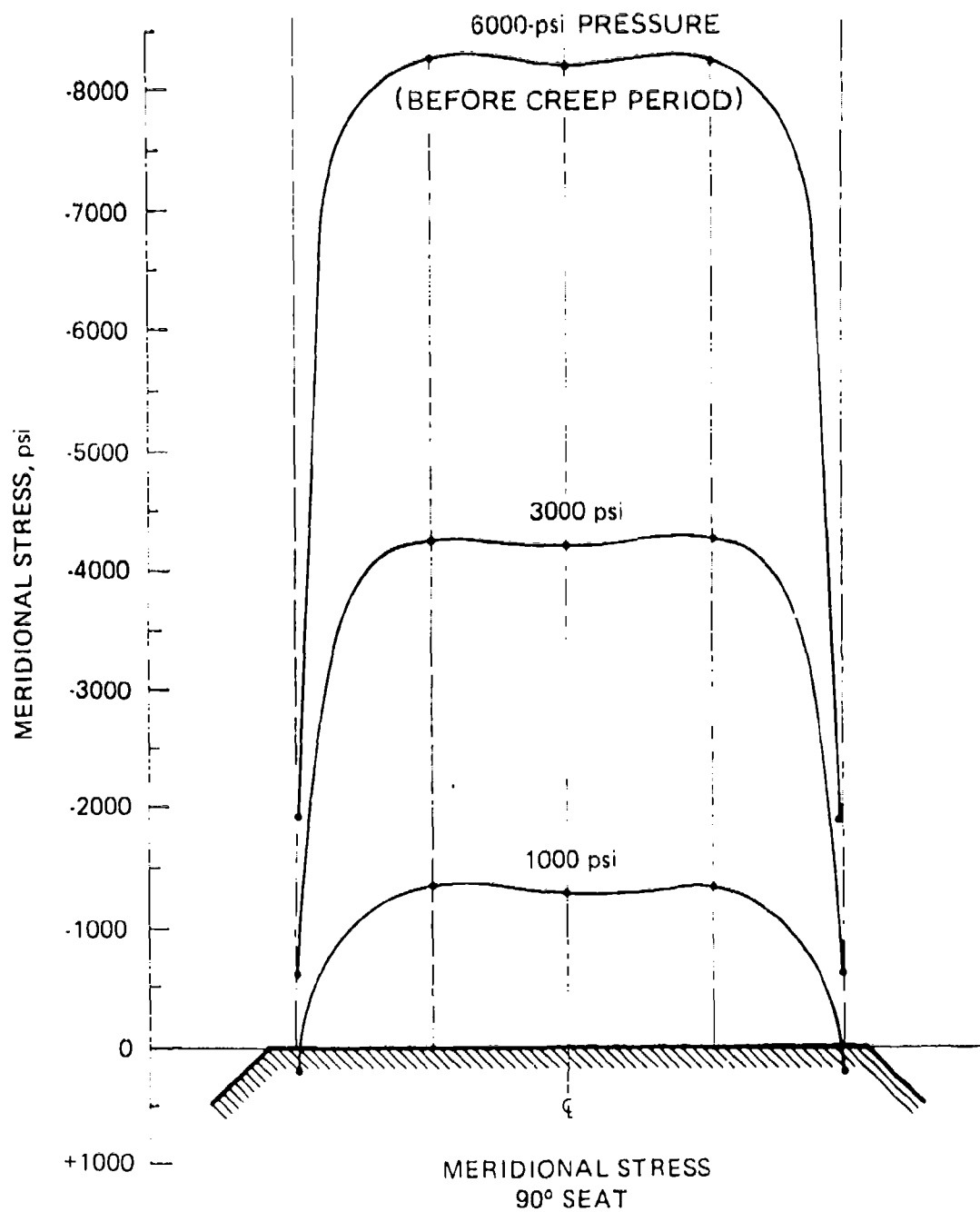
Figure 22C. Distribution of meridional stresses on window in figure 22A.

60
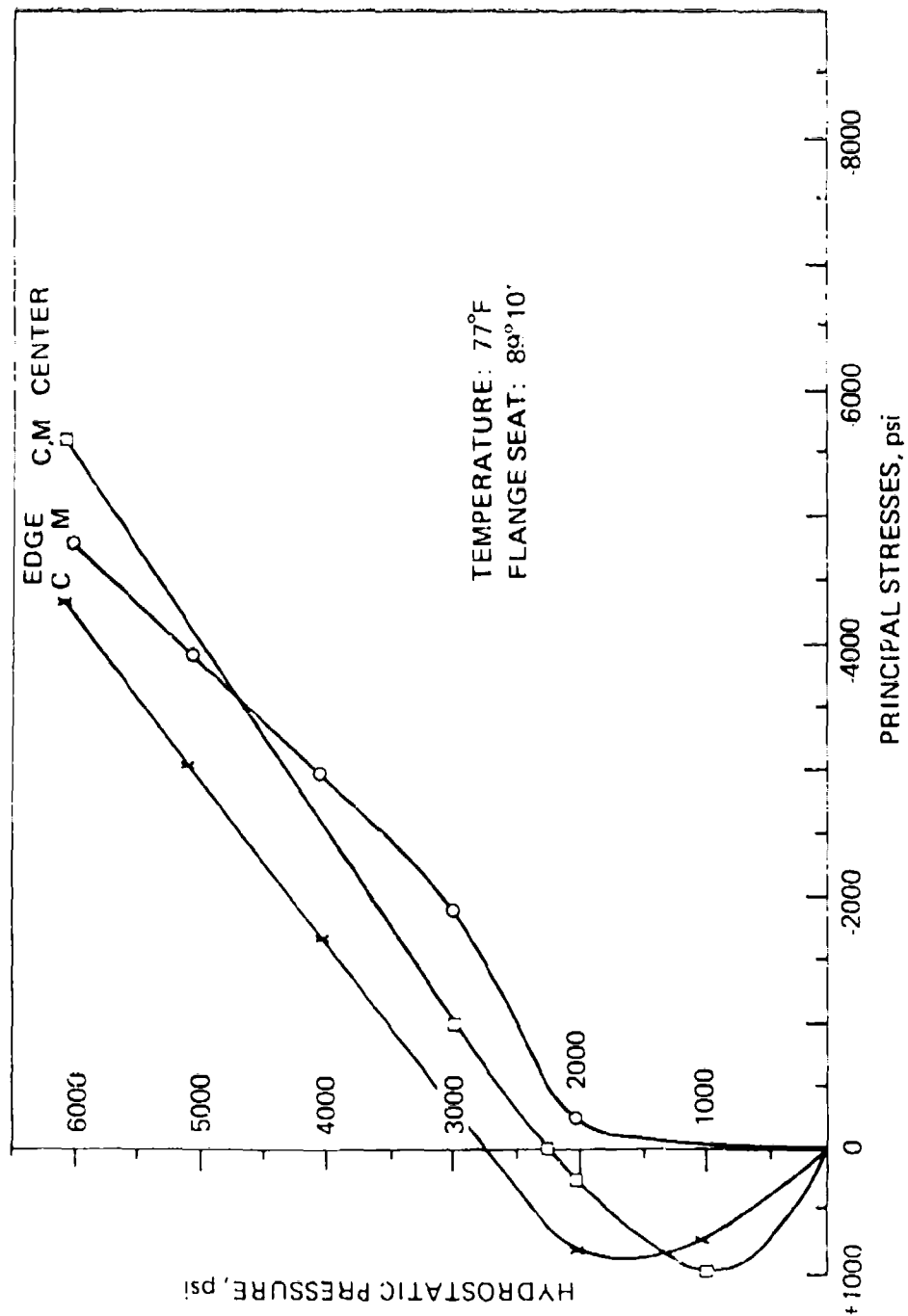
Figure 23A. Principal stresses on low-pressure face of spherical sector window 4 during short-term pressurization to 6000 psi in a flange seat with 89°10' included angle. (C, circumferential; M, meridional.)

61
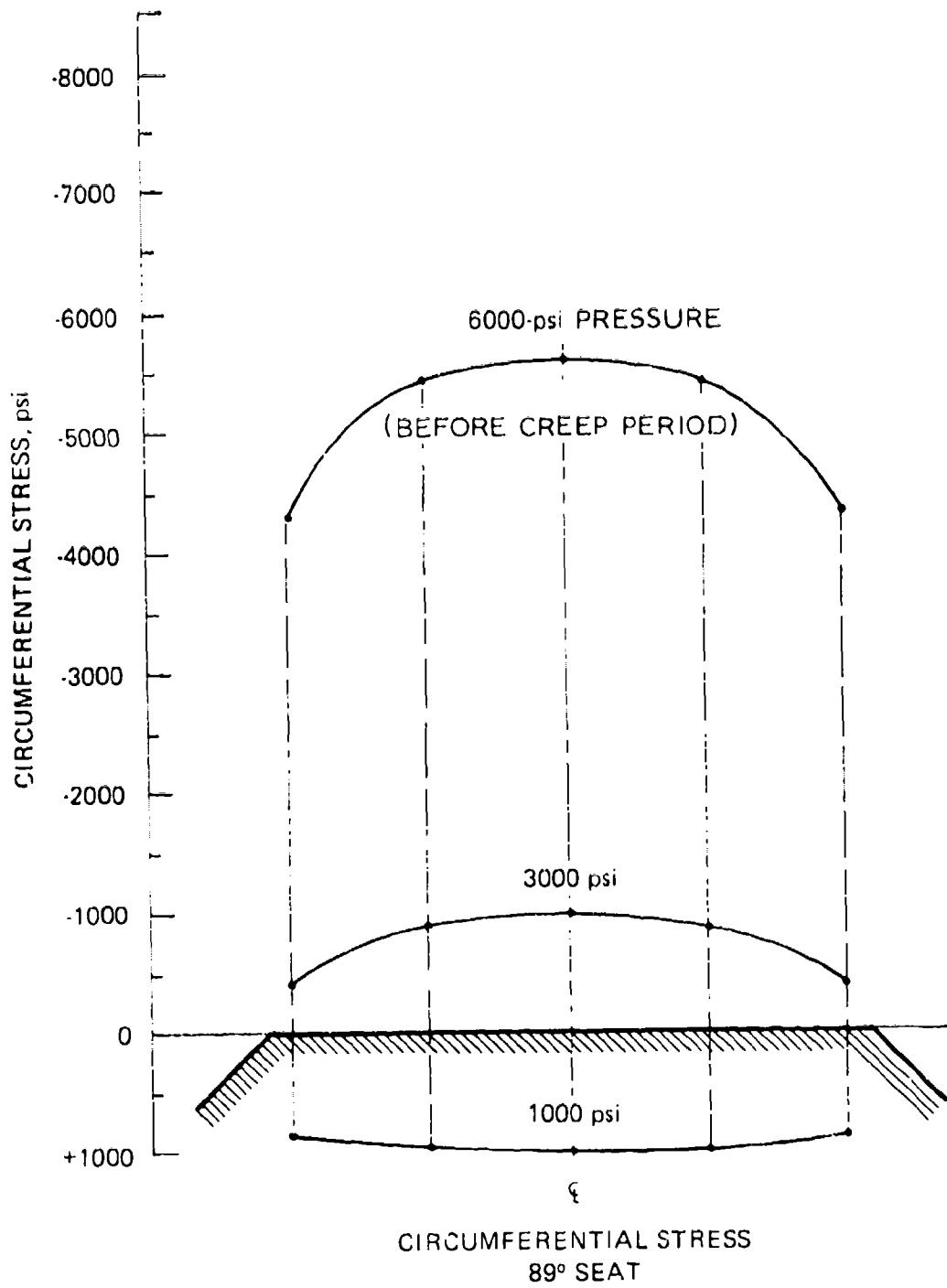
Figure 23B. Distribution of circumferential stresses on window in figure 23A.
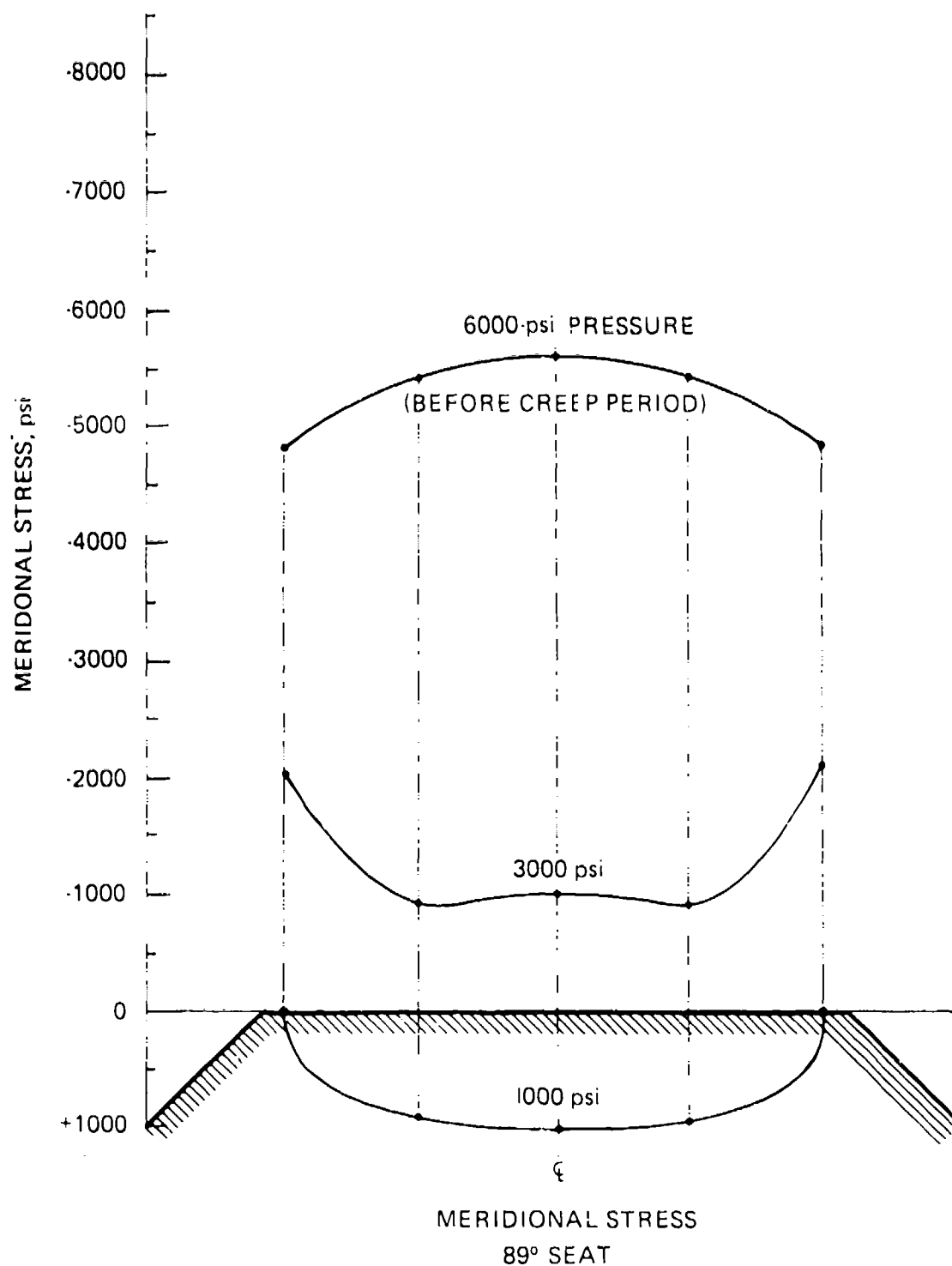
Figure 23C. Distribution of meridional stresses on window in figure 23A.

LAME'S EQUATION FOR HOLLOW SPHERES

$\nu = 0.3$

$E = 450,000$ psi

$$\frac{\epsilon_t}{P} = \frac{\Delta R_i}{R_i \cdot P} = \frac{1-\nu}{E}\left\{\frac{1.5}{1-\left[1/(1+t/R_i)\right]^3}\right\}$$

▲ NCEL R-631
● ALVIN, MEASURED $\Delta R_i/(R_i \cdot P)$
○ ALVIN, MEASURED ε_{Ti}/P
□ NUC TP 355, MEASURED ε_{Ti}/P
■ CEL (TYPE 1 AND 6 DOMES), MEASURED ε_{Ti}/P
✱ NUC TP 410, MEASURED $\dfrac{\Delta R_i}{R_i P}$

ALVIN

y-axis: $\Delta R_i/(R_i \cdot P)$, in^2/lb $\times 10^{-5}$

y-axis values: 0, 0.2, 0.4, 0.6, 0.8, 1.0, 1.2, 1.4, 1.6, 1.8

x-axis: t/R_i

x-axis values: 0, 0.1, 0.2, 0.3, 0.4, 0.5, 0.6, 0.7, 0.8, 0.9, 1.0, 1.1, 1.2, 1.3, 1.4, 1.5, 1.6
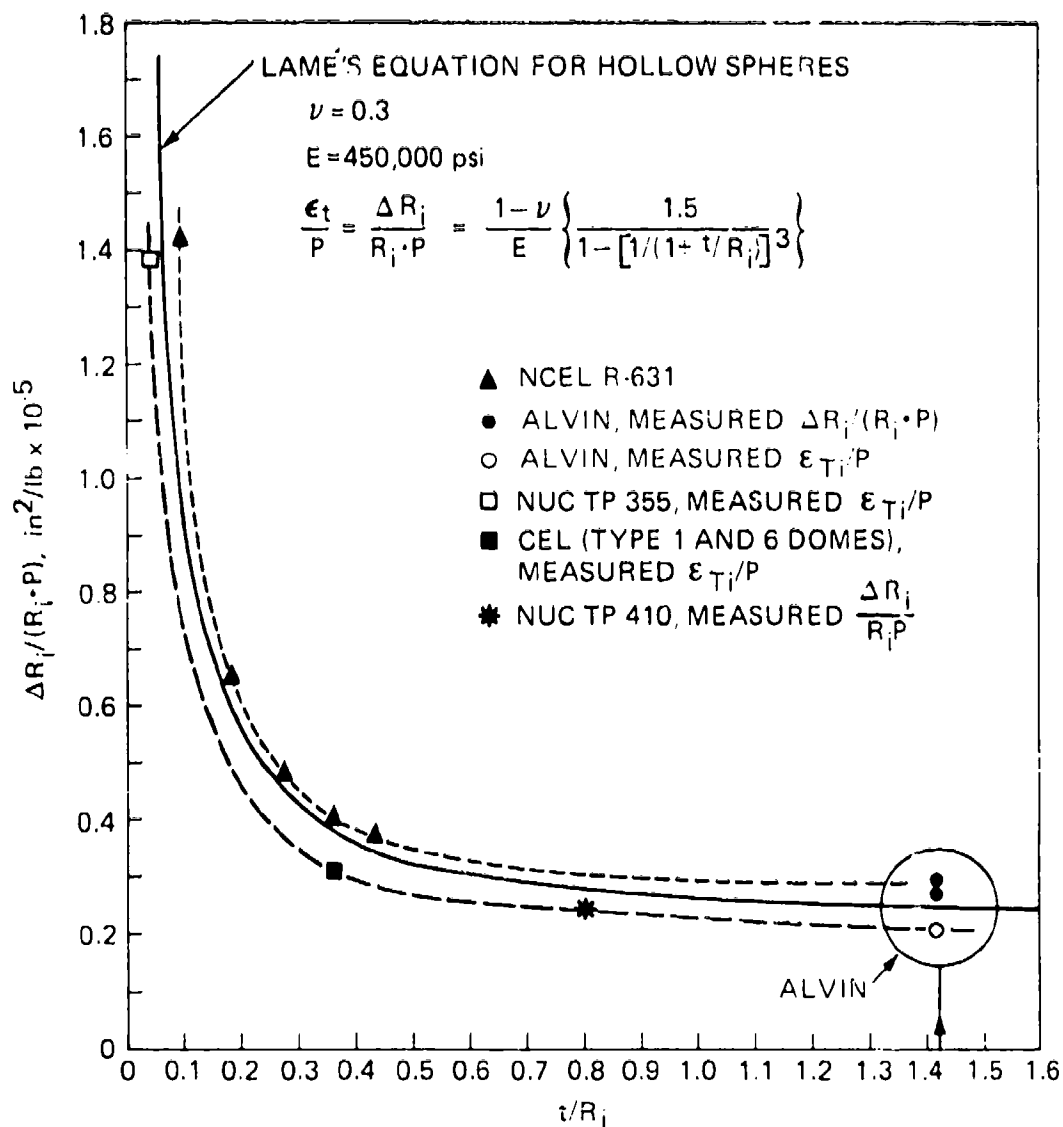
Figure 24. Comparison of measured strains and displacements on low-pressure face of spherical sector windows (included angle ≥ 90°). Values calculated from Lamé's equation.

64

At maximum operating depth, the radial displacement of the low-pressure face approaches about 0.12 inch at the end of a 7-hour dive where the initial mismatch, in terms of included spherical angles, is about 50'. In the cold water of abyssal depths, the displacement would be appreciably less, presumably down to about 0.08 inch. If the windows were made to fit the flanges completely, the displacement would further decrease to presumably 0.05 inch in the cold water. Since the displacement is uniform over most of the low-pressure face, there is reason to believe that the optical properties of the window would still be retained with little distortion, even down to the maximum diving depth of the submersible.

From a structural point of view, the measurements indicate that the windows will operate well within their elastic range. The creep rate at maximum pressure is low, causing an increase in tangential strains in the low-pressure face of about 20 percent during the 7-hour dive, half of which occurs during the first hour. After the dive, the strains relax during the night; this prevents a cumulative buildup of residual strain even if the submersible were to perform a 7-hour dive every day for 30 days. After such a diving schedule, no permanent deformation, crazing, or other structural deterioration of the window is expected, i.e., the test window was subjected to a similar schedule in the laboratory and was found to be flawless when removed for inspection, except for stress corrosion crazing and cracking on chemically sensitized areas. The latter statement applies only when there is a mismatch of 50' in the included spherical angles of the window and seat. There are, however, engineering reasons to support the premise that the window seated without mismatch will perform equally well. It would be more difficult to extend this argument to cases where the mismatch is the other way, i.e., with initial seating occurring at the low-pressure face of the window. This condition should, therefore, be avoided unless further tests are performed to confirm its adequacy under pressure cycling.

To confirm the capability of the new window design to withstand extreme emergency conditions, the 100-hour 20,000-psi test was carried out. Although the window was permanently damaged by the test, the large reserve capacity of the window, even at the greatest existing ocean depth, was demonstrated. Previous experiments on similar windows (reference 19) have shown that 90° conical frustum windows blow out when the axial displacement reaches a magnitude approximately equal to the original thickness of the window.

Applying this criterion to the window tested at 20,000 psi for 100 hours, it appears that the window will last at least another 4000 hours before catastrophic failure. In fact, it would probably last longer, since the 4000-hour prediction is based on the creep rate after 80 to 100 hours of creep. Earlier tests (references 13, 14, and 15) have shown that the creep rate decreases further until it stabilizes at a constant rate (after about 500 hours).

It is also useful to consider the foregoing results in relation to the following criteria for safe, economical, and optically acceptable performance of an acrylic window in a deep diving submersible.

1. The strain and displacement generated during a full day's dive (7 to 8 hours) to the maximum operating depth should be completely gone the next morning, i.e., after 7 hours of relaxation, prior to initiation of another dive.

2. During dives to the maximum operating depth, the window should retain its shape to minimize optical distortion through the window — even after 7 hours at the maximum operational depth.

3. The seating of the window should avoid stress concentrations that can cause premature cracking of the seating surface and hence a reduced working life of the window.

4. The window mounted in its actual flange should be capable of withstanding, for a length of time well in excess of the capacity of the life-support system, the greatest ocean depth to be encountered in the probable area of operation of the submersible. On the basis of the tests performed on the new spherical ALVIN windows, they completely satisfy these criteria. The allowable geographical area of operation, as far as the windows are concerned, is not restricted in any way.

SHORT-TERM CRITICAL PRESSURE

The blowout pressure of windows under continuous pressurization of about 650 psi per inch is often used as a measure to determine the safe operating condition of a window. For these windows, this criterion was used because the STCP* exceeds the capacity of any available test facility. For complete discussion, however, it is important to know how the STCP of the ALVIN's windows compares with STCP data from other tests. For this purpose, figure 25, showing the computed tangential stress on the low-pressure face of spherical windows at STCP (subjected to a constant pressurization of 650 psi per inch at 70°F), has been included.

Except for the very thin windows which fail by elastic instability, the STCP increases linearly with thickness; very little difference is seen between $90°$ and $180°$ windows. Also, as the t/R_i exceeds about 0.1, the computed tangential stress on the low-pressure face at the STCP exceeds the uniaxial compressive yield of the material. For the spherical window with the highest recorded STCP ($t/R_i = 0.436$ and $90°$ angle), the tangential stress at failure is 2.5 times the uniaxial compressive yield. Figure 25 shows that the spherical sector window for ALVIN does not lie in the range of existing experimental data, since its t/R_i is 300 percent greater than the last experimental point on the curve. If the straight-line relationship were extrapolated to $t/R_i = 1.43$, it would predict a short-term critical pressure in excess of 70,000 psi with an accompanying tangential stress on the low-pressure face of about 120,000 psi. The stress is of such magnitude that one might expect other factors to override it (references 1 and 10).

In a triaxial compressive stress field, the compressive strength of acrylic has experimentally been shown to be in excess of 500,000 psi (reference 22). This is not the case for biaxial stress fields, where the compressive strength must be less but still significantly higher than for a uniaxial stress field. Since the compressive strength of acrylic in a biaxial stress field has not been experimentally determined, its magnitude can only be estimated to be in excess of 50,000 psi, the ultimate compressive strength of acrylic under uniaxial compression.

The stress field in a spherical sector window during plastic flow is extremely complex, but there is no doubt that triaxial stress fields exist everywhere except on the low-pressure face where a biaxial stress is present. If the spherical sector were thinner, it would fail by plastic instability (reference 1) at compressive stresses equal to or less than uniaxial compressive yield. However, because of the high t/D_i ratio, plastic instability failure is not likely to occur. Thus, the controlling factor that determines when the window is catastrophically ejected becomes the D_i/D_f ratio (figure 6).

STCP, short-term critical pressure.

EXPERIMENTAL DATA

NCEL R631 ●
NUC TP 355 ■

ALVIN WINDOW:

ACTUAL t/R_i = 1.408

EXTRAPOLATED σ_{ti} = 117,600 psi

EXTRAPOLATED STCP = 72,800 psi

(FOR D_i/D_f > 2)

NOTES:

TANGENTIAL COMPRESSIVE STRESS
ON LOW-PRESSURE FACE σ_{ti}

SHELL THICKNESS   t

INTERNAL RADIUS R_i

LAMÉ'S EQUATION σ_{ti} = k (STCP)

$$k = \frac{1.5}{1 - \left[1/(1 + t/R_i)\right]^3}$$

TANGENTIAL COMPRESSIVE STRESS, thousands of psi

t/R_i
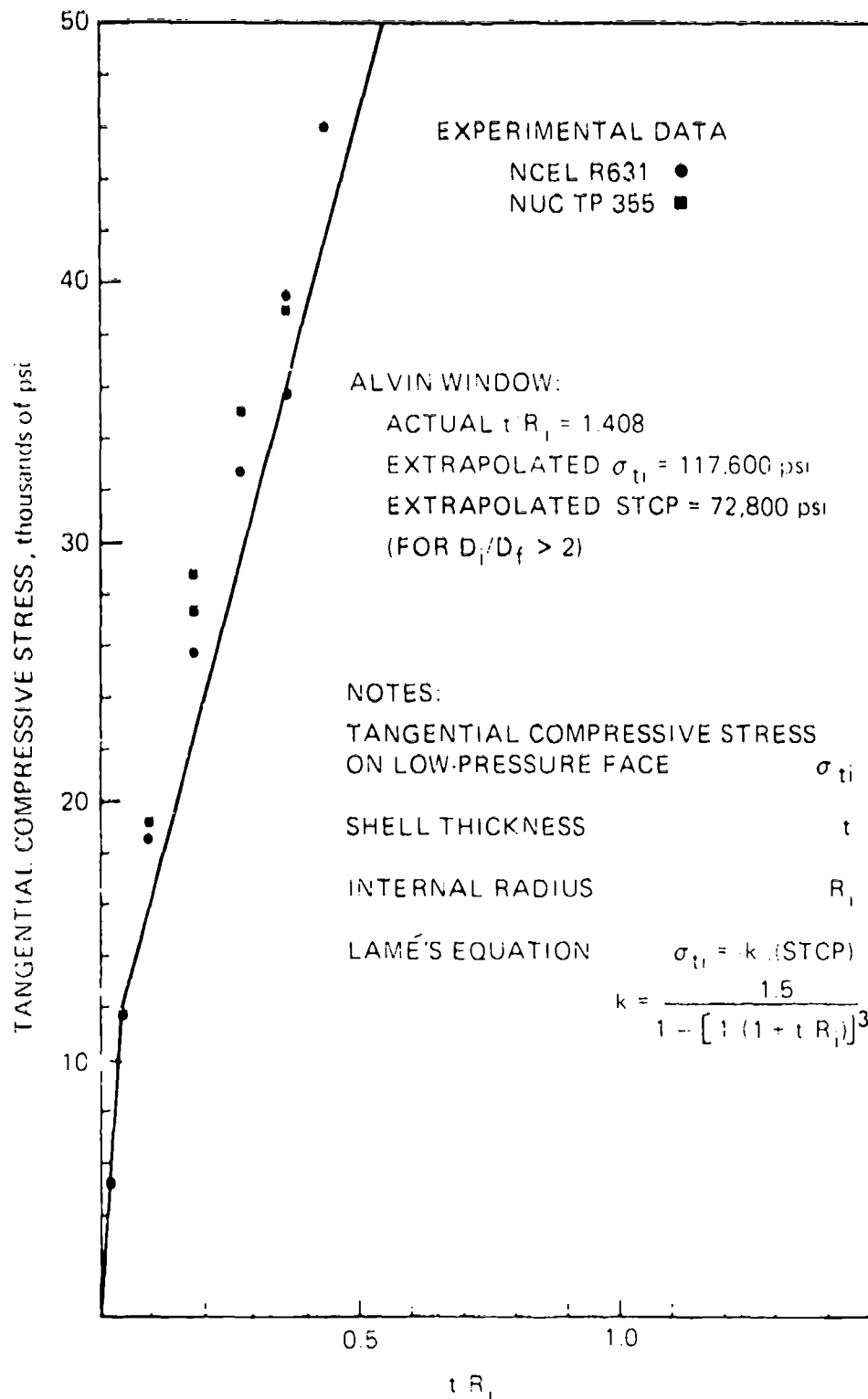
Figure 25. Tangential stresses (circumferential and meridional) on low-pressure face of spherical sector windows prior to catastrophic failure under STCP loading.

67

For a thick spherical sector window located in a flange with a low D_i/D_f ratio,* e.g., for the ALVIN window, the STCP is determined primarily by the loss of support for the radial flange seat after the window displaces more than $0.1 D_i$. This loss is also the primary reason for generation of the conical fracture plane whose apex extends to the center of the high-pressure face. Although increasing the D_i/D_f relationship would increase the STCP significantly, most window flanges are not designed with high D_i/D_f ratios, since increasing this ratio drastically decreases the window's field of view. The ratio of $D_i/D_f = 1.1$, encountered in many submersibles, is simply a good engineering compromise between high STCP and the field of view for the occupants of the submersible.

If the spherical sector window were placed in a test flange with a ratio of $D_i/D_f \geqslant 2$, it is quite probable that the STCP would reach, and maybe exceed, the projected 70,000-psi hydrostatic pressure. There is even a basis for an engineering estimate that when $D_i/D_f \geqslant 10$ the STCP may exceed 500,000 psi. Such a high D_i/D_f ratio would decrease the field of view to such a degree that the windows would become essentially useless for operating the submersible.

Based on the above discussion, it can be postulated that the STCP of the window can be made to vary from about 50,000 to 500,000 psi, depending on the D_i/D_f flange seating arrangement. The ratio of $D_i/D_f = 1.12$, found in the ALVIN submersible, is a practical compromise that provides the spherical sector window a projected STCP of about 50,000 psi.

COMPARISON OF PERFORMANCE OF CONICAL FRUSTUM WINDOW AND SPHERICAL SECTOR WINDOW

To serve its dual functions as a structural part of the hull and as an optical window, the acrylic viewport must possess some unique properties. It must withstand the hydrostatic pressure without excessive displacement; it must have ample strength under extreme loading conditions; it must have a long working life; and it must possess good optical properties. This section is an account of the comparative study performed to assess the relative merits of the plane window previously used in ALVIN and the new spherical windows (figures 2 and 4).

DISPLACEMENT UNDER HYDROSTATIC PRESSURE

For the same increase in pressure, the axial displacement of the center on the conical frustum window's low-pressure face is more than twice that of the spherical window's displacement. This statement is based on the comparison between the results generated in the present study for the spherical window and the previously published results for conical frustum windows under short-term loading (figure 26) (references 10 and 11).

It should be noted that the measurements on the spherical window were made at 75°F and those for the conical frustum window at 35°F. Thus, the deflection per unit pressure measured on plane windows should be increased by at least 20 percent to compensate for the lower temperature used in those tests. Also, the spherical window displaces radially

---

*Low ratios are considered those where $D_i/D_f \leqslant 1.1$
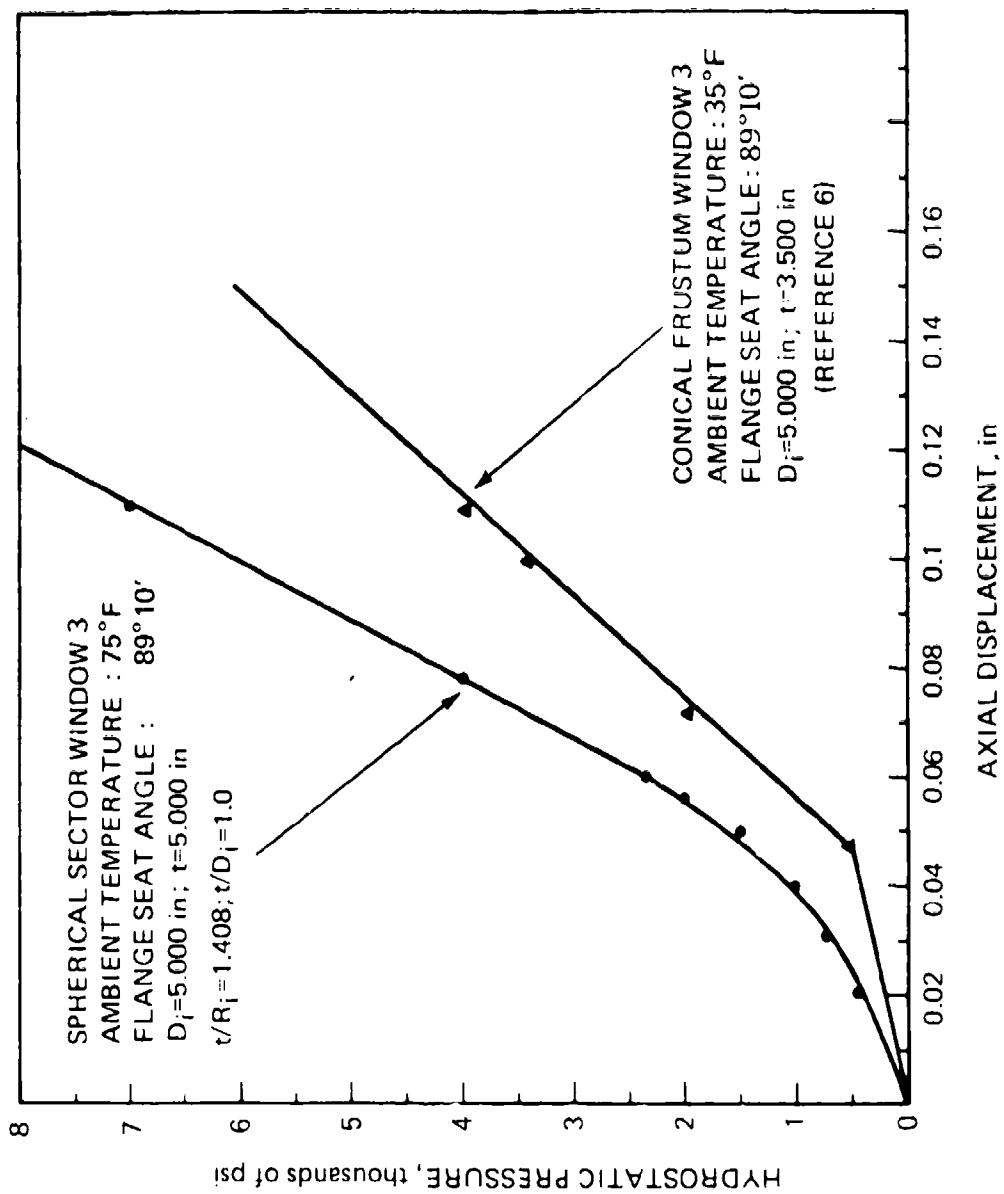
Figure 26. Comparison between experimentally determined displacements of spherical sector windows and conical frustum windows for ALVIN under short-term hydrostatic loading.

69

by approximately the same amount over most of its curved face,* while the displacement of the conical frustum window is much less uniform. The reason for the latter is that the external pressure in the spherical sector window is transferred to the window seat as membrane stresses, while bending and shear stresses are also important in the conical frustum window. The comparison of the measured strains and displacements on the faces of the conical frustum window (reference 11) indicates that only about half of the total displacement is caused by membrane stresses. Of the remaining half, a theoretical consideration shows that at least 75 percent is caused by shear stresses (reference 19). It can thus be postulated that the conical frustum window displaces at least twice as much in the center as near the seat (figure 27). This makes it reasonable to expect that the spherical sector window will retain the same optical properties, even at the maximum operating depth. The conical frustum window, however, will experience significant changes in its optical performance.

This comparison is only strictly true if both windows completely fit their flanges. If there is an initial mismatch, the windows will obviously displace more during the initial phase of the dive.

RESERVE STRENGTH

The reserve strength of the windows is of great importance because it generally decides the ability of the windows to withstand extraordinary loading conditions. If, for example, the submersible were to sink out of control in very deep water and hit the rocks on the sea bed with one of its windows, reserve strength would obviously be necessary.

Four parameters can be used to judge reserve strength: (1) short-term critical pressure; (2) long-term critical pressure; (3) impact strength; and (4) fatigue life.

Short-Term Critical Pressure

Previous studies (reference 16) show that about 32,000 psi can be expected for the conical frustum window with $t/D_i = 0.7$ (at $\cong 70°F$ and 650 psi per minute pressurization). For spherical sector windows with $t/D_i = 1.0$, the value is not accurately known, but is estimated to be 56,000 psi. It is significantly higher than 32,000 psi because of the following.

1. All available test results show that for the same t/D_i ratio the 90° spherical sector window generally fails at pressures that are at least twice the STCP of the comparable conical frustum window (references 1 and 10).

2. The spherical sector window displaces less than the conical frustum window for the same increase in hydrostatic pressure, and will thus start to lose radial support on the flange seat at a higher pressure (references 1 and 10).

Both the spherical sector and conical frustum windows in the high t/D_i range tend to develop cracks in the conical seating surface under high loads (references 1 and 10). The cracks are approximately normal to the bearing surface. It is also well established that these cracks are the incipient sign of failure. However, catastrophic failure is much more imminent in the conical frustum window after the cracks appear than in the spherical sector window

---

*This is known from the uniform distribution of meridional and circumferential strains measured on the low-pressure face.
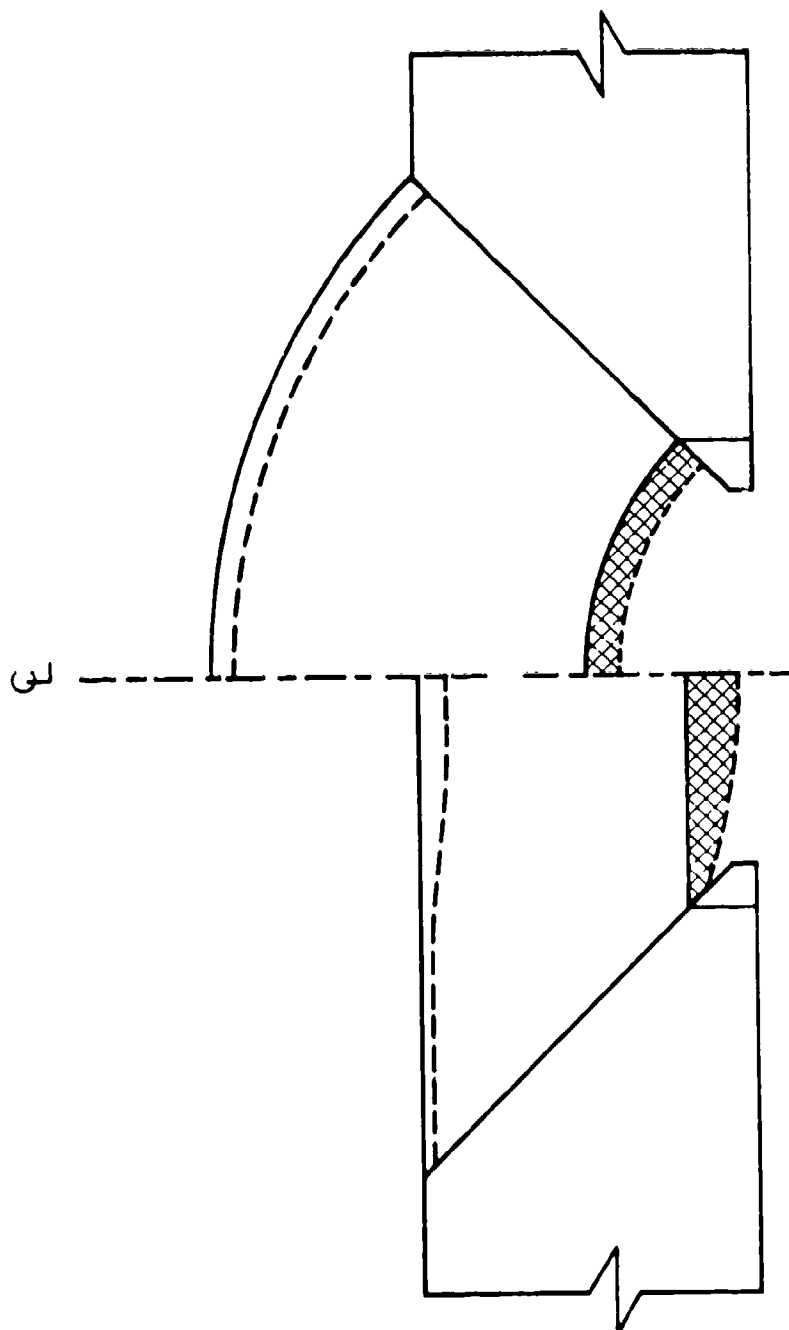
Figure 27. Qualitative comparison between the displacement patterns of spherical sector windows and conical frustum windows.

$\mathfrak{C}$

71

because of the difference in shape and direction of the fracture plane's propagation (figure 28). The cracks in the conical frustum window extend linearly across the thickness of the window causing early failure, while the cracks in the spherical sector window are somewhat more parallel to the spherical surfaces which does not immediately alter the window's capability to withstand external pressure. Thus, one can expect the conical frustum window to fail catastrophically by ejection of a central, conical plug whose apex penetrates through the high-pressure face, a process demonstrated in earlier tests (references 10 through 16 and figure 29).

Earlier studies have shown that the failure mode of spherical sector windows, with an included angle of $90°$ to $180°$, results from elastic or plastic instability after a local flat spot forms at the center of its surface (references 1 and 18). Because it takes a much higher external pressure for the plastic of the thick spherical sector window to become unstable than it takes to have the cracks in the seating surface of the plane window penetrate the window from the bearing surface to the high-pressure side, the spherical sector window is considered to be stronger than the conical frustum window (identical D_i and D_o).

Long-Term Critical Pressure

The long-term critical pressure of spherical sector windows with an included angle $< 150°$ has not been experimentally established. Data from windows with $\alpha = 180°$ show that the endurance at a given pressure is significantly longer than that for the conical frustum window (reference 5). It is also known for $90°$ spherical sectors that (1) the rate of displacement is less than that for conical frustum windows and (2) the volume of acrylic material that must be forced through the opening flange is substantially larger.

Displacement rates established during earlier long-term model tests (reference 13) show the magnitude of displacement of the conical frustum window at the end of a 100-hour test at 20,000 psi to be about 1.40 inches and the rate of displacement to be 1.5×10^{-3} to 2×10^{-3} inches per hour. When the magnitude and rate of displacement of conical frustum windows are compared to those of the spherical sector it is found that they are approximately 100 percent larger (figure 30). Because catastrophic failure of the conical frustum window generally occurs only after the magnitude of displacement equals the original thickness of the window, it is apparent that the thinner and more rapidly displacing conical frustum window will eject sooner, by an order of magnitude, than the spherical sector window fitted for and tested in the same flange.

Impact Resistance

Because the spherical sector window is thicker, has a higher STCP, and larger volume of window material than the conical frustum window, it can be theorized that the spherical sector window has a higher impact resistance than the conical frustum window. Impact tests on pressurized spherical sector windows at the Southwest Research Institute have substantiated the postulate that the impact resistance of a window is related to the window's thickness (reference 20). Thus, there is no doubt that the 5-inch thick spherical sector window has a significantly higher impact resistance than the 3.5-inch thick conical frustum window.

$T/t = 1.428$
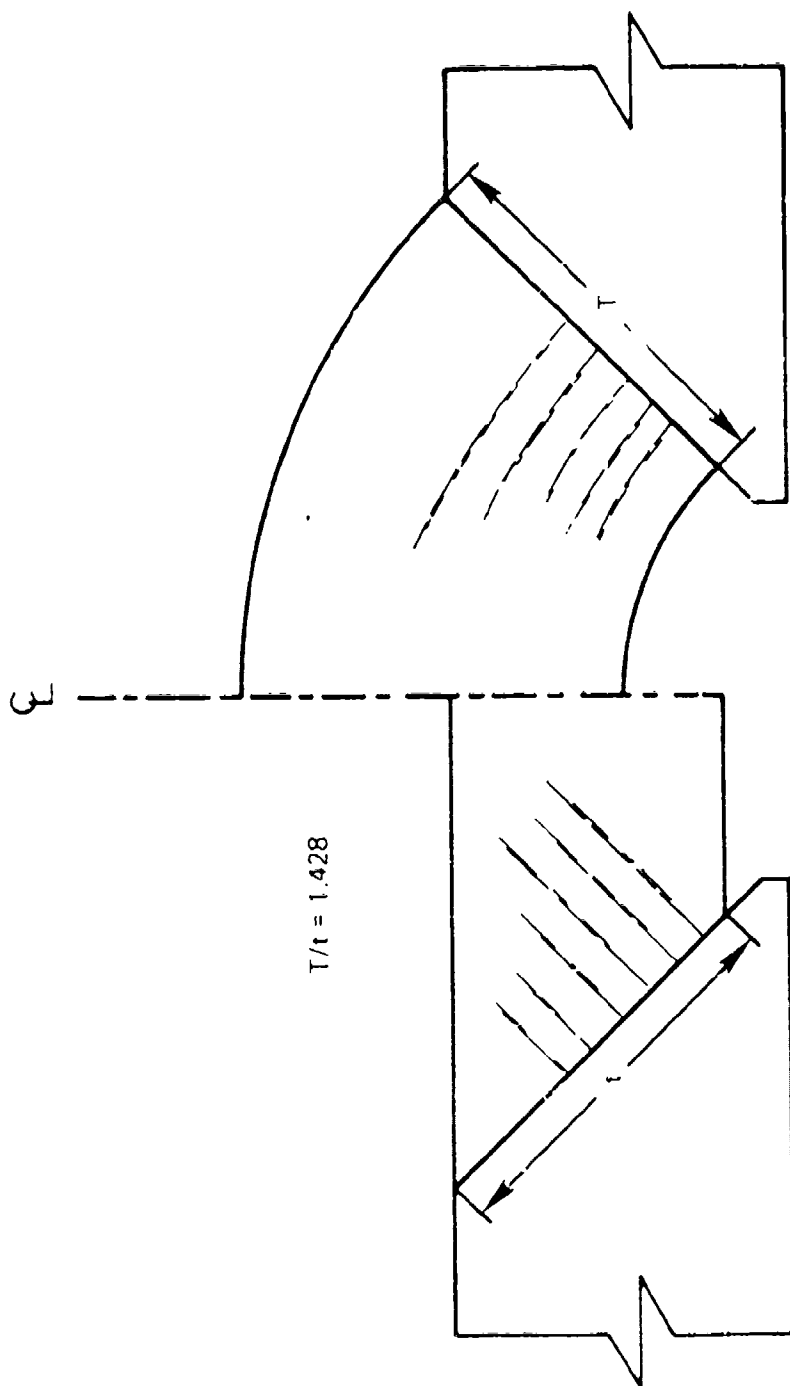
Figure 28. ...elative comparison between the fracture patterns in the spherical sector window
and the conical frustum window.

Figure 29A. Arrested failure pattern in conical frustum window with a ratio of $t/D_i = 0.5$. Tested in flange seat with $D_i/D_o = 1.5$ under short-term loading condition (reference 16). Close-up view of high-pressure face.

74
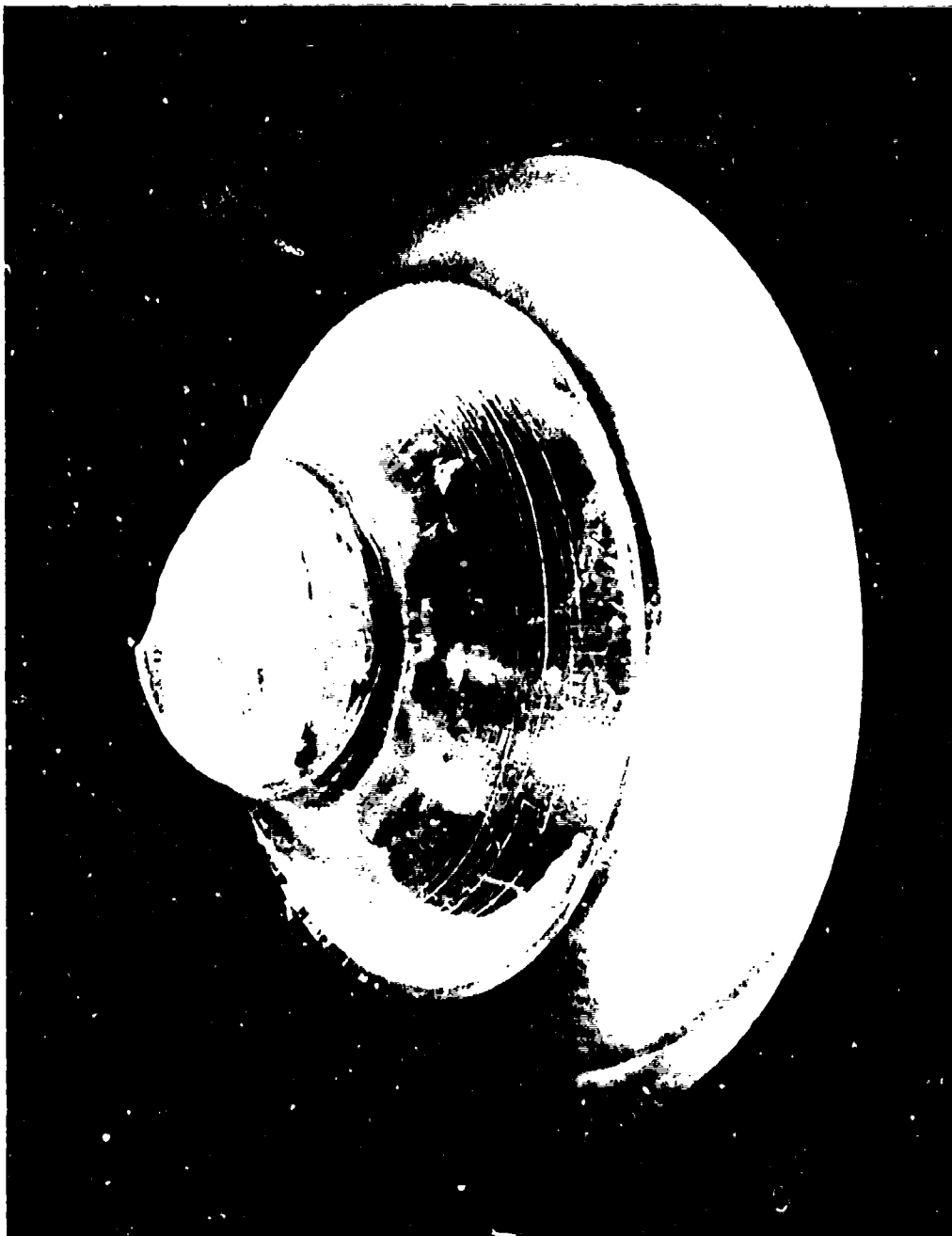
Figure 29B. Close-up view of low-pressure face and bearing surface of window in figure 29A.

Figure 29C. Close-up view of high-pressure face after removal of central plug from window in figure 29A.
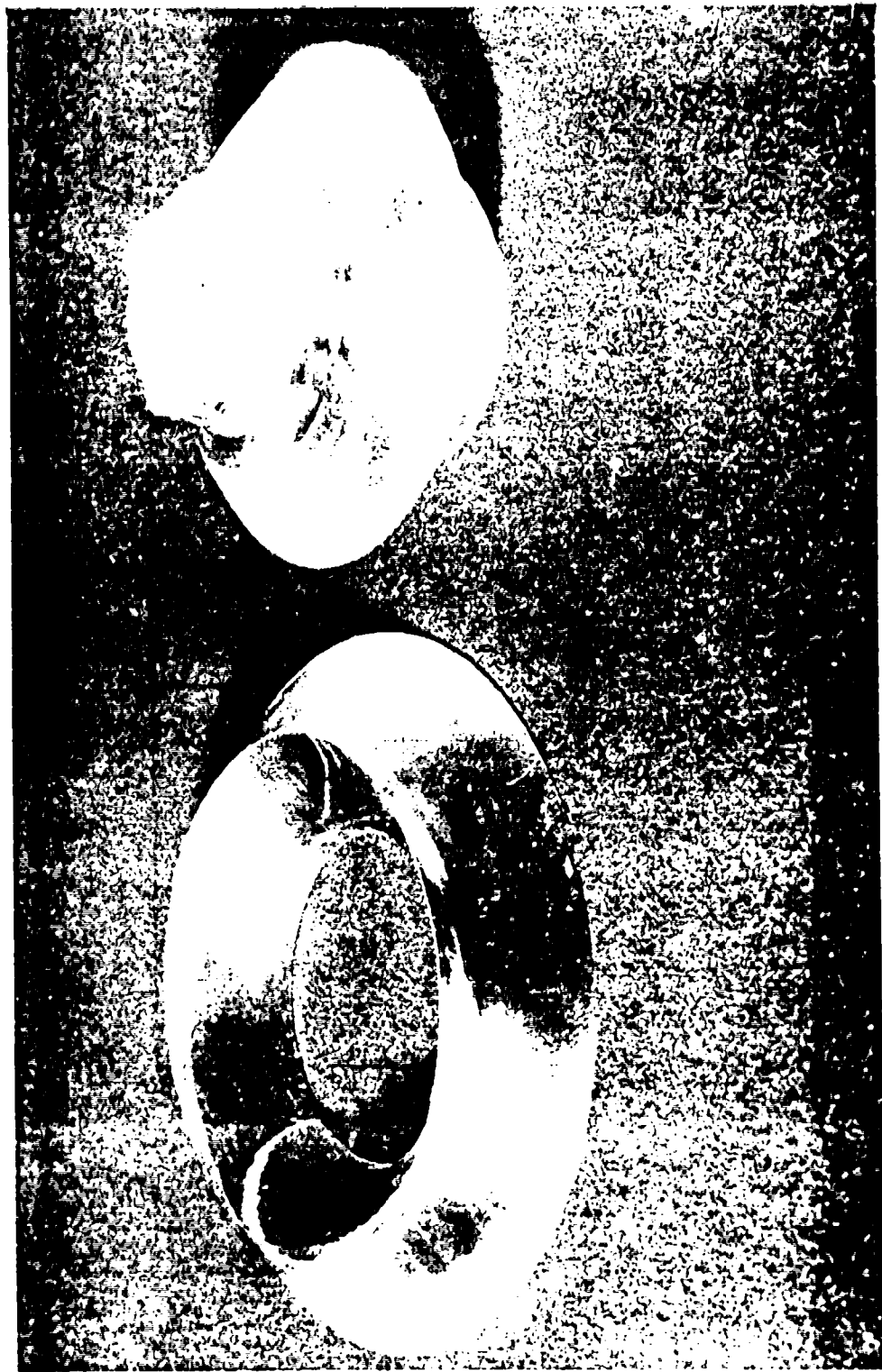
Figure 29D. Close-up view of low-pressure face and bearing surface after removal of central plug from window in figure 29A.
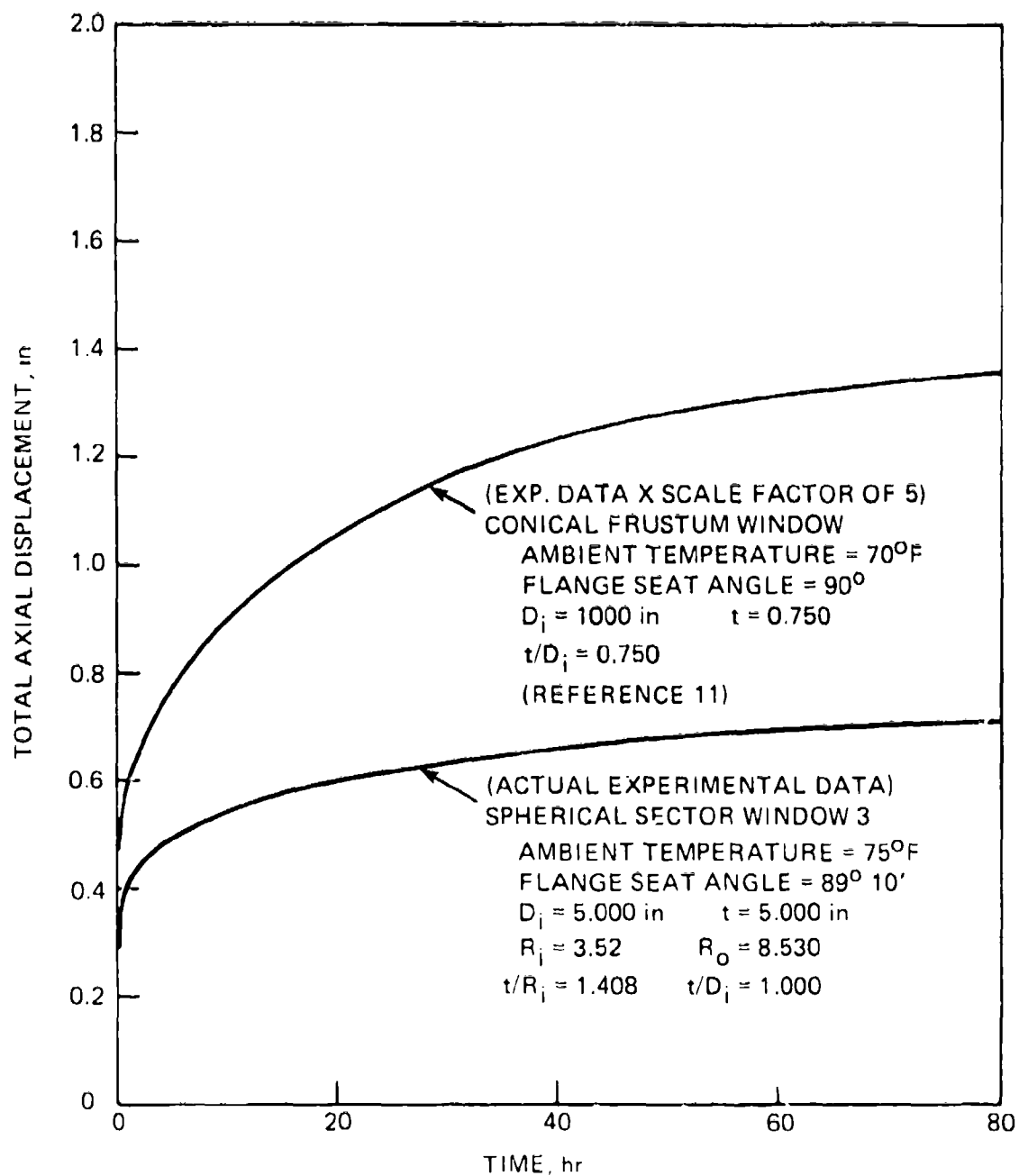
Figure 30A. Comparison between experimentally determined total axial displacements generated by 20,000-psi sustained loading of spherical sector window and conical frustum window of approximately the same t/D_i ratio as the ALVIN's cone frustum windows.
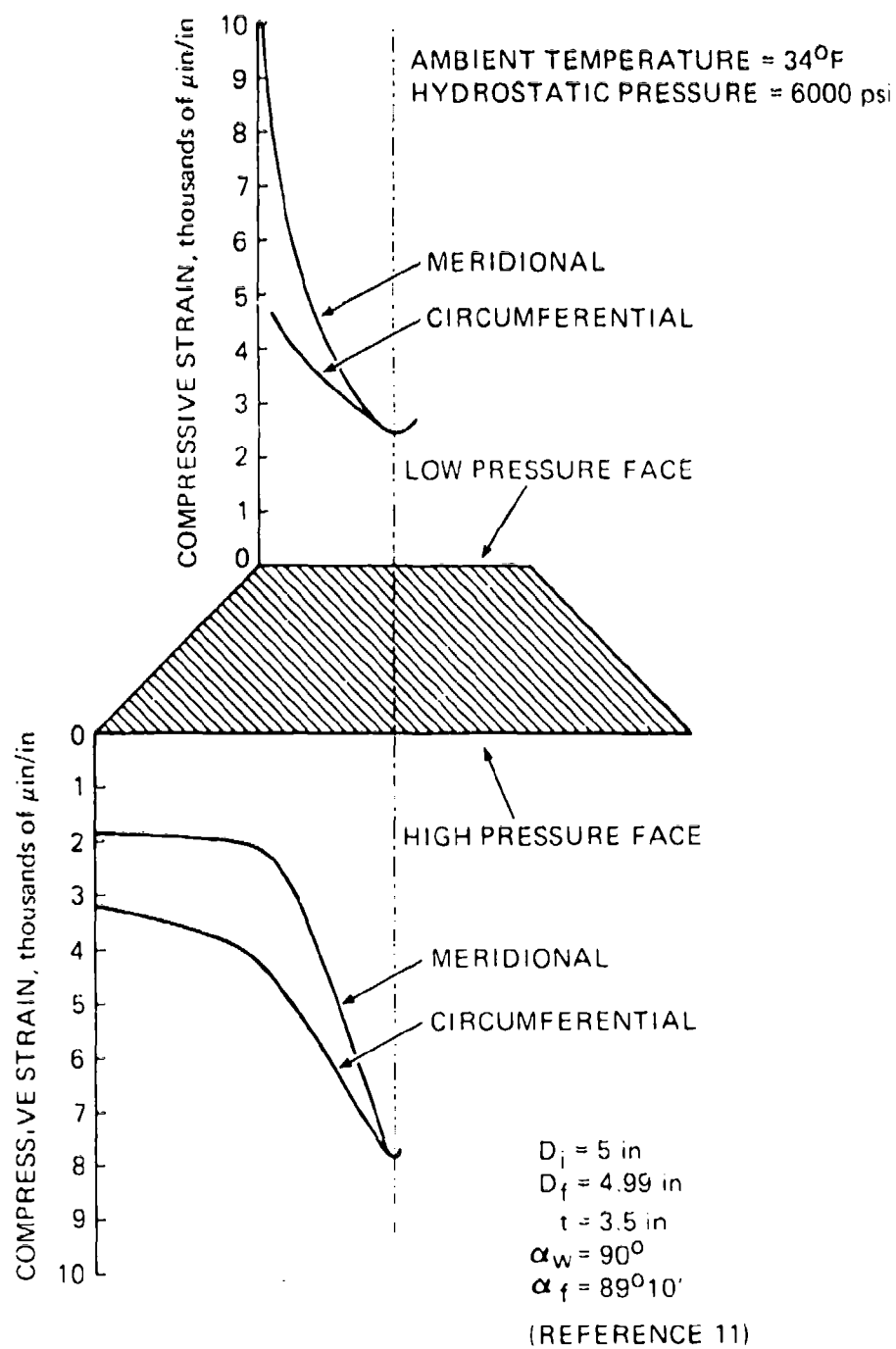
Figure 30B. Distribution of strains on high- and low-pressure faces of conical frustum window for ALVIN under 6000-psi hydrostatic loading.

Fatigue Life

This is the number of 7- to 8-hour dives that can be made to the submersible's maximum operating depth before cracks appear in the window. Once substantial cracks have appeared on a plane window's bearing surface, catastrophic failure can occur within a few dives; however, the spherical sector window is probably safe for a significantly larger number of dives.

Prior fatigue data exist only for a spherical window with a ratio of $t/D_i = 0.172$ and with $\alpha = 150°$ cycled 100 times to 4500 psi without the appearance of cracks (reference 23). The spherical window for ALVIN can survive at least 33 7-hour dives to 13,500 feet with no less than 17 hours of rest between each dive. Since the initiation of cracks on the seating surface is a function of the bearing pressure and friction, it is probable that the window with the most uniform distribution of bearing pressure will last longer. Finite element analysis of conical frustum windows has shown that there is a pronounced stress concentration on the seating surface near the edge of the low-pressure face (reference 21). This is expected, since the conical frustum window reacts to hydrostatic loads by bending. However, the spherical sector window does not react in this manner, and thus does not experience the high stress concentration on the bearing surface at the edge of the low-pressure face. There is only a small stress gradient on the bearing surface of thick spherical sector windows, resulting in slightly higher stresses near the low-pressure face. On the basis of these considerations it is reasonable to conclude that the fatigue life of the spherical sector window is significantly longer than that of the conical frustum window; however, the difference is not expected to be as large as the difference in ultimate strength.

RESULTS

1. Spherical sector acrylic plastic windows with a 90° included angle and thickness-to-diameter ratio of 1.00 can withstand 20,000-psi sustained hydrostatic loading for at least 100 hours without catastrophic failure.

2. The windows showed no permanent deformation after being subjected to 33 pressure cycles, where the maximum pressure was 6000 psi and the duration of an individual cycle 24 hours (7 hours of sustained loading followed 17 hours of relaxation).

3. The magnitude of maximum stress measured at the apex of the window's low-pressure face varied with the fit between the window and seat in the steel flange.

4. When the included angle of the flange seat was 1° less than that of the window, the maximum stress measured at the center of low-pressure face decreased by 46 percent from the maximum stress value measured for a perfectly fitted window.

5. The flange seat overhang ratio of 1.12 (minor window diameter divided by minor flange seat diameter) is adequate for 6000 psi of external pressure service, since the maximum axial displacement of the window in the flange seat for 100 hours is extrapolated to be about 0.140 inch.

6. Custom-cast acrylic blocks supplied by Polymer Products, Inc., for machining of windows possess the minimum mechanical properties specified by the Navy and ASME for man-rated windows.

7. During prooftesting of four windows to 6000 psi, the measured axial displacements were found to be within 5 percent of the calculated mean, indicating excellent reproducibility of mechanical properties from one casting to another.

8. The field of view through a 90° spherical sector with $t/D_i \doteq 1.0$ is 50 percent larger in area than through a 90° conical frustum with $t/D_i = 0.7$ when measured underwater at a 7.5-foot distance from the window.

CONCLUSIONS

Acrylic plastic conical frustum windows with $t/D_i = 0.7$ and a 90° included angle can be replaced in existing submersibles with spherical sectors of the same material, if the major and minor diameters of both shapes are the same and the spherical radii intersect the conical bearing surface at right angles. By replacing conical frustum windows with spherical sector windows that fit the existing window seat (figure 31) a larger field of view (figure 32) and greater implosion depth are assured.

Figure 31A Mating the spherical sector window to the ALVIN submersible at Woods Hole Oceanographic Institute.

Figure 31B. Close-up view of figure 31A.

23 in
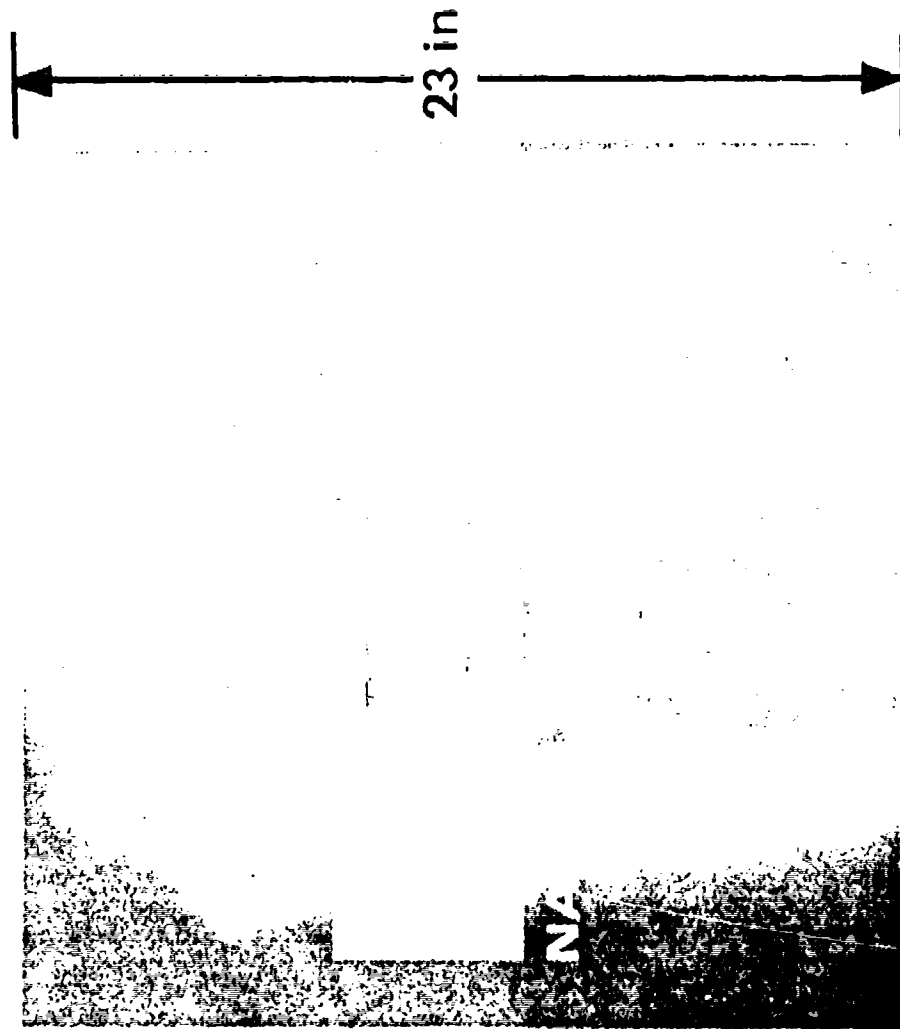
Figure 32A. Fields of view at 7.5-ft distance for windows in ALVIN. Photographs taken with 50mm camera lens at 6-in. standoff from center of window's low-pressure face. Plane frustum window.

94

23 in
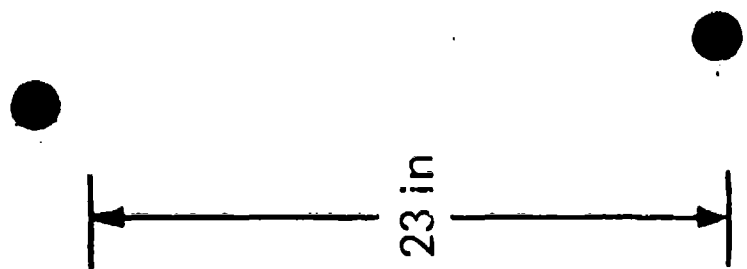
Figure 32B. Same data in figure 32A, but spherical sector window.

Figure 32C. Same data as figure 32A, but showing arrangement for photographing the bottom of a 7.5-foot deep swimming pool through conical frustum and spherical sector windows.

Figure 32D. Same data as figure 32A, but showing the placement of conical frustum window into the floating holding fixture.

DESIGN RECOMMENDATIONS

In the spherical shell sector the bearing stresses are distributed fairly uniformly across the conical seat. The presence of an o-ring groove on the conical seat represents an unacceptable stress riser that leads to early fatigue cracks in the window's bearing surface underneath the groove. This is distinctly different from conical frustum windows where an o-ring groove can be reasonably tolerated in the bearing surface as long as it is located within one-third of the bearing surface's length, measured from the high-pressure face of the window. At this location, the bearing compressive strains in a conical frustum are usually so low that they can tolerate the presence of a stress riser in the form of an o-ring groove without causing fatigue cracks.

Since o-ring grooves are not recommended either in the steel seat or in the spherical sector acrylic window, the seal must be accomplished by a gasket or an o-ring squeezed against both the metallic seat and high-pressure face (figures 33 and 34). Because of this, the window's high-pressure face must be either flush with the outside edge of the flange or a known distance below the outside edge. The diameter of the high-pressure face must be held within a tight dimensional tolerance. The maximum diametral tolerance is considered to be +0.000/-0.030 inch.

To seal successfully around the edge of the high-pressure face, there must be an assured contact between its edge and the conical flange seat. Since the experimental data described in this report have shown that a slight angular mismatch (where the angle of the window is larger than that of the flange seat) is not only acceptable but probably beneficial, the angular tolerance on the window's angle should be in the positive direction. The angular tolerance for machining should be less than 15' and shown as +15 minutes -0 minutes. If the windows are to be installed in new pressure hulls, the diametral and angular tolerances on the flange seats should be of the same magnitude but opposite in sign, i.e., +0.030/-0.000 for the major diameter and -15 minutes +0 minutes for the seat angle. Using these dimensional tolerances, the maximum diametral mismatch between the window's high-pressure face and the flange seat's major diameter is 0.060 inch, while the maximum mismatch in the included angle is 0.5°.

Although the STCP for thick spherical sector windows is a function of the D_i/D_f ratio, too high a ratio will decrease the field of view so that the window loses its value as a panoramic viewport. A D_i/D_f ratio of 1.1 is considered a good engineering compromise between high STCP and optical field of view. A ratio of $D_i/D_f = 1.0$ is to be avoided, since it will lower the STCP below the value used in its design (reference 1).

CORNER OF WINDOW FLUSH WITH
OR SLIGHTLY BELOW THE EDGE OF FLANGE

0.375-in NEOPRENE,
COMPRESSED TO
0.250-in, BONDED
TO RETAINER RING

D_f

D_i

$D_i/D_f \geq 1.1$

DETAIL A
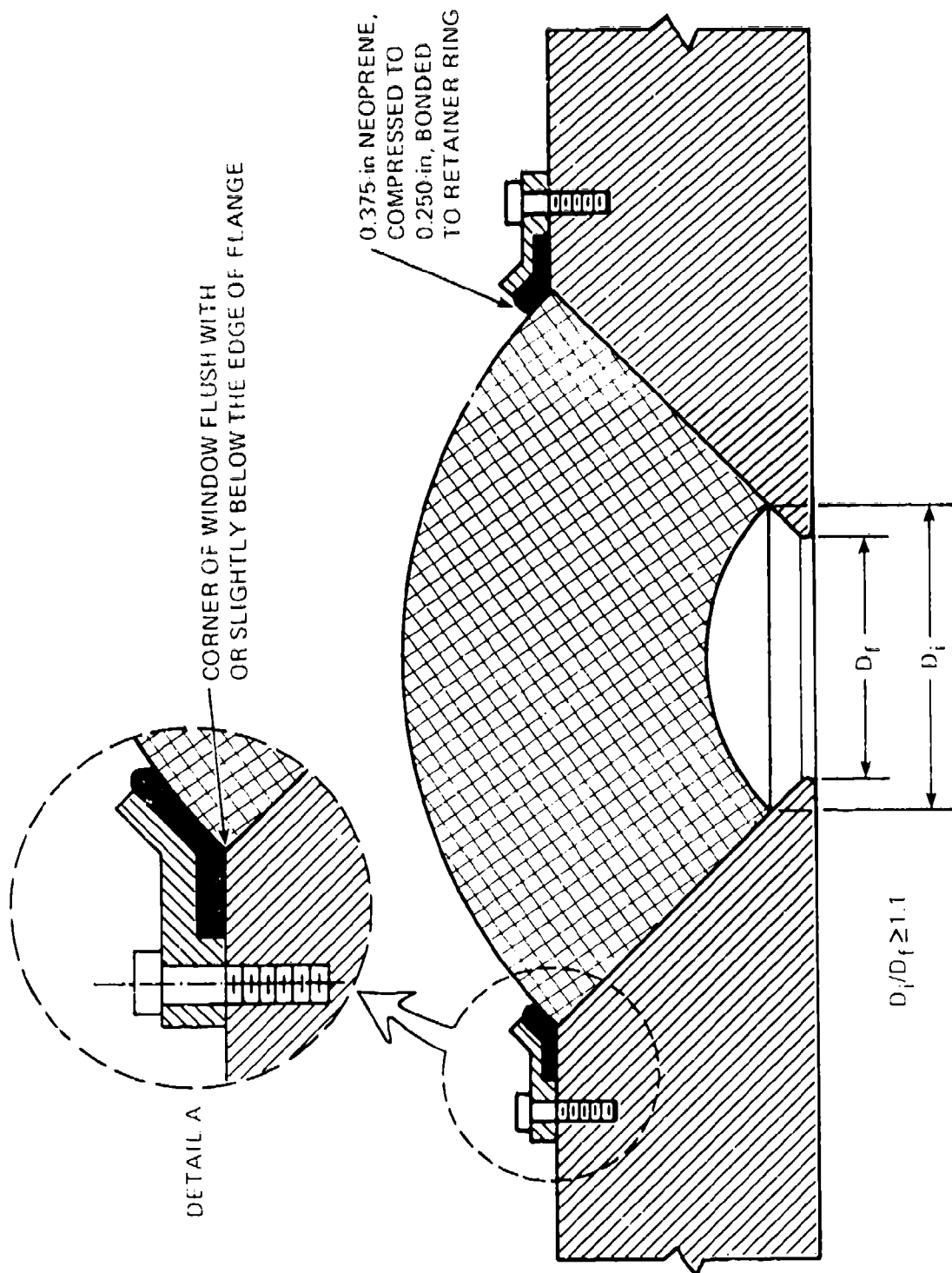
Figure 33. Recommended gasket seal design for acrylic plastic spherical sector window with 12,000-foot operational capability.

DETAIL A

1/16-in MAX. CLEARANCE

1/4-in O-RING, 60 DUROMETER
(5/16-in O-RING MAY BE USED ALSO)

0.3 ± 1

D_f

D_i

$D_i/D_f \geq 1.1$
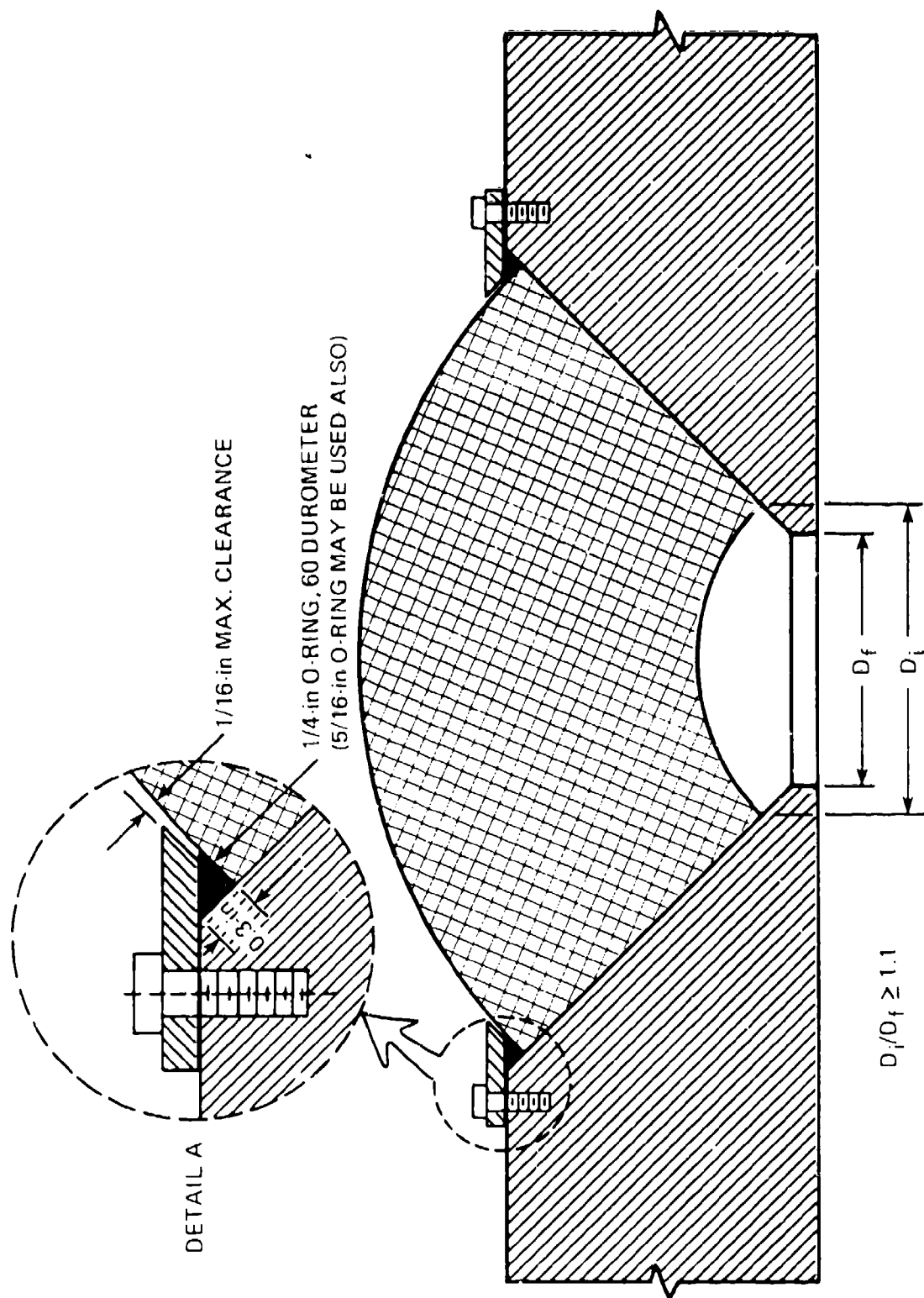
Figure 34. Recommended o-ring seal design for acrylic plastic spherical sector window with 12,000-foot operational capability.

90

REFERENCES

1. Naval Civil Engineering Laboratory, Technical Report R-631, Windows for External or Internal Hydrostatic Pressure Vessels; Part 3. Critical Pressure of Acrylic Spherical Shell Windows Under Short Term Pressure Application, by J. D. Stachiw, F. W. Brier, June 1969 (AD 689789).

2. Naval Undersea Center, NUC TP 383, Cast Acrylic Dome for Undersea Applications, by J. D. Stachiw, January 1974.

3. Naval Undersea Center, NUC TP 410, Development of a Precision Casting Process for Acrylic Plastic Spherical Shell Windows Applicable to High Pressure Service, by J. D. Stachiw, May 1974.

4. Naval Undersea Center, NUC TP 315, Acrylic Plastic Hemispherical Shells for NUC Undersea Elevator, by J. D. Stachiw, September 1972 (AD 749029).

5. a. Naval Civil Engineering Laboratory, Technical Report R-676, Development of a Spherical Acrylic Plastic Pressure Hull for Hydrospace Application, by J. D. Stachiw, April 1970 (AD 707363).

    b. Naval Civil Engineering Laboratory, Technical Note N-1113, The Spherical Acrylic Pressure Hull for Hydrospace Application; Part 2. Experimental Stress Evaluation of Prototype NEMO Capsule, by J. D. Stachiw, K. L. Mack, October 1970 (AD 715772).

    c. Naval Civil Engineering Laboratory, Technical Note N-1094, The Spherical Acrylic Pressure Hull for Hydrospace Application; Part 3. Comparison of Experimental and Analytical Stress Evaluations for Prototype NEMO Capsule, by H. Ottsen, March 1970 (AD 709914).

    d. Naval Civil Engineering Laboratory, Technical Note N-1134, The Spherical Acrylic Pressure Hull for Hydrospace Application; Part 4. Cyclic Fatigue of NEMO Capsule #3, by J. D. Stachiw, October 1970 (AD 715345).

6. Naval Undersea Center, NUC TP   , Impact Loading of Acrylic Spherical Shell Windows Under Hydrostatic Pressure, by J. D. Stachiw (under preparation).

7. Naval Undersea Center, NUC TP   , Explosive Loading of Acrylic Spherical Shells Under Hydrostatic Loading, by J. D. Stachiw (under preparation).

8. American Society of Mechanical Engineers, ASME Paper 63-WA-160, ALVIN on Oceanographic Research Submarine, J. B. Walsh and William O. Rainnie, Jr., December 1963.

9. Woods Hole Oceanographic Institution, Technical Report WHOi-74-60, Deep Submergence Research Conducted During the Period 16 June 1961-31 December 1973, Staff Report, August 1974.

10. Naval Civil Engineering Laboratory, Technical Report R-512, Windows for External or Internal Hydrostatic Pressure Vessels; Part 1. Conical Acrylic Windows Under Short Term Pressure Application, by J. D. Stachiw, K. O. Gray, January 1967 (AD 646882).

11. Journal of Ocean Technology, Volume 1, No. 1, Observation Windows of the Deep Submersible ALVIN, by James W. Mavor, Jr., 1966.

12. Naval Undersea Center, NUC TP 378, Recommended Practices for the Design, Fabrication, Prooftesting and Inspection of Windows in Man-rated Hyperbaric Chambers, by J. D. Stachiw, December 1973 (AD 773737).

13. Naval Civil Engineering Laboratory, Technical Report R-645, Windows for External or Internal Hydrostatic Pressure Vessels; Part 4. Conical Acrylic Windows Under Long Term Pressure Application of 20,000 psi, by J. D. Stachiw, October 1969 (AD 697272).

14. Naval Civil Engineering Command, Technical Report R-708, Windows for External or Internal Hydrostatic Pressure Vessels; Part 5. Conical Acrylic Windows Under Long Term Pressure Application of 10,000 psi, by J. D. Stachiw, W. A. Moody, January 1970 (AD 718812).

15. Naval Civil Engineering Laboratory, Technical Report R-747, Windows for External or Internal Hydrostatic Pressure Vessels; Part 6. Conical Acrylic Windows Under Long Term Pressure Application of 5,000 psi, by J. D. Stachiw, K. O. Gray, June 1971 (AD 736594).

16. Naval Civil Engineering Command, Technical Report R-773, Windows for External or Internal Hydrostatic Pressure Vessels; Part 7. Effect of Temperature and Flange Configuration on Critical Pressure of 90 Degree Conical Acrylic Windows Under Short Term Loading, by J. D. Stachiw, J. R. McKay, August 1972 (AD 748583).

1. Roark, Raymond J., "Formulas for Stress and Strain," McGraw-Hill Book Company, New York, 1965, Fourth Edition.

18. Naval Undersea Center, NUC TP 355, Flanged Acrylic Plastic Hemispherical Shells for Undersea Systems, by J. D. Stachiw, August 1973 (AD 769213).

19. Timoshenko, S., Strength of Materials, Part II, Third Edition, Van Nostrand Inc., Princeton, New Jersey, March 1956.

20. Southwest Research Institute, Final Report SWRI 03-4090-001, "Finite Element Analysis of an Acrylic Spherical Window Impacting a Rigid Wall, by O. H. Burnside, February 1975.

21. Snoey, M. R. and Crawford, J. E., "Stress Analysis of a Conical Acrylic Viewport," Naval Civil Engineering Laboratory, Technical Report R675, April 1970, Port Hueneme, California, April 1970.

22.   Naval Ordnance Laboratory, NOLTR 66-45, The Compressibility of Polymers to 20,000 Atmospheres, by R. W. Warfield, June 1966.

23.   Naval Undersea Center, NUC TP 393, Glass or Ceramic Spherical Shell Window Assembly for 20,000 psi Operational Pressure, by J. D. Stachiw, May 1974.

24.   Trowbridge, Taylor, "Optical Properties of a Spherical Plastic Underwater Observatory NEMO," ASME Paper No. 70-UnT-A, December 1970.

ACRYLIC PLASTIC HEMISPHERICAL SHELLS FOR NUC UNDERSEA ELEVATOR

by

J. D. Stachiw

Ocean Technology Department

September 1972

ADMINISTRATIVE STATEMENT

The work described in this report was performed by the Ocean
Technology Department in 1971 under the sponsorship of the Independent
Exploratory Development (IED) program at the Naval Undersea Center.

Released by
H. R. TALKINGTON, Head
Ocean Technology Department

ii

SUMMARY

PROBLEM

Free-blown acrylic plastic hemispherical shells with equatorial flanges have been incorporated into the underwater elevator capsule assembly mounted on the Naval Undersea Center (NUC) offshore tower. Since the wall thickness of a free-blown hemisphere decreases significantly at its apex, classical expressions for stress distribution and elastic instability of spheres with uniform wall thickness did not apply. For this reason an empirical approach was utilized to determine the required thickness of the hemispheres for a 56-ft operational depth.

RESULTS

An empirical approach to the prediction of local elastic instability in free-blown acrylic hemispheres was developed that utilized the measured minimum local thickness on the hemisphere for extrapolation of implosion pressure from available data on the implosion pressure of uniformly thick acrylic spheres. Equatorial flanges were found to contribute significant bending stresses during hydrostatic loading of hemispheres, particularly if the heel of the flange was rounded. The free-blown hemisphere incorporated into the underwater elevator capsule withstood successfully a 100-percent overload proof-test of 6 hours' duration without any permanent deformation.

RECOMMENDATIONS

Free-blown acrylic plastic hemispherical shells may be safely utilized in shallow-submergence, 1-atm manned submersible systems provided that the thinning of the shell at the apex is taken into consideration. The equatorial flange resulting from the free blowing process should be either trimmed off or provided with a cast-in-place interior ring supporting the rounded heel of the flange.

CONTENTS

INTRODUCTION

Acrylic plastic, because of its low cost and ease of fabrication, has found application as the ideal material for construction of submersible hulls with continental shelf depth capability. The precision-built NEMO-type (Ref. 1) spherical acrylic plastic pressure hulls in the NEMO (Ref. 2), Johnson-Sea-Link (Ref. 3), and MAKAKAI (Ref. 4) submersibles provide the crews with panoramic visibility at lesser cost than would be the case for metallic hulls with viewports rated for the same operational depth.

Still, for harbor-depth applications, even the economical fabrication costs of a precision-made NEMO-type acrylic plastic hull may appear to be too high. For such applications, valid economical inducements exist to substitute less precise fabrication techniques if the safety of the crew can still be assured. One of such less precise but very inexpensive fabrication techniques for spherical hulls is the free-forming technique.

BACKGROUND

Free-forming is the most economical technique for fabricating acrylic plastic hemispheres. The technique consists of clamping a sheet of acrylic plastic between two sheets of plywood, one of which has a circular cutout whose diameter is equal to that desired for the finished hemisphere. After the assembly is heated to 320°F in an air-heated oven, the space between the sheet of acrylic and the bottom sheet of plywood is pressurized with compressed air, causing the softened plastic to expand through the circular opening like a soap bubble. When the bubble assumes the shape of a hemisphere, the pressure of air expanding the plastic is reduced and the whole assembly removed from the oven. When the assembly has cooled down to room temperature, the pressure inside the acrylic bubble is dropped to atmospheric pressure, the two sheets of plywood are unclamped, acrylic bubble is removed, and the remnants of acrylic sheet are trimmed down to form an external flange around the equator of the hemisphere.

The resulting acrylic plastic bubble has very smooth inside and outside surfaces that do not require any further polishing to achieve the potential transparency of acrylic plastic. There is, however, considerable variation from one point to another on the shell in wall thickness and sphericity. The wall thickness, as a rule (Ref. 5), decreases by as much as 55 percent at the pole (Fig. 1), while the deviation in sphericity can be large or small depending on the technical capability of the fabricator, thickness-to-diameter ratio of the sphere, temperature, and many other factors. For hemispheres in the 4- to 6-ft-diameter range, the sphericity deviations generally are of a 0.5 to 1.0-in. magnitude.

When one compares the typical deviations in thickness (6 percent of nominal thickness) and sphericity (0.7 percent of nominal radius) of NEMO-type acrylic spheres with
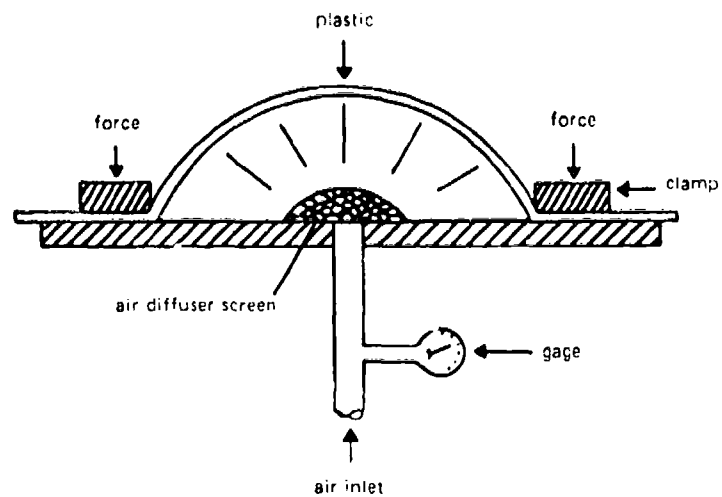
Figure 1a. General arrangement for free-forming of acrylic plastic shells through differential pressure method.
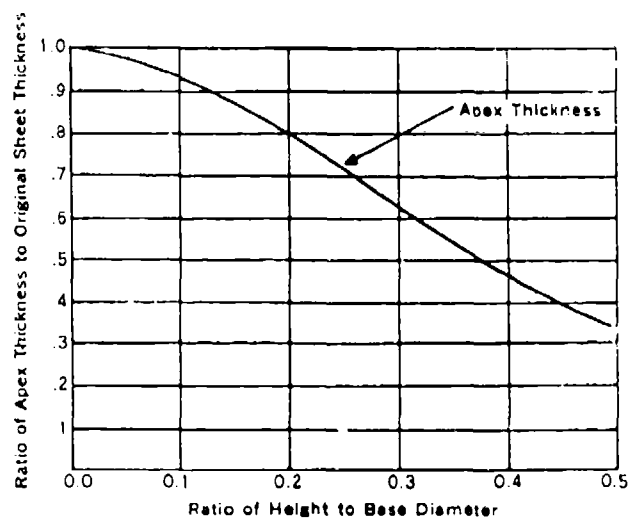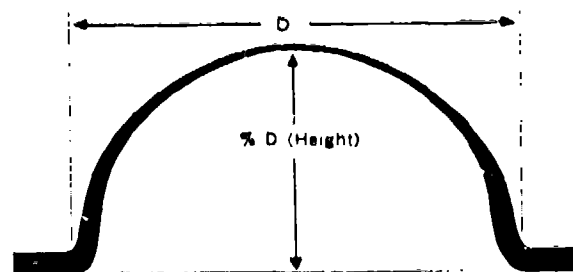
Figure 1b. Maximum stretching of acrylic plastic shells free-formed by the pressure differential between the interior and the exterior of the bubble.

those of the free-formed spheres (55 percent of thickness and 3 percent of nominal radius), one immediately notices that both sphericity and thickness deviations of free-formed hemispheres are significantly higher. The effect of large thickness and sphericity deviations on the elastic stability of the shell requires that the depth rating of free-formed hemispheres be considerably shallower than of NEMO-type spheres of the same nominal dimensions.

But besides a decrease of elastic stability in free-formed hemispheres, there is also an increase in magnitude of stresses because of the thin spot at the pole and the molded-in flange at the equator. Both of these deviations from a perfect hemisphere add considerable bending stresses to the compressive membrane stresses. Because of this, the principal meridional and circumferential stresses in the free-formed hemisphere are significantly higher than for ideal hemispheres of the same nominal dimensions. As a result, when rating the safe-depth capability of a free-formed hemisphere with molded-in flange, one must take into account not only its reduced elastic stability but also the increase in peak stresses.

DISCUSSION

The Naval Undersea Center operates an offshore tower that serves as a stationary platform for performance of studies in the optical and acoustical properties of shallow seas. An undersea elevator (Fig. 2) with panoramic visibility has been incorporated into the framework of the tower (Fig. 3) to provide opportunity for scientists and engineers to perform their own undersea experiments, and to inspect the condition of the tower framework from the interior of a 1-atm capsule with unrestricted vision. Since the depth of water at the tower is only 56 ft, a very inexpensive acrylic capsule was needed to keep the price of the elevator in line with its limited depth capability.

Although a precision-made NEMO-type spherical hull of only 0.500 in. nominal wall thickness would probably satisfy the requirement for a sphere with a median 54-in. diameter, the cost of fabrication still would be comparable to that of NEMO-type hulls for greater depths ($10,000–$15,000). Thus, only by substituting a fabrication process that inherently produces a dimensionally less precise but still satisfactory spherical shell would it be possible to significantly reduce the price of fabrication. The free-forming fabrication technique was chosen because it met the criteria of very low cost and acceptable performance for harbor-depth operations. Selecting the free-forming technique reduced the cost of fabricating a 54-in.-diameter acrylic capsule to a very economical level ($2000–$4000) even though the thickness of the acrylic plate from which it was to be formed would be much greater than that required for a precision-made NEMO-type hull with the same depth rating.

DESIGN

Since design criteria were not available at that time for free-formed acrylic hemispheres, the design had to be based on the extrapolation of short-term critical pressures from previous Navy programs, and the use of an apparent safety factor of 4 based on short-term critical pressure. This minimum apparent safety factor was previously established
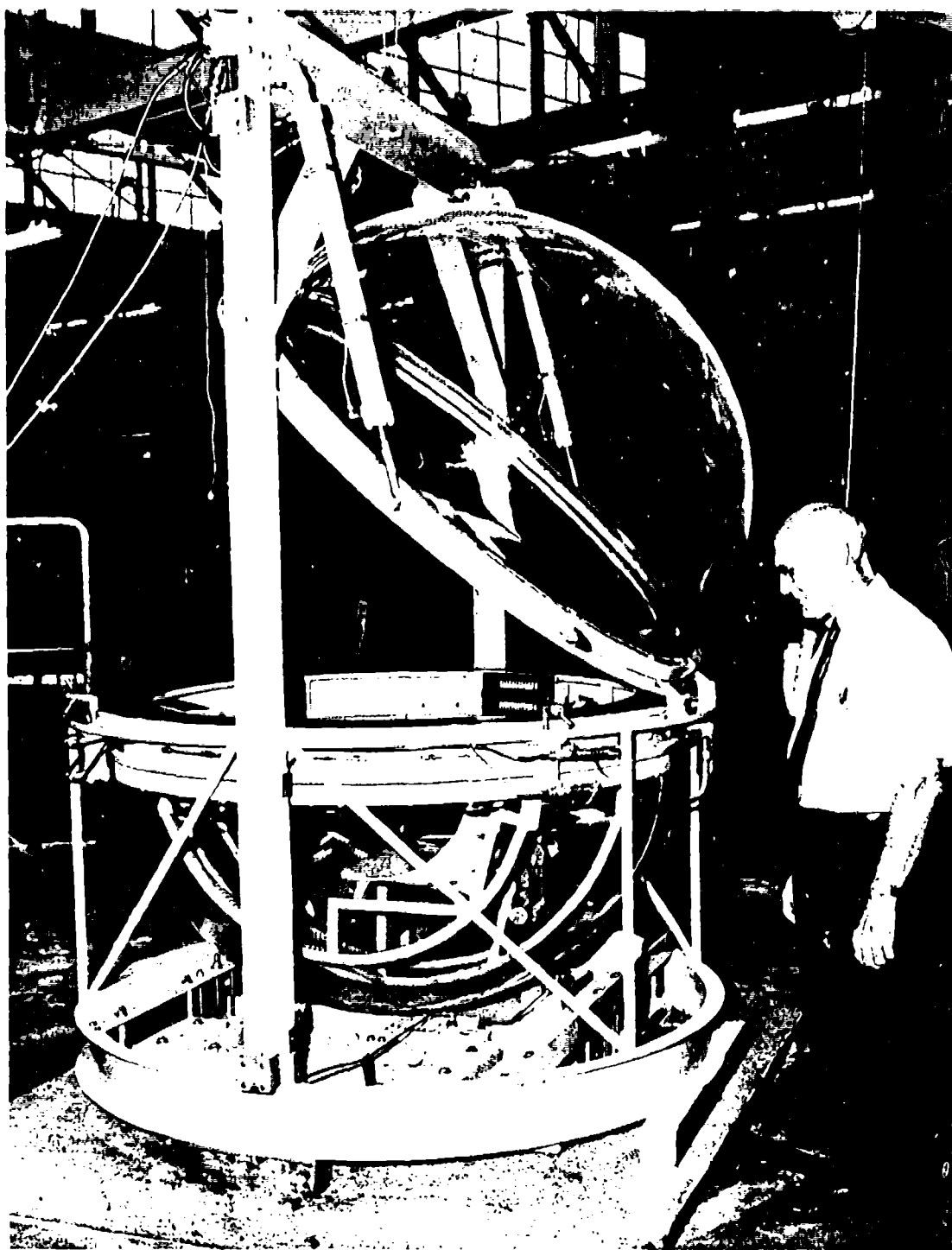
Figure 2a. Undersea elevator capsule with the lid open.

4
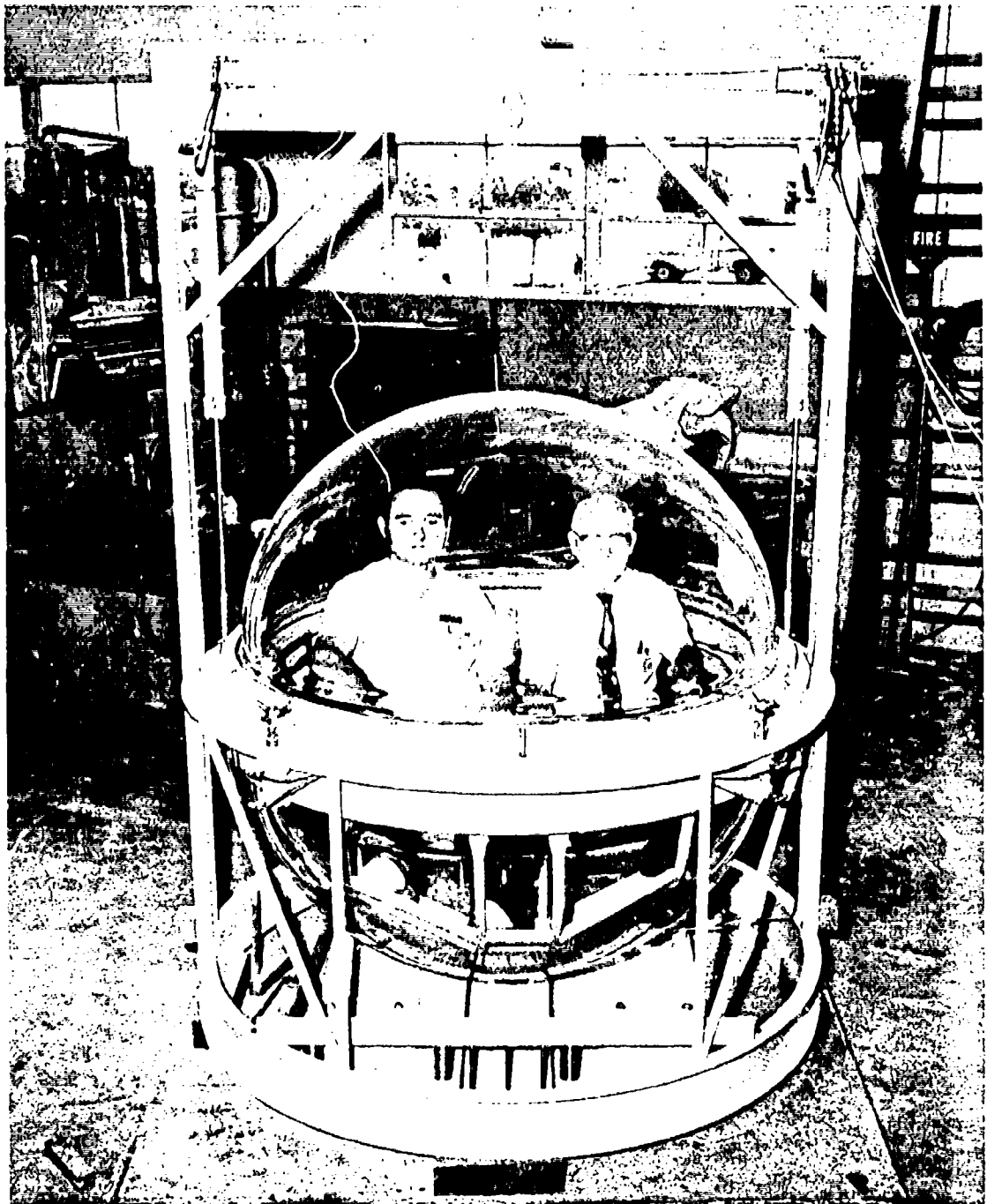
Figure 2b. Undersea elevator capsule with passengers after closing of the lid.

5
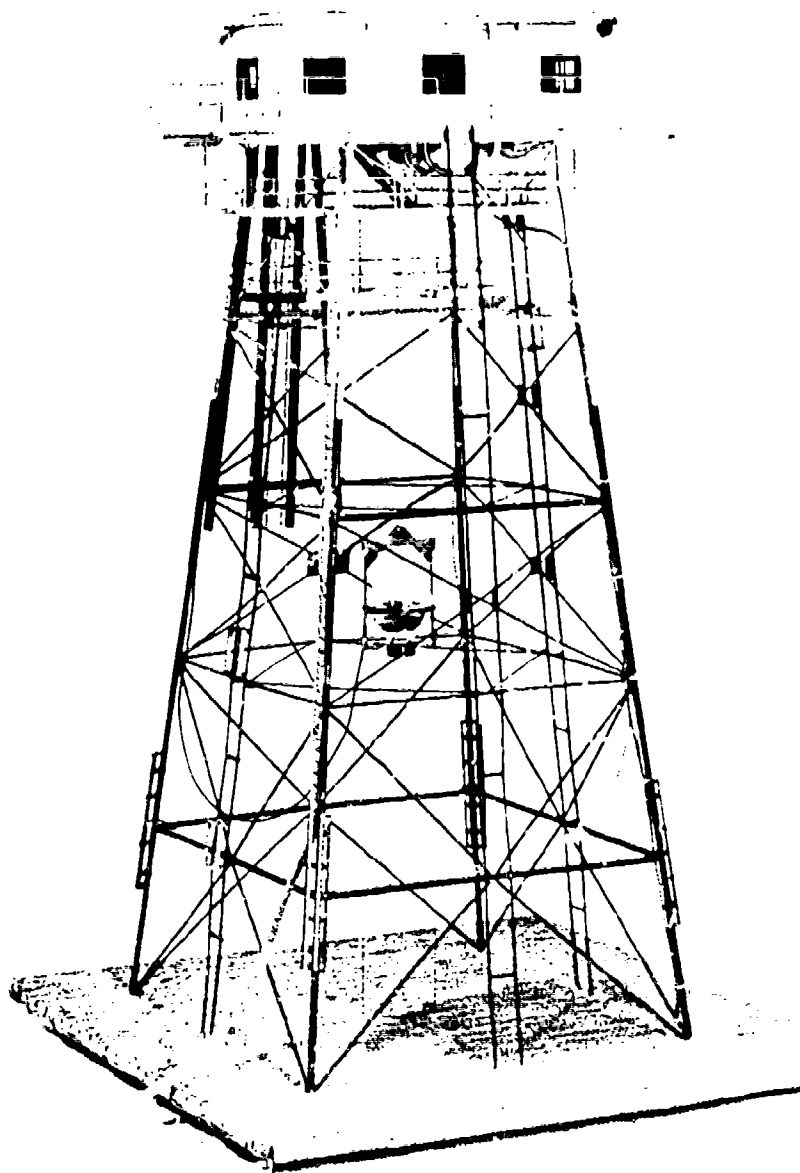
Figure 3a. Display model of the undersea elevator installation

Figure 36. Undersea elevator capsule after completion of a dive.

experimentally during the testing of spherical acrylic windows and NEMO hulls for the Navy's plastic material test program (Refs. 1, 6).

Since the short-term critical pressure and an apparent safety factor of 4 were to serve as the guideline for choosing the minimum shell thickness, the first step was to calculate the minimum acceptable short-term critical pressure for the capsule. It was calculated by multiplying the maximum operational pressure of 25 psi* by a factor of 4. The second step was to calculate the minimum shell thickness needed to withstand 100 psi prior to failure under short-term loading.

The minimum shell thickness for 100 psi critical pressure was established by extrapolation from NEMO hull model data (Ref. 1). By extrapolation from the 350-psi short-term collapse pressure of NEMO spheres with $t/R_0 = 0.0334$ (thickness-to-external-radius ratio), a t/R_0 of 0.0178 was obtained for a short-term collapse pressure of 100 psi. The extrapolation was based, in this case, on the elastic instability formula $p_c = K(t/R_0)^2$ where K was empirically established as 3.15×10^5. By means of this extrapolation, a nominally 0.5-in.-thick acrylic sphere would appear to satisfy the requirements for a 100-psi short-term collapse depth, provided the tolerances on sphericity and thickness were the same as for NEMO hulls (Ref. 1).

This is not the case, however, for free-formed hemispheres, where the dimensional tolerances are one order of magnitude larger. In addition, the existence of the equatorial acrylic flange and the method of clamping the hemisphere to the steel equatorial ring would introduce severe bending stresses not present in the NEMO hull structure. The two above-mentioned structural conditions, which tend to lower the critical pressure of the free-formed spheres, could be counteracted, however, by selecting as basic construction material acrylic plate stock with greater nominal thickness than the one calculated by extrapolation from the NEMO experimental data

The increase in thickness would have to be accomplished in a rather arbitrary manner since its effect on the short-term collapse pressure of a free-formed acrylic sphere was unknown. As a minimum, a nominal thickness could be chosen for the plate that, after free-forming, would result in a thickness, at the pole, obtained from extrapolation of NEMO data. Since a 55-percent reduction in wall thickness at the pole during free-forming of the hemisphere was expected, a 100-percent thicker standard plate than needed at the pole was chosen for the minimum-thickness hemisphere specimens (hemispheres 1A and 1B). Thus, the plate selected for the first test to evaluate hemispheres fabricated by free-forming was of 1.0 in. nominal thickness. It was expected to thin out at the pole due to stretching and result in a 0.45-in.-thick hull at that location. Thus, it would approximate the minimum-thickness requirement based on the extrapolation of NEMO data. Besides the minimum-thickness hemisphere specimens, another set of specimens was chosen to represent the conservative wall thickness one might possibly choose for the 56-ft depth application. The second set of hemisphere specimens (hemispheres 2A and 2B) was to be formed from 2.0-in.-thick plate, which during forming would be reduced in thickness at the pole of the hemisphere to about 1.0 in.

---

*All cited pressures are overpressures, i.e., above atmospheric.

8

In addition to the difference in nominal thickness, there was also a major design variation incorporated into the two sets of free-formed hemisphere specimens. The design difference between the first and second set of hemisphere specimens lay in the shape of the flange located at the equator (Fig. 4). Acrylic hemispheres 1A and 1B had a flange design that utilized an internal support ring to give the shell complete axial bearing support. Hemispheres 2A and 2B had a flange design that utilized only the external equatorial flange for axial bearing support. The reason for doing this was fabrication economy. By eliminating the accurately machined internal support ring and the bonding associated with it, sufficient savings accrued to offset the cost of the thicker plate. If incomplete axial bearing support at the equator could be structurally tolerated, free-formed hemispheres with more than minimum thickness would become economically feasible.

FABRICATION

Both sets (1.0 and 2.0 in. nominal thickness) of hemispheres were free-formed from Plexiglas G grade acrylic plastic satisfying MIL-C-24449 specification for plastic submersible windows (Table 1). After free-forming, the sphericity and wall thickness of the hemispheres were checked and the values recorded (Tables 2 and 3, and Fig. 5).

Subsequently, the hemispheres were machined on the bearing area of the equatorial flange surface. In the case of hemispheres 1A and 1B, internal support rings were machined from 1.0-in. Plexiglas G stock and bonded in place. This completed the fabrication of the hemispheres.

EXPERIMENTAL EVALUATION

Both sets of free-formed acrylic hemispheres were assembled into capsules and were subsequently subjected to hydrostatic testing for experimental evaluation. There was, however, a difference in the loading conditions, because the objectives of the test programs for the two sets of hemispheres differed significantly.

TEST PROGRAM

The objective of the test program for hemispheres 1A and 1B was to determine (1) the stresses in the hull during a single pressurization cycle representing a 100-percent pressure overload and duration of loading to which the elevator capsule may be subjected during a typical dive, and (2) the short-term critical pressure. The profile of the single pressure cycle for hemispheres 1A and 1B was designed to pressurize the capsule assembly at the rate of 100 psi/min to a level of 50 psi, hold it at that pressure for 6 hours, depressurize to 0 psi at the rate of 100 psi/min, and permit the assembly to relax at 0 psi for 24 hours prior to the short-term implosion test. This test was conducted at the rate of 100 psi/min also, except that the pressurization continued until implosion took place.

The test program for hemispheres 2A and 2B was identical to the test program for hemispheres 1A and 1B, except that the implosion test was omitted. The objective of

A

ACRYLIC HEMISPHERE

27.5 NOMINAL RADIUS

26.5 NOMINAL RADIUS

0.75 R

NEOPRENE
PRESSURE PAD

ACRYLIC SUPPORT RING
BONDED TO THE HEMISPHERE
WITH ACRYLIC CEMENT

0.625

0.9

2.4

29.0 RADIUS

SUPPORT FOR HEMISPHERES 1A & 1B

B

CAST IN PLACE
90 DUROMETER HARDNESS
ELASTOMER

28.0 NOMINAL RADIUS

26.0 NOMINAL RADIUS

3.5 R

NEOPRENE GASKET
BONDED TO ACRYLIC

CAPSULE FRAME

1.0

1.75

29.0 RADIUS

SUPPORT FOR HEMISPHERES 2A & 2B

All dimensions in inches

Figure 4. Support for the equatorial flanges on the acrylic plastic hemispheres for the NUC offshore tower elevator.

10

Table 1. Mechanical Properties of Acrylic Plastic.

Material Property	Test Specification	Specified Values MIL-C-24449	Measured Values				
			Hemisphere 1A	Hemisphere 1B	Hemisphere 2A	Hemisphere 2B
Tensile strength	ASTM-D-638	9,000 psi min	9,400 psi	9,130 psi	10,500 psi	10,500 psi
Tensile modulus		400,000 psi min	465,000 psi	460,000 psi	450,000 psi	440,000 psi
Tensile elongation		2 percent min	4.1 percent	4.1 percent	6.6 percent	5.9 percent
Compressive yield	ASTM-D-695	15,000 psi min	17,000 psi	16,900 psi	18,100 psi	17,400 psi
Compressive modulus		420,000 psi min	512,000 psi	510,000 psi	530,000 psi	530,000 psi
Flexural strength	ASTM-D-790	14,000 psi min	14,100 psi	12,300 psi	16,300 psi	15,800 psi
Flexural modulus		420,000 psi min	515,000 psi	510,000 psi	510,000 psi	500,000 psi
Shear strength	ASTM-D-732	8,000 psi min	10,300 psi	10,200 psi	10,500 psi	10,600 psi
Deformation underload (4000 psi at 122° F)	ASTM-D-621	2 percent max	0.85 percent	0.96 percent	0.81 percent	0.78 percent

NOTE: The experimentally determined mechanical properties are average values based on the test results from a total of 40 test specimens cut from the Plexiglas G sheets used for free-forming of hemispheres.

Table 2A. Thickness (in inches) of Free-Formed Hemisphere 1 A.

Azimuth (deg)	Elevation (deg)												
	4	15	30	45	60	75	90	75	60	45	30	15	4
0	0.910	0.800	0.676	0.576	0.508	0.467	0.450	0.467	0.510	0.582	0.67?	0.804	0.910
15	0.906	0.804	0.678	0.579	0.509	0.462	0.450	0.468	0.510	0.582	0.687	0.814	0.922
30	0.904	0.805	0.678	0.576	0.507	0.464	0.450	0.471	0.515	0.587	0.685	0.816	0.922
45	0.904	0.801	0.678	0.578	0.508	0.463	0.450	0.468	0.510	0.588	0.688	0.817	0.920
60	0.902	0.800	0.676	0.579	0.503	0.463	0.450	0.468	0.514	0.588	0.689	0.813	0.923
75	0.899	0.801	0.677	0.571	0.503	0.464	0.448	0.471	0.513	0.585	0.686	0.813	0.920
90	0.900	0.801	0.676	0.581	0.507	0.467	0.446	0.463	0.510	0.589	0.689	0.813	0.920
105	0.896	0.802	0.676	0.576	0.506	0.464	0.445	0.467	0.510	0.584	0.686	0.812	0.918
120	0.896	0.797	0.673	0.577	0.507	0.467	0.447	0.470	0.514	0.581	0.682	0.809	0.915
135	0.900	0.793	0.668	0.573	0.504	0.463	0.453	0.473	0.511	0.583	0.680	0.801	0.909
150	0.900	0.797	0.677	0.581	0.512	0.471	0.449	0.468	0.510	0.580	0.677	0.799	0.893
165	0.899	0.800	0.675	0.578	0.508	0.466	0.449	0.467	0.508	0.577	0.676	0.797	0.900

NOTES:

- Hemisphere 1A was free-blown from a 1-in.-thick sheet of Plexiglas G to a nominal external radius of 27.5 in.
- The thinnest spot on the hemisphere is 0.445 in. and is located at the apex of the hemisphere.

12

Table 2B. Thickness (in inches) of Free-Formed Hemisphere 1B.

Azimuth (deg)	Elevation (deg)												
	7	15	30	45	60	75	90	75	60	45	30	15	7
0	0.913	0.803	0.671	0.561	0.488	0.448	0.431	0.455	0.507	0.585	0.698	0.840	0.960
15	0.906	0.804	0.675	0.569	0.491	0.449	0.434	0.457	0.502	0.585	0.693	0.832	0.953
30	0.924	0.807	0.679	0.570	0.497	0.452	0.437	0.454	0.504	0.580	0.689	0.824	0.935
45	0.923	0.812	0.686	0.579	0.501	0.453	0.434	0.450	0.494	0.570	0.683	0.811	0.923
60	0.935	0.822	0.692	0.681	0.501	0.453	0.433	0.447	0.493	0.565	0.679	0.804	0.910
75	0.945	0.826	0.694	0.586	0.503	0.455	0.433	0.449	0.490	0.563	0.675	0.803	0.944
90	0.952	0.831	0.693	0.584	0.506	0.457	0.433	0.448	0.496	0.568	0.672	0.800	0.915
105	0.948	0.829	0.698	0.590	0.510	0.459	0.434	0.448	0.491	0.567	0.673	0.802	0.912
120	0.940	0.825	0.689	0.583	0.507	0.457	0.435	0.452	0.493	0.566	0.668	0.800	0.911
135	0.927	0.825	0.696	0.590	0.509	0.459	0.438	0.459	0.485	0.563	0.670	0.806	0.911
150	0.940	0.829	0.698	0.585	0.505	0.458	0.436	0.445	0.488	0.566	0.671	0.802	0.915
165	0.968	0.837	0.702	0.587	0.509	0.461	0.433	0.448	0.487	0.561	0.671	0.800	0.910

NOTES.

• Hemisphere 1B was free-blown from a 1-in.-thick sheet of Plexiglas G to a nominal external radius of 27.5 in.

• The thinnest spot on the hemisphere is 0.431 in. and is located at the apex of the hemisphere.

13

Table 2C. Sphericity of Free-Formed Hemisphere 1A.

Azimuth (deg)	Elevation (deg)												
	4	15	30	45	60	75	90	75	60	45	30	15	4
0	-0.188	+0.438	+0.407	+0.157	-0.125	-0.312	-0.406	-0.375	-0.187	+0.063	+0.344	+0.407	+0.188
15	-0.172	+0.421	+0.391	+0.141	-0.125	-0.312	-0.406	-0.375	-0.187	+0.063	+0.344	+0.407	+0.219
30	-0.188	+0.407	+0.375	+0.125	-0.125	-0.312	-0.406	-0.375	-0.187	+0.063	+0.344	+0.407	+0.219
45	+0.157	+0.375	-0.344	+0.094	-0.156	-0.343	-0.406	-0.375	-0.187	+0.063	+0.344	+0.438	+0.250
60	+0.172	+0.375	+0.313	+0.062	-0.156	-0.359	-0.437	-0.375	-0.187	+0.063	+0.329	+0.438	+0.266
75	+0.172	+0.344	+0.282	+0.062	-0.187	-0.375	-0.437	-0.375	-0.218	+0.032	+0.313	+0.422	+0.250
90	+0.141	+0.344	+0.282	+0.062	-0.187	-0.312	-0.406	-0.343	-0.187	+0.063	+0.313	+0.422	+0.250
105	+0.141	+0.329	+0.282	+0.062	-0.187	-0.343	-0.406	-0.343	-0.187	+0.063	+0.329	+0.438	+0.250
120	+0.157	+0.344	+0.282	+0.062	-0.187	-0.343	-0.406	-0.343	-0.171	+0.110	+0.344	+0.438	+0.250
135	+0.172	+0.344	+0.282	+0.047	-0.187	-0.375	-0.406	-0.343	-0.156	+0.110	+0.375	+0.454	+0.250
150	+0.188	+0.375	+0.313	+0.062	-0.187	-0.375	-0.406	-0.343	-0.140	+0.125	+0.375	+0.438	+0.250
165	+0.188	+0.375	+0.313	+0.062	-0.187	-0.375	-0.406	-0.343	-0.656	+0.125	+0.375	+0.438	+0.219

NOTES:

- Hemisphere 1A was free-blown from a 1-in.-thick sheet of Plexiglas G to a nominal external radius of 27.5 in.
- Measurements shown are in inches and denote deviations from a nominal 27.5-in. external radius.
- Maximum deviations from the nominal 27.5-in. radius are -0.437 in. at the apex, and +0.454 in. at 15-deg elevation.

Table 21. Sphericity of Free-Formed Hemisphere 1B

Azimuth (deg)	Elevation (deg)												
	7	15	30	45	60	75	90	75	60	45	30	15	7
0	+0.172	+0.360	+0.313	+0.079	-0.156	-0.312	-0.406	-0.343	-0.187	+0.063	+0.188	+0.469	+0.282
15	+0.172	+0.344	+0.282	+0.063	-0.187	-0.343	-0.406	-0.343	-0.187	+0.063	+0.375	+0.469	+0.282
30	+0.188	+0.344	+0.250	+0.032	-0.187	-0.343	-0.406	-0.343	-0.187	+0.063	+0.344	+0.407	+0.250
45	+0.188	+0.344	+0.250	0.000	-0.218	-0.375	-0.406	-0.343	-0.156	+0.063	+0.313	+0.375	+0.219
60	+0.157	+0.313	+0.219	-0.031	-0.250	-0.406	-0.390	-0.312	-0.125	+0.110	+0.344	+0.431	+0.250
75	+0.157	+0.313	+0.219	-0.031	-0.250	-0.375	-0.406	-0.312	-0.125	+0.125	+0.344	+0.438	+0.219
90	+0.188	+0.344	+0.219	-0.062	-0.281	-0.406	-0.406	-0.312	-0.125	+0.125	+0.375	+0.407	+0.219
105	+0.219	+0.344	+0.219	-0.031	-0.265	-0.406	-0.406	-0.312	-0.125	+0.125	+0.344	+0.407	+0.219
120	+0.250	+0.344	+0.219	-0.062	-0.281	-0.406	-0.406	-0.312	-0.125	+0.125	+0.344	+0.407	+0.188
135	+0.250	+0.375	+0.250	-0.031	-0.250	-0.375	-0.406	-0.312	-0.125	+0.125	+0.344	+0.375	+0.188
150	+0.282	+0.407	+0.282	0.000	-0.250	-0.375	-0.406	-0.312	-0.125	+0.094	+0.344	+0.375	+0.188
165	+0.282	+0.438	+0.313	+0.032	-0.218	-0.375	-0.406	-0.312	-0.156	+0.094	+0.313	+0.375	+0.157

NOTES:

- Hemisphere 1B was free-blown from a 1-in.-thick sheet of Plexiglas G to a nominal external radius of 27.5 in.
- Measurements shown are in inches and denote deviations from a nominal 27.5-in. external radius.
- Maximum deviations from the nominal 27.5-in. radius are -0.406 in. at the apex, and +0.469 in. at 15-deg elevation.

Table 3A. Thickness (in Inches) of Free-Formed Hemisphere 2A.

Azimuth (deg)	Elevation (deg)												
	7	15	30	45	60	75	90	75	60	45	30	15	7
0	1.730	1.428	1.247	1.109	1.010	0.949	0.910	0.934	0.985	1.065	1.183	1.360	1.630
15	1.673	1.418	1.238	1.113	1.009	0.947	0.915	0.931	0.975	1.053	1.157	1.315	1.570
30	1.642	1.398	1.229	1.105	1.010	0.950	0.918	0.923	0.966	1.038	1.135	1.276	1.518
45	1.591	1.379	1.222	1.102	1.009	0.954	0.915	0.918	0.970	1.036	1.130	1.262	1.505
60	1.565	1.350	1.210	1.105	1.029	0.963	0.929	0.928	0.962	1.029	1.130	1.285	1.529
75	1.558	1.363	1.214	1.093	1.022	0.966	0.927	0.921	0.962	1.045	1.165	1.318	1.557
90	1.577	1.382	1.227	1.103	1.015	0.969	0.921	0.937	0.979	1.055	1.178	1.361	1.630
105	1.585	1.387	1.243	1.112	1.023	0.965	0.918	0.932	0.982	1.076	1.210	1.392	1.623
120	1.582	1.413	1.243	1.108	1.020	0.963	0.918	0.936	0.987	1.081	1.227	1.413	1.655
135	1.617	1.413	1.239	1.105	1.013	0.958	0.918	0.933	0.985	1.087	1.229	1.415	1.675
150	1.632	1.403	1.230	1.098	1.006	0.950	0.918	0.944	1.005	1.101	1.244	1.425	1.697
165	1.618	1.385	1.210	1.087	0.990	0.933	0.919	0.944	1.006	1.104	1.243	1.434	1.707

NOTES:

- Hemisphere 2A was free-blown from a 2 in. thick sheet of Plexiglas G to a nominal external radius of 28.0 in.
- The thinnest spot on the hemisphere is 0.910 in. and it is located at the apex of the hemisphere.

Table 3B. Thickness (in Inches) of Free-Formed Hemisphere 2B.

Azimuth (deg)	Elevation (deg)												
	7	15	30	45	60	75	90	75	60	45	30	15	7
0	1.599	1.418	1.208	0.966	0.955	0.903	0.887	0.917	0.984	1.095	1.237	1.443	1.604
15	1.570	1.403	1.195	1.055	0.962	0.910	0.887	0.918	0.987	1.093	1.230	1.421	1.597
30	1.540	1.375	1.177	1.045	0.956	0.905	0.887	0.917	0.983	1.085	1.224	1.408	1.605
45	1.495	1.328	1.151	1.024	0.943	0.902	0.888	0.917	0.983	1.086	1.227	1.394	1.597
60	1.433	1.287	1.123	1.009	0.937	0.903	0.888	0.913	0.985	1.089	1.223	1.409	1.628
75	1.413	1.249	1.106	1.005	0.937	0.894	0.888	0.913	0.981	1.088	1.222	1.400	1.620
90	1.366	1.235	1.102	1.006	0.940	0.897	0.889	0.908	0.986	1.086	1.220	1.399	1.635
105	1.345	1.245	1.113	1.013	0.947	0.907	0.890	0.921	0.990	1.088	1.223	1.407	1.637
120	1.420	1.305	1.148	1.030	0.953	0.908	0.891	0.908	0.980	1.086	1.230	1.421	1.655
135	1.535	1.377	1.185	1.054	0.960	0.909	0.891	0.912	0.981	1.087	1.233	1.441	1.634
150	1.608	1.444	1.226	1.075	0.973	0.908	0.891	0.917	0.983	1.083	1.233	1.446	1.647
165	1.640	1.454	1.239	1.085	0.980	0.915	0.891	0.914	0.969	1.077	1.223	1.423	1.608

NOTES:
- Hemisphere 2B was free-blown from a 2-in.-thick sheet of Plexiglas G to a nominal external radius of 28.0 in.
- The thinnest spot on the hemisphere is 0.887 in. and is located at the apex of the hemisphere.

17

Table 3C. Sphericity of Free-Formed Hemisphere 2A.

Azimuth (deg)	Elevation (deg)										
	15	30	45	60	75	90	75	60	45	30	15
0	+0.375	+0.681	+0.500	+0.249	+0.032	−0.030	+0.063	+0.313	+0.594	+0.750	+0.402
15	+0.423	+0.750	+0.557	+0.250	+0.094	−0.020	+0.094	+0.360	+0.688	+0.820	+0.469
30	+0.438	+0.766	+0.563	+0.235	0.000	−0.031	+0.094	+0.391	+0.719	+0.735	+0.485
45	+0.438	+0.750	+0.532	+0.219	0.000	−0.031	+0.110	+0.407	+0.745	+0.875	+0.500
60	+0.516	+0.870	+0.835	+0.430	+0.130	−0.030	0.000	+0.188	+0.485	+0.635	+0.344
75	+0.500	+0.844	+0.704	+0.407	+0.125	−0.030	−0.015	+0.157	+0.407	+0.560	+0.282
90	+0.485	+0.797	+0.641	+0.375	+0.125	−0.040	−0.030	+0.125	+0.344	+0.485	+0.250
105	+0.438	+0.719	+0.579	+0.329	+0.079	−0.040	−0.030	+0.110	+0.313	+0.438	+0.235
120	+0.390	+0.640	+0.515	+0.282	+0.063	−0.040	−0.030	+0.110	+0.313	+0.547	+0.235
135	+0.329	+0.579	+0.469	+0.250	+0.063	−0.020	−0.015	+0.141	+0.360	+0.469	+0.266
150	+0.313	+0.570	+0.460	+0.250	+0.063	−0.030	+0.032	+0.204	+0.429	+0.563	+0.313
165	+0.329	+0.610	+0.469	+0.250	+0.063	−0.031	+0.040	+0.250	+0.510	+0.657	+0.370

NOTES:

- Hemisphere 2A was free-blown from a 2-in.-thick sheet of Plexiglas G to a nominal external radius of 28 in.
- Measurements shown are in inches and denote deviations from a nominal 28.0-in. external radius.
- Maximum deviations from the nominal 28.0-in. radius are −0.040 in. at the apex, and +0.875 in. at 30-deg elevation.

18

Table 30. Sphericity of Free-Formed Hemisphere 2B.

Azimuth (deg)	Elevation (deg)												
	7	15	30	45	60	75	90	75	60	45	30	15	7
0	0.000	+0.370	+0.694	+0.620	+0.428	+0.245	+0.147	+0.192	+0.344	+0.538	+0.630	+0.313	-0.035
15	-0.062	+0.282	+0.618	+0.556	+0.375	+0.220	+0.150	+0.188	+0.336	+0.505	+0.594	+0.313	-0.031
30	-0.125	+0.243	+0.618	+0.500	+0.344	+0.212	+0.132	+0.188	+0.312	+0.500	+0.594	+0.344	0.000
45	-0.182	+0.214	+0.505	+0.469	+0.339	+0.193	+0.130	+0.188	+0.318	+0.505	+0.599	+0.344	+0.027
60	-0.250	+0.188	+0.500	+0.490	+0.360	+0.209	+0.140	+0.209	+0.365	+0.563	+0.588	+0.407	0.000
75	-0.291	+0.183	+0.532	+0.500	+0.370	+0.212	+0.140	+0.219	+0.380	+0.594	+0.714	+0.407	+0.032
90	-0.291	+0.219	+0.588	+0.535	+0.375	+0.209	+0.135	+0.240	+0.435	+0.681	+0.803	+0.469	+0.063
105	-0.250	+0.260	+0.651	+0.585	+0.375	+0.193	+0.135	+0.250	+0.464	+0.743	+0.870	+0.532	+0.063
120	-0.193	+0.308	+0.694	+0.615	+0.380	+0.188	+0.135	+0.250	+0.486	+0.760	+0.930	+0.589	+0.094
135	-0.156	+0.339	+0.722	+0.620	+0.375	+0.204	+0.135	+0.255	+0.510	+0.818	+0.943	+0.563	+0.125
150	-0.093	+0.380	+0.745	+0.620	+0.375	+0.190	+0.151	+0.255	+0.498	+0.752	+0.903	+0.532	+0.063
165	-0.057	+0.349	+0.688	+0.594	+0.375	+0.193	+0.150	+0.250	+0.443	+0.688	+0.813	+0.438	+0.032

NOTES:

- Hemisphere 2B was free-blown from a 2-in.-thick sheet of Plexiglas G to a nominal external radius of 28.0 in.
- Measurements shown are in inches and denote deviations from a nominal 28.0-in. external radius.
- Maximum deviations from the nominal 28.0-in. radius are +0.943 in. at 30-deg elevation, and -0.291 in. at 7-deg elevation.
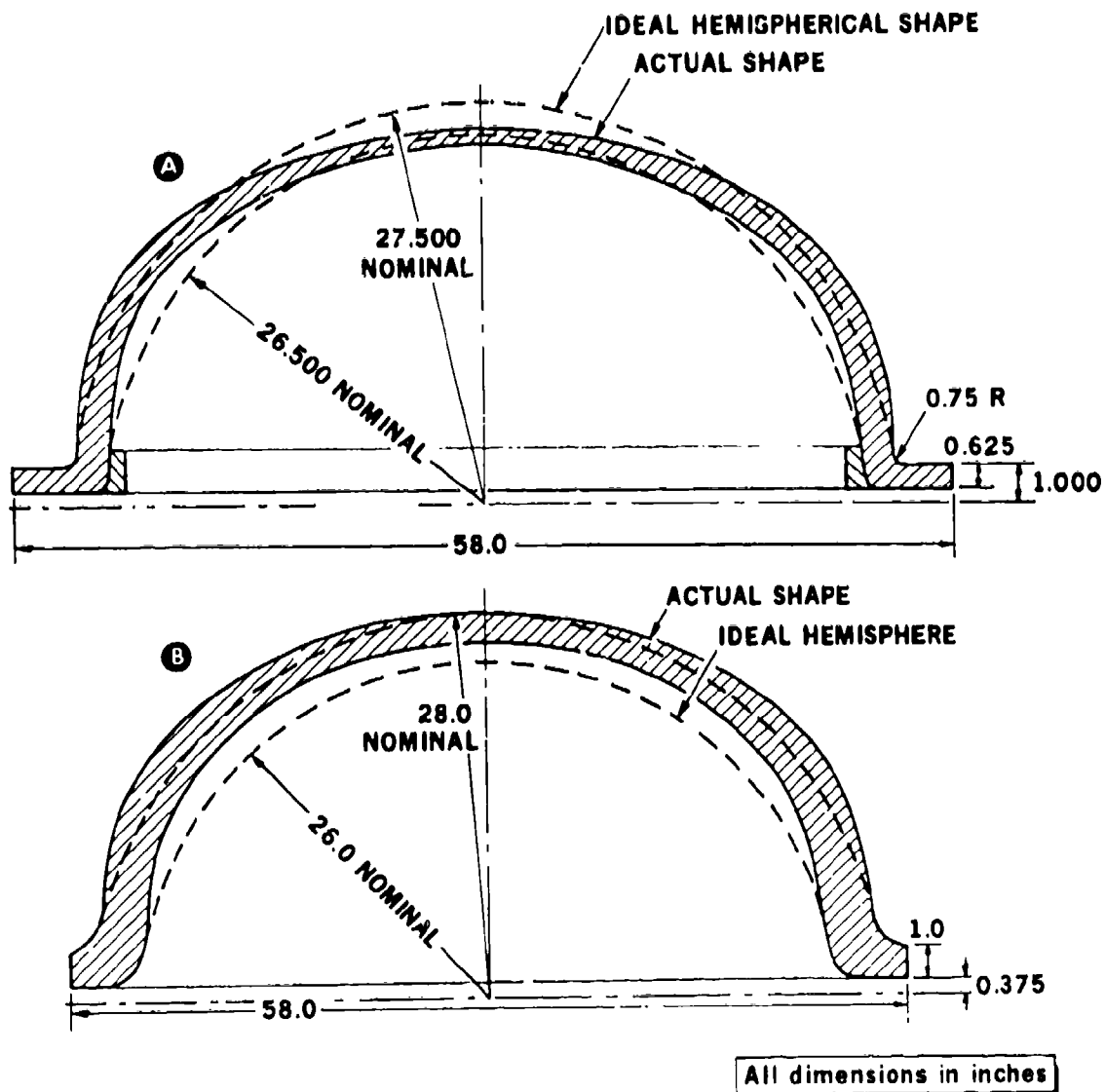
19

Figure 5. Deviations in sphericity observed on the free-formed acrylic plastic hemispheres.

the tests was in this case to determine the stress distribution in the hull, and to compare the stresses with those measured on hemispheres 1A and 1B during a similar pressure cycle.

TEST ARRANGEMENTS

All of the tests were conducted at the pressure test facilities of Southwest Research Institute. Tap water at 70°F served as the pressurizing fluid and was pumped into the pressure vessel with a positive-displacement pump.

The test jig used for evaluation of the hemispheres was the actual (Fig. 6) elevator frame. Several advantages were gained by its use. The major ones were: (1) the measured stresses on the acrylic hemisphere during the test would be indentical to those that the hull would see in service, and (2) the performance of the steel framework would be also evaluated at no additional cost.

The hemispheres were held in place for the test by steel retaining flanges bolted to the elevator frame. Flat neoprene gaskets bonded with contact cement to the acrylic flanges at the equators of the hemispheres acted as seals.

INSTRUMENTATION

The elevator frame assembly with hemispheres mounted on it was instrumented with 22 waterproofed electric-resistance strain gages (Fig. 7). Since the acrylic hull was the critical item under investigation, 16 of the gages were located on it and the balance on the steel frame.

Strain readings were taken with each 25-psi increment in pressure during pressurization, at 60-min intervals during sustained pressure loading at 50 psi, and every 6 hours during relaxation at 0 psi.

DATA REDUCTION

After the testing was completed, the data were reduced by means of a computer program that presented the results in the form of principal strains and stresses. An elasticity modulus (E_t) of 450×10^3 psi and a Poisson's ratio (μ) of 0.35 were used in the conversion of measured strains to stresses on acrylic plastic. For steel $E_t = 30 \times 10^6$ and $\mu = 0.3$ were utilized in data reduction.

OBSERVATIONS

The behavior of capsules under hydrostatic loading was as expected of hemispherical shells with a rigidly restrained equator and a wall thickness that decreased in magnitude with latitudinal distance from the equator. This behavior was characterized by flexure stresses superimposed on compressive membrane stresses (Table 4).

The flexure stresses, as expected, were maximized in the shell near the equatorial flange. This can be readily seen by observing the change in magnitude of meridional stresses as one progresses from the pole of the hemisphere to the heel of the flange. This comparison of meridional stresses shows that at locations remote from the flange, the stresses on the exterior and interior of the shell were approximately equal, whereas near the flange there was a marked dissimilarity between them.

The flexure stresses were greater in hemispheres 2A and 2B than in hemispheres 1A and 1B when compared at the same external hydrostatic loading of 50 psi. Since in both
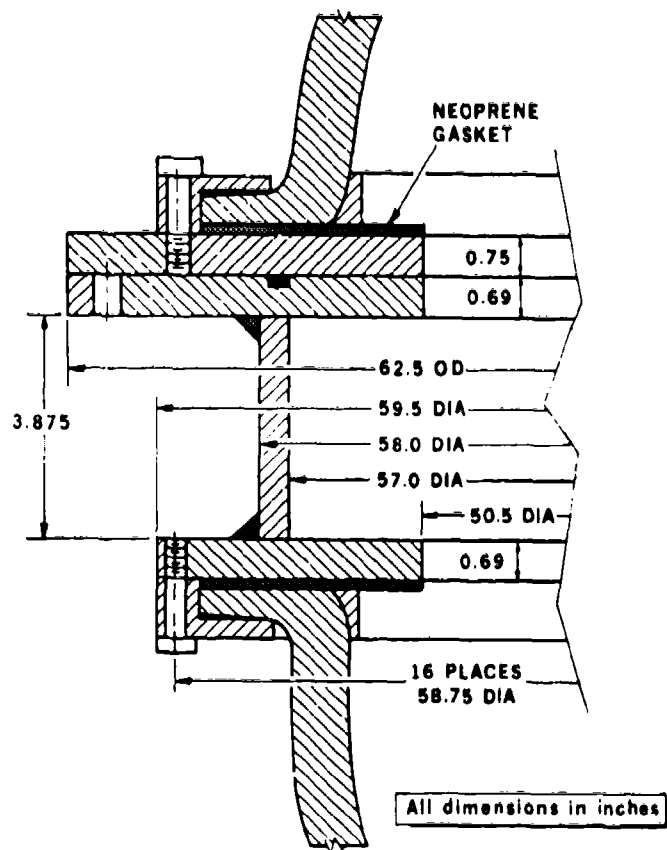
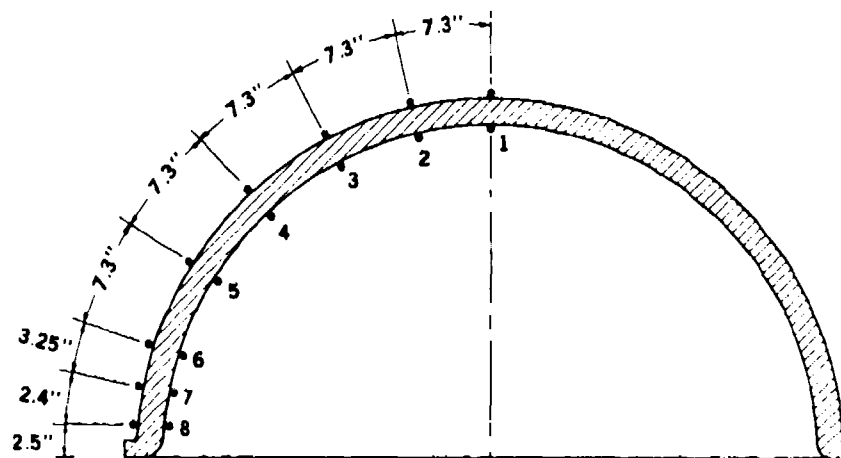Figure 6. Dimensions of the steel equatorial joint for the acrylic plastic hemispheres.

Figure 7. Location of electric-resistance strain gage rosettes on the acrylic hemispheres 1B and 2B prior to hydrostatic testing.

Table 4. Stresses Measured on Hemispheres at 50 psi External Hydrostatic Pressure.

Location	Hemisphere 1B		Hemisphere 2B	
	Meridional Stress (psi)	Circumferential Stress (psi)	Meridional Stress (psi)	Circumferential Stress (psi)
1. Outside	−1577	−1422	−623	−623
Inside	−1408	−1452	−687	−675
2. Outside	−1378	−1367	−668	−624
Inside	−1441	−1420	−692	−692
3. Outside	−1303	−1281	−600	−623
Inside	−1385	−1385	−679	−658
4. Outside	−1220	−1042	−610	−521
Inside	−1153	−1109	−633	−589
5. Outside	−1012	−834	−301	−345
Inside	−812	−779	−695	−573
6. Outside	−812	−779	−671	−760
Inside	−762	−762	−112	−580
7. Outside	−1042	−919	−1277	−1077
Inside	−363	−651	+497	−381
8. Outside	−1398	−909	−2295	−1283
Inside	+140	−371	+1145	+55

NOTE: Location No. 1 is at the pole of the hemisphere, while Location No. 2 is approximately 1 in. above the flange.

cases the flanges and the ratios of wall thickness at the flange to that at the pole were about the same, this increase in flexure stresses can only be explained by the absence of the internal equatorial support ring in hemispheres 2A and 2B. Because of the absence of these support rings, the heels of the external acrylic flanges were not supported, and thus bending moments in the shell at the flange were increased.

The increase in shell thickness near the equator as well as at the equatorial flange imposed a considerable constraint on the shell in the equatorial region. As a result, the magnitude of circumferential stresses as a rule decreased as one progressed from the strain gages at the pole to those near the flange. Because of this, the hemispheres contracted radially in a nonuniform manner under external hydrostatic loading. The contraction was very large at the pole, where the shell thickness was the thinnest and the edge constraint the least.

The unequal contraction of the acrylic hemispheres eventually led to failure of the sphere by elastico-plastic instability, with the center of the dimple located at the pole of the hemisphere. There should be no doubt that this was the failure mode of hemisphere 1B, since the maximum measured stress at the moment of implosion at 147 psi was only −5000 psi. This stress level at the pole was not sufficiently high to cause material failure (Fig. 8).
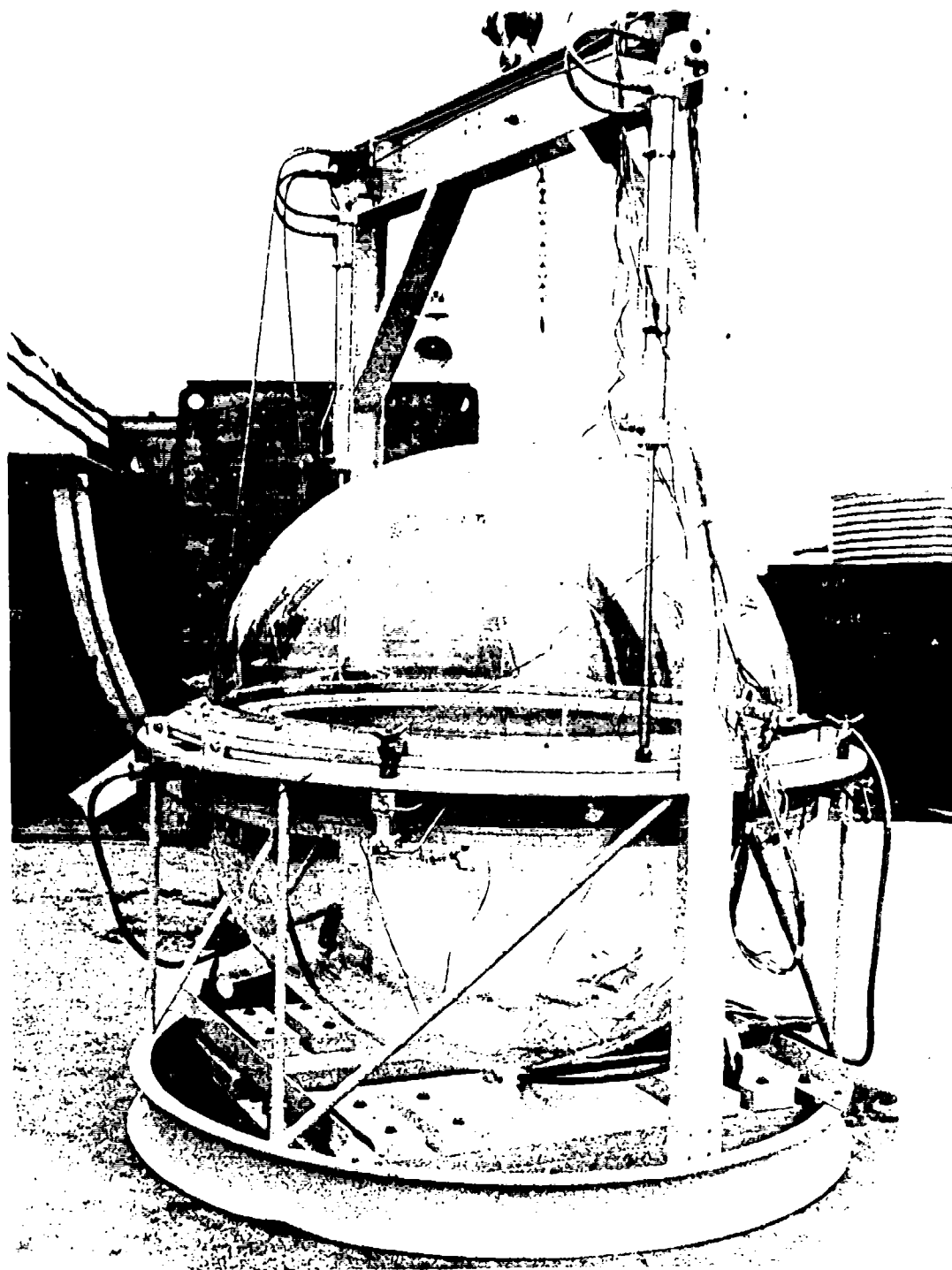
Figure 8a. Acrylic hemisphere 1B after 6-hour pressurization to simulated 112-ft depth.
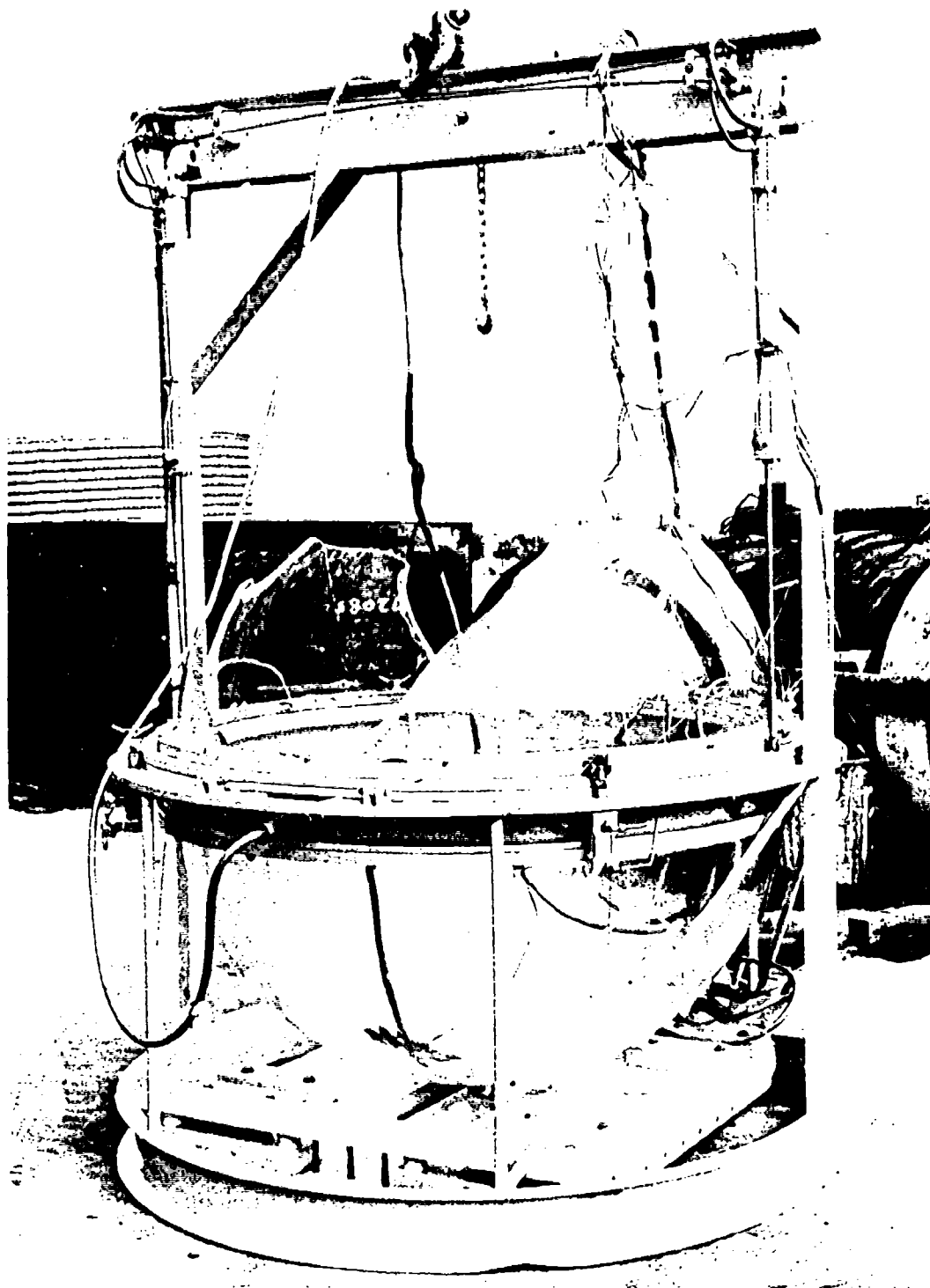
24

Figure 8b. Acrylic hemisphere 1B after short-term pressurization to 330-ft simulated depth.

No leakage was observed in capsules 1 and 2, indicating that the use of contact cement for retention of thick neoprene gaskets under the acrylic flange was satisfactory. No separation between gasket and flange was observed even in the imploded capsule 1.

FINDINGS

ACRYLIC CAPSULE NO. 1 (NOMINAL DIMENSIONS: 27.0 IN. MEDIAN RADIUS AND 1.0 IN. THICK)

Hemispheres 1A and 1B, representing the assumed minimum hull thickness for a 56-ft depth, appeared to be satisfactory for that service. This finding is based on the following observations: Long-term sustained pressure loading of 50 psi (equivalent to a proof-test with 100-percent pressure overload) resulted only in a maximum principal stress of −1577 psi. This principal stress was measured along the meridian on the exterior of the hull at the pole. Maximum tensile stress due to bending was measured at the heel of the flange, and its magnitude was found to be only +140 psi. Creep at all locations on the hull was less than 50 μin for the 6 hours of sustained loading.

The magnitudes of both compressive stress and creep were less than for the Navy-certified NEMO hull. For the NEMO Model 600 hull, the maximum compressive stress on the interior of the shell at 100-percent pressure overload was −3650 psi, and the creep after 6 hours of sustained loading was −300 μin. Since the tensile stress of +140 psi is less than +1500 psi, the proven safe long-term tensile stress for acrylic, it is considered to be acceptable also.

Relaxation of the acrylic hull at 0 psi after 50-psi long-term pressure loading showed a return of all the strains on the acrylic hull to zero. This indicates that even at 100-percent hydrostatic overload, no permanent plastic deformation took place after a 6-hour sustained loading.

Short-term implosion at 147 psi showed that the acrylic hull possesses an apparent safety factor of 6 for an operational depth of 56 ft. The apparent safety factor of 6 compares favorably with the 6 to 7 range of apparent safety factors previously experimentally established as very conservative in the NEMO acrylic hull program.

ACRYLIC CAPSULE NO. 2 (NOMINAL DIMENSIONS: 27.0 IN. MEDIAN RADIUS AND 2.0 IN. THICK)

The acrylic hemispheres 2A and 2B representing the assumed adequate hull thickness for 56-ft depth appeared to be satisfactory for that service. There appeared to be, however, some disadvantages over Sphere No. 1. This finding is based on the following observations: Long-term sustained pressure loading of 50 psi resulted in a maximum principal stress of −2295 psi measured at the instep of the equatorial flange. Tensile stress due to bending was +1145 psi, and it was located at the heel of the equatorial flange. Creep at all locations after a 6-hour sustained loading was less than 50 μin. Since the maximum

26

compressive stress was less than in the NEMO Model 600 hull at 100-percent pressure over-load (−3650 psi) and the tensile stress less than the acceptable safe limit for plastic in tension (+1500 psi), the existing stress levels were found to be acceptable.

Relaxation at 0 psi after the long-term sustained pressure loading at 50 psi showed a return of all the strains to zero. This indicated that no permanent plastic deformation took place in the shell after the long-term loading.

Short-term testing pressurization was not continued to implosion, and because of this there is no experimentally established implosion pressure for Sphere No. 2. A brief review of pertinent parameters, however, seems to indicate that the implosion of this sphere will be caused by material failure at approximately 390 psi, which would provide the very ample apparent safety factor of 16 for a 56-ft operational depth.

The predicted implosion pressure was arrived at by considering independently both the elastico-plastic instability and material failure. When the instability failure was con-sidered, the implosion pressure was predicted to be 620 psi. This prediction was based on the extrapolation of Sphere No. 1 minimum thickness and instability failure pressure (0.431 in. and 147 psi) to Sphere No. 2 thickness (0.887 in.) and utilized the well-established $p_c = K(t/R_0)^2$ instability relationship for spheres. Since the spherical deviations and loca-tion of the thin spots on the hemispheres are about the same for both Sphere No. 1 and Sphere No. 2, the extrapolation of instability failure pressure is reasonably valid.

When material failure was considered, the implosion pressure was predicted to occur at 390 psi. This prediction was based on the linear extrapolation of stresses measured at 50 psi to higher pressure values. The maximum compressive stress of −2295 psi and tensile stress of +1145 psi measured at 50 psi when extrapolated to −18,000 psi and +9000 psi stress values will initiate material failure at 390 psi external hydrostatic loading. Since material failure will produce implosion at a lower pressure than instability, it is con-sidered to be the controlling mode of failure for Sphere No. 2.

COMPARISON OF SPHERE NO. 1 WITH SPHERE NO. 2

Doubling the thickness of Sphere No. 2 should have resulted not only in a fourfold increase in the stability of the shell, but should have also reduced the stresses by approxi-mately 50 percent at the proof-test pressure of 50 psi. This reduction of stresses would have been achieved in Sphere No. 2 if the equatorial acrylic support ring present on the interior of hemispheres 1A and 1B had not been omitted on hemispheres 2A and 2B. Lack of the interior support rings on hemispheres 2A and 2B caused the stresses near the equator to double instead of decreasing by 50 percent. Near the pole, where the influence of the equatorial discontinuity is not felt, the stresses in hemispheres 2A and 2B were as predicted, approximately 50-percent less than in hemispheres 1A and 1B.

Omitting the equatorial support ring at the equator negated to a large degree the decrease of stresses expected from an increase of nominal thickness in a hemisphere. It would thus appear that if the equatorial support ring is to be omitted from the free-formed

hemispheres because of the additional cost that it represents, the hemisphere should be deflanged. In that manner, the excessive bending moments that are created by axial load on the curved heel of the equatorial flange are eliminated.

CONCLUSIONS

Free-formed acrylic hemispheres may be successfully utilized for undersea applications provided the following precautions are taken:

1. The actual thickness at the pole after forming should be used in the instability and material failure calculations. If the actual thickness measurement at the pole is not available, the conservative value of 0.4 times nominal thickness of sheet used in forming can be substituted for it.

2. The apparent safety factor based on experimentally or analytically established short-term critical pressure must be at least 6.

3. The maximum deviation in sphericity and thickness from nominal value should not exceed 2 percent of radius and 60 percent of thickness, respectively.

4. Either equatorial support rings must be bonded to the heel of the flange, or the equatorial flange has to be trimmed away above the curved heel prior to mating the hemispheres with the equatorial support structure.

28

REFERENCES

1. Stachiw, J. D. "Spherical Acrylic Pressure Hulls for Undersea Exploration," *Trans. ASME/Journal of Engineering for Industry*, Series B, No. 2, Vol. 93, May 1971.

2. Snoey, M. R., and E. M. Briggs. "The NEMO Submersible," ASME paper 70-Unt-C, 1970.

3. Kelsey, R. A. "The Johnson-Sea-Link, the First Deep Diving Welded Aluminum Submersible," ASME paper 70-WA/Unt-6, 1970.

4. Stachiw, J. D. *Window in the Sea*, Smithsonian Institution Press, Washington, D.C., 1971.

5. Rohm and Haas Co. Handbook. "Plexiglas Design and Fabrication Data," 1971.

6. Stachiw, J. D. "Critical Pressure of Spherical Shell Acrylic Windows Under Short-Term Pressure Loading," *Trans. ASME/Journal of Engineering for Industry*, Series B, No. 3, Vol. 91, August 1969.

DOCUMENT CONTROL DATA - R & D

(Security classification of title, body of abstract and indexing annotation must be entered when the overall report is classified)

1. ORIGINATING ACTIVITY (Corporate author)	2a. REPORT SECURITY CLASSIFICATION
Naval Undersea Center San Diego, Calif. 92132	UNCLASSIFIED
	2b. GROUP

3. REPORT TITLE

ACRYLIC PLASTIC HEMISPHERICAL SHELLS FOR NUC UNDERSEA ELEVATOR

4. DESCRIPTIVE NOTES (Type of report and inclusive dates)

Research report—1971-72

5. AUTHOR(S) (First name, middle initial, last name)

J. D. Stachiw

6. REPORT DATE	7a. TOTAL NO. OF PAGES	7b. NO. OF REFS
September 1972	34	6

8a. CONTRACT OR GRANT NO	9a. ORIGINATOR'S REPORT NUMBER(S)
b. PROJECT NO. ZFXX-412-001 Task Area Number 00000-0-05530 Work Unit Number	NUC TP 315
c.	9b. OTHER REPORT NO(S) (Any other numbers that may be assigned this report)
d.	

10. DISTRIBUTION STATEMENT

Distribution of this document is unlimited.

11. SUPPLEMENTARY NOTES	12. SPONSORING MILITARY ACTIVITY
	Naval Undersea Center San Diego, Calif. 92132

13. ABSTRACT

Free-formed, flanged, acrylic hemispherical shells with a nominal 27-in. median radius have been experimentally evaluated for service as external pressure hulls with a nominal 56-ft depth. Because the free-forming fabrication technique produces hemispheres with significant variation in thickness and sphericity, uneven stress distribution results during external hydrostatic loading. As a result, extreme care must be exercised when utilizing free-formed acrylic hemispheres because their elastic instability pressure and magnitude of stresses cannot be predicted on the basis of equations for ideal acrylic spheres. Using an experimental approach to the evaluation of 54-in.-median-diameter hemispheres, it was found that nominally 1-in.-thick acrylic plate stock is adequately thick for free-forming of shells that will be utilized as pressure hulls for an operational depth of 56 ft

14 KEY WORDS	LINK A		LINK B		LINK C	
	ROLE	WT	ROLE	WT	ROLE	WT
Submersibles						
Pressure hull						
Plastic						
Panoramic visibility						
Undersea elevator						

CAST ACRYLIC PLASTIC DOME FOR UNDERSEA APPLICATIONS

by

Jerry D. Stachiw
Ocean Technology Department
January 1974

ADMINISTRATIVE STATEMENT

ACKNOWLEDGEMENT

Released by
H. R. TALKINGTON, Head
Ocean Technology Department

ii

SUMMARY

PROBLEM

Large, acrylic plastic domes for deep submergence applications have been built primarily by bonding small, thermoformed structural modules. Tne large amount of hand labor required by this approach makes such domes relatively expensive.

RESULTS

A casting technique utilizing a glass fiber-reinforced plastic mold system composed of male and female molds filled with monomer/polymer casting syrup has been shown to be capable of producing massive domes of at least 78-inch diameter and 6.375-inch thickness with significant saving in labor over domes built by bonding small structural modules. The dimensional deviations of massive domes cast by this technique are higher than those of machined massive modular dornes but less than those of thin domes free-formed by compressed air.

RECOMMENDATIONS

The casting of massive acrylic plastic domes in glass fiber-reinforced plastic molds should be considered as an economically attractive technique for production of massive domes for deep submergence application.

CONTENTS

INTRODUCTION

Many ocean engineering systems require transparent structural components that serve as windows. Since the size of the window directly influences the field of view that the window provides, a premium is placed on size. However, large sizes require that windows be quite thick.

Thick, plane, acrylic plastic windows can be readily manufactured either by laminating many thin sheets or by casting massive blocks. In either case the technology is well developed and plane, acrylic plastic windows of almost any thickness and size can be obtained from industrial suppliers on a fixed-price basis. Still, plane windows are not as much in demand as are spherical shell windows, whose shape makes them structurally superior (references 1-10).

Unfortunately, the technology for the fabrication of spherical shell windows is not so advanced as is that for plane windows. Thin windows can be readily fabricated by blowing with compressed air, with or without a mold, but the resulting hemispheres are of varying thickness and must be limited in their operation to shallow depths. Thick windows have been fabricated only (1) by laminating many thin, blown shells; (2) by hogging-out massive castings; or (3) by assembling and bonding many small structural segments. Of these three approaches, the laminating produces shells of varying thickness, while the hogging-out is prohibitively expensive. Only the bonding of small, identical segment assemblies has produced thick, spherical shell windows of uniform thickness at a tolerable price. It was this technique which was used to fabricate spherical hulls for the NEMO, MAKAKAI, and JOHNSON SEA LINK deep submergence vehicles. Bonding left a lot to be desired in terms of cost, because it entailed an inordinate amount of hand labor. Obviously, another technique was needed that would require significantly less hand labor while producing thick, spherical windows with acceptable dimensional tolerances.

A fabrication technique which seemed promising was the casting of monolithic hemispheres. It was thought that if problems of excessive shrinkage, cracking and generation of bubbles during the polymerization process could be surmounted without excessive investment in tooling, this process would permit the production of inexpensive, spherical, acrylic plastic windows of large size.

Realizing the potential savings if an inexpensive casting technique could be developed, the Naval Undersea Center initiated studies of two casting techniques. The first would minimize the cost of tooling in exchange for allowing (1) large dimensional tolerances in the sphericity, diameter and thickness of the casting and (2) a large amount of hand labor for polishing of the cast surfaces. The second would (1) minimize the amount of hand labor for polishing and (2) keep the thickness, sphericity and radius within tight dimensional tolerances, but would require expensive tooling. This paper describes the first study.

1

DISCUSSION

DESIGN OF DOME

The objective of the casting technique study was the fabrication of an acrylic plastic hemisphere with a nominal 78-inch outer diameter, 65.25-inch inner diameter and 7-inch cylindrical skirt. This dome was dimensioned to serve as an undersea observation chamber for the small waterplane area hull vehicle SSP KAIMALINO. Since the observation chamber was to be mounted only approximately 12 feet underwater, the hydrostatic pressure was not of sufficient magnitude to control the structural design of the dome.

Instead, the thickness of the dome was chosen on the basis of the dynamic impact to which the hull could be subjected when accidentally striking a water-logged floating log. The 6.375-inch thickness chosen for the dome represented a good compromise as it gave the dome a reasonable impact resistance (roughly equivalent to that of 0.375-inch mild steel) while at the same time keeping its weight and cost at an acceptable level.

An additional benefit of such a thick wall was that the dome could also serve as a panoramic window for submersibles and ocean bottom habitats operating to a depth of 1,000 feet. In this manner, once the tooling was fabricated for casting of the dome, the output of the tooling would not be limited to impact-resistant transparent bows for surface ships, but also would provide relatively inexpensive observation cupolas for submersibles and undersea habitats.

ATTACHMENT FOR THE DOME

Besides operational parameters like hydrostatic pressure and dynamic impact, the method of attaching the 3,000-pound acrylic casting to the metallic hull of the SSP KAIMA-LINO had to be considered. The pitching of the hull in rough water, depending on its amplitude and frequency, could subject the acrylic casting to gravitational forces in excess of 10,000 pounds. Forces of such magnitude and the presence of seawater eliminated adhesives from the consideration for attachments.

Several mechanical attachment systems were considered before settling on the chosen design. Those that were considered, but ultimately rejected, were attachments that required either straps or retaining bars pressing against the convex surface of the dome and thus restricting the panoramic view from inside the dome. The design finally chosen relied on mechanical fastening like those rejected, but because of its layout did not obstruct in any manner the view from inside the dome.

The basic features of the attachment chosen for fabrication (figures 1 and 2)* are these:

1. A metallic, U-shaped flange restrains the dome against vertical static and dynamic forces and provides the foundation to which the metallic hull of the vehicle and the split ring of the dome attachment are fastened. The dome fits into the flange rather loosely

*The figures and table 1 are grouped at the end of the text.

2

(approximately 0.125-inch clearance between the surfaces of the dome and interior of the flange) to allow room for (a) thermal expansion and contraction of the dome under typical conditions and (b) contraction of the dome under hydrostatic loading encountered at 12 feet.

2. A metallic split-ring restrains the dome against static and dynamic horizontal forces. The split ring fits rather snugly against the inner surface of the flange but rather loosely (approximately 0.125-inch clearance) against the acrylic surface. Because of this arrangement, the split ring can be fastened quite securely with bolts to the flange while still allowing for limited radial and axial displacement of the dome due to thermal expansion and hydrostatic loading.

3. An elastomeric filler (silicone rubber) between the acrylic dome and the metallic components of the attachment serves both as a seal against water and as a compliant cushion preventing high stress concentrations at point contacts.

4. A cylindrical skirt on the dome mates with the metallic components of the attachment. To fit properly with the mating metallic parts of the attachment all surfaces of the skirt have been machined to close tolerances. This was necessary as the casting process chosen would not produce surfaces on the skirt to the desired close tolerances.

CASTING TECHNIQUE

The casting technique chosen* required that (1) a mix of acrylic monomer resin and polymer granules be placed into (2) glass-fiber reinforced epoxy molds that were subsequently subjected to (3) elevated temperature and pressure inside an autoclave. Since acrylic spherical castings of such magnitude had never been cast before and a very distinct possibility existed that the first attempt would be an expensive failure, a scale model of 24 inches outside diameter and 2 inches wall thickness was cast first. When this casting was successful it was decided to proceed with the full scale 78-inch-diameter casting.

The distinctive feature of the casting arrangement chosen was the use of a sprue located at the apex of the dome to concentrate all gas bubbles in a part of the casting that would be subsequently cut off without decreasing the size of the finished dome. An alternative approach to removal of the gas bubbles from the casting would be to place the molds upright and to pour the casting mix between the male and female molds. In this arrangement the bubbles would rise and concentrate in the base of the cylindrical skirt. After polymerization several inches of the skirt base containing the bubbles would be machined off, leaving behind a bubble-free casting.

The basic reason for not choosing the alternative casting arrangement was the 7-inch length of the skirt required to attach the finished dome to the vehicle hull. If bubbles were to be concentrated in the base of the skirt, an additional 3 to 5 inches of skirt length would have to be added to the rough casting. The resulting 10- to 12-inch cylindrical skirt probably would make the removal of the male mold very difficult as the casting mix shrinks approximately 8 to 10 percent upon polymerization and would grip the cylindrical portion of the mold quite securely.

---

*The casting process is a proprietary development of Cadillac Plastics and Chemical Company of Kalamazoo, Michigan.

MACHINING OF DOME

The successfully cast dome (figures 3 and 4) contained gas bubbles only in the upper 5 inches of the sprue; the dome casting proper was virtually bubble-free. The first operation was to machine the sprue flat so that it would serve subsequently as the base for the dome during machining of the skirt surfaces (figure 5) in a vertical mill. Next, the sprue was completely removed and the exterior surface was sanded (figure 6). Material test samples were also cut from the sprue and used to test the mechanical properties of the casting (figure 7, table 1). Finally, the interior surface of the dome was sanded and all surfaces were polished (figure 8). The completed dome was then carefully inspected (figure 9) and its dimensions recorded.

FABRICATION OF ATTACHMENT

The U-shaped flange was fabricated by rolling and welding strips of mild steel. The rough U-channel structure was machined to final shape on the same vertical mill (figure 10) that was used for machining of the cast dome. Bolt holes for fastening of the flange to the hull and for attachment of the split ring to the flange were drilled with a portable drill held in a magnetic clamp fixture.

The split ring was fabricated by rolling, welding and rough grinding of mild steel strip. The ring (figure 11) was cut with a hacksaw in one place just prior to mating of the attachment components to the dome.

MATING OF ATTACHMENT TO THE DOME

The first step in mating of the attachment to the dome consisted of plugging the holes in the U-shaped flange so that the liquid elastomer would not leak out prior to its polymerization (figure 12). The holes in the base were covered with 0.25-inch-thick neoprene patches that not only covered the bolt holes but also served as spacers between the dome and the bottom of the U-shaped flange. Without the presence of the neoprene spacers the heavy dome would displace the liquid elastomer completely and the base of the skirt would bottom against the steel surface.

The second step in the mating procedure was to compress and insert the split ring into the machined groove in the casting skirt (figure 13). Now the dome was ready for mating with the U-shaped flange.

The third step was filling of the U-shaped flange with the elastomeric compound (Dow Corning Two-Part Room Temperature Polymerizing 3110RTV Compound) and immediately lowering the dome into the flange until the skirt bottomed on the neoprene spacers and the surplus elastomer was squeezed out (figure 14).

The fourth and final step of the mating procedure after the elastomer solidified was to draw up the split ring against the U-shaped flange with the help of radially oriented bolts. Removal of the extruded elastomer and external dome lifting clamp completed the mating of the attachment to the dome.

OBSERVATIONS

The mechanical properties of the acrylic plastic casting described in this paper differ significantly from those of acrylic sheets and plates (Plexiglas G, Acrylite, Swedlow 310) cast solely from monomer resin (table 1). A general statement can be made that the cast acrylic in the dome has lower tensile, flexural and compressive strength; lower modulus of elasticity; and higher creep than typical cast acrylic sheets and plates. This is typical of acrylic plastic castings formed by polymerization of a mixture containing both the monomer resin and polymer granules. The lower mechanical properties of such castings must be taken into account in the calculation of allowable working stresses for structures fabricated from them. This is particularly true when the design of cast spherical domes or sectors is based on empirical data generated previously by the destructive testing of scale models of spherical windows machined from thick Plexiglas plates that have higher mechanical properties than the full scale cast spherical dome.

Dimensions of the rough dome casting deviated noticeably from specified nominal dimensions (figure 9). The deviations were not serious enough to hamper the dome's use as a transparent bow on a surface ship but they would place serious restrictions on its operational depth as a potential panoramic window for submersibles. The most serious deviation from specified nominal dimensions occurred near the apex, where there was a visually noticeable thinning out of the dome shell around the circumference of the sprue base. This was caused by the difference in shrinkage between the 6.375-inch-thick dome and the 20-inch-diameter sprue during the polymerization process. If the outer surface of the dome had been machined to eliminate any optical distortion in the dome by smoothing out the shrinkage valley, the thickness at the apex of the dome would have decreased from the specified 6.375 inches to 5.0 inches.

This observation suggests that to produce domes with only minor thickness variations using this technique it is necessary to either (1) modify the existing molds at the intersection between the sprue pipe and the female mold so that when the shrinkage takes place the thickness of the shell at the base of the sprue pipe does not decrease below the specified nominal thickness, or (2) remove the sprue pipe, patch the sprue pipe opening, invert the molds, increase their skirt length and pour the casting mix into the annular space between male and female molds. Of these two modifications to the existing molds, the former is the more economical and, besides, attempting to remove a dome casting with increased skirt length from an inverted mold might meet with failure.

Quality of the casting was very high except for some minor imperfections on the exterior surfaces. These imperfections were caused by putting too thick a layer of mold-release agent on the interior surfaces of the glass fiber-reinforced molds; this formed ridges and drops in some places on the mold which were subsequently faithfully reproduced in the acrylic casting. In general it appears that the rough surface finish of the molds, coupled with uneven application of the mold release agent, required an extensive amount of hand labor for sanding and polishing of surfaces on the dome.

FINDINGS

1. Molds made of plastic reinforced with glass fibers present an economical approach to tooling for the production of large, spherical shell acrylic castings providing that the permissible tolerances on thickness, diameter and sphericity are at least ±0.250 inches. To achieve tighter dimensional tolerances than ±0.250 inches the dome casting must be made slightly oversize and subsequently machined down to the desired size.

2. The quality and mechanical properties of the acrylic plastic dome cast n glass-reinforced plastic molds by Cadillac Plastic is acceptable for hydrospace applications providing that the lower mechani al properties of the casting as compared to properties of commercially availatle cast acrylic plate are taken into account.

3. The design developed for the attachment of a hemispherical acrylic plastic dome to the metallic hull of a ship has been found to be economical to fabricate and easy to assemble with the dome.

CONCLUSIONS

It is feasible to cast very large acrylic plastic domes that do not require any subsequent machining on the viewing surfaces at a reasonable investment in tooling and hand labor for polishing providing that one can accept deviations from nominal dimensions which exceed those customarily associated with machined domes but are significantly less than those associated with vacuum- or pressure-formed domes from flat acrylic sheets.

RECOMMENDATIONS

It is recommended that the casting technique described in this report be utilized for those hydrospace applications where (1) only one or two very large, thick acrylic plastic domes of the same size are required and (2) the hydrostatic loading of the dome will be of such magnitude that the dimensional tolerances of ±0.250 inch on the thickness, diameter and sphericity can be readily accepted. If the casting technique is used for the applications enumerated above it will provide the hydrospace engineer with very large domes at a rock bottom price.

6

SECTION

DETAIL A

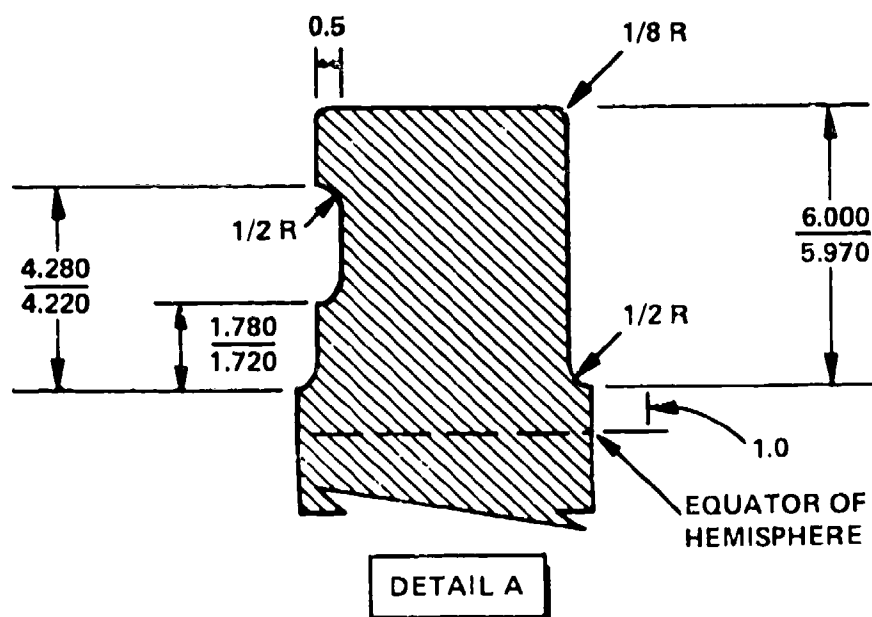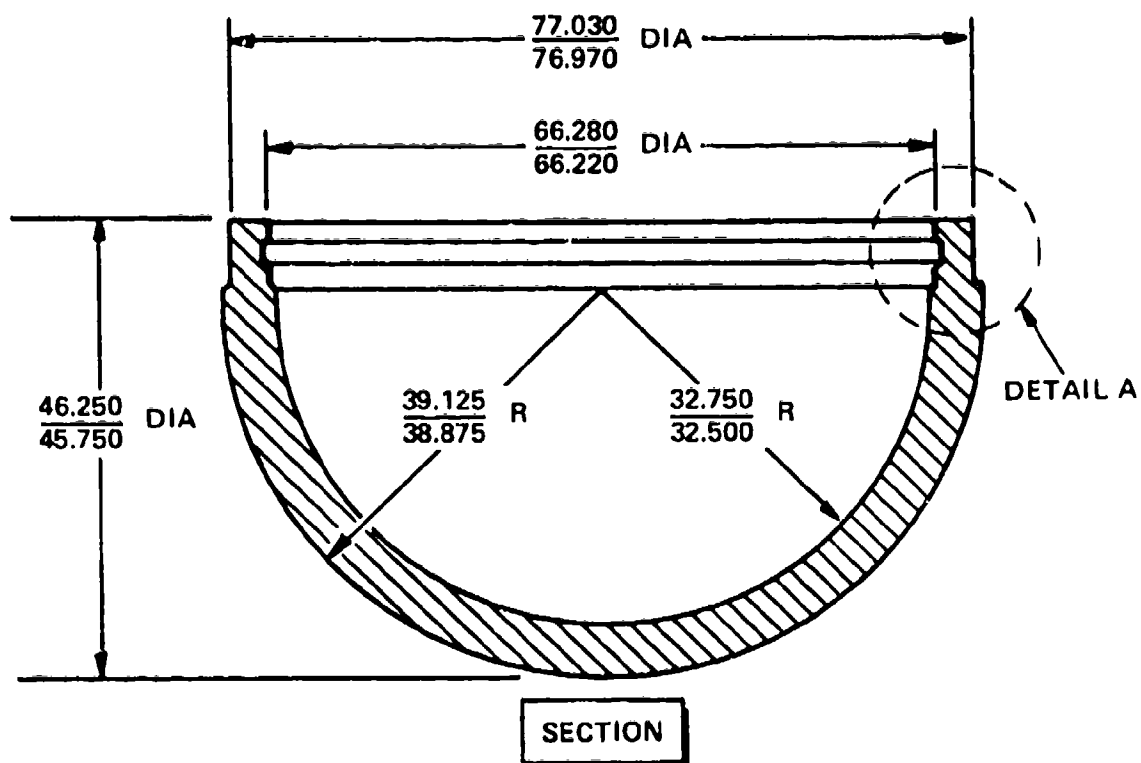Figure 1. Dimensions specified for the finished acrylic plastic dome casting.
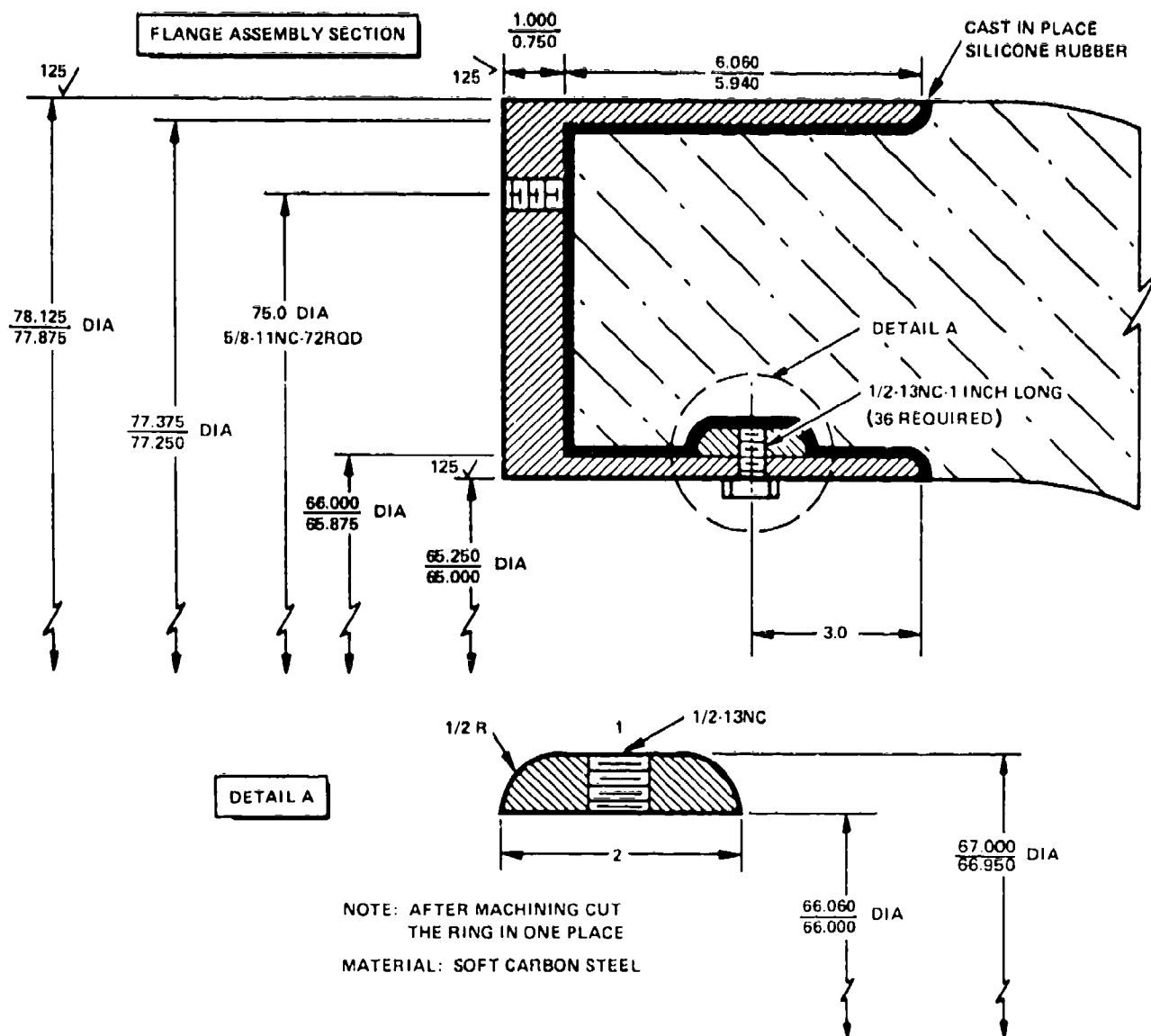
Figure 2. Attachment for fastening the acrylic plastic dome to vehicle hull.

8
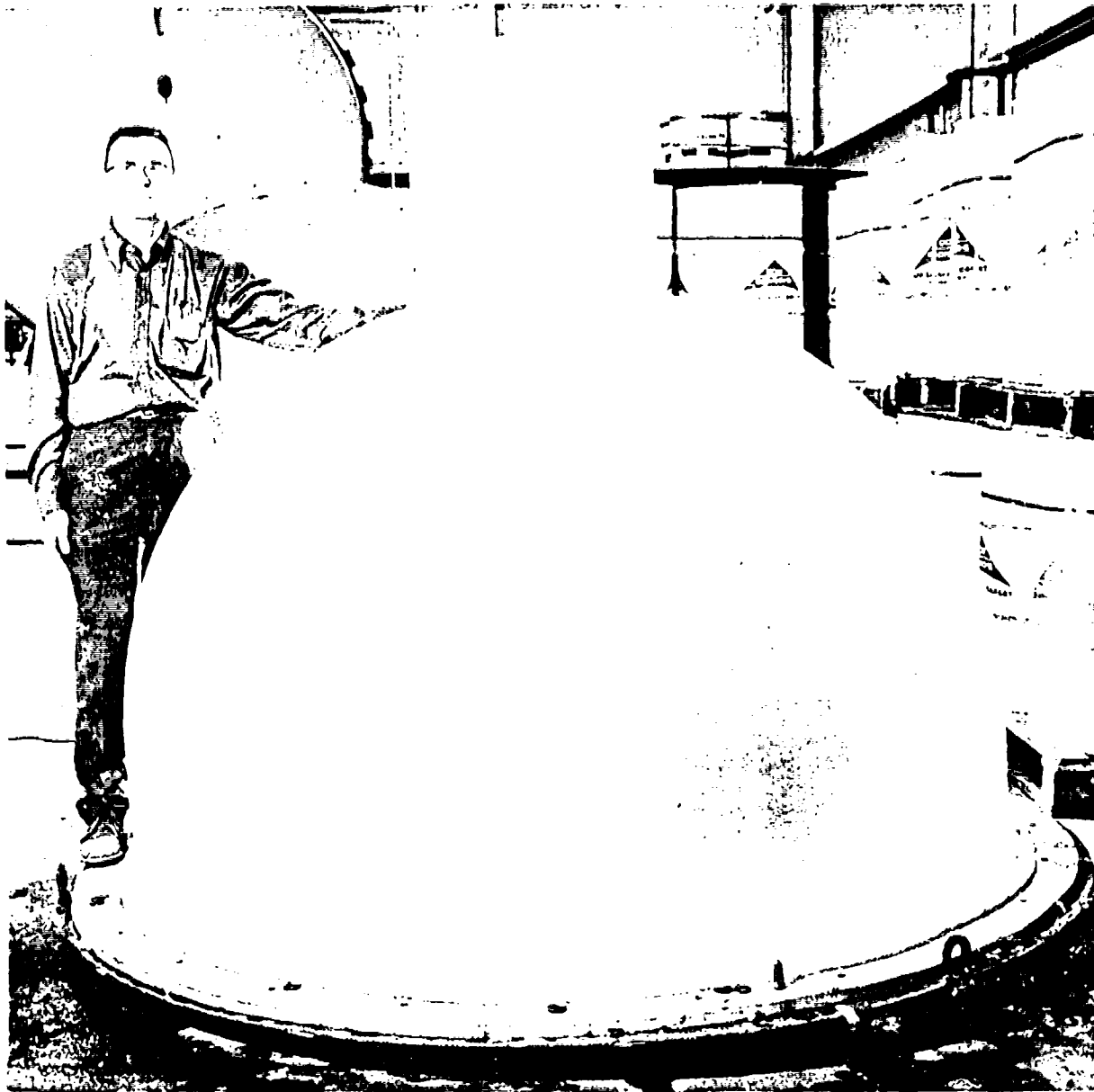
Figure 3. Rough casting of the dome after removal from the molds.
Note the big sprue at the apex of the dome.

9
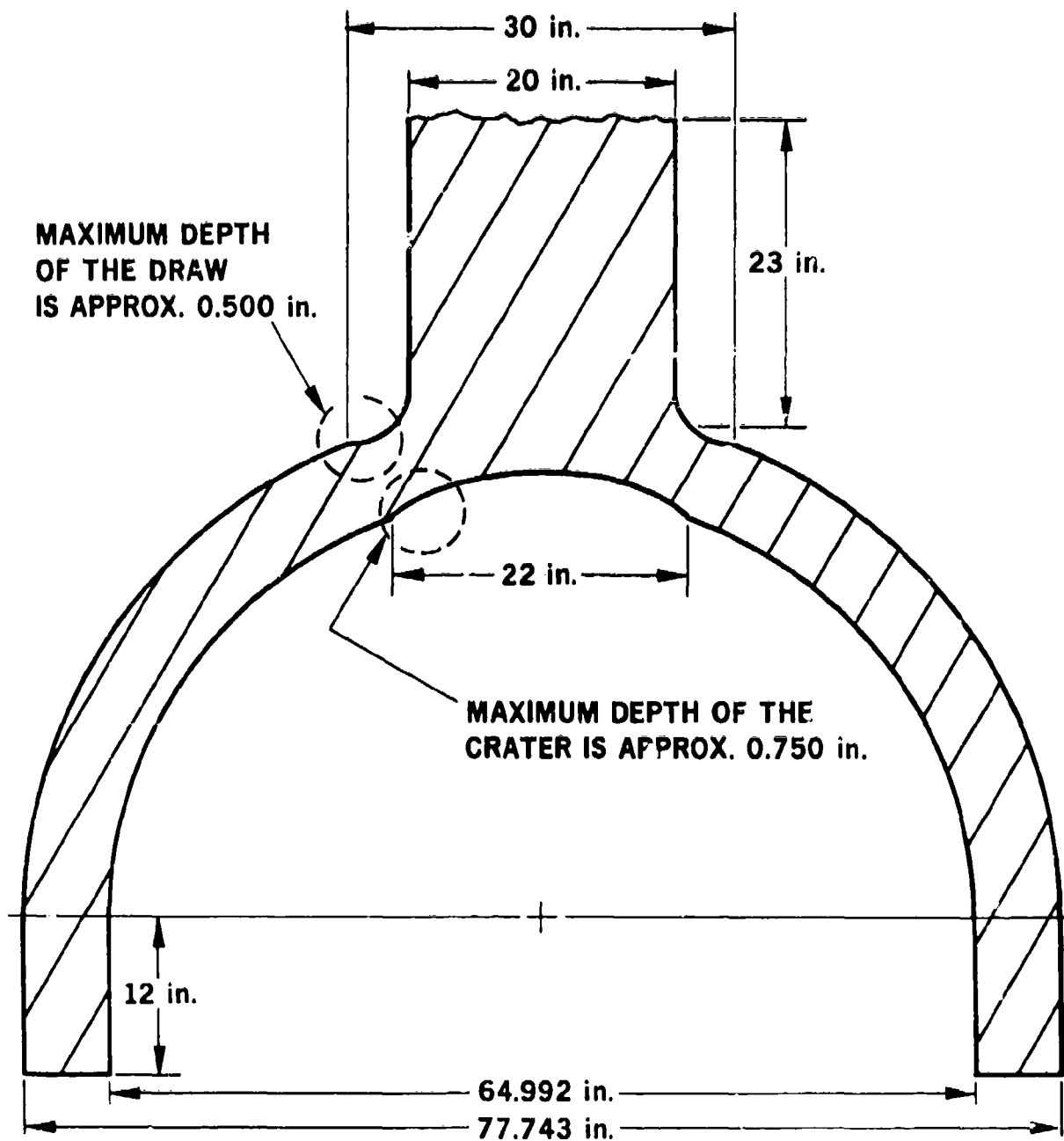
Figure 4. Dimensions of the dome casting prior to machining.
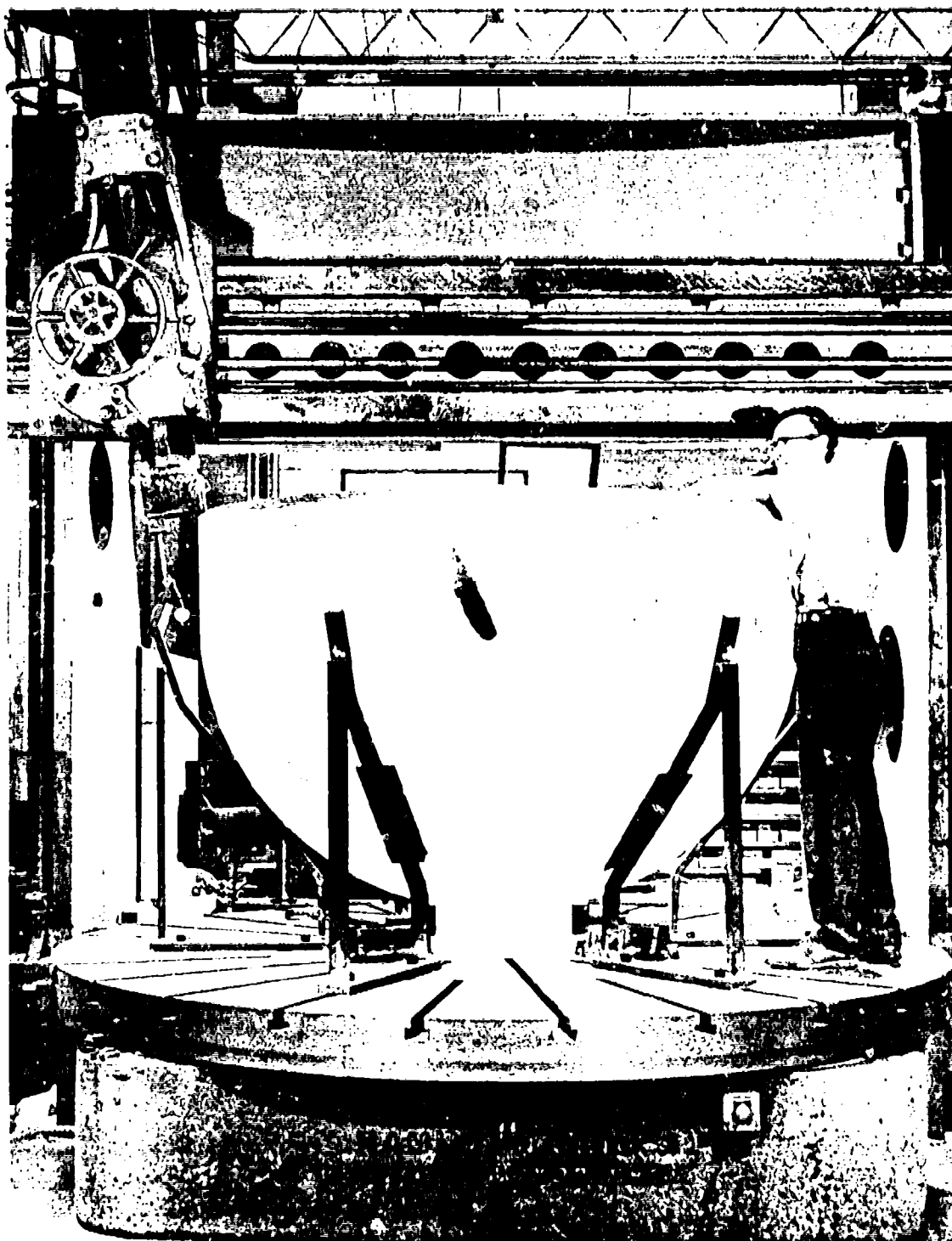
Figure 5. Machining the skirt on the dome.
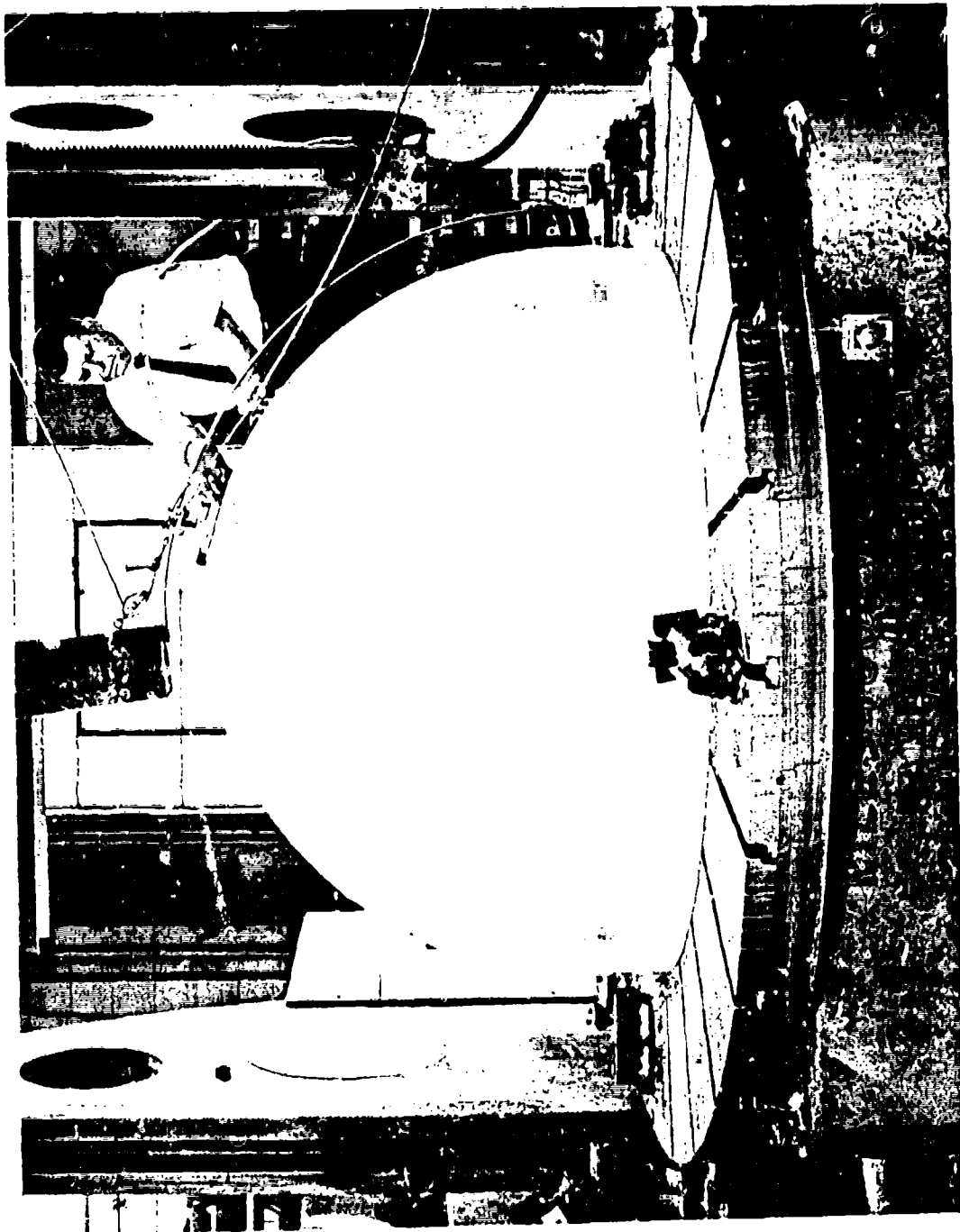
Figure 6. Machining off the sprue on the dome.
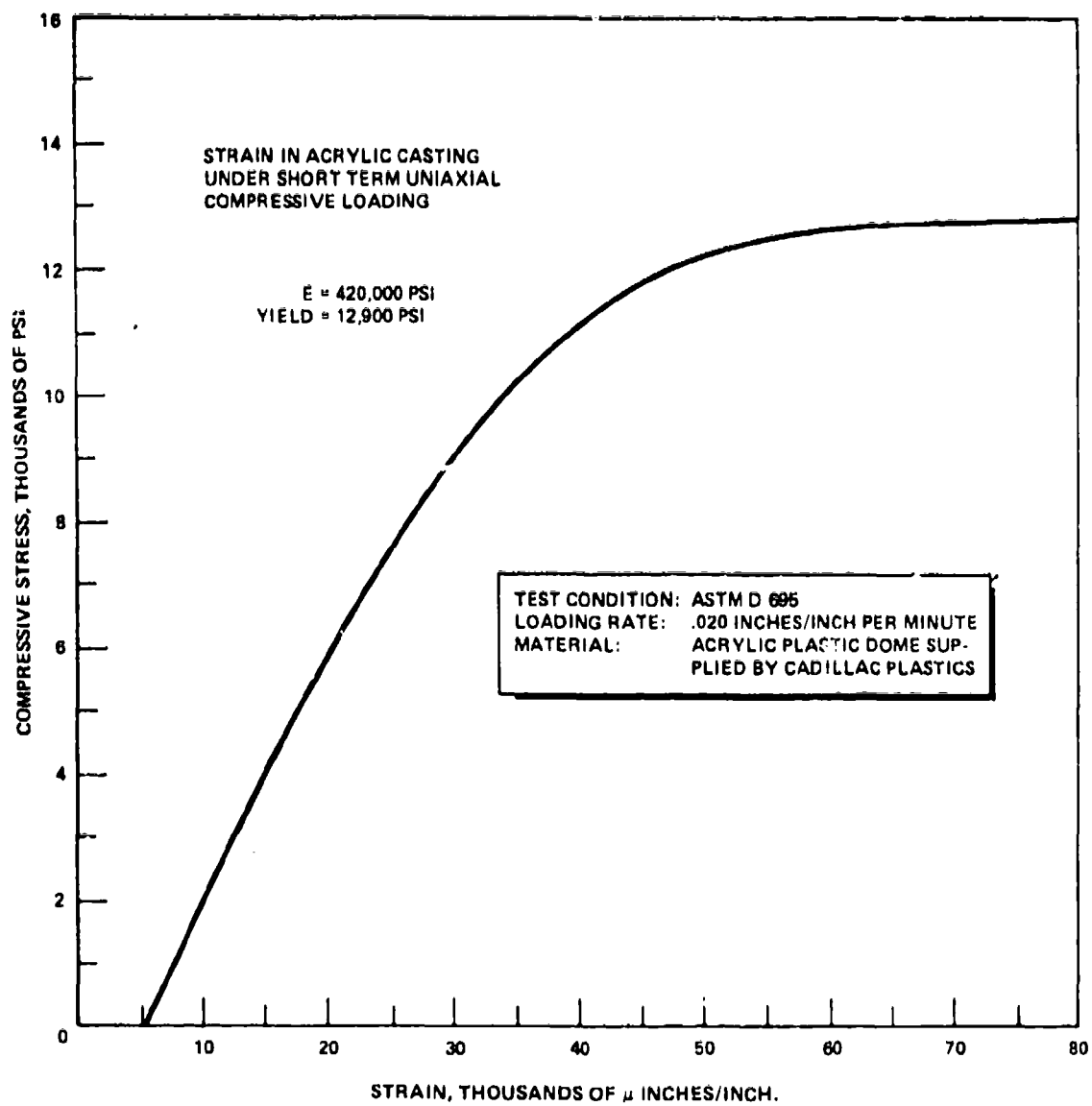
Figure 7. The stress-strain relationship of a material test specimen under uniaxial compressive loading; the test specimen was cut from the sprue adjacent to the dome.

Figure 8. Polishing of the dome with power-driven buffing wheel.

14
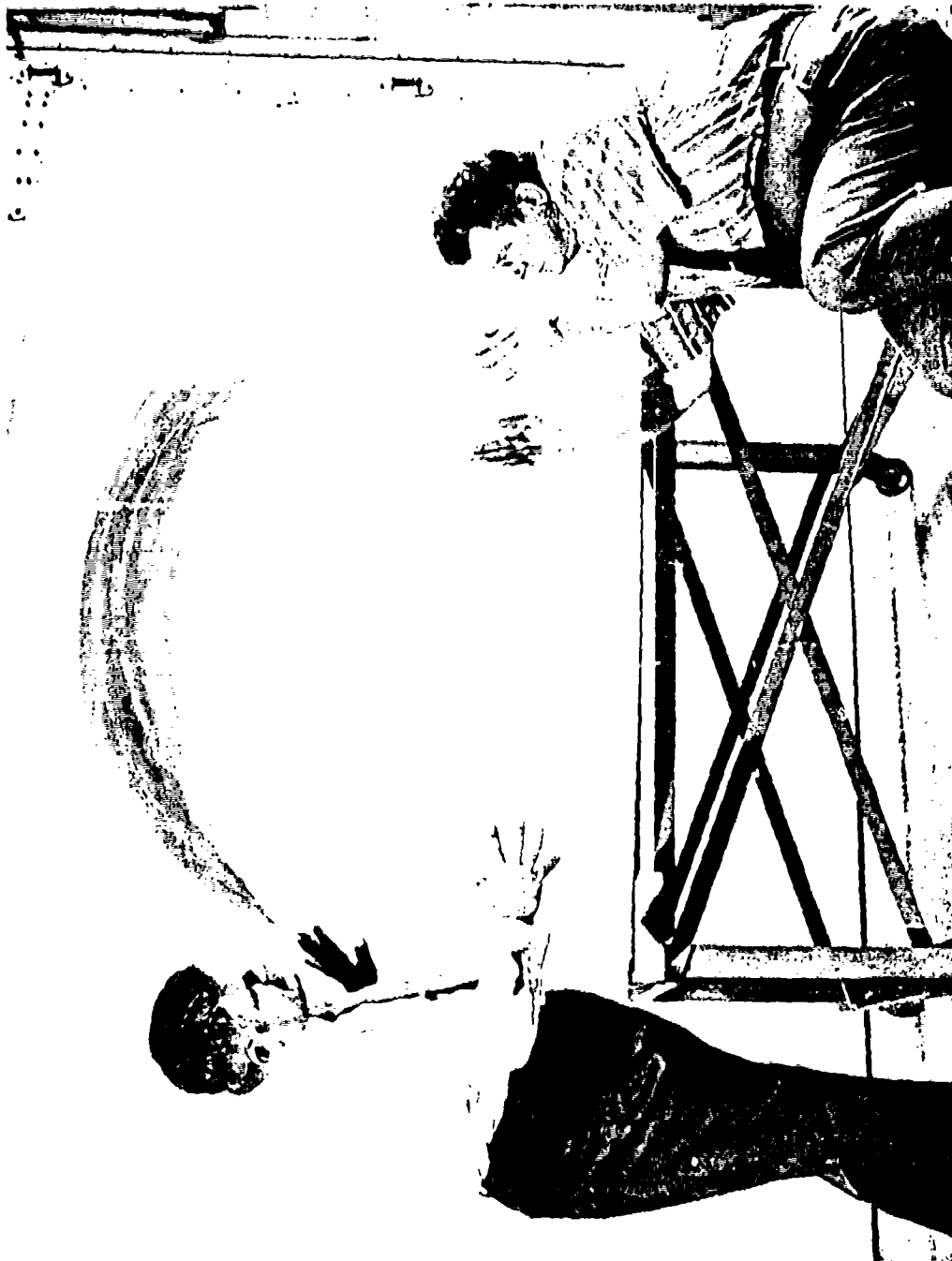
Figure 9. The finished acrylic plastic dome is inspected by Dr. J. D. Stachiw, acrylic plastic structure expert at NUC, and Mr. A. Nichols, casting specialist at Cadillac Plastic.
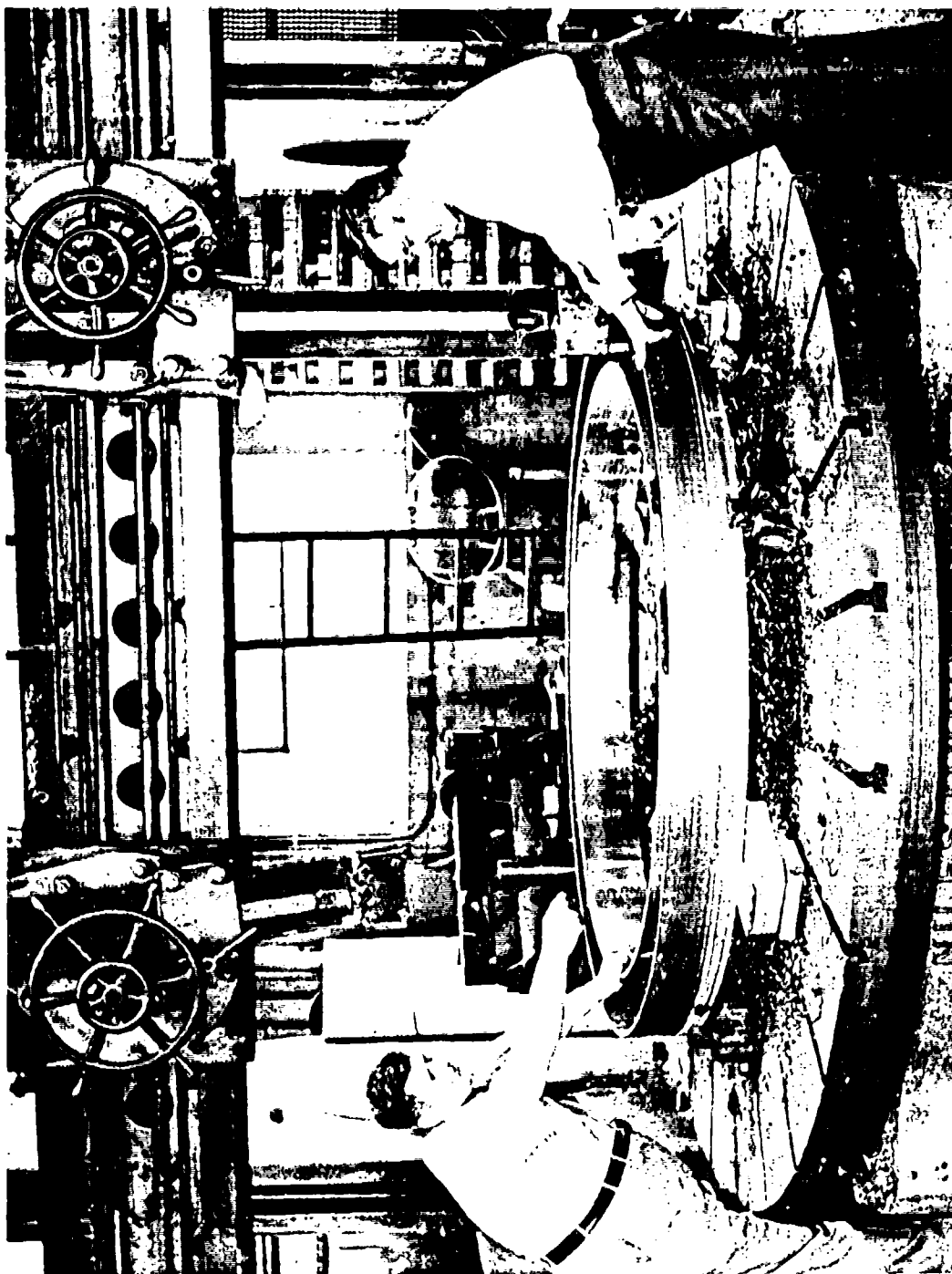
Figure 10. Machining of the U-shaped flange.

16
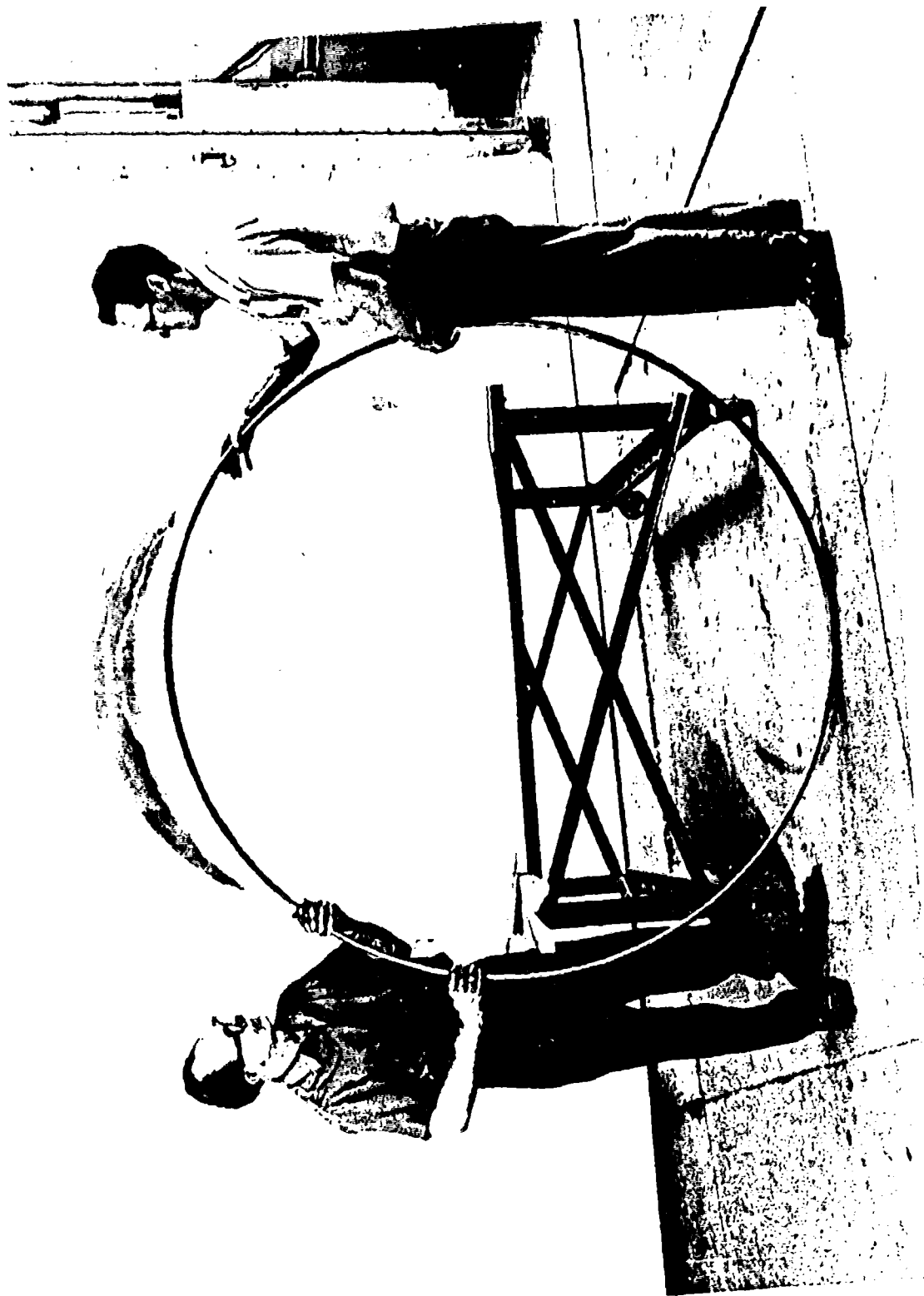
Figure 11. Finished split ring that locks the dome's skirt in the U-shaped flange.
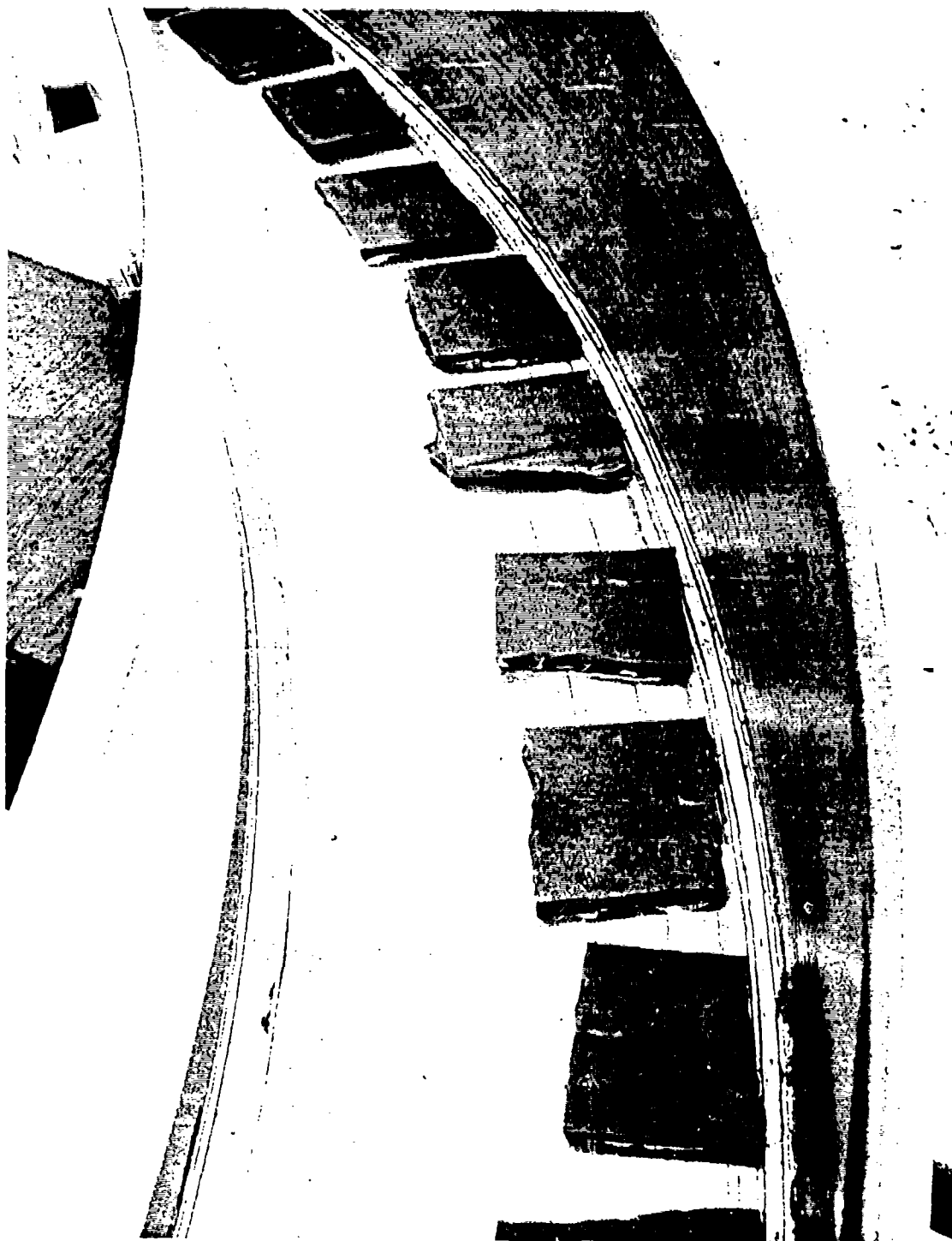
Figure 12. U-shaped flange just prior to pouring of the elastomeric sealant. Note the stoppers plugging the radial bolt holes in the left side of the flange and the neoprene bearing pads covering the axial bolt holes in its bottom.
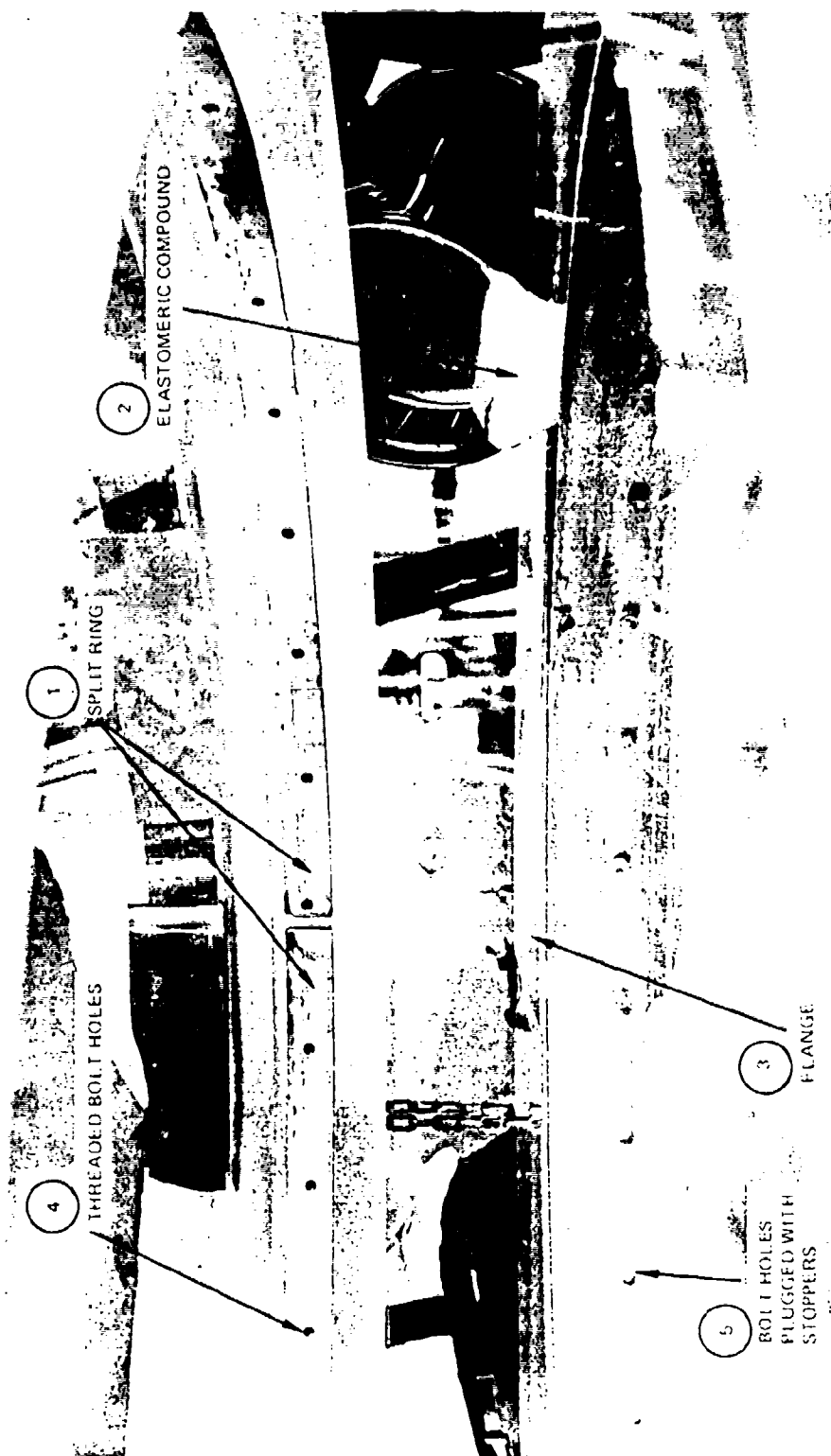
Figure 13. Mating the dome to the U-shaped flange. The split ring[1] is already resting in the groove machined for it in the dome skirt and the elastomeric compound[2] is being poured into the U-shaped flange[3] prior to insertion of the skirt into the flange. Note the threaded bolt holes[4] in the split ring and the stoppered bolt holes[5] in the flange.
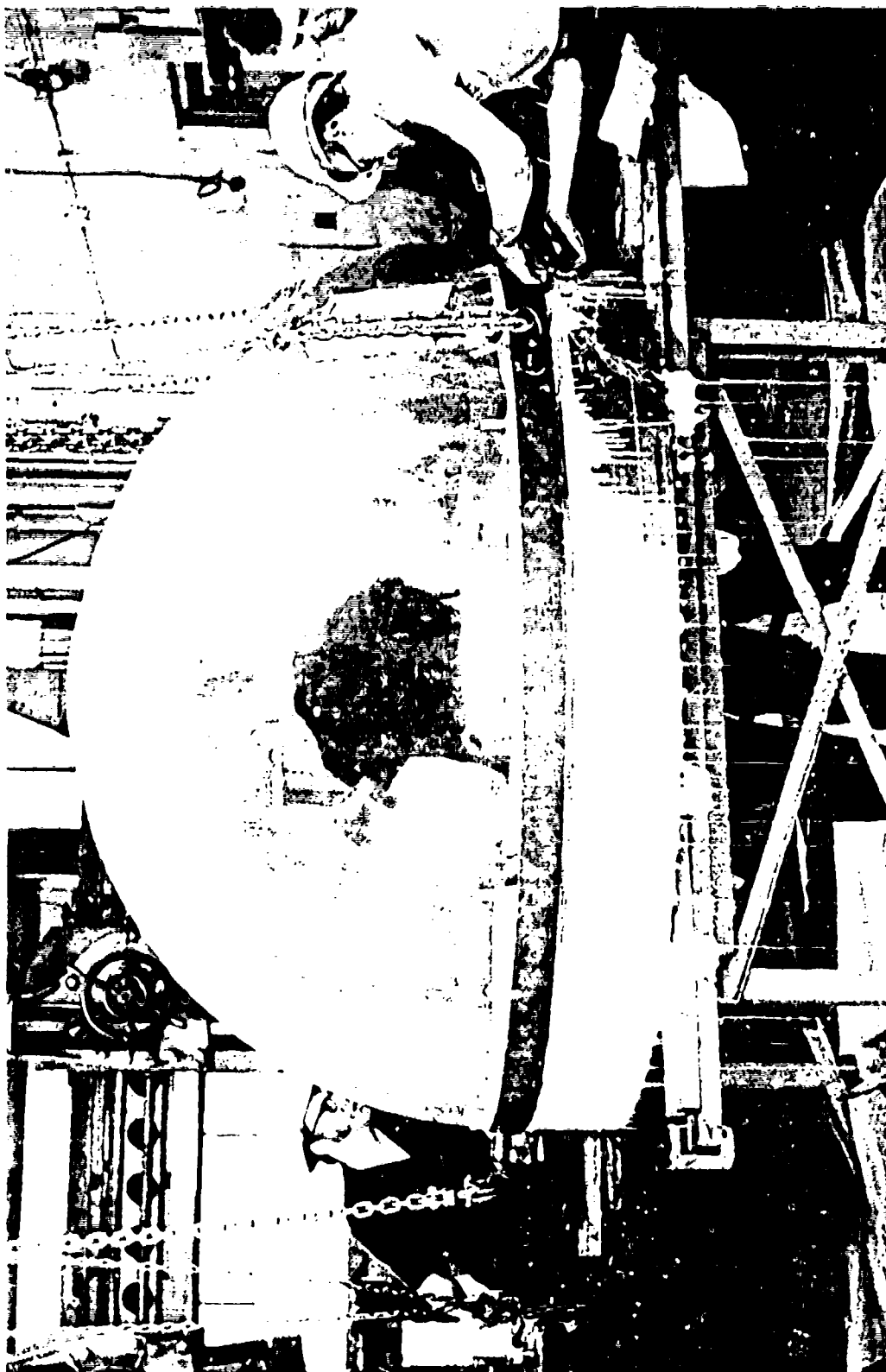
Figure 14. Dome after the mating with the flange has been completed. The displaced elastomeric compound signifies that all spaces between the dome skirt and the flange have been filled. Note the external lifting clamp surrounding the dome's base and the chains by which the dome is lowered into the flange.

Table 1. Mechanical Properties of Material.

A. Acrylic Plastic Casting.

Type of test	[a]Cast acrylic plastic sheets and plates	[b]Massive hemisphere casting
Compressive yield	15,000 psi	12,900 psi
Compressive modulus	420,000 psi	415,000 psi
ASTM-D-695		
Tensile strength	9,000 psi	8,100 psi
Tensile modulus	400,000 psi	410,000 psi
Tensile elongation	2 percent	4.8 percent
ASTM-D-638		
Flexural strength	14,000 psi	not available
Flexural modulus	420,000 psi	not available
ASTM-D-790		
Shear strengths ASTM-D-732	8,000 psi	not available
Deformation under load (4000 psi at 122°F for 24 hours) ASTM-D-621	1 percent maximum	0.96 percent

NOTES:

[a]Minimum properties specified for acrylic plastic viewports fabricated from sheets or plates — MIL-C-24449.

[b]Actual values obtained by testing of coupons cut from the massive hemisphere casting.

Table 1. (Continued)

B. Silicone elastomeric compound[c] (Dow Corning 3110 RTV)	
Color[2]	White
Deep section cure, 1-in. depth in metal can	Yes
Recommended Primer	1201
ASTM D 445. Viscosity at $25°C$ ($77°F$), poises	125
ASTM D 792. Specific gravity at $25°C$ ($77°F$)	1.17
MIL-S-23586. Corrosion resistance	Good/Pass
ASTM D 412. Tensile strength, psi	350
ASTM D 412. Elongation, percent	200
ASTM D 676. Durometer hardness, Shore A	45
Linear shrinkage, percent, 3 days at $25°C$ ($77°F$)	0.4
Radiation resistance, cobalt 60 source, $25°C$ ($77°F$), megarads	100
ASTM D 570. Water absorption, percent, 7 days at $25°C$ ($77°F$)	0.4
Temperature range, degrees	-65 to $200°C$ (-85 to $392°F$)
Thermal conductivity, Cenco-Fitch, $25-100°C$ ($77-212°F$, gm cal/cm^2-sec-($°C$/cm)	5.0×10^{-4}
MIL-I-16923C. Thermal shock, 10 cycles	Pass
Weight loss 96 hrs/$200°C$ ($392°F$), percent	6
Volume expansion $25-150°C$ ($77-302°F$) cc/cc/$°C$	7.5×10^{-4}
Specific heat, cal/gm/$°C$	0.35
ASTM D 746. Brittle point, degrees	$-100°C$ ($-143°F$)
Fire resistance	Self-extinguishing

[c]Typical values supplied by Dow-Corning for 3110 RTV.

APPENDIX: DESIGN HINTS

For those engineers interested in utilizing the casting technique for acrylic plastic domes or the design developed for the attachment of these domes to vehicle hulls, some brief discussion of their limitations is in order.

CAST MATERIAL

Because the mechanical properties of cast massive acrylic plastic domes differ significantly from those of domes formed and subsequently machined from thick, commercially available plastic plates (for example. Plexiglas G, Acrylite or Swedlow 310), lower stress levels must be utilized in their operation. Appropriate stress levels can be determined using the ratio of the mechanical properties of the dome casting to those of flat plates. For example, the ratio of the compressive strength of the dome casting to that of flat plate is approximately 6/7 or 0.85. Therefore, the maximum working stresses in cast domes should relate to the working stresses in domes fabricated from plates by roughly the same factor.

Since the maximum compressive working stress allowed at the present time for spherical Plexiglas manned capsules with a minimum proven 1,000 cycles and 10^6 hours static fatigue life is only 4,000 psi,* the maximum allowable compressive working stress in a cast dome having the mechanical properties shown in table 1 should not exceed 3,400 psi (arrived at by multiplying 4,000 psi by 0.85). The maximum allowable tensile working stress in a cast dome should, by the same token, not exceed 1,800 psi (arrived at by multiplying the accepted 2,000-psi value for thick plates by a factor of 0.9, the ratio of the tensile strength of a cast dome to that of typical flat plate).

In those cases where the casting does not form a dome but has the shape of a spherical sector and the design is based on empirical short-term implosion data of scale model sectors machined from Plexiglas G plates, a different approach must be used. Since the operational depth of spherical sector windows is generally only a known fraction of their short-term implosion pressure, the only modification to their design procedure is to multiply the maximum operational pressure allowed for spherical sector Plexiglas G windows by the same factor that was used in the previous paragraph to reduce allowable maximum compressive working stresses in domes.

ATTACHMENT

The attachment (figure 2) for affixing the dome to the vehicle hull has been specifically designed for shallow depths of 100 feet or less. A similar attachment could be used for depths to 1,000 feet, but the clearance between the U-shaped flange and the skirt would have to be increased to allow for greater radial contraction under the larger hydrostatic pressure.

---

*Based on the results of the NPMO hull testing program at the Naval Civil Engineering Laboratory, reported in references 11 through 15.

For depths beyond 1,000 feet the cylindrical skirt and the attachment developed for it (figure 2) would have to be eliminated altogether, as the bending stresses at the intersection of the hemisphere and the cylindrical skirt become quite high. By elimi. ating the cylindrical skirt on the casting its operational depth can be readily increased from 1,000 feet to about 2,500 feet. For mating the hemisphere to the hull of an undersea vehicle a different attachment would have to be devised.

A typical attachment for a hemispherical dome is shown in figure A.1. Its characteristics are (1) lack of restraint to the radial contraction of the sphere under hydrostatic pressure; (2) lack of an O-ring groove under the acrylic bearing surface; (3) presence of a smooth, metallic bearing surface on which the acrylic bearing surface can slide; and (4) an externally located rubber sealing gasket.

24

HEMISPHERE RETAINING RING

FIBERGLASS FAIRING

SYNTACTIC FOAM

STEEL HULL

STEEL FLANGE WITH WELD DEPOSITED MONEL FACING ON THE BEARING SURFACE FOR ACRYLIC

SQUARE OR ROUND SOFT NEOPRENE O-RING UNDER AXIAL AND RADIAL COMPRESSION

NEOPRENE BEARING GASKET BONDED WITH CONTACT CEMENT TO THE STEEL RETAINING RING
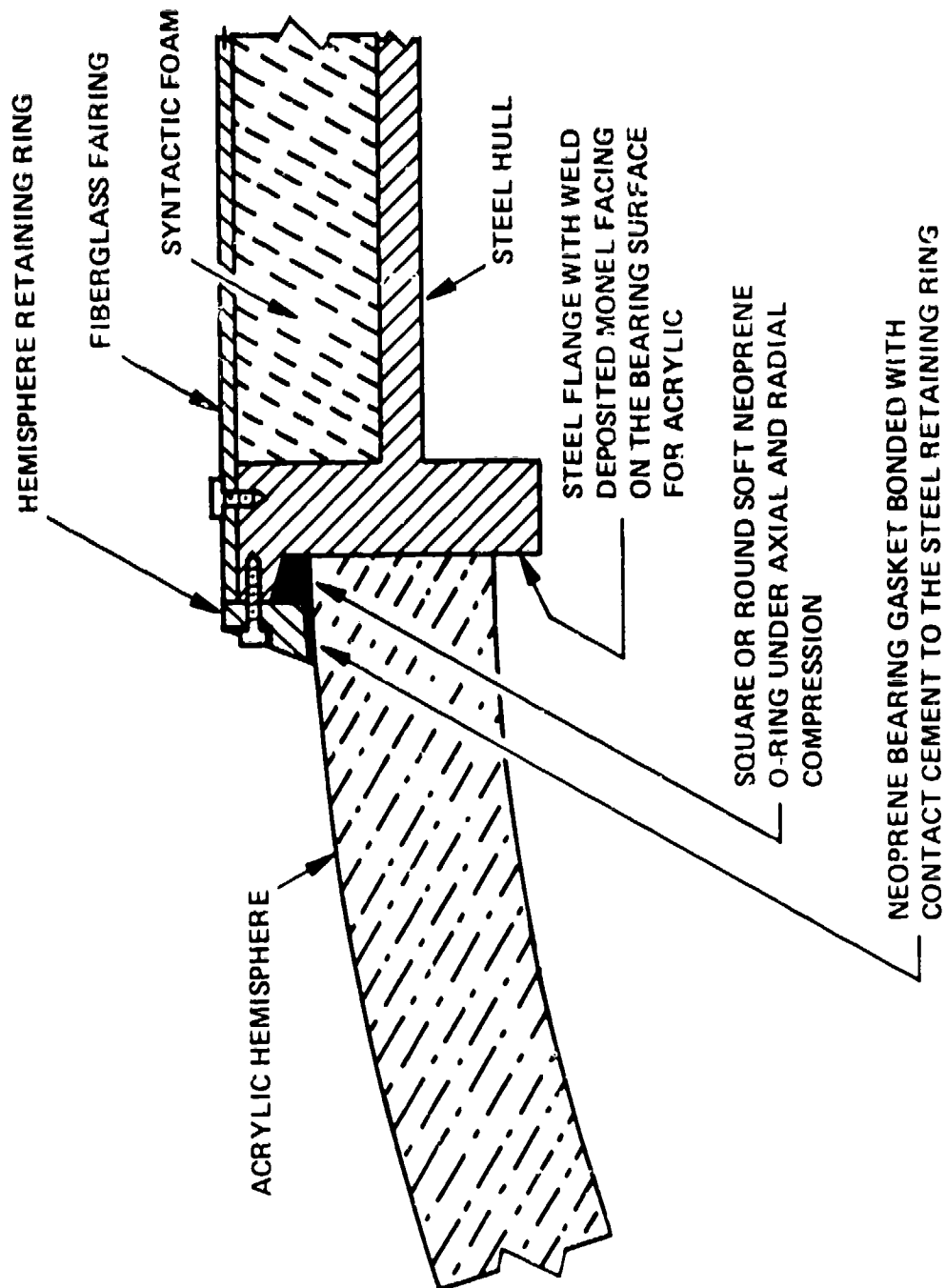
ACRYLIC HEMISPHERE

Figure A.1. Attachment for fastening a geometrically true plastic hemisphere to the hull of a deep diving submersible.

25

REFERENCES

1. Naval Civil Engineering Laboratory. Technical Report R-512, Windows for External or Internal Hydrostatic Pressure Vessels, pt. 1. Conical Acrylic Windows Under Short Term Pressure Application, by J. D. Stachiw and K. O. Gray. Port Hueneme, California, January 1967 (AD 646882).

2. _____ Technical Report R-527, Windows for External or Internal Hydrostatic Pressure Vessels, pt. 2. Flat Acrylic Windows Under Short Term Pr ure Application, by J. D. Stachiw, G. M. Dunn and K. O. Gray. Port Huene California, May 1967 (AD 652343).

3. _____ Technical Report R-645, Windows for External or internal Hydrostatic Pressure Vessels, pt. 4. Conical Acrylic Windows Under Long Term Pressure Application of 20,000 psi, by J. D. Stachiw. Port Hueneme, California, October 1969 (AD 697272).

4. _____ Technical Report R-708, Windows for External or Internal Hydrostatic Pressure Vessels, pt. 5. Conical Acrylic Windows Under Long Term Pressure Application of 10,000 psi, by J. D. Stachiw and W. A. Moody. Port Hueneme, California, January 1970 (AD 718812).

5. _____ Technical Report R-747, Windows for External or internal Hydrostatic Pressure Vessels, pt. 6. Conical Acrylic Windows Under Long Term Pressure Application of 5,000 psi, by J. D. Stachiw and K. O. Gray. Port Hueneme, California, June 1971 (AD 736594).

6. _____ Technical Report R-773, Windows for External or Internal Hydrostatic Pressure Vessels, pt. 7. Effect of Temperature and Flange Configuration on Critical Pressure of 90 Degree Conical Acrylic Windows Under Short Term Loading, by J. D. Stachiw and J. R. McKay. Port Hueneme, California, August 1972 (AD 748583).

7. _____ Technical Report N-1127, Flat Disc Acrylic Plastic Windows for Man-Rated Hyperbaric Chambers of the U. S. N. Experimental Diving Unit, by J. D. Stachiw. Port Hueneme, California, November 1970 (AD 716751).

8. _____ Technical Report R-631, Windows for External or Internal Hydrostatic Pressure Vessels, pt. 3. Critical Pressure of Acrylic Spherical Shell Windows Under Short Term Pressure Application, by J. D. Stachiw and F. W. Brier. Port Hueneme, California, June 1969 (AD 689789).

9. Naval Undersea Center. NUC TP 315, Acrylic Plastic Hemispherical Shells for NUC Undersea Elevator, by J. D. Stachiw. San Diego, California, September 1972 (AD 749029).

10.   _____ NUC TP 355, Flanged Acrylic Plastic Hemispherical Shells for Undersea Systems by J. D. Stachiw. San Diego, California, August 1973 (AD 769213).

11.   Naval Civil Engineering Laboratory, Technical Report R-676, Development of a Spherical Acrylic Plastic Pressure Hull for Hydrospace Application, by J. D. Stachiw. Port Hueneme, California, April 1970 (AD 707363).

12.   _____ Technical Note N-1113, The Spherical Acrylic Pressure Hull For Hydrospace Application, pt. 2. Experimental Stress Evaluation of Prototype NEMO Capsule, by J. D. Stachiw and K. L. Mack. Port Hueneme, California, October 1970 (AD 715772).

13.   _____ Technical Note N-1094, The Spherical Acrylic Pressure Hull for Hydrospace Application, pt. 3. Comparison of Experimental and Analytical Stress Evaluations for Prototype NEMO Capsule by H. Ottsen. Port Hueneme, California, March 1970 (AD 709914).

14.   _____ Technical Note N-1134, The Spherical Acrylic Pressure Hull for Hydrospace Application, pt. 4. Cyclic Fatigue of NEMO Capsule #3, by J. D. Stachiw. Port Hueneme, California, October 1970 (AD 715345).

15.   Naval Undersea Center. NUC TP 305, Effect of Bubble Inclusions of the Mechanical Properties of Cast Polymethyl Metacrylate, by J. D. Stachiw. San Diego, California, August 1972 (AD 746862).

DOCUMENT CONTROL DATA · R & D

(Security classification of title, body of abstract and indexing annotation must be entered when the overall report is classified)

1. ORIGINATING ACTIVITY (Corporate author)	2a. REPORT SECURITY CLASSIFICATION
Naval Undersea Center San Diego, California 92132	UNCLASSIFIED
	2b. GROUP

3. REPORT TITLE

CAST ACRYLIC PLASTIC DOME FOR UNDERSEA APPLICATIONS

4. DESCRIPTIVE NOTES (Type of report and inclusive dates)
Research and Development, July 1972 – June 1973

5. AUTHOR(S) (First name, middle initial, last name)

Jerry D. Stachiw

6. REPORT DATE	7a. TOTAL NO. OF PAGES	7b. NO. OF REFS
January 1974	32	15

8a. CONTRACT OR GRANT NO.	9a. ORIGINATOR'S REPORT NUMBER(S)
b. PROJECT NO. Funded internally through the Independent Exploratory c. Development Program	NUC TP 383
	9b. OTHER REPORT NO(S) (Any other numbers that may be assigned this report)
d.	—

10. DISTRIBUTION STATEMENT

Approved for public release; distribution unlimited.

11. SUPPLEMENTARY NOTES	12. SPONSORING MILITARY ACTIVITY
	Director of Navy Laboratories Washington, D. C. 20390

13. ABSTRACT

    An acrylic plastic hemispherical dome with a 78-inch outer diameter, 65.25-inch inner diameter and 7-inch-long skirt has been successfully cast, machined, and equipped with a metallic mounting flange. The mounting flange will allow mating of the cast plastic dome to a surface ship hull, where it will serve as an impact-resistant undersea observation chamber that will afford its occupants panoramic vision of subsurface hydrospace. Other potential applications for such cast domes are in deep submergence vehicles, continental shelf ocean bottom habitats, pressurized aquaria, and hyperbaric chambers. This dome is applicable to depths in the 0- to 2,500-foot range providing that the right method is used for attaching the dome to the vehicle or habitat. The mechanical properties of the massive dome casting have been found to be significantly less than the typical properties of flat plates cast solely from acrylic monomer.

14. KEY WORDS	LINK A		LINK B		LINK C	
	RÔLE	WT	RÔLE	WT	ROLE	WT
Acrylic resins						
Acrylic casting						
Viewports						
Submersible windows						
Spherical shells						
Windows						
Submersibles						
Habitats						
Observation chambers						

DD FORM 1 NOV 1473 (BACK)

(PAGE 2)

Technical Note N-1127

FLAT DISC ACRYLIC PLASTIC WINDOWS FOR MAN-
RATED HYPERBARIC CHAMBERS AT THE USN EXPERIMENTAL

DIVING UNIT

By

J. D. Stachiw

November 1970

NAVAL CIVIL ENGINEERING LABORATORY
Port Hueneme, California 93041

FLAT DISC ACRYLIC PLASTIC WINDOWS FOR MAN-RATED HYPERBARIC CHAMBERS AT
THE USN EXPERIMENTAL DIVING UNIT

Technical Note N-1127

56-020

by

J. D. Stachiw

ABSTRACT

Flat disc acrylic plastic windows have been designed, fabricated,
evaluated and delivered to EDU for replacement of glass windows used to
date. The large (D_o = 6.950 inches; t = 1.650 inches) and the small
(D_o = 4.450 inches, t = 1.040 inches) windows have been found on the
basis of an extensive evaluation program to be more than adequate for
man-rated service under 450 psi maximum operational pressure in steel
flanges with D_i (diameter of opening in flange) of 5.000 and 3.000
inches. All windows were prooftested to 675 psi pressure at 120°F
ambient temperature prior to delivery.

ii

INTRODUCTION

The Supervisor of Salvage, USN, requested the Naval Civil Engineering Laboratory to design, fabricate, evaluate and deliver flat disc acrylic plastic windows for replacement of glass windows currently utilized by the EDU (Experimental Diving Unit) at Washington, D. C. In view of the fact that the pressure vessels into which the windows were to be installed are man-rated, the windows also had to be subjected to a sufficiently exhaustive testing program that would justify man-rating them. This report is a brief summary of the systematic window and material testing program to which the acrylic plastic windows for the EDU chambers were subjected to insure their acceptability for man-rated service in a USN installation.

DISCUSSION

Since the main objective of an evaluation program for windows applicable to man-rated service is establishment of confidence in the installed windows, all the phases of the evaluation program had to contribute to the attainment of this objective. Thus, confidence had to be established in the design, material, fabrication, quality control and service life of such windows under stated operational conditions; 450 psi maximum pressure and $120^\circ F$ ambient temperature.

Design

The design of the windows was based on the destructive short-term hydrostatic tests performed previously by NCEL in $75^\circ F$ ambient environment on flat disc acrylic plastic windows.[1] Since the short-term loading conditions are distinctly different from long-term sustained or cyclic pressure tests, a conservative conversion factor had to be used in applying the short-term test data to the design of windows for the more severe sustained and cyclic pressure operational service conditions at $120^\circ F$ temperature. The conversion factor chosen was 12, considered to be sufficiently large to take into account not only the difference in loading conditions (short-term vs. cyclic and long-term loading) but also the need for a safety margin of at least 300 percent. Using the conversion factor of 12, the t/D_i (thickness to flange opening diameter ratio) was found* to be 0.325. This value gave the

---
*When the 450 psi operational pressure is multiplied by the conversion factor of 12, the result is 5400 psi. Using Figure 10 in NCEL Technical Report TR-527, one finds that a t/D_i (thickness to flange opening diameter) ratio of about 0.325 is required in order for windows to fail at 5500 psi under short-term loading conditions at $75^\circ F$.

1

proper design ratio between the window thickness and the unsupported diameter of the window. Because acrylic plastic plate stock varies in thickness from specified values, the actual t/D_i ratio of finished windows varies from the specified one (Figure 1). Since previous tests have shown that a 1.5 ratio between the flange opening and the outer window diameters is desirable the existing EDU window flanges (Figure 2) were checked for conformance. They were found to conform approximately to this ratio. It was found, however, that modification of the existing retaining ring (Figure 3) for the EDU chamber flange with the 7.000-inch diameter seat was required to accommodate the 1.650-inch thick acrylic plastic window. No further changes in the EDU window flanges were found to be necessary to accommodate the acrylic plastic windows chosen on the basis of 0.325 t/D_i ratio. The sealing arrangement consisting of flat rubber gaskets used previously with glass windows was retained unchanged for acrylic plastic windows.

Material Selection

Since the utility grade of acrylic plastic Plexiglas G (MIL-P-21105C) has been found in previous studies to be acceptable for man-rated windows under hydrostatic loading, it could be utilized for EDU windows without any further material selection tests. But if the fabricator of windows would rather supply an equivalent or better grade of acrylic plastic for the windows, it could be utilized also, providing the typical window performance evaluation tests were performed with windows fabricated from that material.

Because Swedlow Inc., the fabricator of the windows, indicated that he would rather use Swedlow 350 grade (MIL-P-8184) acrylic plastic, it was chosen for the EDU windows. The advertised mechanical properties of Swedlow 350 acrylic were approximately the same as of Plexiglas G acrylic. Therefore, no fear existed that it may not pass the NCEL specifications (Table 1) for man-rated acrylic plastic windows. The basic difference between Swedlow 350 and Plexiglas G was in the former's better resistance to (1) surface crazing when exposed to harmful chemicals, and (2) deformation at elevated temperatures. Since this difference between Swedlow 350 and Plexiglas G was to EDU's advantage, it was accepted as a desirable feature.

Material Quality Control

Material quality control was exercised by cutting test specimens from the center of the acrylic plastic plates serving as machining stock for the windows. Since the existing specification MIL-P-8184 covered the optical and physical properties of the Swedlow 350 material no need existed to repeat these tests on the plate in stock. Thus, only mechanical properties tests were run on the material test specimens cut from each acrylic plastic plate used as stock for machining of the windows. If the tests showed that the mechanical properties were lower than specified, the acrylic plastic plates from which the test specimens were taken

2

Table 1. Specified* Properties of Acrylic Plastic
For Man-Rated Structures.

Physical Properties		
Property	Typical	Test Method
Hardness, Rockwell M	90	ASTM-D785-62
Hardness, Barcol	90	ASTM-D2583
Specific gravity	1.19 ± 0.01 (2 tests within 0.005)	ASTM-D792-64T
Refractive index; 1/8 inch	1.50 ± 0.01	ASTM-D542-50
Luminous transmittance; 1/8 inch	91%	ASTM-D1003-61
Haze, 1/8 inch	2.3	ASTM-D1003-61
Heat distortion temperature +3.6°F/min at 264 psi +3.6°F/min at 66 psi	200°F 220°F	
Thermal expansion/°F at 20°F	35×10^{-6}	Fed. Stan. 406 Method 2031
Water absorption; 1/8 inch (a) 25 hours at 73°F (b) to saturation	0.3% 1.9%	ASTM-D570-63T
Mechanical Properties		
Tensile strength, rupture (0.2 in./min)	9,000 psi (min)	ASTM-D638-64T
Tensile elongation, rupture	2% (min) - 7% (max)	ASTM-D638-64T
Modulus of elasticity, tension	400,000 psi (min)	ASTM-D638-64T
Compressive strength, (0.2 in./min)	15,000 psi (min)	ASTM-D695-63T
Modulus of elasticity, comp.	420,000 psi (min)	ASTM-D695-63T
Flexural strength, rupture	14,000 psi (min)	ASTM-D790-63
Shear strength, rupture	8,000 psi (min)	ASTM-D732-46
Impact strength, Izod (per inch of notch)	0.4 ft-lb (min)	ASTM-D256-56
Compressive deformation under load (4,000 psi at 122°F for 24 hours)	2% (max)	ASTM-D621-64

*Specification developed by NCEL for procurement of acrylic plastic
plates to be utilized in the fabrication of man-rated pressure
resistant windows and pressure hulls.

3

would be rejected, new plates would be selected from the warehouse, and the material quality control tests repeated.

The acrylic plastic plates chosen for the machining of EDU windows met (Table 2b) the NCEL specification for man-rated acrylic plastic windows and the plates were released for machining of windows.

Window Performance Evaluation

The aim of window performance evaluation tests was to establish the fact that the combination of window dimensions, window material and window flange chosen for EDU hyperbaric chambers is adequate for the service to which the windows are to be subjected. The evaluation tests chosen for a series of EDU windows selected at random from the lot of windows supplied by Swedlow Inc. were: (1) Short-term tests, (2) Long-term tests, and (3) Cyclic tests.

Short-term tests were identical to those performed previously[1] during exploratory evaluation of acrylic plastic flat disc windows. The objective of the short-term hydrostatic tests performed at this time was (1) to confirm the validity of the t/D_i vs p_c (where p_c denotes catastrophic failure pressure) curve for Swedlow 350 acrylic plastic established in previous NCEL tests with Plexiglas G acrylic plastic windows, and (2) to establish the effect of $120^\circ F$ ambient temperature on p_c established previously at $70^\circ F$ ambient temperature.

Long-term sustained hydrostatic tests had the objective of establishing that (1) the catastrophic failure of flat disc acrylic plastic windows under long-term sustained hydrostatic loading is predictable, and that (2) the window system chosen for EDU chambers is adequate to withstand any unforeseeable single sustained hydrostatic loading. Proving the first point would permit extrapolating into the future the results of few tests of less than a month's duration. Proving the second point would assure the operators of the hyperbaric chambers at EDU that even if the divers remained inside the chamber for a period of one year, the windows would not catastrophically fail due to visco-elastic creep.

Cyclic hydrostatic tests had the objective of (1) establishing that failure of flat disc acrylic plastic windows under cyclic pressure loading is predictable, and to (2) determine the cyclic fatigue life of the window system selected for EDU chambers. Proving the first point would permit extrapolating into the future the results of few tests of less than a month duration. Establishing the cyclic fatigue life of windows in EDU chambers would permit the chamber operators to establish a window replacement schedule with an adequate margin of safety.

Product Assurance

To assure that each window was indeed safe for operation under stated service conditions all windows were to be subjected for 1 hour to a 50 percent hydrostatic overload proof test at $120^\circ F$ ambient temperature. After the test, each window was to be carefully inspected for

4

Table 2. Mechanical Properties of Acrylic Plastic* Plate
Used for the Fabrication of EDU Windows.

Property Measured	Minimum	Average	Maximum
Compressive Yield, psi (ASTM D-695)	18,000	18,300	18,700
Compressive Modulus of Elasticity, psi (ASTM D-695)	4.8×10^5	5.4×10^5	6.2×10^5
Deformation Under Compressive Load, percent (ASTM D-621-64; 4000 psi at 122°F for 24 hrs)	0.36	0.51	0.63
Tensile Ultimate Strength, psi (ASTM D-638-64)	11,300	11,600	11,800
Tensile Modulus of Elasticity, psi (ASTM D-638-64)	4.5×10^5	4.7×10^5	4.9×10^5
Tensile Elongation at Failure, percent (ASTM D-638-64)	3.6	4.0	4.3
Flexure Strength, psi (ASTM D-790)	16,900	17,000	17,100
Flexure Modulus of Elasticity, psi (ASTM D-790)	4.9×10^5	4.96×10^5	5.0×10^5
Shear Strength, psi (ASTM D-732)	10,200	10,200	10,200

*Swedlow 350 acrylic plastic meeting MIL-P-8184 specification.

5

presence of cracks and packed for shipment. This final test just prior to delivery of the windows to EDU was intended to remove any remaining doubts about the quality and safety of the supplied windows.

EXPERIMENTAL TEST PROGRAM

Testing Arrangement

The experimental test program for evaluation of the chosen window design for EDU consisted of testing to destruction under hydrostatic pressure a series of EDU windows. While the type of loading differed from test to test depending on whether the tests were of short-term, long-term, or cyclic nature, the method of loading and the test arrangements were the same in every case (Figure 4).

The 9-inch diameter NCEL pressure vessels were used in every case for the containment of windows. The pressure was raised with positive displacement air operated pumps at 650 psi/minute rate. For long-term tests the desired pressure level was maintained inside the vessel by closing valves leading to the vessel. Only periodically were they opened to adjust the pressure if it deviated more than 50 psi from the desired pressure setting. During cyclic tests the sustained pressure was maintained for 7 hours followed by depressurization proceeding at a rate equal to the pressurization rate. The depressurization was followed always by a 17-hour long relaxation period. The overall 24-hour length of the cycle was patterned on a typical working day.

To eliminate as many extraneous variables as possible from the tests, the windows rested on a 0.025-inch thick nylon fiber reinforced gasket (DuPont's Fairprene 5722A) and no retaining rings were used for clamping the windows inside the test flanges.* The sealing was accomplished by placing a bead of room temperature curing silicone rubber around the circumference of the window.

Test Specimens

Test specimens were windows selected at random from the lot supplied by the manufacturer for installation in the EDU test chamber complex. All of the tests except for 6 short-term tests were conducted for economy with the small (4.450×1.040 inches, $t/D_i = 0.346$) windows. The 6 short tests were conducted with the large windows (6.950×1.650 inches, $t/D_i = 0.330$) to determine whether there was a substantial difference between the strengths of the large and the small windows. Also for economy only one window was tested for each of the many chosen long-term and cyclic loading conditions making any subsequent statistical reliability analysis of data impossible.

---

*Clamping sometimes tends to strengthen the windows. Testing unclamped windows always produces conservative data.

6

Table 3. Catastrophic Failure of EDU Acrylic Plastic* Windows Under Short-Term Hydrostatic Loading

Window Diameter D_o	Flange Opening D_i	Thickness t	Temperature	Failure Pressure psi
4.445 inches	3.000 inches	1.042 inches	32°F	7,420
6.957 inches	5.000 inches	1.645 inches	32°F	7,800
4.457 inches	3.000 inches	1.035 inches	54°F	8,100
6.948 inches	5.000 inches	1.640 inches	54°F	7,970
4.453 inches	3.000 inches	1.053 inches	76°F	7,000
6.959 inches	5.000 inches	1.635 inches	76°F	6,960
4.469 inches	3.000 inches	1.030 inches	98°F	7,550
6.950 inches	5.000 inches	1.650 inches	98°F	6,530
4.454 inches	3.000 inches	1.043 inches	120°F	· 7,000
6.960 inches	5.000 inches	1.630 inches	120°F	6,050

*Swedlow 350 acrylic plastic

NOTE: 1. All windows were pressurized at 650 psi/minute rate till catastrophic failure took place.

2. All windows were tested with 0.025-inch thick neoprene impregnated nylon cloth serving as the bearing gasket on the flange seat.

3. No retaining ring was used to restrain the window in the flange.

FINDINGS

The window evaluation study has conclusively shown that (1) the performance of windows is predictable, and that (2) the window system chosen is more than adequate for the 450 psi 120°F operational service in EDU chambers.

Both the large (t/D_i = 0.330) and the small (t/D_i = 0.346) windows chosen for the EDU chambers imploded (Table 3) under short-term hydrostatic loading at room temperature (70-75°F) in approximately the same pressure range (6900-7200 psi) as Plexiglas G windows tested in previous study (7000-8500 psi). This proved that Swedlow 350 acrylic plastic windows performed as well as Plexiglas G acrylic plastic on which the NCEL specifications for acrylic plastic windows were based.

The mode of failure for the windows tested at 120°F ambient pressure was found to be the same (Figures 5 and 6) as that for windows tested at 70°F ambient pressure (see NCEL Technical Report[1] R-527 Appendix B). First there formed a star shaped system of cracks propagating radially outward from the center of the window's low pressure face. The cracks were the deepest in the center of the window face. The depth of these cracks even at the center of the window face was less than the thickness of the window. Second, the leading edges of the cracks inside the body of the window curved towards the horizontal plane of the window coalescing in a single conical fracture plane. The apex of the cone was centered just below the center of the window's high pressure face. Third, a small hole was punched through the center of the window relieving the hydrostatic pressure inside the vessel.

Comparisons between the 7200 psi implosion pressure of small EDU windows at 76°F and 7000 psi implosion pressure at 120°F has shown that the effect of 120°F temperature on the short-term strength of EDU windows is insignificant. It was found, however, that the temperature appears to have some effect on crack initiation (Figure 7a). There appears to be some difference between the failure pressure of large and small EDU windows as could be predicted from the small difference in their t/D_i ratios. The EDU windows can withstand with confidence a momentary pressure loading of approximately 3600 psi without initiation of major cracks giving the windows a proven safety factor of about 8 under short-term overload (less than 1 minute duration). The displacements of the large EDU windows were larger than those of the small windows, but almost in direct proportion to the ratio of their t/D_i diameters (Figure 7b).

Long-Term Loading

The catastrophic failure of EDU windows has been found to be very predictable (Table 4). The relationship between implosion pressure and duration of a single sustained loading was found to be graphically expressable as a straight line on log-log coordinates (Figure 8) and thus easily to extrapolate into the future. The windows were found capable of withstanding a long-term pressure loading of at least 2250 psi without

8

Table 4. Catastrophic Failure of EDU Acrylic Plastic
Windows Under Sustained Long-Term Hydrostatic Loading

Window Diameter inches (D_o)	Thickness inches (t)	Sustained Pressure psi	Duration of Loading minutes
4.453	1.039	7000	1
4.460	1.042	6000	1.7×10
4.454	1.042	5000	1.275×10^3
4.459	1.036	4500	4.5×10^3
4.460	1.034	4000	3.57×10^4
4.458	1.025	2000	$1.02 \times 10^5*$

NOTE: 1. All windows were pressurized at 650 psi/minute
rate till specified pressure was reached, this
pressure was subsequently maintained till failure
took place.

2. Ambient temperature for all tests was $120^{\circ}F$.

3. 0.025-inch thick neoprene impregnated cloth was
used as the bearing gasket on the flange seat
under the window.

4. No retaining ring was used to restrain the window
in the flange.

5. *Test was terminated; no cracks were observed in
the window.

6. The windows were fabricated from Swedlow 350
acrylic plastic.

7. The opening in the flange (D_i) was 3.000 inches
in diameter.

catastrophic explosion failure giving the windows a proven safety factor of 5 under a single sustained long-term overload (approximately 10^{10} minutes duration).

The mode of failure under long-term loading was found to be similar to the mode of failure under short-term loading and thus will not be discussed here in any detail. There was, however, a significant difference in the magnitude of window deformation prior to catastrophic failure. While under short-term loading the maximum displacement of the 1.040-thick window's center just prior to failure was approximately 0.250 to 0.350 inches, for long-term loading the displacement was 0.400 to 0.500 inches (Figure 9). Surprisingly enough, the maximum displacement prior to catastrophic failure under long-term loading was the same regardless of the magnitude of sustained hydrostatic pressure loading. This substantially proves that the ultimate strength of acrylic windows is not a function of stress but of strain and that calculations of window failure under long-term loading based on stress alone are of little value.

Cyclic Loading

The catastrophic failure of EDU windows under cyclic pressure loading was found to be very predictable (Table 5). The mode of failure was similar to short-term and long-term loadings. The relationship between the implosion pressure and number of cycles could be graphically represented as a straight line on log log coordinates (Figure 10), and thus easy to extrapolate. The windows were found capable of withstanding more than 10^{10} cycles each (7 hours duration at 450 psi pressure) prior to requiring replacement due to catastrophic failure. How many cycles they will withstand at longer, or shorter than 7 hour cycle loadings is not quantitatively known. It is, however, qualitatively known from the NEMO experimental program[2] that if the duration of an individual fatigue cycle on acrylic plastic is less than 7 hours then the fatigue damage to the window for each cycle fatigue will be less, and if the duration of a cycle is longer, the fatigue damage accomplished by each cycle will be greater. But even if the duration of individual cycles was 100 hours, it is estimated that it still would take at least 1000 cycles to failure.

Proof Testing

All windows were proof tested (Figures 11 and 12) under 50 percent overload prior to shipment for installation at EDU. All windows withstood the 1-hour long proof test successfully without visual or photoelastic detectable permanent deformation or cracks.

CONCLUSIONS

The design, material, and fabrication method chosen for EDU windows have been found more than adequate for the service in man-rated hyperbaric chambers designed to operate under 450 psi maximum operational pressure and ambient temperature not to exceed $120^{\circ}F$.

Table 5.   Catastrophic Failure of EDU Acrylic Plastic
Windows Under Cyclic Pressure Loading

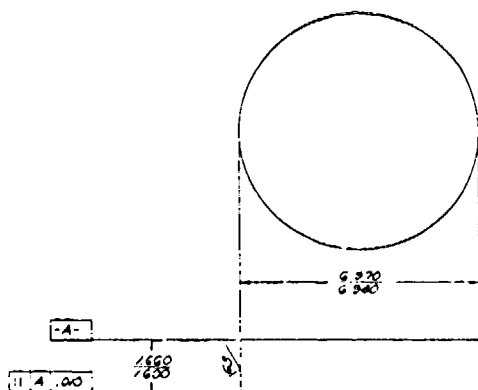| Window Diameter inches (D_o)	Thickness inches (t)	Peak Pressure (psi)	Number of Cycles at Failure
4.446	1.025	5500	1
4.430	1.027	5000	3
4.505	1.038	4500	9
4.460	1.024	4000	14
4.461	1.040	3500	120

NOTE: 1.   Duration of a typical pressure cycle was 24 hours.
The window was alternately 7 hours under sustained
hydrostatic loading and 17 hours under zero pressure.

2.   Ambient temperature for all tests was $120^{o}F$.

3.   0.025-inch thick neoprene impregnated cloth was used
as the bearing gasket on the flange seat under the
window.

4.   No retaining ring was used to restrain the window in
the flange.

5.   The opening in the flange (D_i) was 3.000 inches in
diameter.

6.   The windows were fabricated from Swedlow 350 acrylic
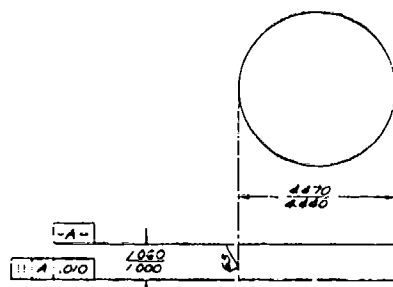plastic.

11

RECOMMENDATIONS

The acrylic plastic windows supplied by NCEL to EDU should be periodically inspected for presence of cracks. Upon visual discovery of a crack in the window it should be replaced. If properly installed and cleaned only with cleaning solutions approved for acrylic plastic, the minimum crack-free life of the windows should be at least 1000 chamber pressurizations to 450 psi.

ACKNOWLEDGEMENT

The setting up of test equipment and supervision of tests was performed by Mr. K. O. Gray, General Engineer. His assistance in the accomplishment of the tests is appreciated.

Figure 1.   Fabrication drawing for EDU windows.
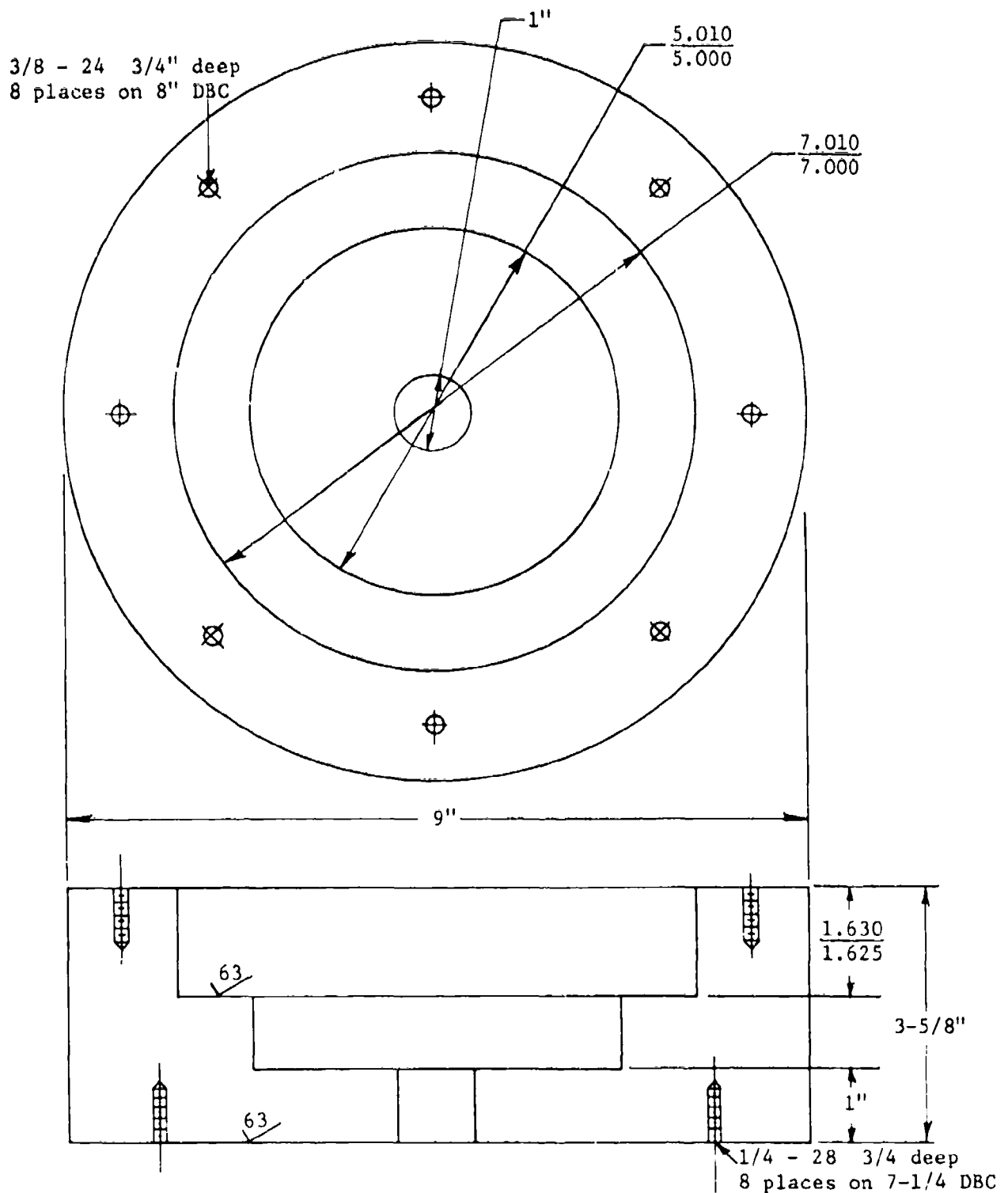
Figure 2a.   Dimensions of window seat and opening diameter in the test
             flange for the 7-inch diameter EDU window, the seat and
             opening in the test flange are the same as in the EDU chamber
             window flanges.

14
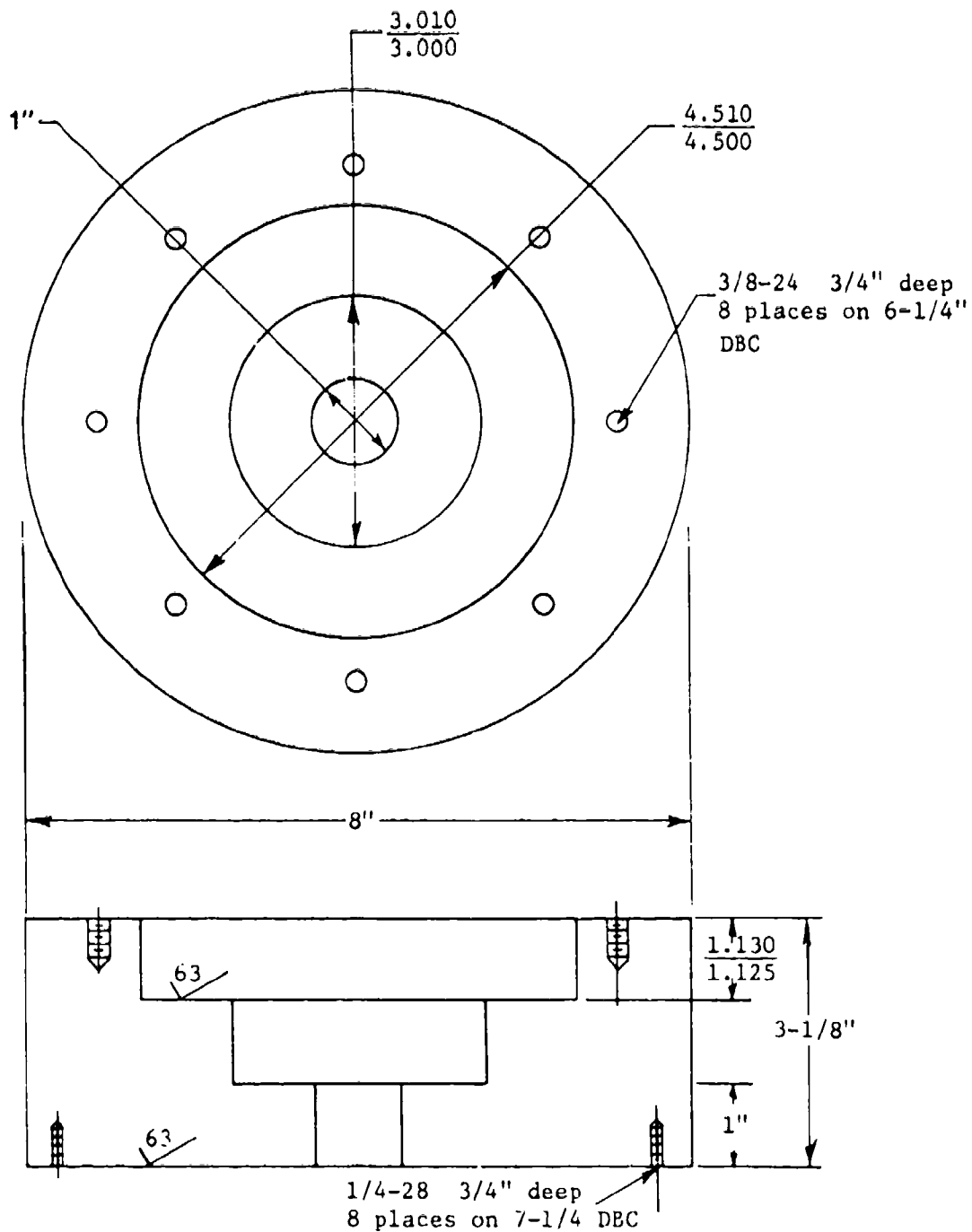
Figure 2b. Dimensions of window seat and opening diameter in the test flange for the 4.5-inch diameter EDU window; the seat and opening in the test flange are the same as in the EDU chamber window flanges.

15
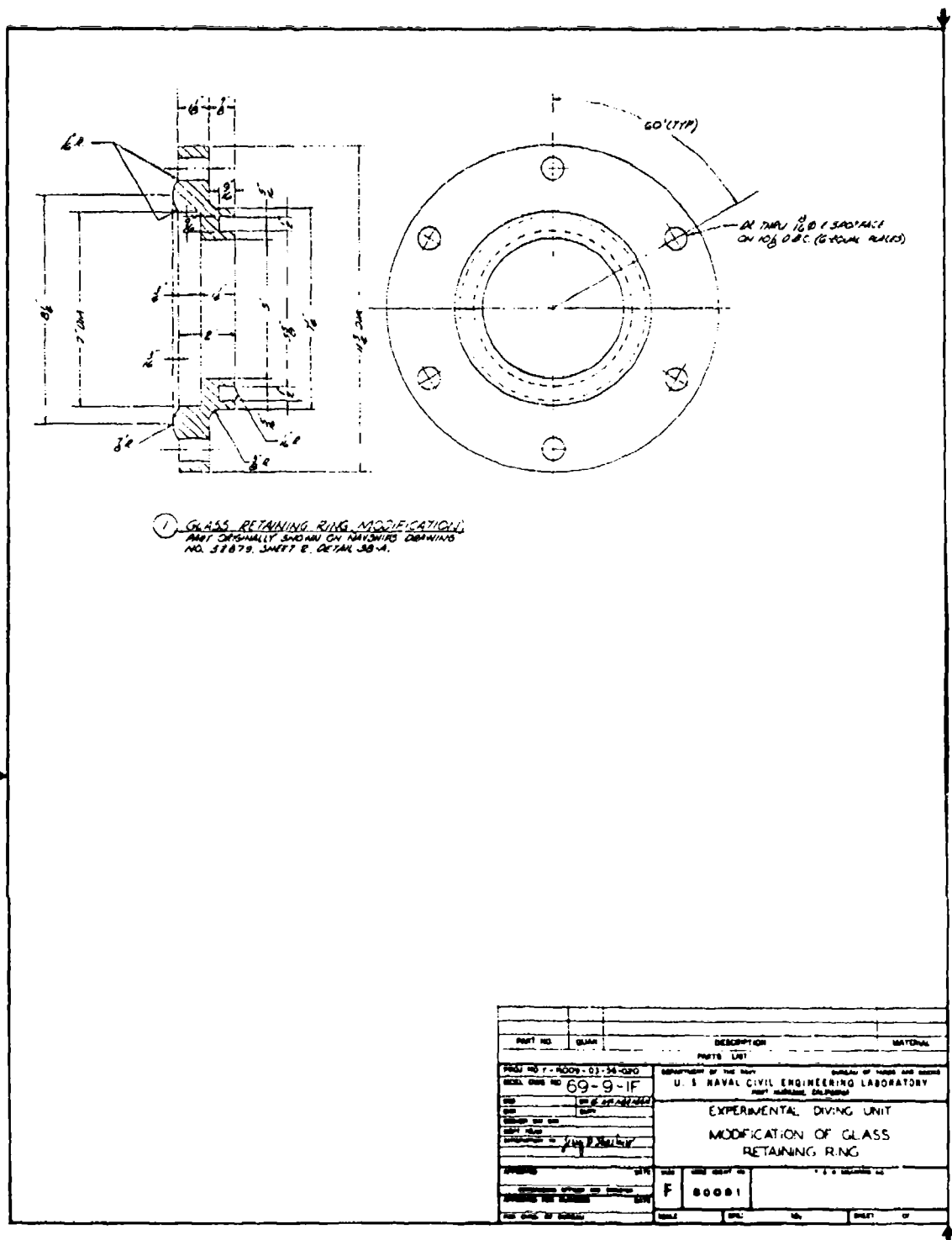
Figure 3.   Modified retaining ring for holding the 7-inch diameter
           acrylic windows in EDU chamber flanges.
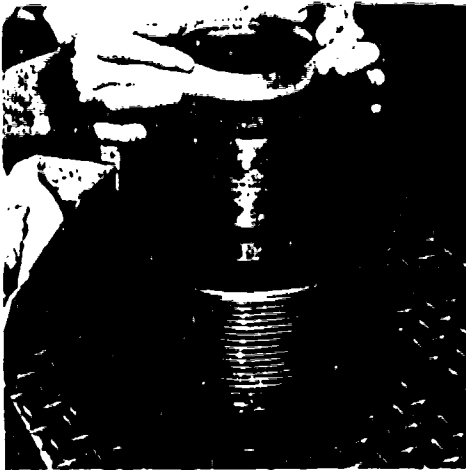
Figure 4a. Placement of window into the flange mounted on the pressure vessel end-closure.
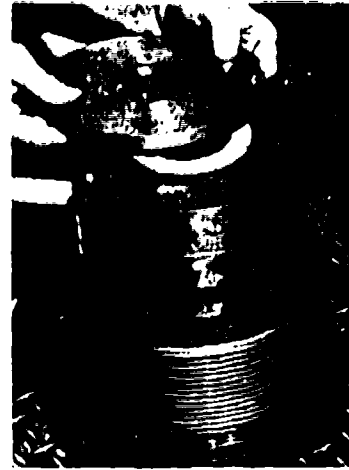
Figure 4b. Placement of retaining ring and retaining ring bearing gasket on the window.

Figure 4c.
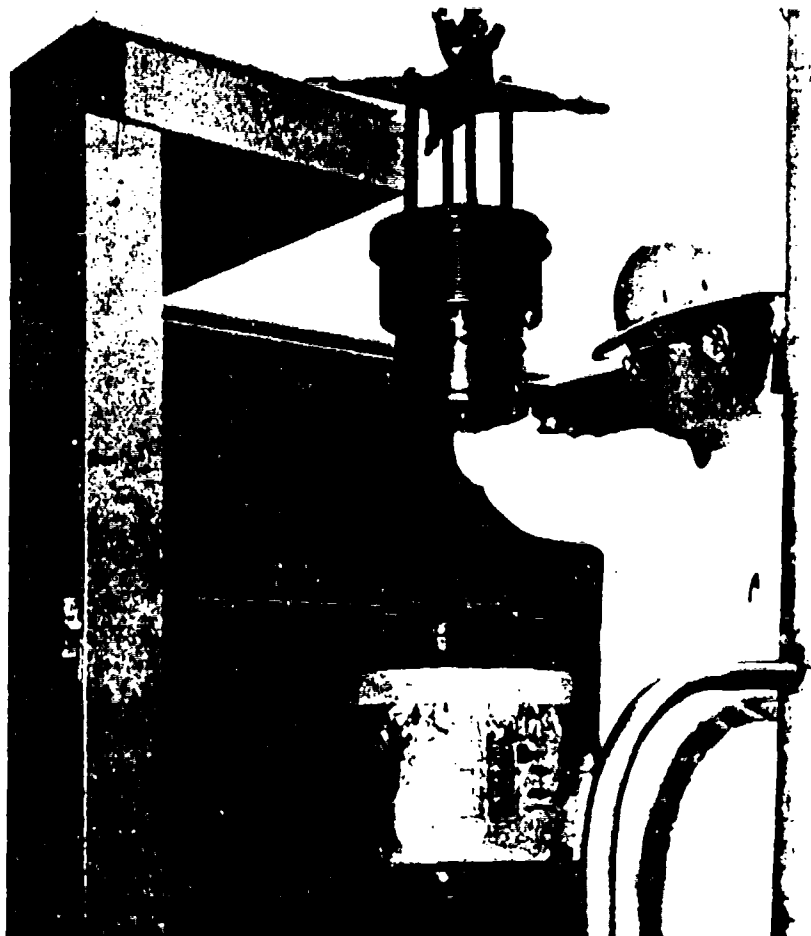
Figure 4d Lowering the end-closure assembly into the pressure vessel.
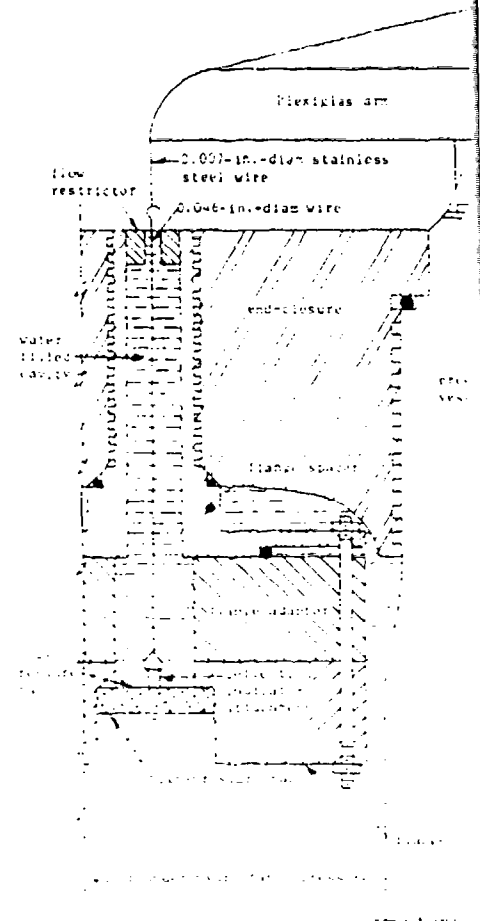
Figure 4e. Schematic drawing of deflection flange mounting used in the test

17

1 of 2
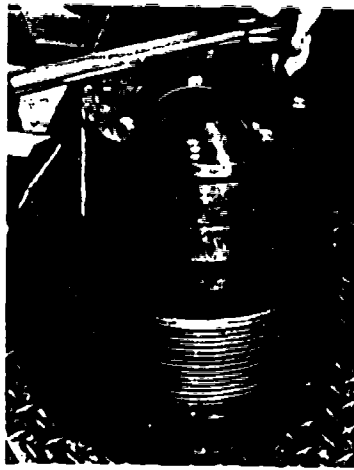
ent of retaining ring
aining ring bearing
on the window.

Figure 4c. Torqueing down
the retaining ring.
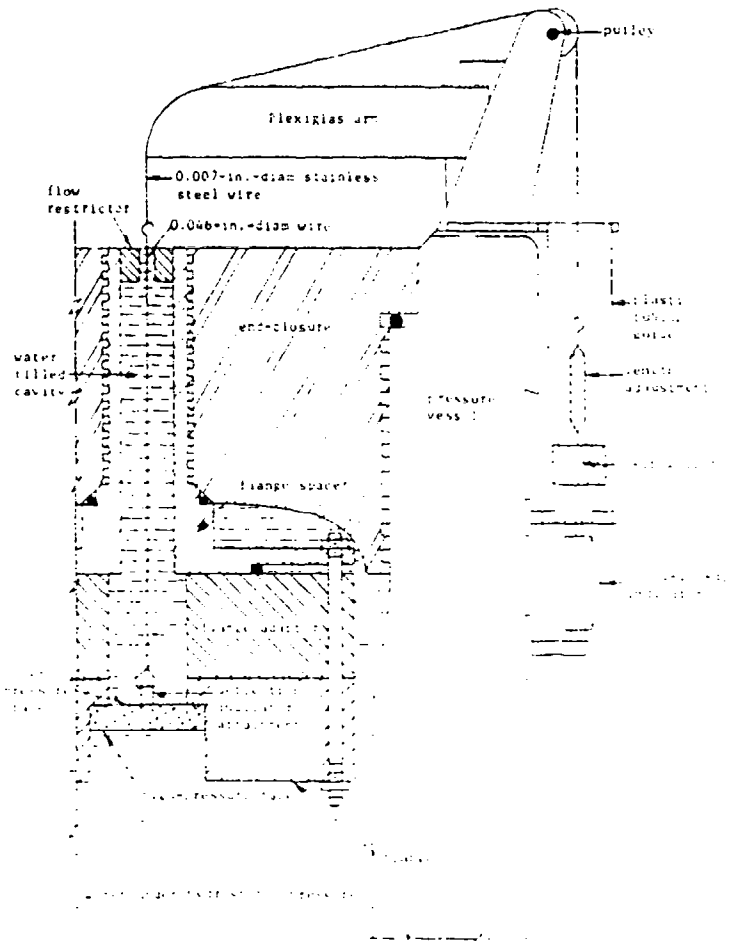
Figure 4e   Schematic drawing of deflection measuring apparatus and
flange mounting used in the testing of windows.

292
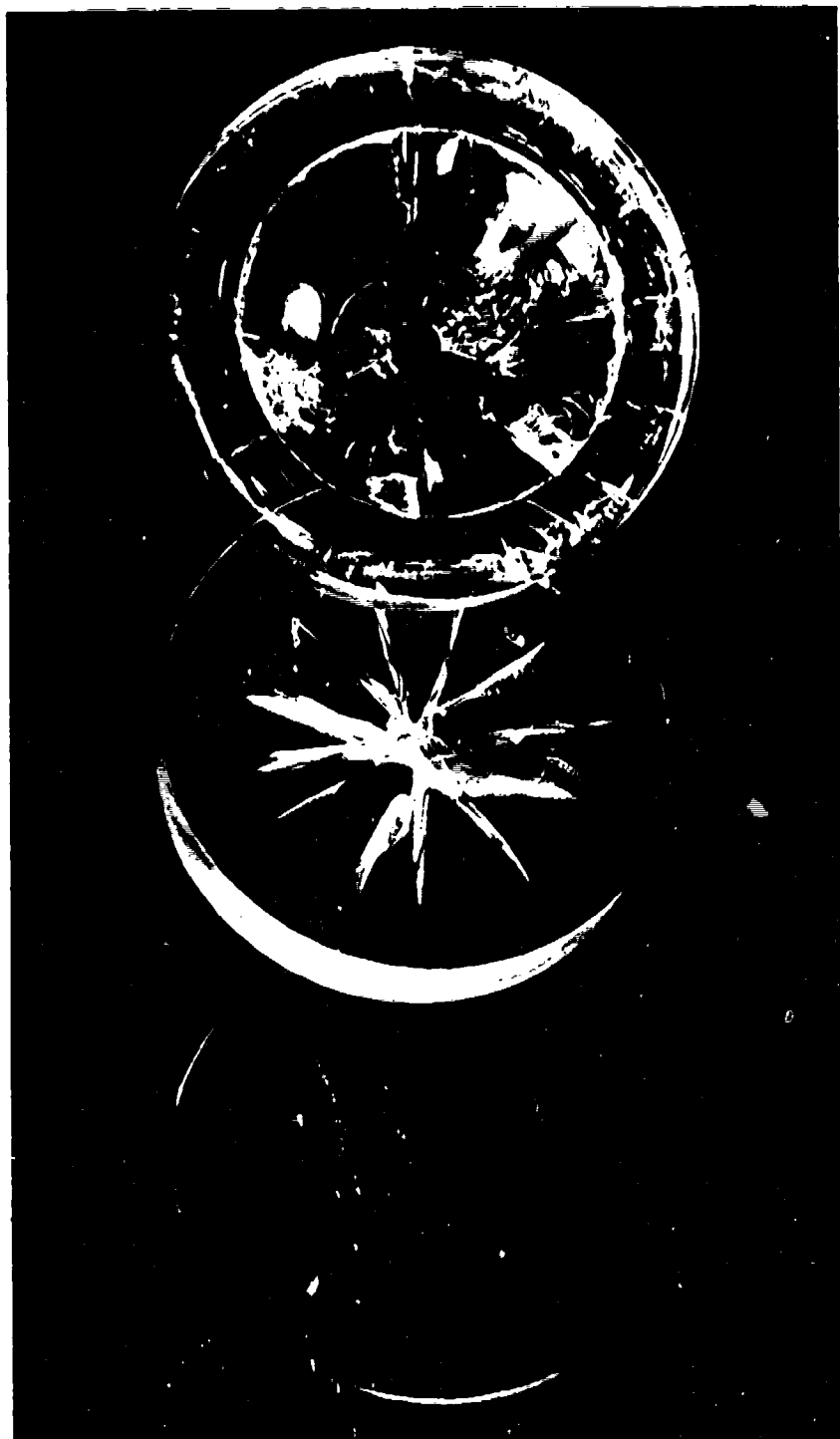
Figure 5. Three conditions of windows during their short-term testing to catastrophic failure; (1) Window under operational pressure of 450 psi, (2) Window under 800 percent overload of 4000 psi, (3) Window after 1400 percent overload of 6900 psi.
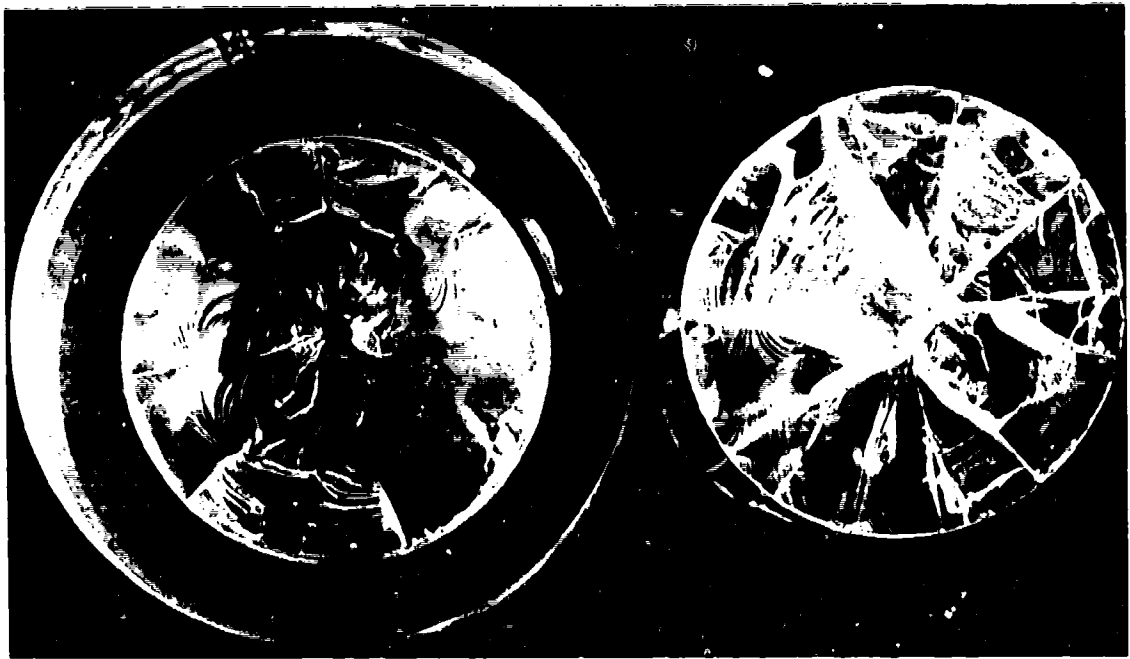
Figure 6a.   High pressure face of a failed window; note the small opening through which the compressed water penetrated into the conical fracture cavity on the low pressure face of window.
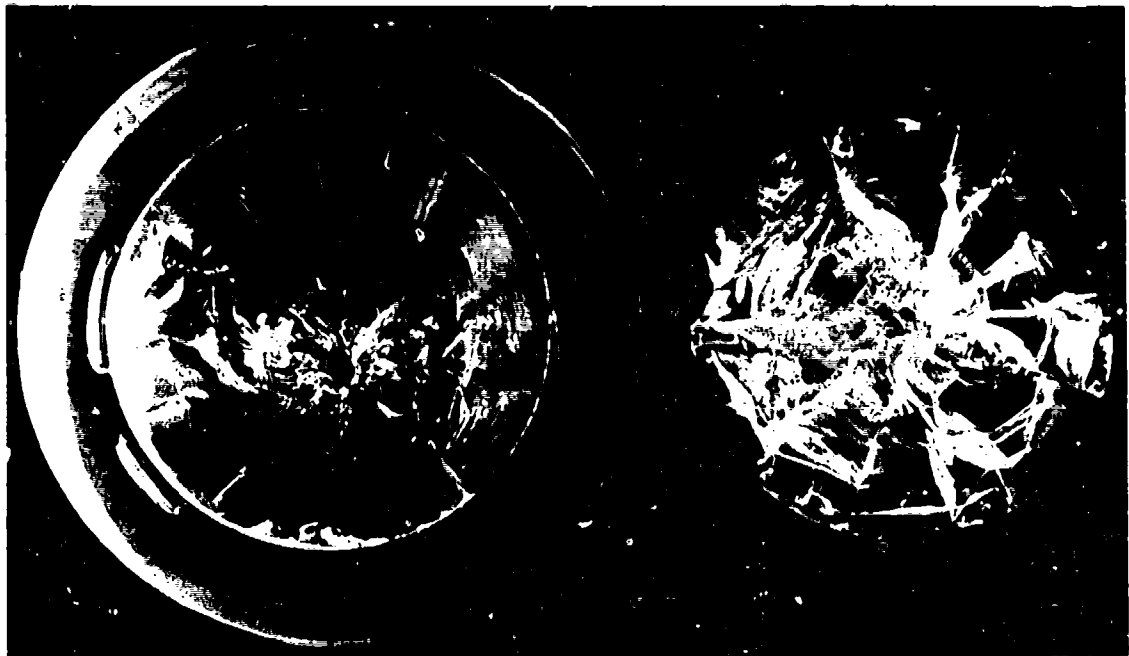
Figure 6b.   Low pressure face of a failed window; note the conical fracture cavity from which the cone-shaped plug was ejected by the compressed water entering the cavity through the small hole at its apex.
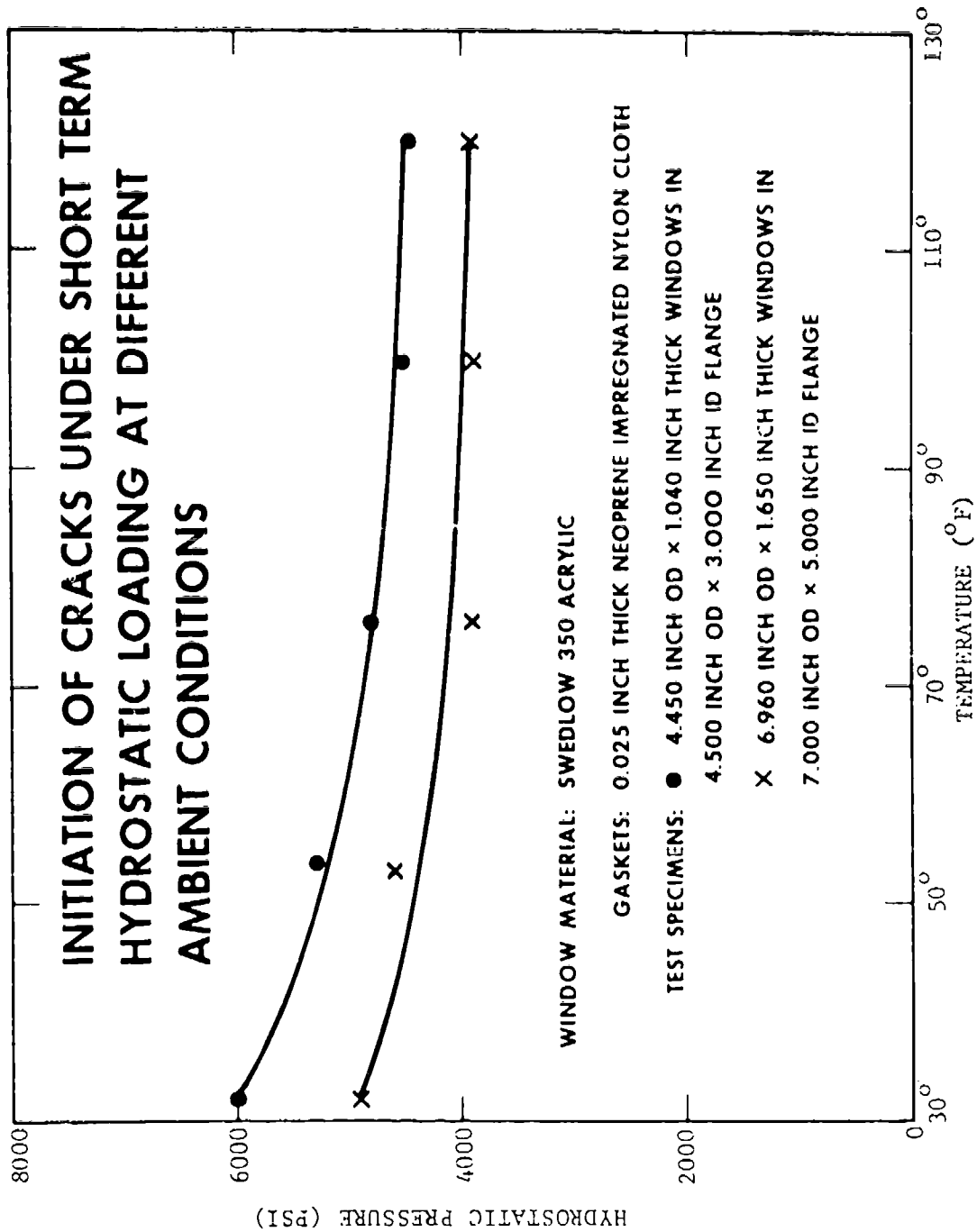
Figure 7a. Effect of temperature on the strength of EDU windows under short-term hydrostatic loading.

21
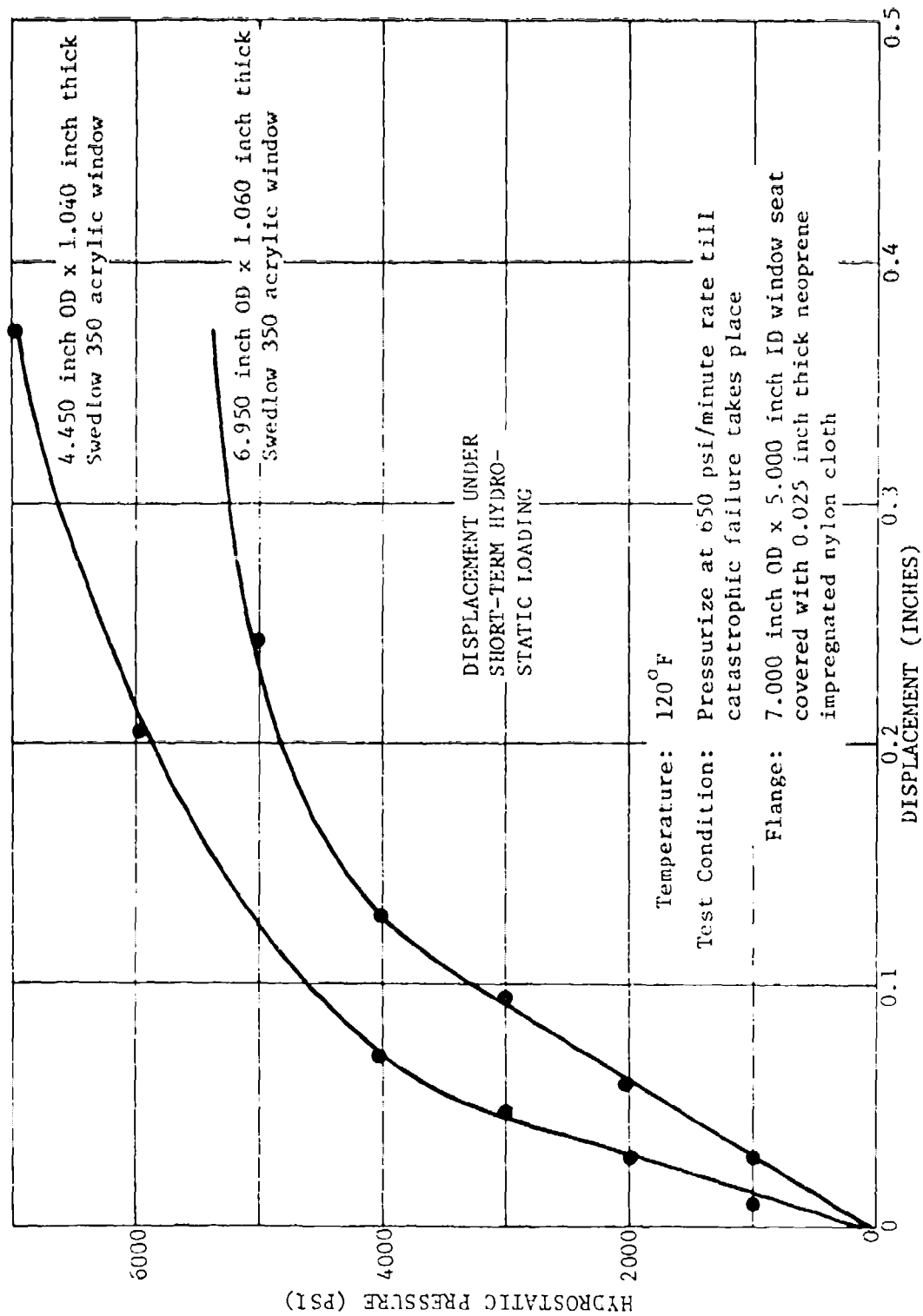
Figure 7b. Displacement of window's low pressure face center under short-term hydrostatic loading to catastrophic failure.

22
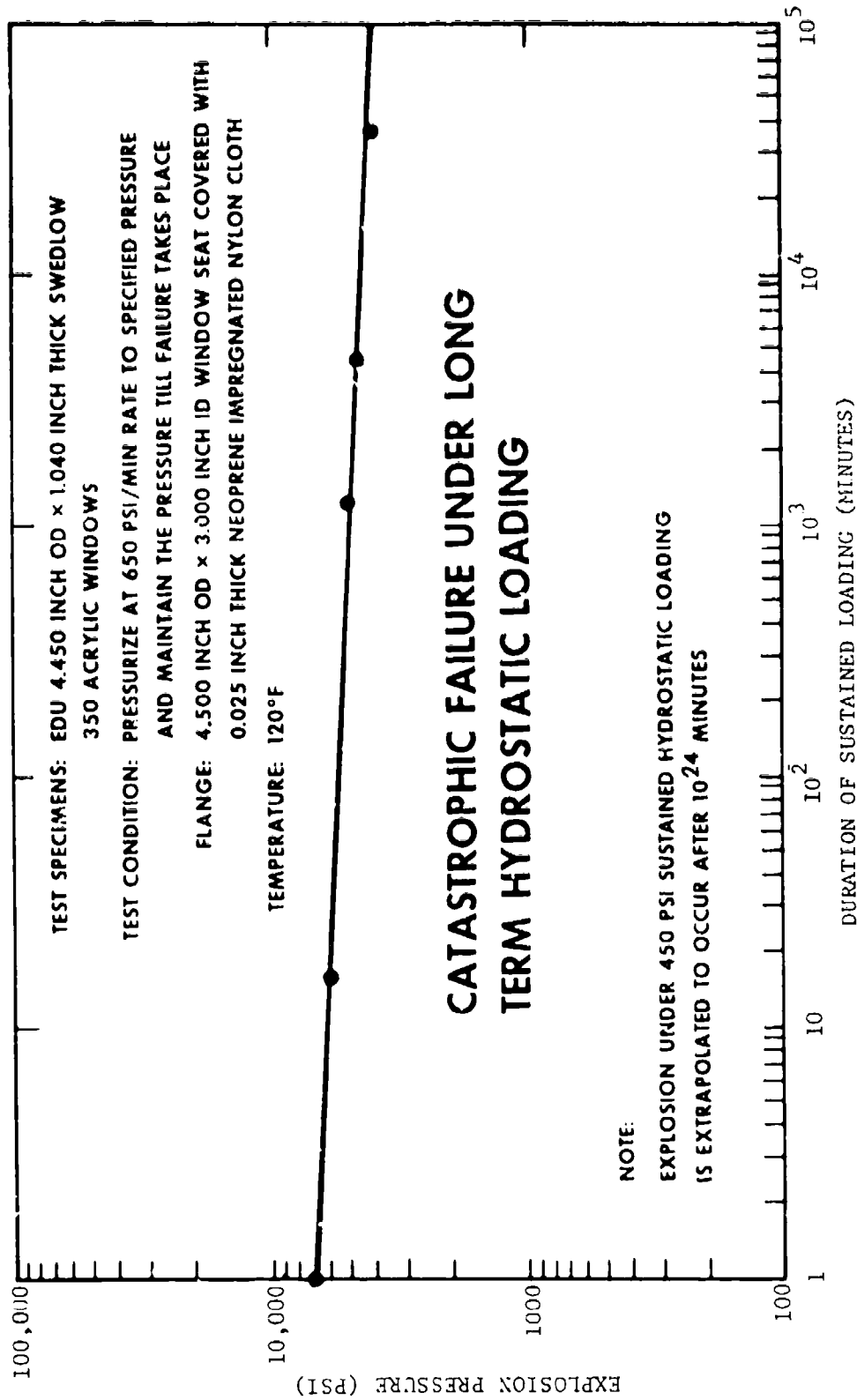
Figure 8. Effect of sustained loading on the catastrophic failure pressure of EDU 4.5-inch diameter windows.

DISPLACEMENTS UNDER LONG TERM HYDROSTATIC LOADING

TEST SPECIMENS: EDU 4.450 INCH OD × 1.040 INCH THICK SWEDLOW 350 ACRYLIC WINDOWS

TEST CONDITION: PRESSURIZE AT 650 PSI/MIN RATE TO SPECIFIED PRESSURE AND MAINTAIN THE PRESSURE TILL FAILURE TAKES PLACE

FLANGE: 4.500 INCH OD × 3.000 INCH ID WINDOW SEAT COVERED WITH 0.025 INCH THICK NEOPRENE IMPREGNATED NYLON CLOTH

TEMPERATURE: 120°F

7000 PSI

6000 PSI

5000 PSI

4000 PSI

2000 PSI

MAXIMUM OPERATING PRESSURE OF 450 PSI

DURATION OF SUSTAINED LOADING (MINUTES)

DISPLACEMENT (INCHES)

10.0 1.0 0.1 0.01

10^1 10^2 10^3 10^4 10^5

Figure 9. Displacements of window's low pressure face center under sustained hydrostatic loadings of different magnitudes; 4.5-inch diameter EDU windows.

24

CATASTROPHIC FAILURE UNDER
CYCLIC PRESSURE LOADING

TEST SPECIMENS: EDU 4.450 INCH OD × 1.040 INCH THICK SWEDLOW 350 ACRYLIC WINDOWS

TEST CONDITION: PRESSURIZE AT 650 PSI/MIN RATE TO SPECIFIED PRESSURE, MAINTAIN THAT PRESSURE FOR 7 HOURS, DEPRESSURIZE AT 650 PSI/MIN RATE TO 0 PRESSURE, AND MAINTAIN 0 PRESSURE FOR 17 HOURS BEFORE REPEATING THE CYCLE

FLANGE: 4.500 INCH OD × 3.000 INCH ID WINDOW SEAT COVERED WITH 0.025 INCH THICK NEOPRENE IMPREGNATED NYLON CLOTH

TEMPERATURE: 120°F

NOTE:
EXPLOSION UNDER CYCLIC SERVICE TO 450 PSI PRESSURE WITH 7 HOUR INDIVIDUAL CYCLE DURATION IS EXTRAPOLATED TO OCCUR AFTER 10^{10} CYCLES

NUMBER OF PRESSURE CYCLES TO EXPLOSION

MAXIMUM HYDROSTATIC PRESSURE IN THE CYCLE (PSI)

Figure 10. Effect of cyclic loading on the catastrophic failure pressure of EDU 4.5-inch diameter windows.

25

Figure 11. Arrangement for proof testing of EDU windows in NCEL's 72-inch diameter pressure vessel.
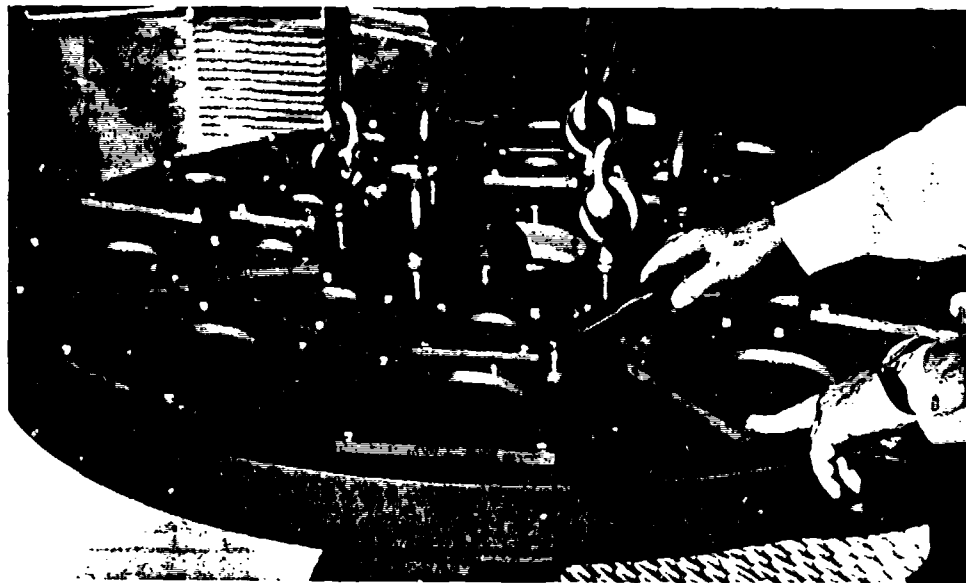
Figure 12. Flange for simultaneous proof testing of 20 EDU windows.

EFFECT OF IMPACT CRACKS ON ACRYLIC PLASTIC HYDROSPACE WINDOWS

The performance of flat disc acrylic plastic windows under short-term loading has been researched in sufficient detail[1] to establish accurately the implosion pressure of such windows. In these tests, considerable pains were taken to insure that no cracks or scratches were present in the windows prior to their implosion testing. Under operational conditions, however, it is very often impossible to prevent the generation of scratches or cracks in the surface of windows. In such cases, a real fear exists that the crack introduced initially into the high pressure face of the window by impact of an external object may serve as the source of catastrophic crack propagation failure at lesser hydrostatic pressures than the window is rated.

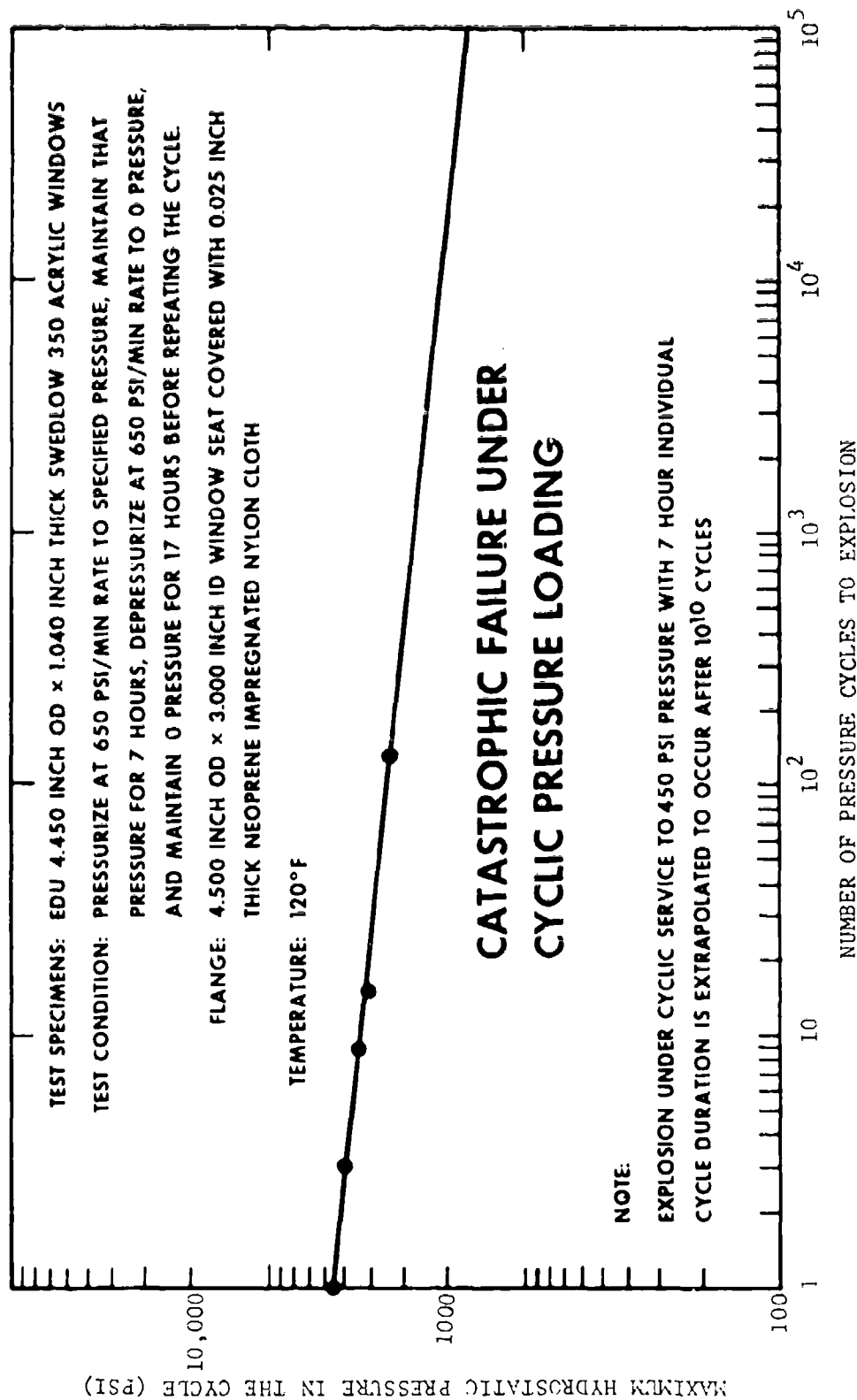For this reason, an exploratory study was conducted. As test specimens four flat disc acrylic plastic windows were used of 6-inch diameter and approximately 1¼-inch thickness (Figure A-1). Two of the windows were of monolithic construction, having been machined from 1.250 thick Plexiglas "G" plate. The other two windows were of laminated construction. The inner layer of the laminated window was 31/32 of an inch thick Plexiglas "G", the outer layer was 7/32 of an inch thick Plexiglas "G", while the layer bonding together the inner and the outer acrylic sheets was cast-in-place Swedlow SS-3330M of 3/32 of an inch thickness. One each of the monolithic and laminated windows were impacted in air with a bullet (.22 caliber long rifle Super X), fired from a distance 6 feet from the window. The other two windows were left untouched for comparison. The laminated window developed a star shaped crack that penetrated only the outer 7/32-inch thick layer, (Figure A-2), while the monolithic window was penetrated by a family of cracks 22/32 of an inch deep (Figure A-3).

All four windows were subjected to hydrostatic pressure in a typical flat window flange with a clear opening of 4 inches, and a 0.005-inch radial clearance between the edge of the window and the flange. The laminated windows were tested with the thin outer acrylic plastic layer serving as the high pressure face, while the fractured monolithic window was placed to have the cracked surface serve as the high pressure face. In this manner, both cracked windows were tested with the cracked surface acting as the high pressure face. Testing of all windows was conducted at 650 psi/min pressurization rate in 68-69°F temperature range.

The windows failed at the following pressures:

<div align="center">

Laminated window, no impact crack   = 5500 psi
Laminated window, with impact crack = 5100 psi
Monolithic window, no impact crack   = 6560 psi
Monolithic window, with impact crack = 6400 psi

</div>

All failed windows exhibited a cone shaped failure surface, with the apex of the cone being located just below the center of the high pressure face of the window. Very little difference was observed between the fracture patterns in the windows with impact cracks and those without (Figure A-4). The comparison of implosion pressures shows that no significant decrease in the window's critical pressure occurred due to the presence of cracks generated prior to pressurization by impact of rifle bullets on the high pressure face. Also the implosion pressures of laminated windows were somewhat lower than those of monolithic windows.

Several tentative conclusions can be drawn from this data. First, a crack on the high pressure face of an acrylic window does not necessarily lead to a catastrophic failure by rapid crack propagation at lesser pressures than the critical pressure of a window without such a crack. Such a crack, however, must not penetrate more than 50 percent of the window thickness and must be located in the center of the window. Second, in view of the fact that the operational pressure rating of an acrylic window generally is only about 1/10 to 1/12 of its critical pressure under short-term loading, no danger exists if the window with cracked high pressure face is inadvertently subjected only once to its operational depth. Third, a laminated window with a soft bonding layer does not possess as high a critical pressure as a monolithic window of identical diameter and thickness. Fourth, a laminated window with an impact crack on the high pressure face does not possess a higher critical pressure than a monolithic window with an impact crack.

Although it is understood that those conclusions apply directly only to specimens tested under short-term loading, they also apply, in all probability, to flat disc windows of different proportions, as well as to conical windows. It must be emphasized, however, that the above conclusions apply only to cracks on the high pressure face of the window. What the behavior of windows with impact cracks on the low pressure face is has not yet been explored in any detail.

Still, regardless of the encouraging results from this very brief study all impact cracks should be avoided on either the high or the low pressure faces of the window. If cracks do occur, the window should be replaced immediately.
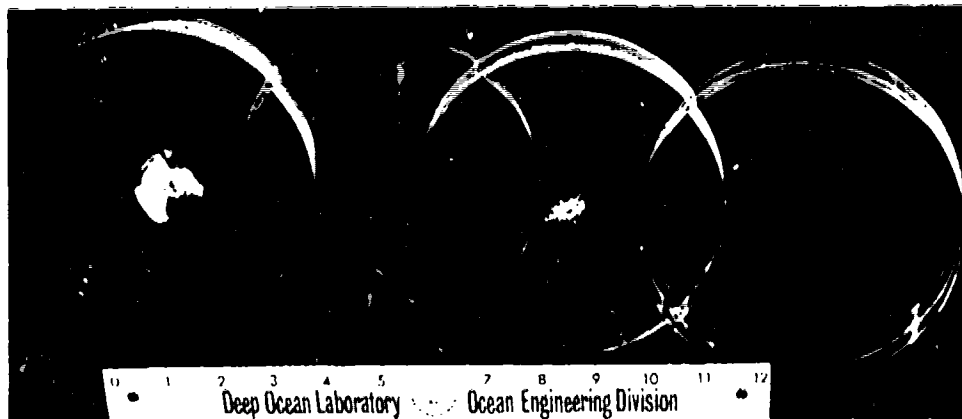
Figure A-1. Flat acrylic disc windows prior to implosion testing. The impacted window on the left is monolithic, while the impacted window on the right is of laminated construction.

Figure A-2. Impacted laminated window prior to hydrostatic testing.

Figure A-3. Impacted monolithic window prior to hydrostatic testing.
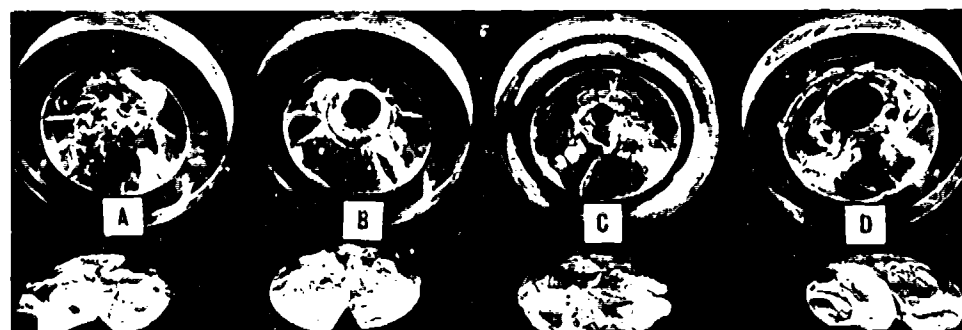
Figure A-4. Flat acrylic disc windows after implosion testing; low pressure faces
A — non-impacted laminated window
B — impacted laminated window
C -- non-impacted monolithic window
D — impacted monolithic window

29

Appendix B

EFFECT OF GASKETS ON THE SHORT-TERM STRENGTH
OF FLAT DISC ACRYLIC WINDOWS

DISCUSSION

Flat disc acrylic plastic windows require for satisfactory perform-
ance gaskets either for sealing, or cushioning in the flange. Although
sealing may be accomplished by other means besides a gasket, like for
example a radially compressed o-ring[1], gaskets are still generally
required on the high and low pressure faces of the window for cushioning
the window against contact with the metallic flange and the metallic
retaining ring. When gaskets are used, the dimensional tolerances on
flatness of the flange seat and retaining ring can be relaxed lowering
the cost of the flange assembly appreciably. Also, the use of gaskets
almost completely eliminates the danger of unforeseen point loads by
the flange and retaining ring on the window surface that may serve as
crack initiators.

Before the gaskets are chosen for a given window, some consideration
has to be given to their effect on the structural performance of the
window. Since gaskets may vary in thickness, hardness, and viscoelasti-
city, some knowledge of their effect on the catastrophic failure of windows
is required so that proper gaskets can be specified for each application.
A brief review of existing meager literature on flat disc acrylic plastic
windows revealed the absence of any experimental or analytical work
dealing with the subject of gaskets for such windows. In view of this,
a few exploratory tests with different gasket materials were performed
at NCEL on flat disc acrylic plastic windows.

TEST PROGRAM

The objective of the test program was to explore the effect of
(1) gasket thickness, (2) gasket material, and (3) retaining ring on
the short-term strength of flat disc acrylic plastic windows. The
scope was limited to only (1) one window thickness, (2) one window
diameter, (3) acrylic plastic, (4) three kinds of gasket materials, and
(5) three gasket thicknesses (Table B-1 and Figure 3-1).

Test specimens were fabricated from shrunk and unshrunk Plexiglas
"G" and Swedlow 350 flat disc acrylic plastic windows of 4.450-inch
diameter and nominal 1-inch thickness (Table B-2). Because of manufac-
turer's casting tolerance on thickness, the actual measured thickness
varied from 0.944 to 1.092 inches. Thus, the actual thickness of test
specimens was sometimes less than thickness of the windows supplied to
EDU. Still for the purposes of this exploratory investigation on gaskets,
the findings of this exploratory study are applicable directly to the
EDU windows.

Test arrangement was identical to the one described in the main body of the report except that a retaining ring was used to restrain the window in the flange (Figure 2) during the hydrostatic tests. The reasons for it were two-fold: (1) to determine whether the presence of the retaining ring has a significant effect on the pressure at which catastrophic failure occurs, and (2) the actual installation of windows in the EDU chamber does require retaining flanges.

The testing of windows was performed at 650 psi/minute rate in $120^{\circ}F$ ambient environment till catastrophic failure of the windows took place. Only the failure pressure was recorded for each test.

FINDINGS

All of the following findings apply directly only to EDU windows, although it can be postulated that they may apply also to windows with other t/D_i and t/D_o ratios.

1. There appears to be no significant difference in failure pressure of windows tested with, or without, bearing gaskets on the window seat in the flange.

2. There appears to be no significant difference in failure pressures of windows tested on thin or thick bearing gaskets.

3. There appears to be no significant difference between failure pressures of windows tested on bearing gaskets fabricated from different materials.

4. There appears to be no significant difference between failure pressures of windows fabricated from shrunk Plexiglas "G", unshrunk Plexiglas "G", or Swedlow 350 plastic.

5. There appears to be no significant difference between failure pressures of windows held in flanges with or without retaining rings.

CONCLUSION

In the selection of bearing gaskets for flat disc acrylic windows, other criteria than failure pressure of the window should be used in the selection of gasket material and its thickness.

RECOMMENDATIONS

For future hyperbaric chamber window assembly designs it is recommended that the bearing gaskets on the high and low pressure faces of the window be made of 0.125 thick commercial cork material. The sealing of the window is to be accomplished by radially compressed o-ring contained in a groove around the circumference of the window. A properly bolted retaining ring is to constrain the window inside the flange cavity. A proposed window design for service at 1000-foot simulated depth utilizing the EDU window dimensions is shown in Figure B-3.

Table B-1. Catastrophic Failure Under Short-Term Hydrostatic
Loading of Flat Disc Acrylic Windows Resting on
Different Gaskets.

Diameter (psi)	Thickness (psi)	Acrylic Plastic In Windows	Bearing Gasket Material	Implosion Pressure (psi)
4.443	0.995	shrunk Plexiglas G	none	5890
4.446	1.025	shrunk Plexiglas G	none	5620
4.451	1.035	shrunk Plexiglas G	none	6000
4.442	1.072	shrunk Plexiglas G	none	5770
4.443	1.021	unshrunk Plexiglas G	0.025 inches	6100
4.440	0.992	unshrunk Plexiglas G	thick nylon	6050
4.443	0.976	unshrunk Plexiglas G	fabric impregnated	6105
4.441	0.955	unshrunk Plexiglas G	with Neoprene	5855
4.451	1.011	shrunk Plexiglas G	0.025 inches thick	5710
4.437	1.026	shrunk Plexiglas G	nylon fabric im-	6405
4.435	1.000	shrunk Plexiglas G	pregnated with	6100
4.439	1.041	shrunk Plexiglas G	Neoprene	5850
4.450	0.946	shrunk Plexiglas G		5350
4.465	0.944	Swedlow 350		5300
6.965	1.534	Swedlow 350		5390
6.946	1.537	shrunk Plexiglas G		5400
4.447	1.011	shrunk Plexiglas G	0.125 thick	5720
4.458	1.035	shrunk Plexiglas G	Neoprene of 90	7110
4.446	1.001	shrunk Plexiglas G	durometer hardness	7580
4.446	1.028	shrunk Plexiglas G		6380
4.448	0.997	shrunk Plexiglas G	0.125 thick	6120
4.443	1.092	shrunk Plexiglas G	cork gasket	5510
4.442	1.016	shrunk Plexiglas G		6000
4.495	1.001	shrunk Plexiglas G		6430
4.442	1.052	shrunk Plexiglas G	0.250 thick	5740
4.441	1.030	shrunk Plexiglas G	Neoprene of	5640
4.445	1.091	shrunk Plexiglas G	90 durometer	5710
4.446	1.049	shrunk Plexiglas G	hardness	5780

NOTE: 1. All windows were tested at 650 psi/minute rate in 119-120°F
ambient temperature environment.
2. The opening in the flange for small windows is 3.000 inches,
while for large windows it is 5.000 inches.
3. All bolts on the retaining ring were torqued down to 20-foot lbs.
4. The compression gasket under the retaining ring was in every case
0.125 thick cork gasket.

Table B-2. Mechanical Properties of Acrylic Plastic[*]
Plate Used for the Fabrication of Test Windows

Property Measured	Minimum	Average	Maximum
Compressive Yield, psi (ASTM D-695)	17,300	17,300	17,300
Compressive Modulus of Elasticity, psi (ASTM D-695)	5.1×10^5	5.2×10^5	5.3×10^5
Deformation Under Compressive Load, percent (ASTM D-621-64; 4000 psi at 122°F for 24 hrs.)	0.36	0.51	0.63
Tensile Ultimate Strength, psi (ASTM D-638-64)	10,200	10,500	10,900
Tensile Modulus of Elasticity, psi (ASTM D-638-64)	4.4×10^5	4.5×10^5	4.6×10^5
Tensile Elongation at Failure, percent (ASTM D-638-64)	3.3	3.4	4.2
Flexure Strength, psi (ASTM D-790)	11,500	15,000	16,700
Flexure Modulus of Elasticity, psi (ASTM D-790)	4.7×10^5	4.8×10^5	4.9×10^5
Shear Strength, psi (ASTM D-732)	9,340	9,410	9,470

[*]Plexiglas G acrylic plastic meeting MIL-P-21105C specification.
Test specimens were cut from plate prior to shrinking it at 300°F.

33
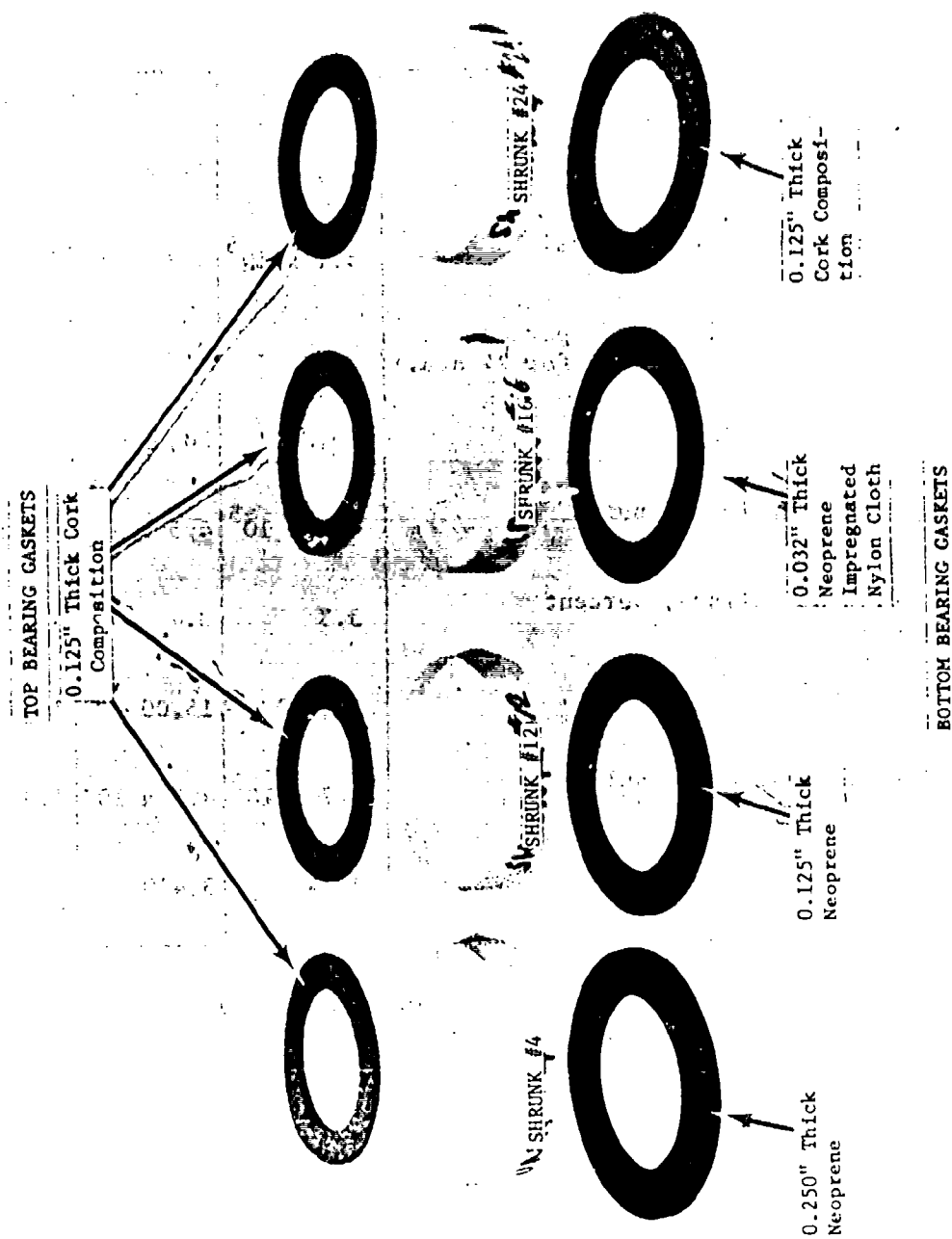
Figure B-1. Typical gaskets used with windows during the gasket evaluation tests.

34
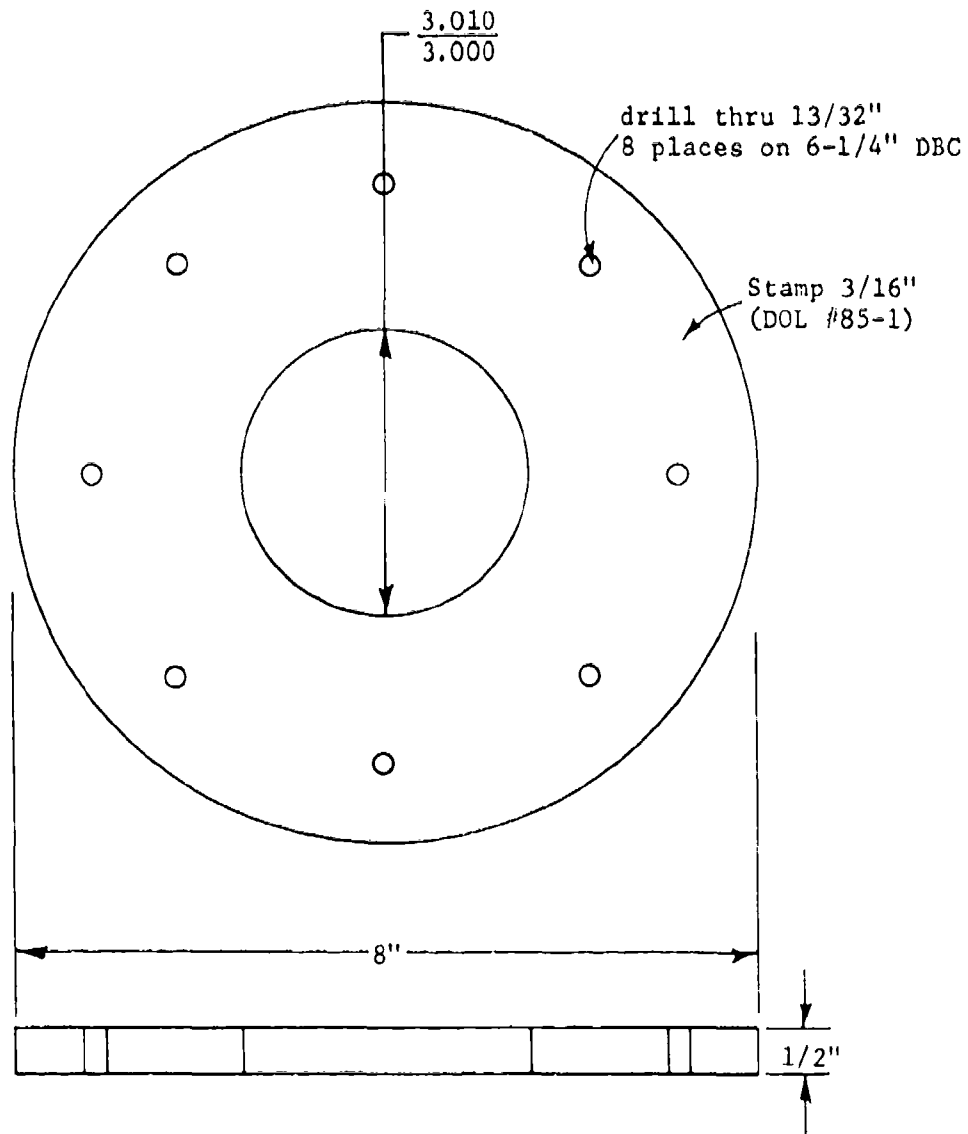
Figure B-2. Retaining ring used in the gasket evaluation tests for
compressing the gaskets on the high and low pressure
faces of the windows.

35
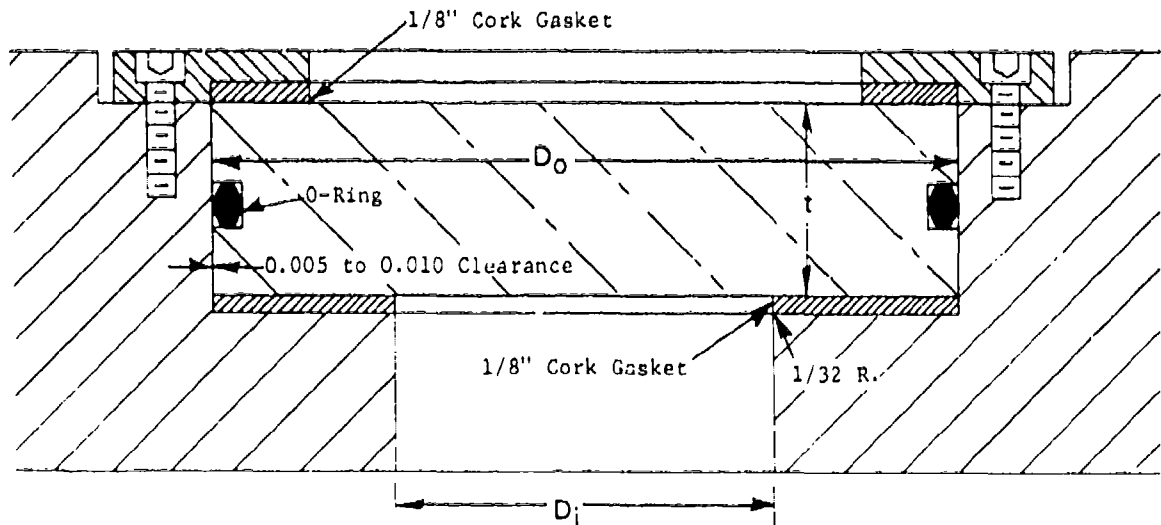
Notes for Windows:

1. Use acrylic plastic MIL-P-21105C, MIL-P-5425 or MIL-P-8184 with mechanical properties satisfying NCEL specifications.

2. All machined surfaces to have $\sqrt{63}$ or better finish.

3. Use a 1/32-inch radius on all corners, particularly the groove.

4. Anneal after machining for 24 hours at $165^{\circ}F$.

5. For 450 psi service, use $t/D_i \geq 0.325$.

Notes for Flange:

1. D_o/D_i must be in 1.250 - 1.500 range.

2. The surface contacting the O-ring should be $\sqrt{63}$ or better.

Notes for Gaskets:

1. Use cork, or neoprene with 90 durometer hardness.

2. Do not use grease on bearing surfaces of windows.

3. Bond one gasket to flange seat, the other to retaining ring.

Figure B-3. Proposed window assembly design for future applications in hyperbaric chambers operating at 450 psi.

REFERENCES

1.   Technical Report R-527, "Windows for External or Internal Hydrostatic Pressure Vessels; Part II - Flat Acrylic Windows Under Short-Term Pressure Application," by J. D. Stachiw, G. M. Dunn, and K. O. Gray, Naval Civil Engineering Laboratory, May 1967.

2.   Technical Report R-676, "Development of A Spherical Acrylic Plastic Pressure Hull for Hydrospace Application," by J. D. Stachiw, Naval Civil Engineering Laboratory, April 1970.

DOCUMENT CONTROL DATA · R & D

(Security classification of title, body of abstract and indexing annotation must be entered when the overall report is classified)

1. ORIGINATING ACTIVITY (Corporate author)	2a. REPORT SECURITY CLASSIFICATION
Naval Civil Engineering Laboratory Port Hueneme, California 93041	Unclassified 2b. GROUP

3. REPORT TITLE

FLAT DISC ACRYLIC PLASTIC WINDOWS FOR MAN-RATED HYPERBARIC CHAMBERS AT THE USN EXPERIMENTAL DIVING UNIT

4. DESCRIPTIVE NOTES (Type of report and inclusive dates)

5. AUTHOR(S): (First name, middle initial, last name)

J. D. Stachiw

6. REPORT DATE	7a. TOTAL NO. OF PAGES	7b. NO. OF REFS
November 1970	37	2

8a. CONTRACT OR GRANT NO	9a. ORIGINATOR'S REPORT NUMBER(S)
b. PROJECT NO 56-020	TN-1127
c.	9b. OTHER REPORT NO(S) (Any other numbers that may be assigned this report)
d.	

10. DISTRIBUTION STATEMENT

This document has been approved for public release and sale; its distribution is unlimited.

11. SUPPLEMENTARY NOTES	12. SPONSORING MILITARY ACTIVITY
	Supervisor of Salvage

13. ABSTRACT

Flat disc acrylic plastic windows have been designed, fabricated, evaluated and delivered to EDU for replacement of glass windows used to date. The large (D = 6.950 inches; t = 1.650 inches) and the small (D = 4.450 inches, t = 1.040 inches) windows have been found on the basis of an extensive evaluation program to be more than adequate for man-rated service under 450 psi maximum operational pressure in steel flanges with D_i (diameter of opening in flange) of 5.000 and 3.000 inches. All windows were prooftested to 675 psi pressure at 120°F ambient temperature prior to delivery.

DD FORM 1473 (PAGE 1)
1 NOV 65

S/N 0101-807-6801

14 KEY WORDS	LINK A		LINK B		LINK C	
	ROLE	WT	ROLE	WT	ROLE	WT
Acrylic resins						
Plastics						
Windows						
Hyperboric chambers						
Performance tests						
Pressure vessels						
Undersea						
Diver						

RECOMMENDED PRACTICES FOR THE DESIGN, FABRICATION, PROOFTESTING AND INSPECTION OF WINDOWS IN MAN-RATED HYPERBARIC CHAMBERS

by

J. D. Stachiw

Ocean Technology Department
December 1973

NAVAL UNDERSEA CENTER, SAN DIEGO, CA. 92132

AN ACTIVITY OF THE NAVAL MATERIAL COMMAND

ROBERT H. GAUTIER, CAPT, USN
Commander

Wm. B. McLEAN, Ph.D.
Technical Director

ADMINISTRATIVE STATEMENT

ACKNOWLEDGEMENTS

SUMMARY

PROBLEM

Hyperbaric chambers require windows for chamber interior observation during their manned operations. Pressure-resistant windows are not covered by any existing national codes, and the designers, fabricators and operators of hyperbaric chambers frequently must use their own judgment to achieve and maintain a safe window system in a hyperbaric chamber. Inasmuch as most of them are not familiar with the acrylic plastic material used for the windows, they can easily err in specifying windows wi   . inadequate safety margin.

RESULTS

Existing data on the design, fabrication and inspection of windows in hyperbaric chambers have been reviewed and checked for applicability to the use of these windows. Based on this study, a set of recommended practices has been proposed and if these practices are followed they will lead to safe window systems in hyperbaric chambers.

RECOMMENDATIONS

The practices recommended in this report for the design, fabrication and inspection of windows in hyperbaric chambers should receive careful consideration and be used as guidelines when new hyperbaric chambers are being specified or old ones overhauled. Radical deviations from the recommended practices should be used only after a thorough review of all pertinent engineering parameters and experimental validation of the design.

PREFACE

Most designers, fabricators, and operators are unfamiliar with the acrylic plastic material used in the construction of observation windows for hyperbaric chambers. For this reason they could inadvertently specify and procure windows with inadequate safety margins for manned operations.

This report discusses the range of practices recommended for use of the acrylic plastic material in windows of hyperbaric chambers. The information covers material, magnitude of pressure service, type of pressure service and range of ambient temperatures. The plastic discussed is methyl metacrylate, commonly known as acrylic plastic. The pressure service is limited to 3500 psia pressure differential between internal and external pressures, which are understood to be of static or cyclic nature. Temperature service is limited to temperatures in the -60 to +150°F range.

These practices follow the cookbook approach, making their use feasible even by personnel with limited technical background in plastic materials. The recommended practices are not set forth to stifle competent structural engineers in their imaginative research and development designing of window systems for hyperbaric chambers. The recommendations are made, rather, to advise and provide specifications for those engineers who need immediate specifications to procure economical observation chambers with proven state of technological construction. For the engineer experienced in this field, the report provides him with guidelines of what has been done successfully thus far.

For pressure differentials in excess of 3500 psi and window shapes not discussed in this report, consult the Safety Standard for Pressure Vessels for Human Occupancy available from the American Society of Mechanical Engineers as publication ASME/ANSI PVHO-1. The above safety standard follows closely the recommended practices of this report and, because of it, can be safely utilized to extend its scope.

CONTENTS

SECTION 1

SERVICE CONDITIONS

Design of windows must be determined by the projected service to which they will be subjected. Only three pressure service conditions are foreseen for the manned chambers in which the windows are located: internal pressurization only, external pressurization only and hybrid pressurization service, in which both internal and external pressurizations are encountered.

In addition to pressure service conditions, there are also temperature service conditions that must be considered. Three temperature service conditions have been established as standard for manned chambers: they are frigid, temperate and tropic. In each case, the type of service is defined by the maximum temperature that ever may be encountered by the hyperbaric chamber *when pressurized*.

1.1 PRESSURE SERVICE CONDITIONS

1.1.1 Internal Pressurization Service

Internal pressurization service is a loading condition that subjects the chamber solely to internal pressure which is always higher than the external pressure. The internal pressure may be of short duration, long duration, or cyclic. In no case will the interior of the vessel be at a lower pressure than its exterior. The magnitude of the most severe expected pressure loading will be established by computing the maximum absolute difference between the internal and external pressure to which the chamber may be subjected during its projected operational life. This absolute pressure differential will be referred to as the "maximum internal loading."

1.1.2 External Pressurization Service

External pressurization is a loading condition that subjects the chamber solely to external pressure that is always higher than the internal pressure. The external pressure may be of short duration, long duration, or cyclic. In no case will the interior of the vessel be at higher pressure than its exterior. The magnitude of the most severe expected pressure loading will be established by computing the maximum absolute difference between the internal and external pressure to which the chamber may be subjected during its projected operational life. This absolute pressure differential will be referred to as the "maximum external loading."

1.1.3 Hybrid Pressurization Service

Hybrid pressurization service is a service in which, during the chamber's life, the internal pressure may be higher at times than the external pressure, while at other times the external pressure is higher. To define quantitatively the hybrid pressurization service, it is necessary to know both the maximum internal and maximum external loadings to which the chamber may be subjected during its projected operational life.

1.2 TEMPERATURE SERVICE CONDITIONS

1.2.1 Frigid Temperature Service

Frigid temperature service is the range of ambient temperatures acting upon one or both faces of the windows where the highest temperature encountered is below +75°F.

1.2.2 Temperate Temperature Service

Temperate temperature service is the range of ambient temperature acting upon one or both faces of the windows where the highest temperature encountered is below +120°F.

1.2.3 Tropic Temperature Service

Tropic temperature service is the range of ambient temperatures acting upon one or both faces of the windows where the highest temperature encountered is below +150°F.

SECTION 2

WINDOW CONFIGURATIONS

Pressure-resistant acrylic plastic windows are available in three standard shapes: circular flat discs, conical frustums and regular spherical sectors (figure 2.1). Depending on the foreseen service conditions to which the chamber will be subjected, the window configuration may employ a single shape or a combination of shapes.

2.1 CONFIGURATIONS FOR INTERNAL PRESSURE SERVICE

For internal pressurization only, three standard window configurations are available. Each of these configurations utilizes only a single circular window element (figure 2.2).

2.1.1 Flat Disc Configuration

Uses a single circular flat disc set inside a mounting with a cylindrical cavity (figure 2.2).

2.1.2 Conical Frustum Configuration

Uses a single conical frustum set inside a mounting with a cone shaped cavity whose minor diameter is on the exterior of the chamber (figure 2.2).

2.1.3 Spherical Sector Configuration

Uses a single spherical sector set inside a mounting with a true spherical cone bearing surface whose apex coincides with the center of the sphere (figure 2.2). When set inside the mounting, the window has the concave surface on the exterior of the vessel.

2.2 CONFIGURATIONS FOR EXTERNAL PRESSURE SERVICE ONLY

For external pressurization, only three standard window configurations are available. Each of these configurations utilizes only a single circular window element (figure 2.3).

2.2.1 Flat Disc Configuration

Uses a single circular flat disc set inside a mounting with a cylindrical cavity (figure 2.3).

2.2.2 Conical Frustum Configuration

Uses a single conical frustum set inside a mounting with a cone-shaped cavity whose minor diameter is on the interior of the vessel (figure 2.3).

Spherical Sector Window With Conical Edge
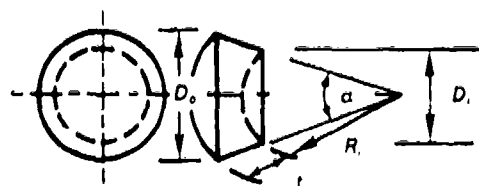
$t \geq 1/2$ in. (12.5 mm)
$\alpha \geq 60$ deg.
$t/R_i \geq 0.09$ for $\alpha \geq 60$ deg.
$t/R_i \geq 0.06$ for $\alpha \geq 90$ deg.
$t/R_i \geq 0.03$ for $\alpha = 180$ deg.
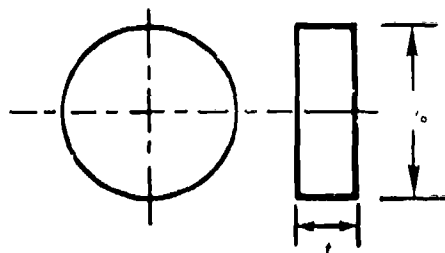
Flat Disk Window

$t \geq 1/2$ in. (12.5 mm)
$t/D_o \geq 0.125$

Conical Frustum Window
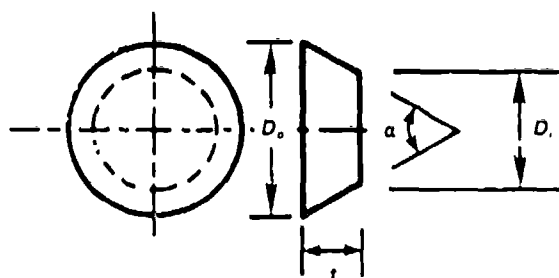
$t \geq 1/2$ in. (12.5 mm)
$t/D_i \geq 0.125$
$\alpha \geq 60$ deg.

Double Beveled Disk Window
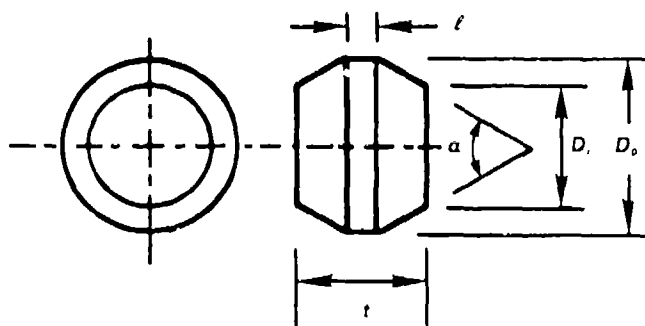
$t \geq 1/2$ in. (12.5 mm)
$t/D_i \geq 0.250$
$\alpha \geq 60$ deg.
$\ell \leq 0.25t$

FIG. 2. 1 STANDARD WINDOW GEOMETRIES
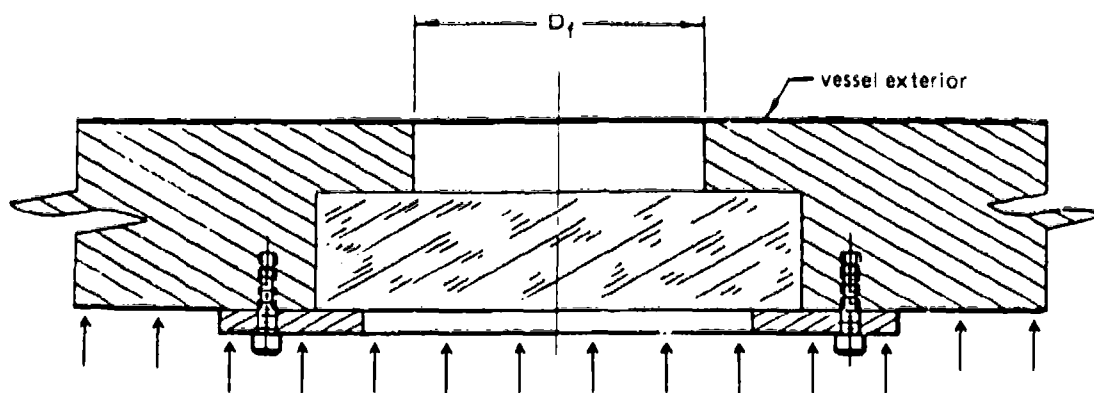
flat disc window configuration
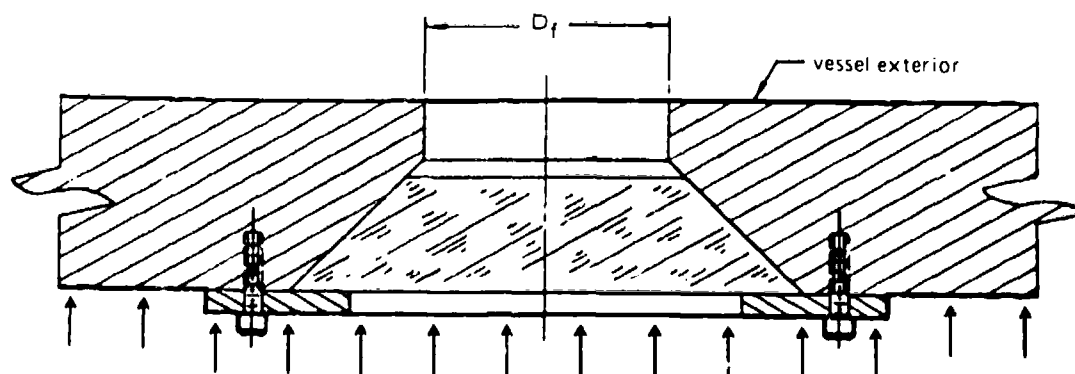
conical frustum configuration
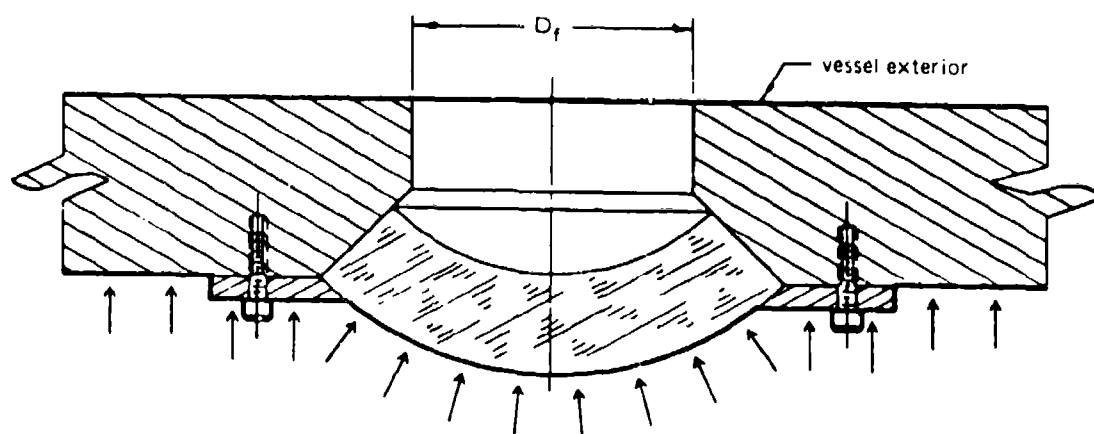
spherical window configuration

Figure 2.2. Configurations for internal pressure.
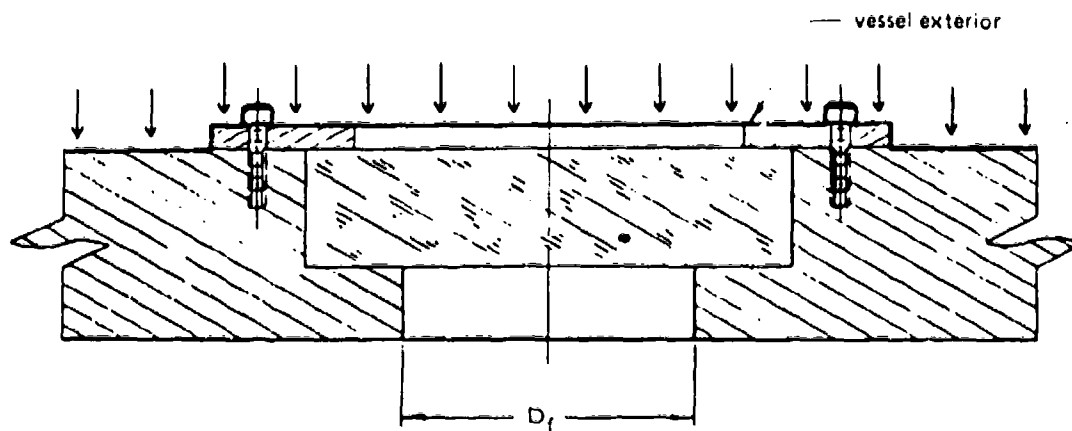
flat disc window configuration
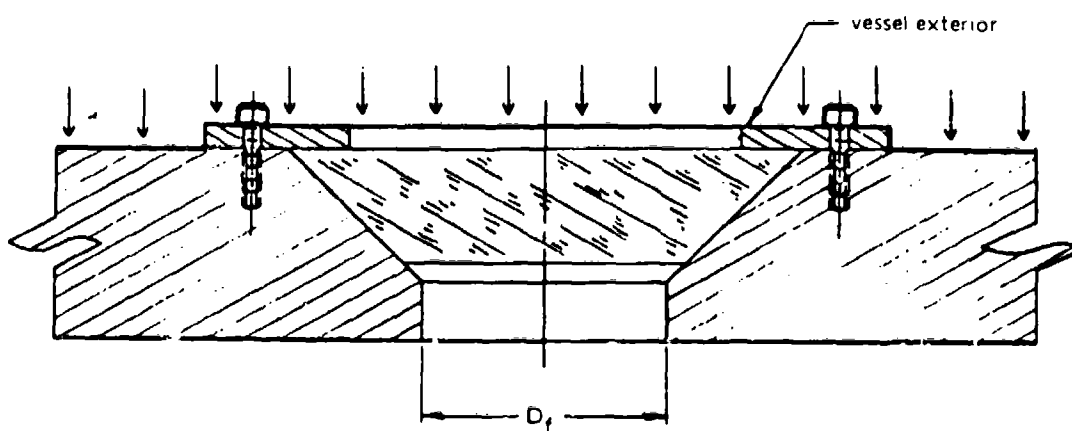
conical frustum configuration
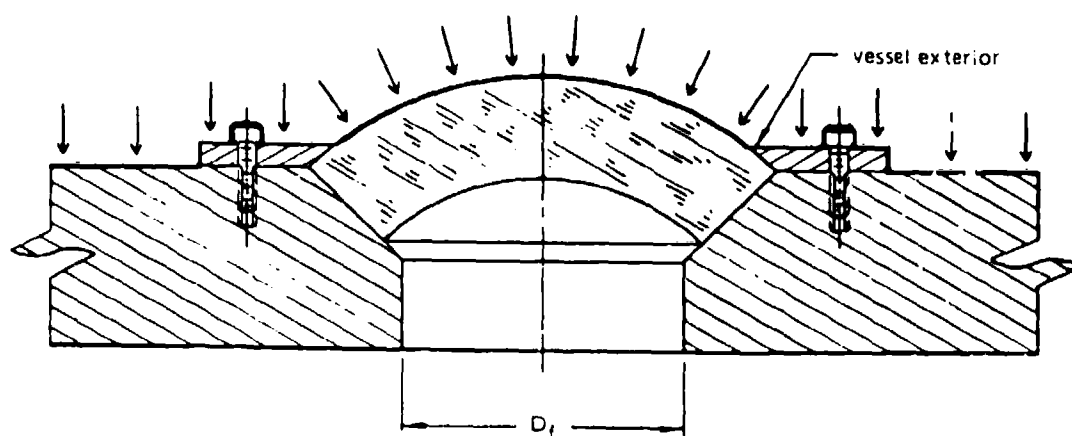
spherical window configuration

Figure 2.3. Configurations for external pressure.

2.2.3 Spherical Sector Configuration

Uses a single spherical sector set inside a mounting with a true spherical cone bearing surface whose apex coincides with the center of the sphere (figure 2.3). The concave surface of the window is on the interior of the vessel.

2.3 CONFIGURATIONS FOR HYBRID PRESSURE SERVICE

There are only three standard window configurations available for hybrid pressure service. Two of the configurations utilize a single window element, while the third uses two (figure 2.4).

2.3.1 Flat Disc Configuration

Uses a single circular flat disc set inside a mounting with a cylindrical cavity (figure 2.4).

2.3.2 Beveled Disc Configuration

Uses a single circular flat disc with beveled edges set inside a mounting with a matching cavity (figure 2.4).

2.3.3 Twin Conical Frustum Configuration

Uses two conical frustums set in a single mounting. The conical frustums are arranged to have their minor diameters facing each other in the mounting.
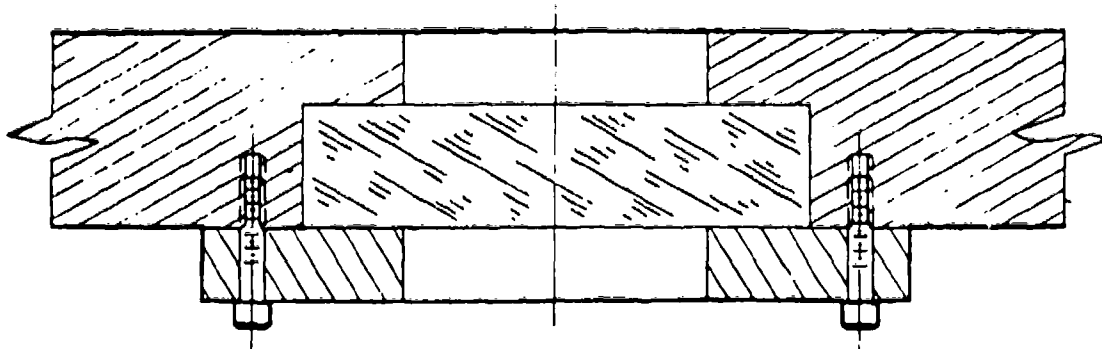
flat disc window configuration
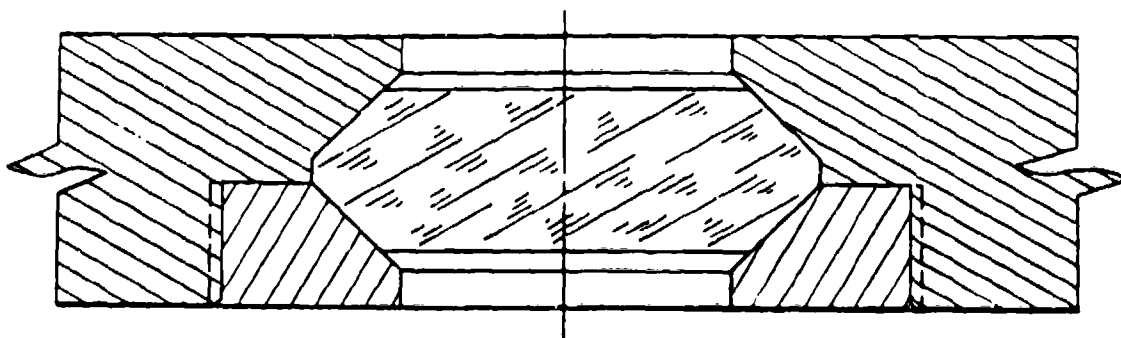
beveled disc window configuration
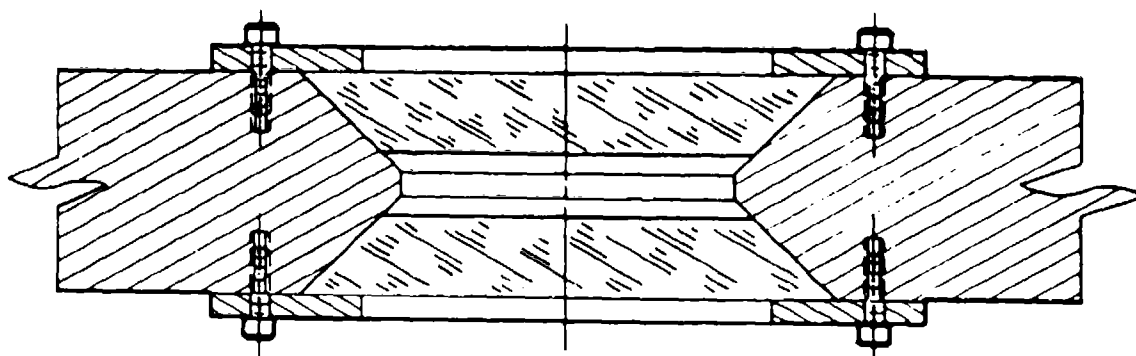
double conical frustum configuration

Figure 2.4. Configurations for hybrid pressure loading.

SECTION 3

WINDOW DESIGN CONSIDERATIONS

The determination of window dimensions is based on the optical requirements, projected future service conditions and window configuration. Optical requirements are beyond the scope of these design recommendations; they will not be considered here. Window configurations and pressure and temperature service conditions, discussed in Section 2, may be referred to for further information. Service conditions which include not only direction of pressure but also ambient temperatures, also discussed in Section 1. are important and the designer should acquaint himself with the different classifications established for them.

This section addresses itself to the selection of window thickness, dimensional tolerances and surface finishes required to withstand safely the pressure and temperature service conditions encountered during the life of the hyperbaric chamber.

3.1 DETERMINATION OF SERVICE CONDITIONS

3.1.1 Type of Pressure Service Condition

The pressure service condition controlling the window design will be determined by establishing whether the hyperbaric chamber under design is subjected to internal, external or hybrid pressurization service.

3.1.2 Magnitude of Pressure Service Condition

The *magnitude* of pressure service condition controlling the window design will be established by determining the maximum internal and/or external pressures the window will encounter during its operational life. Pressures met by windows during proof testing of the whole hyperbaric chamber or individual windows will not be taken into consideration if they do not exceed the maximum operational pressure by 50 percent.

3.1.3 Magnitude of Ambient Temperature

The magnitude of ambient temperature condition controlling the window design will be established by determining the maximum ambient temperature acting upon the window when it is pressurized. Peaks of ambient temperature fluctuations lasting less than 60 seconds and separated by at least a 30 minute interval are disregarded for consideration as maximum temperatures.

3.2 METHODS FOR SELECTION OF WINDOW THICKNESS

3.2.1 Nondimensional t/D_i Ratio

The nondimensional overall thickness to minor window diameter ratio (t/D_i) is the basic parameter used to establish the required window thickness for a specific set of pressure and ambient temperature service conditions. The validity of t/D_i ratio has been established both analytically and experimentally in scaling window dimensions from model to full scale for hydrostatic pressure service for the three windows recommended for hyperbaric chamber service.

3.2.2 Short-Term Critical Pressure

The short-term critical pressure experimentally established on window test specimens at 70°F ambient temperature will serve as the basis for establishing safe operational pressure of windows in hyperbaric chambers. The critical pressure is the hydrostatic pressure on the high-pressure face of the window that will cause a release of pressure and catastrophic structural failure of the window. "Short term" denotes that the pressurization rate is 650 psi/min during destructive testing of windows.

The critical short-term pressures have been experimentally established for the three standard window shapes and their average values have been plotted as a function of t/Di ratios (figures 3.1, 3.2 and 3.3). Since a plot of short-term critical pressure for beveled discs (figure 2.4) is not available, the critical pressures of conical frustums (figure 3.2) will be utilized with the provision that the cylindrical land (l) on the beveled disc does not exceed 0.25t of the beveled window. For other window shapes, consult the ASME/ANSI PVHO-1 publication.

3.2.3 Conversion Factors

Factors designated as conversion factors, correlate the maximum operational pressure with the short-term critical pressure to serve as the basis of window design. The magnitude of a conversion factor expresses the relationship between a window's maximum operational pressure and its short-term critical pressure at 70°F. In practice, the maximum operational pressure is multiplied by the conversion factor to arrive at the required short-term critical pressure for the window.

The magnitudes of allowable conversion factors fall in the range of 4 to 16. The exact magnitude of conversion factor chosen will depend both on the temperature service conditions and on the extent of the additional testing program contemplated for window certification.

Where no additional testing program of windows is contemplated prior to request for certification, the conversion factors will be chosen from the range 6 to 16, the exact magnitude depending upon the temperature service condition. Frigid temperature service condition requires a minimum conversion factor of 6, temperate service condition, a minimum conversion factor of 10 and tropic, a minimum conversion factor of 16. Larger conversion factors
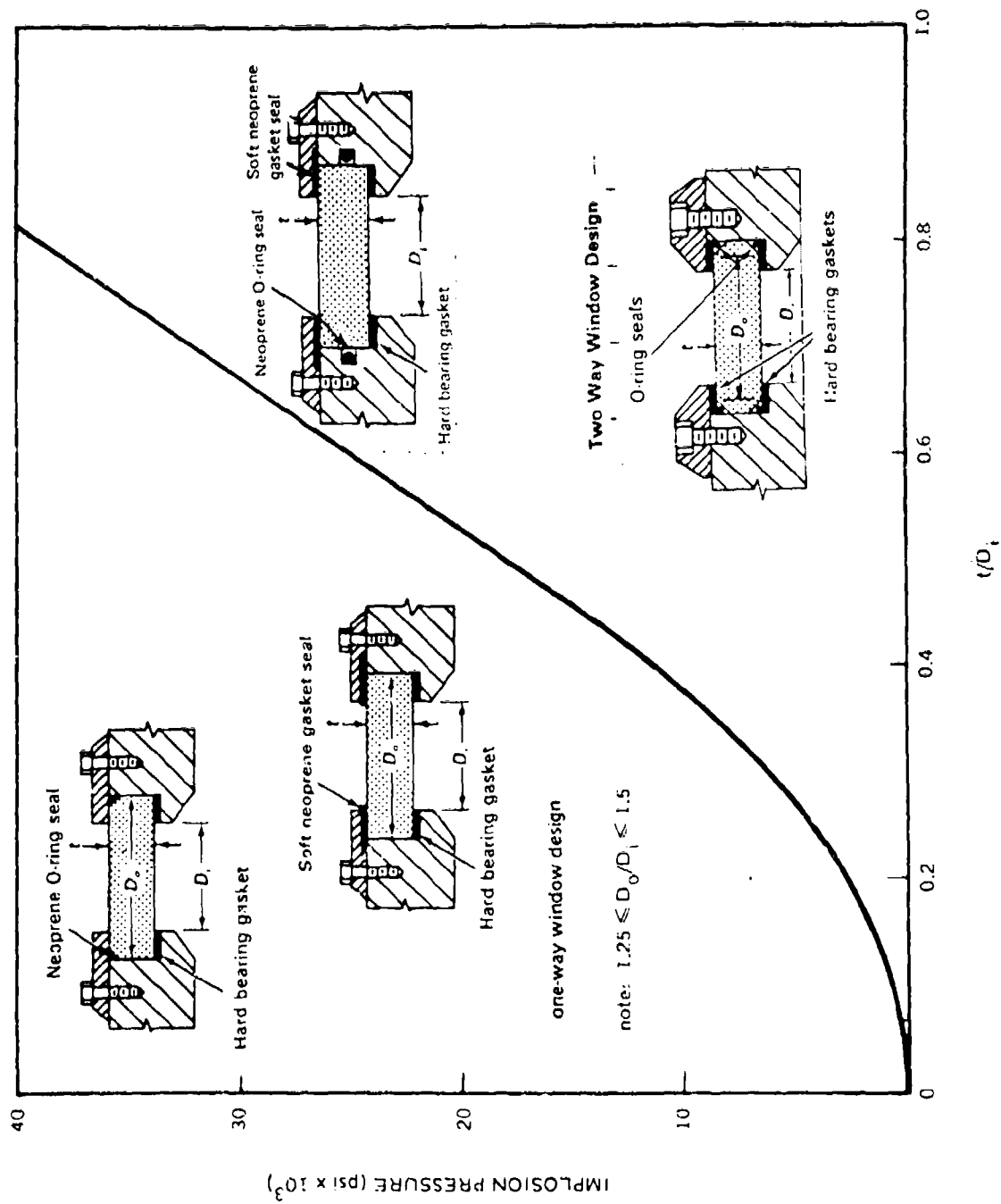
Figure 3.1. Short-term critical pressure of flat disc acrylic windows.
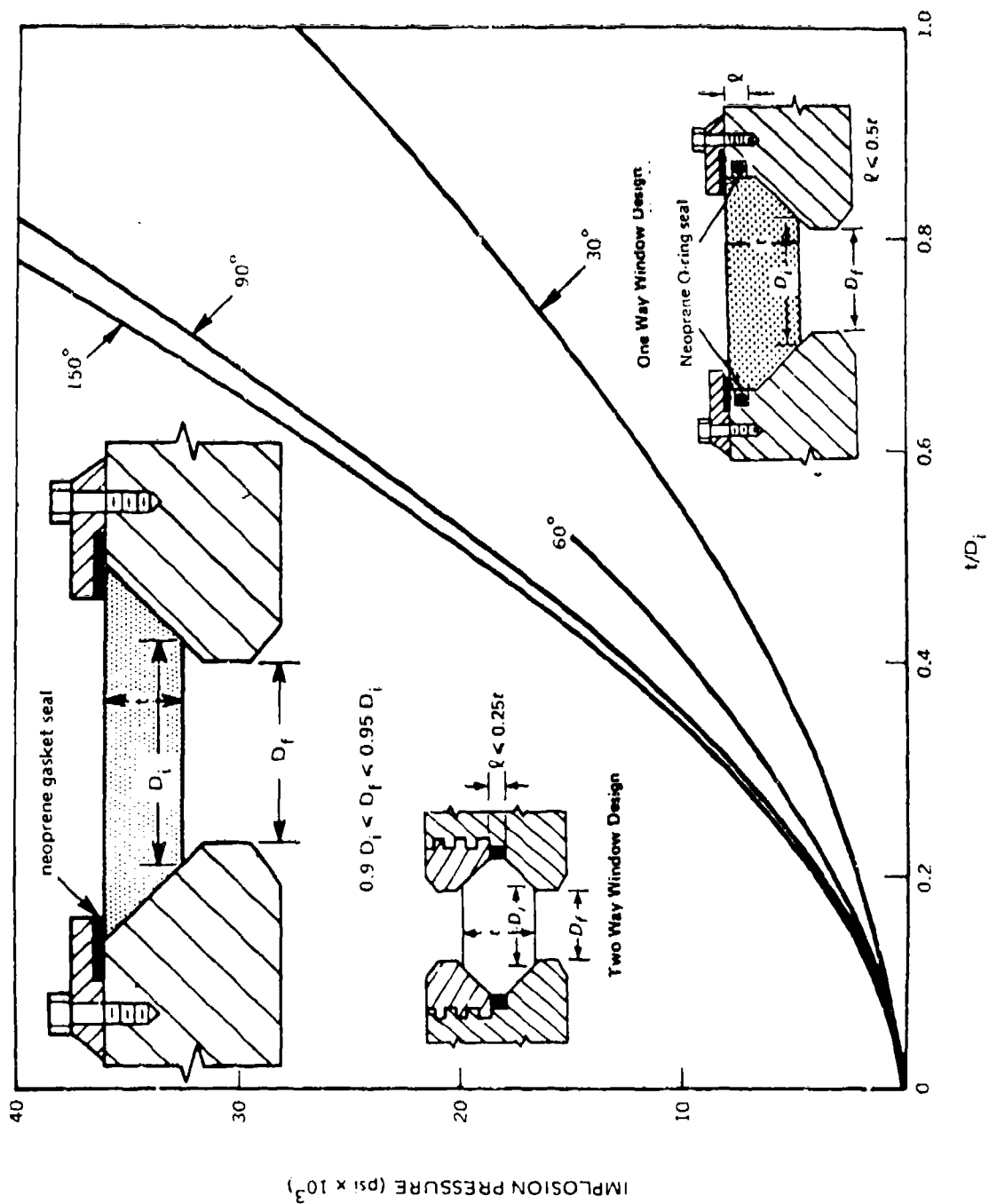
Figure 3.2. Short-term critical pressure of conical frustum acrylic windows.

3-4
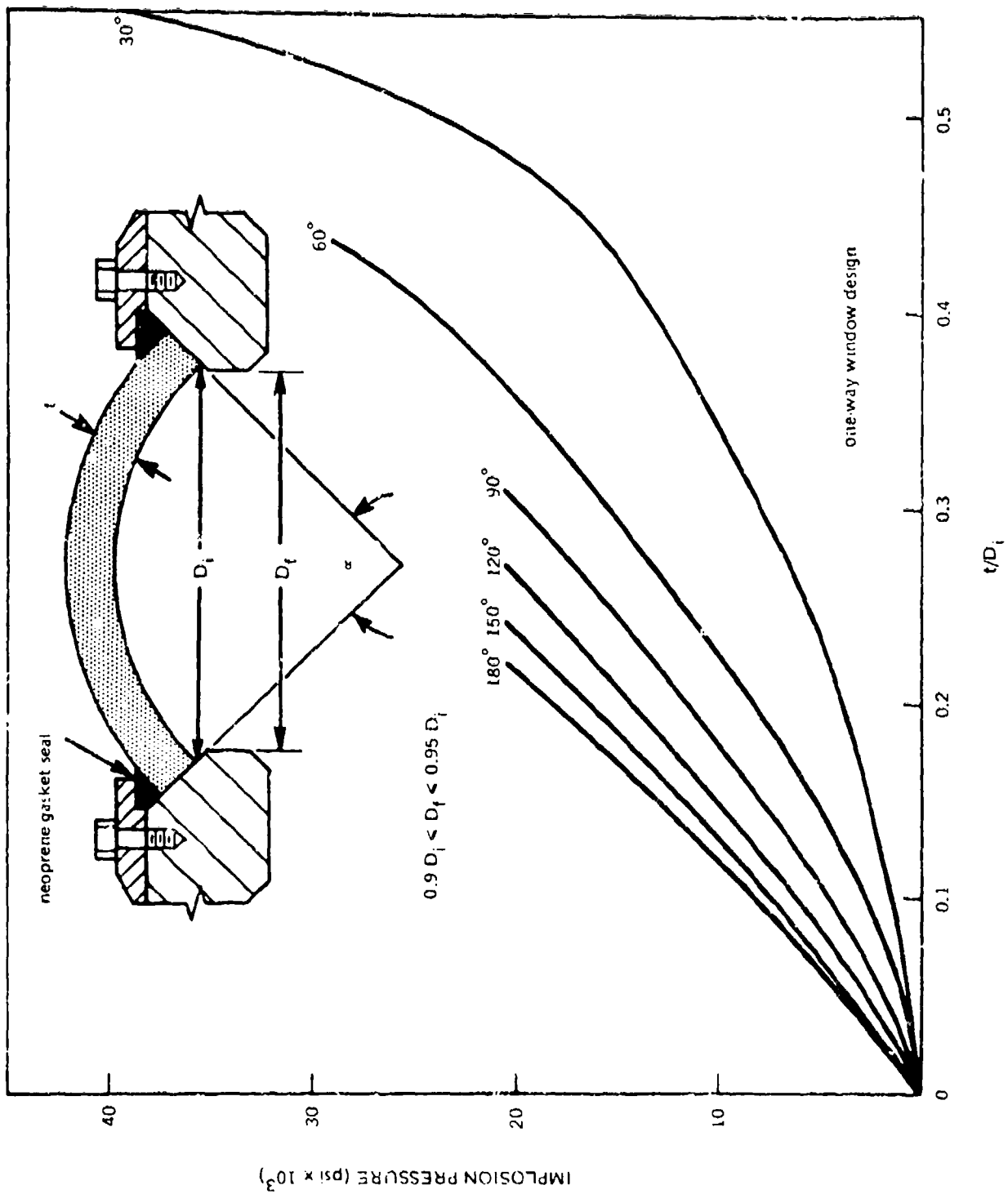
Figure 3.3. Short-term critical pressure of spherical sector acrylic windows.

one-way window design

$0.9 D_i < D_f < 0.95 D_i$

t/D$_i$

IMPLOSION PRESSURE (psi x 10^3)

are permitted but not required, because those specified are adequate for the temperature service conditions shown.

Where additional testing of windows prior to request for certification is contemplated, the magnitude of conversion factors may be decreased to 4, provided the testing follows the requirements discussed next.

3.2.4 Validation of Window Design

Where the designer of the windows desires to utilize lower conversion factors than those cited, the burden of proving the window's performance rests upon him. At a minimum, the test program will have to incorporate the following elements:

3.2.4.1 Short-term pressure tests must be conducted on at least five full-scale windows to prove that the average short-term critical pressure of the windows is above a pressure value equal to the maximum operational pressure multiplied by a factor of 4. The tests must be conducted at the highest ambient temperature predicted for the operation of the hyperbaric chamber.

If any of the original five windows fail at a pressure that is 25 percent below the average pressure, an additional five windows must be subjected to short-term tests. If among the additional five windows another specimen fails at a pressure 25 percent below the average value, the average of the two low values will be considered as the accepted average.

3.2.4.2 Long-term pressure tests must be conducted on a minimum of five full-scale windows to prove that the long-term failure of the window under operational pressure and temperature will take place only after a minimum of 10^6 minutes. In the long-term tests, extrapolated, rather than actual, values may be used to establish the long-term life of the window.

The testing program consists of subjecting individual windows to different sustained pressure loadings and recording the elapsed time to catastrophic failure. If only five windows are used, then the first window should be subjected to 90 percent; the second, to 85 percent; the third, 80 percent; the fourth, 75 percent; and the fifth, 70 percent of average short-term critical pressure established for these windows by prior tests. The tests must be conducted at the maximum ambient temperature predicted for the operation of the hyperbaric chamber.

3.2.4.3 Cyclic pressure tests conducted on a minimum of five full-scale windows must prove that the cyclic fatigue life under operational pressure, temperature and duration of cycle will be in excess of 10^4 cycles. If the projected average length of an operational pressure cycle is not known, a 24-hour period will be used in its place. In the cyclic pressure tests, extrapolated, rather than actual, values may be used to establish the cyclic fatigue life of the window. The testing program consists of pressure cycling individual windows to different pressure levels until catastrophic fatigue failure occurs. If only five windows are used, then the first window should be cycled to 90 percent; the second, to 85 percent; the third, 80 percent; the fourth, 75 percent; and the fifth, 70 percent of short-term critical pressure established

3-6

for these windows by prior tests. The tests must be conducted at the maximum ambient temperature predicted for the operation of the hyperbaric chamber.

3.2.4.4 The extrapolation method allowed for the static long-term and cyclic fatigue tests under operational pressure is based on plotting the experimental data on log-log coordinates and extending the linear graph to infinity. For long-term static tests, the parameters plotted on log-log coordinates are catastrophic failure pressure vs time to failure. For cyclic fatigue tests, catastrophic failure pressure *vs* number of cycles to failure is plotted. In each case, catastrophic failure is defined as leakage of water through the window.

3.3 WINDOW DIMENSIONAL TOLERANCES

The proper performance of an acrylic plastic window depends not only on proper design dimensions, but also on machining tolerances.

3.3.1 Conical Frustum Window Tolerances

The important dimensions whose deviation from nominal values must be restricted during design are thickness, minor diameter, included conical angle and parallelism of viewing surfaces.

3.3.1.1 The thickness of conical frustum windows must be always equal to or larger than the specified nominal value.

3.3.1.2 The minor diameter of conical frustum windows must be within $\pm 0.002 \times D_i$ inch of the specified nominal value.

3.3.1.3 The included conical angle of conical frustum windows must be within ± 15 minutes of the nominal value.

3.3.1.4 Parallelism of the viewing surfaces should be within 0.030 inch. Measurement should be conducted at least at four points around the windows' circumference.

3.3.2 Flat Disc Window Tolerances

The important dimensions whose deviation from nominal values must be restricted during design are thickness, outer diameter and parallelism of viewing surfaces.

3.3.2.1 The thickness of flat disc windows must be always equal to or larger than the specified nominal value.

3.3.2.2 The outer diameter of flat disc windows must be within +0.000/-0.010 inch of nominal value (which is the same as the nominal diameter of the cavity in the flange) if a radial O-ring is to be used as the secondary or tertiary seal. If a radial O-ring is not employed for sealing the windows, the diametral tolerance on the nominal value may be as large as +0.000/-0.030 inch.

3.3.2.3 The parallelism of viewing surfaces should be within 0.030 inches. Measurements must be made at least at four points around the windows' circumference.

3.3.3 Spherical Shell Sector Windows

For these windows, the important dimensions whose deviation from nominal values must be restricted during design are thickness, sphericity, minor diameter, concentricity and included conical angle. The spherical shell sector acrylic plastic window is more sensitive to dimensional variations than the other window shapes, and because of this, special attention must be paid to its dimensional inspection through use of a set of custom-made measuring tools.

3.3.3.1 The thickness of spherical shell sector acrylic plastic windows must always be equal to or larger than the specified nominal value.

3.3.3.2 Sphericity of spherical shell sector acrylic plastic windows must be within ±0.5 percent of specified nominal external radius of the window.

3.3.3.3 Concentricity of spherical shell sector optical surfaces must be always within ±2 percent of the wall thickness.

3.3.3.4 Minor diameter of spherical shell acrylic plastic window must be within $±0.002 \times D_i$ inches of the specified nominal value.

3.3.3.5 Included conical angle of spherical shell acrylic plastic window must be within ±15 minutes of the specified nominal value.

3.4 WINDOW SURFACE FINISHES

The surfaces of acrylic plastic windows must receive proper finish to give the windows the desired optical properties and impart the necessary resistance against initiation of cracks on their bearing surfaces.

3.4.1 Conical Frustum Window Finish

In conical frustum windows, the optical finish considerations apply only to the two parallel flat viewing surfaces, while the structural finish considerations apply to the conical bearing surface.

The optical finish on the two surfaces utilized for viewing should meet the requirements of ASTM D702-66 paragraph 6.1.15 (clear print of size 7 lines per column inch and 16 characteristics to the linear inch shall be clearly visible when viewed through the window from a distance of 20 inches).

The structural finish requirement for the conical bearing surface specifies as a minimum a 32-rms machined surface. Finer surface finishes, including polishing, are permissible, but not desirable.

3.4.2 Flat-Disc-Window Finish

In flat disc windows, the optical finish considerations apply only to the two parallel flat surfaces. The structural finish consideration applies only to the radial bearing surface around the circumference of the disc.

The optical finish on tne two parallel viewing surfaces and the flat bearing areas should meet the requirements of ASTM D 702-66 paragraph 6.1.15.

The structural finish on the radial bearing surface shall be equal to or better than 32 rms.

3.4.3 Spherical Shell Sector Window Finish

In spherical shell sector windows, the optical finish considerations apply only to the convex and concave viewing surfaces, while the structural finish requirement applies to the edge bearing surface around the circumference of the window.

The optical finish on the convex and concave viewing surfaces should meet the requirements of ASTM D 702-66, paragraph 6.1.15 when the eye of the observer is located in the interior and at the center of curvature.

SECTION 4

WINDOW FLANGES

Flanges for window penetrations have two major functions; they act as structural reinforcement for the window penetration and also serve as a seat for the acrylic window. Because of these dual functions, the flange must satisfy not only the structural requirement of the vessel, but also that of the window.

The selection of flange configuration is based upon the (1) window configuration, (2) the type of pressure service and (3) preferred sealing arrangement. The types of available standard window configurations and the various service conditions have been discussed previously. This section addresses itself to the selection of flange and retainer configuration and sealing arrangements for windows.

4.1 STRUCTURAL CONSIDERATIONS

Regardless of the flange configuration and sealing arrangement chosen, there are certain structural parameters that must be considered in the design of the window flange for acrylic plastic windows.

4.1.1 Flange Stresses and Deformations

Because of the large mismatch between the modulus of elasticity in the plastic window and the metallic flange, it is assumed that the window does not provide any reinforcement for the hull material around the penetration. All of the reinforcement for the hull penetration must be provided by the window flange. Any of the accepted analytical or empirical methods for stress calculations may be used for dimensioning the thickness, width and location of the flange around the window penetration, provided that the resultant flange stresses and deformations meet the following minimum requirements:

4.1.1.1 Radial deformation of the window seat at maximum internal or external operational pressure must be less than $0.003 \times D_f$ inches.

4.1.1.2 Angular deformation of the window seat at maximum internal or external operational pressure must be less than 0.5 degree.

4.1.1.3 The peak stress measured on a window penetration flange at maximum operational pressure shall always be less than one half of the flange material's yield strength under uniaxial tensile loading.

4.1.2 Flange and Retainer Subassembly Configuration

The flange and retainer subassembly configuration will be chosen to match the desired window configuration and sealing arrangement. Once a flange and retainer subassembly

configuration has been chosen for a particular type of pressure service, the hyperbaric chamber becomes limited to that particular type of pressure service. Later changes in the flange configuration are costly and time-consuming. For this reason, considerable thought must be exercised prior to choosing the flange configuration.

In the design of the retainer subassembly, one must consider two types of loading conditions. The *primary* loading consideration is the retention of the window in the flange seat under a specified magnitude of hydrostatic loading. The magnitudes of hydrostatic pressure that the windows must withstand are given in paragraphs 4.1.2.1 through 4.1.2.3. The *secondary* loading consideration is the precompression of elastomeric gaskets serving as the primary seal in the window assembly. A good rule of thumb for estimating the magnitude of loading imposed by precompressed elastomeric gaskets and O-rings is to multiply the outer window diameter in inches by 2000 pounds. If the secondary loading is calculated to be larger than the primary, the design of the retainer subassembly configuration will have to be based on the larger loading value.

4.1.2.1 Internal pressure service requires that the window retaining ring subassembly be located on the interior of the vessel. It must be designed structurally to retain the force generated by an external hydrostatic pressure of 15 psi (figure 2.2). The minimum safety factor specified for the retainer subassembly requires that water leakage may occur through the window penetration only at external hydrostatic pressures higher than 60 psi.

4.1.2.2 External pressure service requires that the window retaining subassembly be located on the exterior of the vessel. It must be designed structurally to retain the force generated by an internal hydrostatic pressure of 15 psi (figure 2.3). The minimum safety factor specified for the retainer subassembly requires that water leakage may occur through the window penetration only at internal hydrostatic pressures higher than 60 psi.

4.1.2.3 Hybrid pressure service requires that the window retaining subassembly be located on the side of the vessel exposed to the *higher* operational pressure It must be designed structurally to retain the force generated by the most severe difference in external and internal pressures acting on the vessel. The minimum safety factor specified for the retainer subassembly requires that water leakage may occur through the window penetration only at a pressure differential 4 times higher than predicted for the operation c the vessel (figure 2.4).

4.2 WINDOW SEAT REQUIREMENTS

Acrylic plastic windows must be supported properly in order to optimize their structural strength. Proper support for the window requires that the seat in the window flange match closely the window bearing surface, allow for movement of the window under load and have a finish adequate for pressure sealing and reducing friction caused by movement between the flange and the window.

4-2

4.2.1 Window Dimensional Tolerances

Since the primary function of the window seat is to give the window adequate support when it is subjected to hydrostatic loading, a close match must be insured between the window seat and the window body. The close match can be attained by close dimensional control of the window and of the window seat.

4.2.1.1 The conical cavity seat must have an included conical angle that is within ± 5 minutes of the nominal value. The minor diameter (D_f) of the window seat must be within $\pm 0.002 \times D_f$ inches of the nominal window penetration diameter.

4.2.1.2 Cylindrical cavity seats must have an outside diameter within $+0.001/-0.000$ inches of nominal value if the radial O-ring is to be used as the secondary seal. If elastomeric gaskets are used as both primary and secondary seals, the tolerance on the outside diameter may be as large as $+0.020/-0.000$ inches. The diametral tolerance on the inside seat diameter is ± 0.020 inch regardless of what kind of secondary seal is used on the window.

4.2.2 Seat Dimensions

The seat dimensions must be adequate to give the window not only sufficient bearing area when it is under zero pressure loading, but also when it is stressed and displacing under proof-test pressure equal to 1.5 times operational pressure.

4.2.2.1 The conical cavity seat has two major requirements. The depth of the conical window cavity must be sufficient to give the window (figure 4.1) support throughout its full length and the minor window seat diameter, D_f, must be smaller than the minor window diameter, D_i. The difference between these diameters assures adequate radial and axial support to the window, which is creeping under hydrostatic loading. The magnitude of the difference is a function of operational pressure, temperature, length of sustained hydrostatic loading and magnitude of conversion factor used in the window design. Since it would be too cumbersome to establish a set of individual guidelines that would cover each possible case, a general rule has been established. This general rule gives D_i/D_f values that are very adequate for most, and very conservative for some, operational window requirements. Shown in figure 4.1 are the minimum D_i/D_f values considered necessary for adequate support of windows using conical seats.

4.2.2.2 Cylindrical cavity seats have three major requirements. The seat will be located in a cylindrical cavity whose depth is equal to or in excess of the window thickness. The maximum nominal diametral clearance between the window and the cavity wall will be $0.005 \, D_o$ inch if no radial O-ring seals are used, and 0.01 in. when they are not used. The ratio between the seat cavity diameter, D_o, and the minor penetration diameter, D_f, must be in the 1.250–1.500 range to give the window adequate bearing support during hydrostatic loading (figure 4.2).

note : the D_i/D_f ratios shown are valid only
for operational pressures ≤ 3500 psi.

α

63

D_i

$\frac{1}{32}$ R

k

D_f

β

β is selected on the basis
of optical requirements.

k ≥ 0.1 D_i
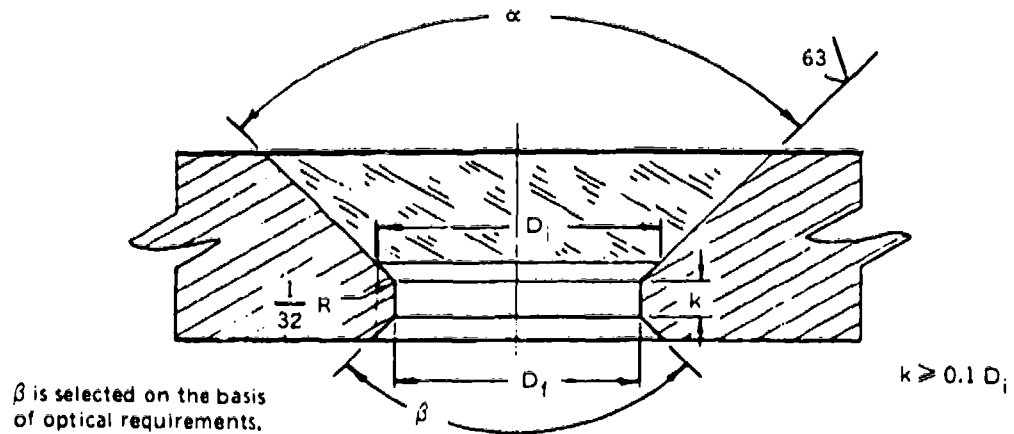
▽▽	included angle (α)	30°	60°	90°	120°	150°
▽	D_i/D_f ratio	1.03	1.04	1.06	1.12	1.28

a. conical frustum window

note : for α between values shown
interpolation is required.

α

63

D_i

$\frac{1}{32}$ R

k

D_f

β

β is selected on the basis
of optical requirements.

k ≥ 0.01 D_i
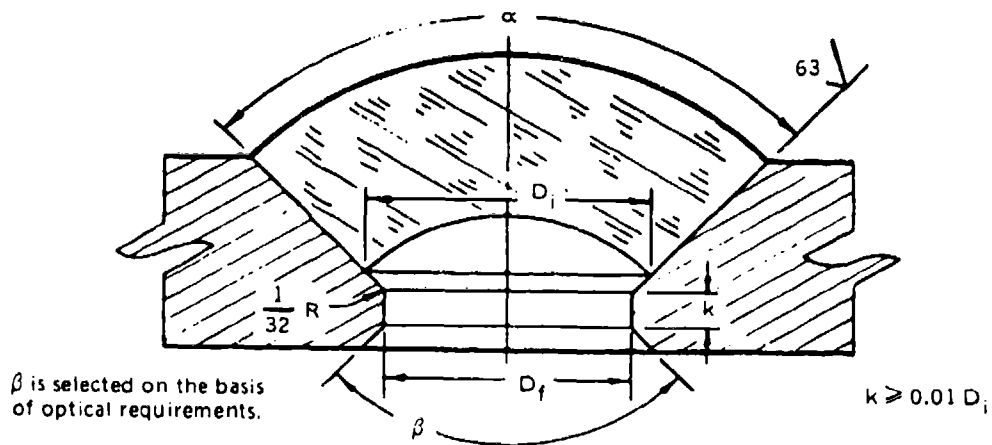
▽▽	included angle (α)	30° thru 90°	120° thru 180°
▽	D_i/D_f ratio	1.05	1.10

b. spherical shell sector window

Figure 4.1. Conical seat cavity requirements.

$$0.000 \leqslant D_s - D_o \leqslant 0.005 \, D_o$$

depending on seal used

$$1.250 \leqslant D_o/D_f \leqslant 1.50$$
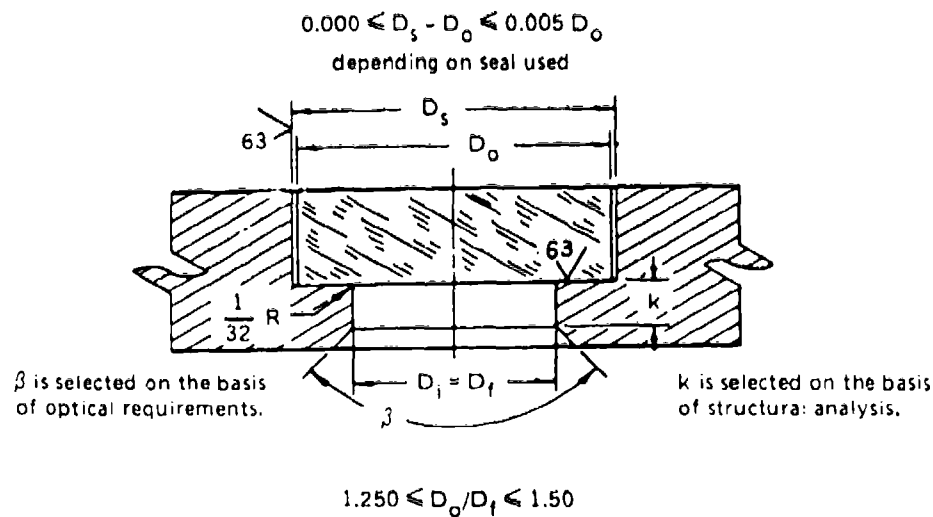
Figure 4.2. Cylindrical cavity seat requirements.

4.2.3 Seat Finish

Proper finish is necessary on the surfaces of the seat to provide a good seal surface and a smooth sliding surface for the extruding window. Without adequate surface finish, the seal may be inoperative and cracks may be generated in the window bearing surfaces prematurely.

4.2.3.1 Conical cavity seats must have a finish that is equal to or better than 63 rms.

4.2.3.2 Cylindrical cavity seats must have a finish on all the internal surfaces that is 65 rms or better.

4.3 SEALING CONSIDERATIONS

Elastomeric seals must be incorporated into the window flange assembly to act as a primary barrier against leakage of gases and water through the window penetration. Since the choice of a particular seal arrangement will require the use of a window retainer subassembly especially suited for that seal arrangement, the designer is advised to choose them at the same time.

In addition to a primary seal, there also must be a secondary seal, which may be of the elastomeric or grease type. Grease seals may act as secondary seals wherever permitted by the window configuration. The window configurations that allow the use of grease seals as a secondary seal are those that have a conical bearing surface mating intimately with a conical window seat. In the case of flat disc windows, the secondary seal must also be of the

4-5

elastomeric type. In other window configurations it is at the option of the designer to choose between the elastomeric and grease type sealing arrangements for the secondary seal.

4.3.1 Conical Frustum Window Seals

The conical bearing surfaces must be equipped with both a primary and a secondary seal. The primary seal must, in addition, act as a bearing gasket for the window retainer ring.

4.3.1.1 The primary seal must be a flat elastomeric gasket (neoprene or similar) bonded to the window retainer ring or an O-ring wedged into a properly dimensioned groove (figure 4.3). The thickness of the gasket will be adequate to allow the necessary precompression specified for installation. In no case will the precompression exceed 50 percent of the original gasket thickness. The precompression specified for the primary seal depends on the conical angle; its value is given in figure 4.3. The hardness of the elastomeric gasket must not exceed 90 Durometer.
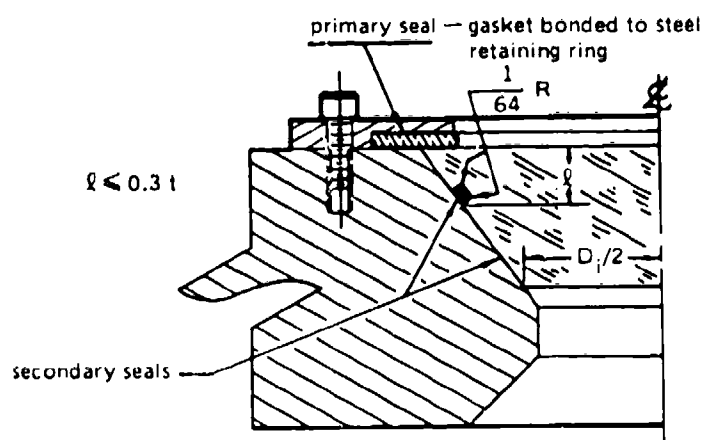
use 60 durometer or softer elastomers

primary seal precompression during assembly					
included angle (∝)	30°	60°	90°	120°	150°
precompression (operational pressure > 1500 psi)	⩾ 0.06 D$_i$	⩾ 0.04 D$_i$	⩾ 0.03 D$_i$	⩾ 0.03 D$_i$	⩾ 0.03 D$_i$
precompression (operational pressure < 1500 psi)	⩾ 0.03 D$_i$	⩾ 0.02 D$_i$	⩾ 0.015 D$_i$	⩾ 0.015 D$_i$	⩾ 0.015 D$_i$

Figure 4.3. Sealing of conical frustum windows.

4.3.1.2 The secondary seal may either be grease between the mating conical surfaces or an elastomeric O-ring located in a groove that has been machined into the conical bearing surface of the window (figure 4.3). O-ring seals are not recommended if the t/D_i ratio of the window is less than 0.25. O-ring should be of $\leqslant$ 60 Durometer hardness.

4.3.2 Flat Disc Window Seals

Flat disc windows with flat bearing surfaces must be equipped both with a primary and a secondary seal. Because of the uniqueness of the cylindrical disc shape, a tertiary seal may be incorporated also.

4.3.2.1 The primary seal must be a flat elastomeric gasket bonded to the retainer ring. The hardness of the gasket must not exceed 90 Durometer unless the window is used in hybrid pressure service, in which case the hardness should be at least 90 Durometer, since the gasket serves then also as a window bearing gasket (figure 4.4).

4.3.2.2 The secondary seal must be a flat elastomeric gasket bonded to the bearing surface on the seat (figure 4.4). Since the secondary seal gasket serves also as a bearing gasket, its hardness should be at least 90 Durometer to keep it from extruding when under load.

4.3.2.3 The tertiary seal (optional) shall be radially compressed O-ring located in a groove machined around the circumference of the window (figure 4.4). If desired, the tertiary seal configuration may be substituted for the secondary seal configuration. The O-ring should be of 90 Durometer hardness.

4.3.3 Spherical Shell Sector Window Seals

Spherical shell sector windows must be equipped with primary and secondary seals (figure 4.5). Since the spherical shell sector windows have low t/D_i ratios as a rule, it is difficult to incorporate O-rings into the conical window bearing surface.

4.3.3.1 The primary seal must be an elastomeric gasket wedged between the external window surface and the flange. The hardness of the O-ring should not exceed 60 Durometer.

4.3.3.2 The secondary seal must be grease trapped between the mating conical surfaces of the window and the flange.

primary seal — gasket bonded to steel
retaining ring

(precompressed > 0.125 in.)

0.005 max.

tertiary seal
O-ring in radial
compression

t/2

t

$D_i/2$

secondary seal — gasket bonded
to flange seat
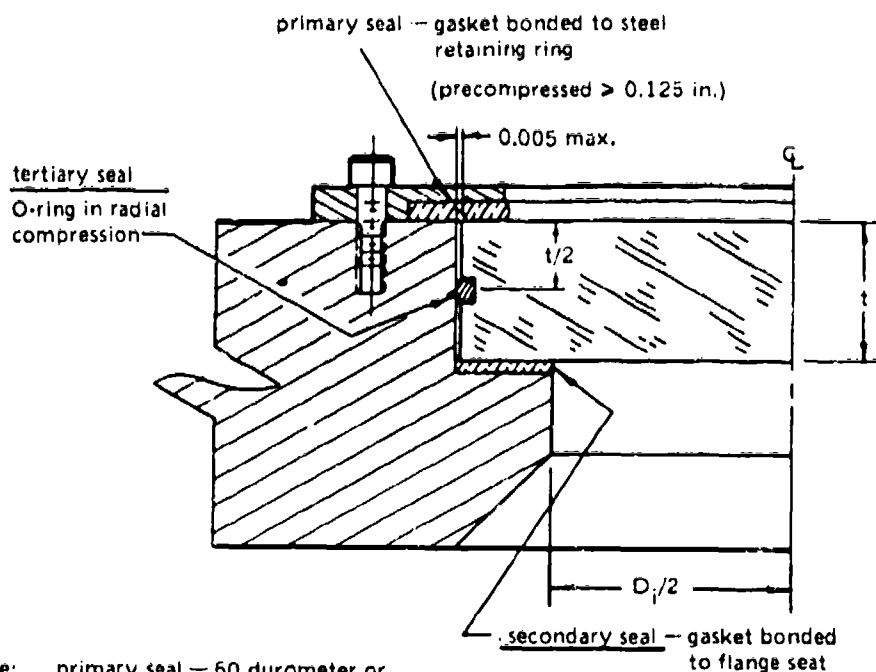
note: primary seal — 60 durometer or
softer elastomer

secondary seal — 90 durometer or harder
(this gasket need not be an elastomer)

Figure 4.4. Sealing of flat disc windows.

primary seal — precompress at assembly
(60 durometer or softer
elastomer)

$D_i/2$

secondary seal
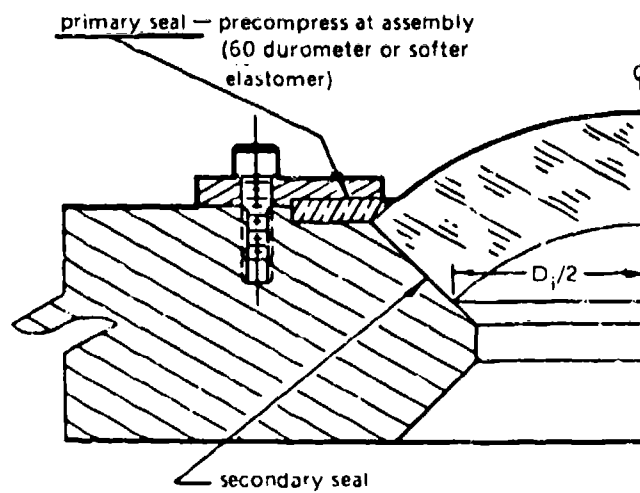
operational pressure	< 1000 psi	< 2000 psi	< 3000 psi
seal precompression	≥ 0.01 D_i	≥ 0.02 D_i	≥ 0.03 D_i

Figure 4.5. Sealing of spherical snell sector windows.

4-8

SECTION 5

FABRICATION

It is necessary that certain basic steps be followed during the fabrication of windows and flanges to insure that the finished product has the structural properties designed into it. Since the procedures for fabricating acrylic plastic windows differ significantly from those which apply to the metallic hull with flanges, they will be discussed separately. The fabrication procedures for flanges are somewhat similar to those for the hull and will be discussed in the section on chamber hull fabrication.

5.1 TRACEABILITY

5.1.1 Material Accounting and Identification System

A material accounting and identification system must be used during fabrication of windows. Identification numbers will be applied to and maintained on each piece of material so it will be possible at any time to trace any piece of raw material, window blank or finished window to the original casting or sheet from which it was cut.

5.1.2 Identification of Finished Windows

Identification of finished windows must be accomplished by using red or black felt tip markers that have no deleterious effect on plastic. Identification of each window will consist of the manufacturer's name, date of fabrication and a number assigned to it by the fabricator to permit tracing it to the stock of material from which it originated. The identification will be placed on the conical bearing surface for conical frustums and spherical sectors and on the cylindrical surface of flat disc windows.

5.2 THERMAL SHRINKING OF STOCK

Windows for service at 150°F must be thermally shrunk prior to machining them to final dimensions. The thermal shrinkage will be accomplished by subjecting the windows to a minimum forming temperature of 325°F for at least four hours. At that time, a lateral shrinkage of approximately two percent and a thickness increase of four percent should occur. The cooling rate from the forming temperature to room temperature should not exceed 15°F/hour.

5.3 MACHINING

5.3.1 Dimensions of Windows

Dimensions of windows will be based on 70°F temperature and 50 percent humidity as produced by soaking in a 70°F air atmosphere with 50 percent humidity for 24 hours.

Because the material expands from frictional heating and contracts under flow of coolant over the machined surface, the contractor will find it necessary to determine experimentally the appropriate dimensions to be used by the machinist during machining.

5.3.2 Lubricants and Coolants

Lubricants and coolants used during the machining operations of acrylic plastic must be water soluble and approved by their manufacturer for such application.

5.4 FORMING

The temperatures used during forming operation must not be less than 300°F or more than 360°F. Forming operation will be employed only for spherical shell sector windows.

5.5 ANNEALING

Annealing of windows must take place at least once and preferably twice. If it is annealed only once, the operation should take place after all the machining and polishing of the windows has been completed. If the annealing operation is performed twice, the first time should be after rough machining, and the second, after final machining. The annealing cycle will consist of a warm-up period (at a maximum 15°F/hour rate) to 175°F, a heat-soaking period of 24 hours duration and a cooling-down period to room temperature (at a maximum 10°F/hour rate).

5.6 PROOF-TESTING

5.6.1 Proof-Testing of Windows

Each window must be proof-tested at least once prior to being approved for service in man-rated hyperbaric chambers. As a minimum, it will be subjected to the overpressure proof-test when the complete hyperbaric chamber is proof-tested prior to its acceptance for man-rated service. It is best to proof-test the window when it is mounted in the hyperbaric chamber since the window is supported during the test by the flanges in which it will see service during its operational life.

A window may be also proof-tested twice before being placed into man-rated service; the first time by the window fabricator in a simulated flange and a second time by the chamber operator when the windows are mounted in the chamber and he proof-tests the whole system. The first proof-test can be conducted in a flange that is not stressed in a manner identical to that of the flange in the hyperbaric chamber. The only requirement for the simulated window flange is that it have the same window seat and retainer dimensions as the operational flange in the chamber.

5.6.2 Magnitude of Pressure

The magnitude of pressure used in the proof-test must be no less than the operational pressure for which the chamber will be rated and no more than 1.5 times the operational pressure. The pressure will be applied at a rate that is not in excess of 1000 psi/minute.

If the window assembly undergoing the tests is designed for hybrid service then one proof-test must be applied to satisfy the internal pressure requirement and another to satisfy the external pressure requirements.

5.6.3 Ambient Temperature

Ambient temperature during the proof-test should not exceed the maximum expected operational temperature for the chamber at any time. If the chamber window design is rated for frigid temperature service, the maximum temperature allowed during the proof-test is 75°F. If the chamber window design is rated for temperate temperature service, the maximum allowable temperature during the proof-test is 120°F. If the chamber window design is rated for tropic temperature service, the maximum allowable temperature during the proof-test is 150°F.

5.6.4 Instrumentation

Instrumentation will be employed during the proof-test only on a single specimen of a given class (design) of windows. The instrumentation will consist either of a simple electrical-resistance strain gage bonded to the center of the window's low-pressure surface or a mechanical dial indicator resting against the center of the window's low-pressure face. The dial indicator must read in 0.001-inch increments.

If the window assembly is intended for hybrid pressure service, the strain gage and dial indicator should be applied consecutively for the internal and external pressure requirements.

5.6.5 Data Recording

Displacement or strain of the window will be recorded at 100-psi intervals during the pressurization and at one hour intervals during relaxation at 0 pressure after the test. The displacements and strains should return to within 0.010 inch and 50 microinches/inch of original values, respectively.

5.6.6 Duration of Proof-Test

Duration of the proof-test must not exceed the maximum length of a typical projected chamber pressurization. In the absence of any other specific recommendation, a four hour pressure hold and four hour relaxation period will be considered standard for proof-test purposes.

5.6.7 Arrangements

Arrangements for the proof-test should never combine the maximum allowable proof-test pressure and temperature simultaneously. If this is done, serious damage may occur in the window during proof-test. It is recommended instead that if 50 percent overpressure is applied to the window, the temperature be kept in the 70-90°F range. On the other hand, if the proof-test entails *no overpressure*, the maximum allowable temperature can be utilized.

5.6.8 Recommended Procedure

To assure that the proof-testing achieves its objective without shortening the fatigue life of the window, it is recommended that the proof-test be performed in two steps:

1. Proof-test the window prior to installation in the hyperbaric chamber by pressurizing it to maximum operational pressure *only* at maximum temperature allowed for that service. The pressure should be sustained for 4 hours.

2. Proof-test the window to 50 percent overpressure when the entire chamber assembly is proof-tested. The temperature during that test should not exceed 75°F nor last longer than 4 hours.

5-4

SECTION 6

ACCEPTANCE OF HARDWARE

It has been assumed that the fabricators of windows and window flanges will strive to comply with the previously recommended practices to produce a reliable viewport for man-rated operation. Still, a written record certifying their compliance with those recommendations helps to crystallize their actions and focus the quality control process on the area vital to safe structural performance.

6.1 WINDOWS

The written records required for certification of windows must show that the design, material, fabrication process and proof-testing complied with the guidelines called out in the preceding recommendations.

6.1.2 Design Record

The design record composed of a fabrication drawing and engineering calculations must show that the following parameters were considered and their magnitude or character established:

    a.   <u>Type of pressure service</u> a..d the magnitude of maximum operational pressure that the chamber will see (e.g., 300 psi maximum, internal pressure only).

    b.   <u>Type of temperature service</u> and the numerical limits of the temperature range (e.g., -20°F to 95°F, temperate zone service).

    c.   <u>Window shape</u> chosen (e.g., 90° conical frustum shape).

    d.   <u>Conversion factor</u> used to arrive at the required window thickness (e.g., conversion factor of 10).

    e.   <u>Short-term critical pressure</u> calculated on the basis of conversion factor and maximum operational pressure (e.g., $10 \times 300 = 3000$ psi short-term critical pressure).

    f.   <u>Thickness-to-diameter ratio</u> (t/D_i) calculated on the basis of operational pressure, conversion factor and empirical design curves (e.g., $t/D_i = 0.20$ for CF = 10, MOP = 300 psi when figure 3.2 is used).

    g.   <u>Dimensional tolerances</u> recommended for the window shape chosen have been entered on the fabrication drawing (e.g., dimensional tolerance on thickness, diameter, and included angle).

    h.   <u>Surface finishes</u> recommended for the window shape chosen have been entered on the fabrication drawing.

6.1.3 Material Qualification Record

The material serving as basic stock for fabrication of windows must comply with the provisions of the specifications recommended for acrylic plastic windows in hyperbaric chambers (see Appendix A). The proof of compliance consists of Material Data Forms 1 and 2, which substantiate the claim that the material is on the Qualified Product List and, subsequently, on the Lot Acceptance List.

6.1.3.1 Qualified product listing for the material must be justified either by the material supplier (he submits a filled-out and notarized Material Data Form 1) or by the window fabricator, who has all the qualification tests done by an independent testing laboratory (the laboratory conducting the tests submits a notarized Material Data Form 1). Not every acrylic casting has to be tested for QPL. The fabricator can qualify a particular acrylic casting product with a single series of tests.

6.1.4 Fabrication Record

The fabrication record, composed of material accounting form, identification tracer, fabrication process rider and quality control certificate, must show that the following items were recorded:

    a.   Material stock used in the fabrication of a window must be positively identified on the material accounting form.

    b.   Lot and item numbers on the identification tracer accompanying a window must correspond to the markings on the window.

    c.   The fabrication process rider accompanying a window must show entries describing the following:

        1.   Thermal regimen used in shrinking of material

        2.   Thermal regimen used in forming of window

        3.   Coolants used during machining

        4.   Thermal regimen used in annealing of window lot

    d.   The quality control certificate accompanying each window must show that the window has been inspected and the following items noted.

        1.   Minor diameter

        2.   Major diameter

        3.   Conical angle (if any)

        4.   Thickness (at three different locations)

        5.   Sphericity (at three locations)

        6.   Optical finish on viewing surfaces

        7.   Structural finish on bearing surface

8. Presence of inclusions in the material

9. Presence of chips and scratches

6.1.5 Proof-Testing Record

The proof-testing record, composed of the test description and window performance data, must show that the following items were recorded.

a. Temperature of water (or gaseous atmosphere) in contact with the window during the test.

b. Pressurization rate used to reach proof-test pressure.

c. Proof-test pressure to which the window was subjected.

d. Duration of constant proof-pressure loading on the window.

e. Depressurization rate used to depressurize the window.

f. Displacement or strain of the window center during the proof-test and subsequent relaxation period (performed only a typical window chosen from the window lot).

g. Visual inspection of the window after the proof-test.

SECTION 7

INSPECTION AND MAINTENANCE OF WINDOWS IN SERVICE

On exposure to harmful cleaners or high temperatures acrylic plastic may deteriorate in service to such an extent that it may lose its optical value and structural strength. Rough handling and repeated overpressurizations may also induce surface cracks and scratches that subsequently initiate fractures which lead to catastrophic failure of the window. For this reason, it is necessary to subject installed windows to periodical visual inspections and maintenance.

7.1 INSPECTIONS

All windows installed in man-rated pressure-resistant vessels must be visually inspected periodically for signs of optical and structural deterioration. Both operational and maintenance inspections must be made.

7.1.1 Operational Inspection

The operational inspection must be conducted by the operator just prior to each pressurization of the hyperbaric chamber. The inspection will be visual and no additional instruments beyond a flashlight are required for its conduct. During this inspection the condition of visually accessible exterior, interior and bearing surfaces will be observed and noted in the hyperbaric chamber logbook. Presence of blemishes in the form of crazing, cracks, scratches, blisters and discolorations require careful evaluation of their effect on the structural integrity of the window and its ability to serve safely under maximum operational pressure.

7.1.1.1 Blemishes on the low-pressure face are a grave source of concern since they can initiate catastrophic failure in flat disc and conical frustum windows. On flat disc and conical frustum windows with $t/D_i < 0.5$, the presence of a crack or scratch deeper than 0.010 inch, crazing, blisters or discoloration will necessitate immediately removing the window and replacing it with another unit. Crazing, blisters, discoloration and cracks or scratches in windows with $t/D_i \geqslant 0.5$ will necessitate immediate window removal if the blemishes penetrate more than $0.01t$ below the low-pressure face. A window having blemishes less than $0.01t$ but more than 0.010 inch will be permitted to serve until next scheduled maintenance inspection, at which time it must be replaced with another unit. Blemishes less than 0.010 inch deep can be tolerated indefinitely.

Blemishes on the low-pressure face of a spherical sector window deeper than $0.02t$ will necessitate the immediate removal of the window and replacement with another unit. A window with blemishes less than $0.02t$ but more than 0.010 inch will be permitted to serve until next scheduled maintenance inspection, at which time it must be replaced. Blemishes less than 0.010 inch deep can be tolerated indefinitely.

7.1.1.2 Blemishes on the high-pressure face as a rule, are not very serious unless they are very deep. Only those blemishes deeper than $0.02t$ will necessitate the immediate replacement of the window. Windows with blemishes less than $0.02t$ but more than 0.020 inch will be permitted to serve until next scheduled maintenance inspection, at which time they must be replaced. Blemishes less than 0.020 inch deep can be tolerated indefinitely.

7.1.1.3 Blemishes on the conical bearing surfaces deeper than 0.060 inch will necessitate the immediate removal and replacement of the window. Windows with blemishes less than 0.060 inch but more than 0.010 inch deep will be permitted to serve until next scheduled maintenance inspection, at which time they must be replaced. Blemishes less than 0.010 inch can be tolerated indefinitely. The same considerations also apply to blemishes in the surface around the circumference of flat disc windows.

7.1.1.4 Chipped edges of windows necessitate the immediate removal of the window only if the chipped high-pressure face edge precludes sealing of the window or the chip missing from the low-pressure face edge is longer than $0.1D_i$ or deeper than $0.02D_i$ inch.

7.1.2 Maintenance Inspection

Maintenance inspection must be conducted at least once every calendar year, and at that time the windows must receive a more thorough inspection than during the operational inspections. During this inspection, *all* surfaces of the windows must be visually inspected. If this cannot be accomplished without removal of retaining rings, then they must be removed.

At the time of the maintenance inspection, it is necessary to remove all the windows on whose surfaces blemishes have been discovered either during the previous operational inspections or the maintenance inspection. All of the windows removed from the hyperbaric chamber can be subsequently placed back in service if the blemishes causing their removal are eliminated by polishing, sanding, machining or patching.

7.2 MAINTENANCE OF WINDOWS

The primary parameter that must be considered prior to repairing a window is its actual thickness. If after repair, the thickness of the window is more than $0.01t$ below the thickness required by Section 3.2, the window will be considered unsuited for the pressure service in which it was previously used. For this reason it is considered prudent to specify as original equipment windows that are 5 to 10 percent thicker than specified by Section 3.2. In this manner some material stock is always available for sanding and machining during window maintenance operations of blemished high- and low-pressure faces.

7.2.1 Annealing

After sanding, machining or recasting of window surfaces, it is recommended that the window be annealed to increase its potential resistance to cracking. The annealing should take

place at 175°F for 24 hours, followed by a cooling-down period in which the temperature is reduced at a maximum of 10°F/hour to room temperature.

7.2.2 Casting and Cementing

If deep blemishes are repaired by patching with a polymerizing acrylic cement, test data must be provided (by the cement supplier) to show the compressive and tensile strength of the cements is not less than 50 percent of the parent material strength. Building up a window's thickness by casting in place is permitted, provided the resulting increase in thickness is less than $0.1t$ and the strength of the casting and its adherence to the window material is not less than 50 percent of the parent material strength.

APPENDIX A
PROPOSED SPECIFICATION FOR ACRYLIC PLASTIC MATERIAL

SECTION 1
SCOPE AND TYPE OF MATERIAL

1.1 SCOPE

1.1.1 This specification covers clear transparent methyl methacrylate castings of nominal 1/2 inch or greater thickness. These sheets or finished shapes are intended to be used as pressure-resistant, structural-component viewing apparatus in manned chambers under internal pressure, external pressure, or both, e.g., submersibles, decompression chambers, transfer capsules, etc. Superior physical and mechanical properties are required in addition to optical properties.

1.1.2 This specification does not cover the finished product, i.e., the window itself.

1.2 TYPES OF MATERIAL

This specification covers three types of cast methyl methacrylate plastics.

1.2.1 **Type 1** — Unshrunk, ultraviolet-light-absorbing and heat-resistant material having greater shrinkage than Types 2 or 3 when heated to thermoforming temperatures.

1.2.2 **Type 2** — Pre-shrunk, ultraviolet-light-absorbing and heat-resistant material.

1.2.3 **Type 3** — Pre-shrunk, ultraviolet-light-absorbing, heat-resistant and craze-resistant material.

SECTION 2

APPLICABLE PUBLICATIONS

Current (as of the date of this specification) issues of the following documents are part of this specification to the extent noted herein.

2.1 TEST METHODS

2.1.1 **ASTM**. The following American Society of Testing Materials (ASTM) test methods shall be used where specified.

Test No.	ASTM Designation	Title or Subject
1	D 256-70	Impact properties of rigid plastics
2	D 542-50	Refractive index of plastics
3	D 570-63	Water absorption in 24 hours of plastics
4	D 621-64	Deformation of plastics under load
5	D 637-50	Surface irregularities of flat transparent plastic sheets
6	D 638-68	Tensile properties of rigid plastics
7	D 648-56	Deflection temperature of plastics under flexural load
8	D 695-69	Compressive properties of rigid plastics
18	D 696-70	Coefficient of linear thermal expansion of plastics
17	D 702-68	6.1.15 clarity, visual rated
9	D 732-46	Shear strength of rigid plastics
10	D 785-65	Rockwell hardness of plastics and electrical insulating materials
11	D 790-70	Flexural properties of rigid plastics
12	D 792-66	Specific gravity of plastics
13	D1003-61	Light transmission of plastics
15	E 308-66	Practice for spectrometry and description of color in CIE 1931 system

Copies of these are available from ASTM, 1966 Race Street, Philadelphia, Pa. 19103.

2.1.2 Military Specifications

Test No.	ASTM Designation	Title or Subject
18	P-8184B	4.5.5 Craze Resistance

Copies available from Naval Supply Depot, 5801 Tabor Avenue, Philadelphia, Pa. 19120.

2.1.3 Other Publications

Test No.		Title or Subject
14	SPE Transactions	Residual Monomer "Gas Chromatography, a New Test for Analysis of Plastics" by Cobbs Samsel, April 1962, p. 150-151.
3.2.2	ASME/ANSI PVH0-1	Safety Standard for Pressure Vessels for Vessels for Human Occupancy

Copies are available from the American Society of Mechanical Engineers, ASME Service Center, 22 Law Drive, Box 2300, Fairfield, NJ 07007-2300, Phone 1-201-882-1167.

SECTION 3

MATERIAL

3.1 GENERAL

The material shall be cast in the form of blocks for individual windows or sheet stock from which several windows may be machined. These should be of sufficient oversize to permit cutting of lot acceptance test specimens prior to machining, thermoforming, etc., of the window(s) from the casting. Qualification test specimens and supplementary lot acceptance test specimens can be taken from material normally shipped to the procurer.

3.2 RAW MATERIALS

The manufacturer is given a wide range in the selection of raw material and in the process of manufacture, provided the material furnished is a transparent plastic conforming to all requirements of this specification and is suitable for the intended use. The supplier is responsible for notifying the procurer of any major formulation changes that might affect qualification test results to the extent that the material would no longer pass these tests. Upon notification the material so designated must be resubmitted for QPL testing.

3.3 LOT DEFINITION

The material shall be supplied in a fully polymerized state (see Table 2, Test 14) and shall be a monolithic homogeneous solid. A lot is that material produced in one pour from the same monomeric material and made at the same time, undergoing identical processing from monomer to polymer. This includes different thicknesses *if* the preceding two statements hold.

A-4

SECTION 4

CLASSIFICATION OF TESTS

4.1 QUALIFICATION TESTS FOR QPL LISTING

Acrylic sheet furnished under this specification should be a product which has been tested and passed the qualification tests specified herein. Qualification tests shall be made on one casting of the first lot (see 3.3 and 4.2) of material furnished under this specification and any subsequent lot of material designated by the specifying agency or the procurer (see 4.6.2). Passing of the qualification test is the basis for listing on the Qualified Products List (QPL). A notarized copy of the test results (see Form 1) should always accompany the shipment of castings from any grade of material. Some qualification tests are lot acceptance tests. Provided qualification test results are available, those tests which are in common need not be rerun for lot acceptance or vice versa.

4.2 THICKNESS CLASSIFICATION

QPL listing of material of one thickness within the thickness ranges shown in Table 1 qualifies other thicknesses within the same range. That is, the QPL lists particular material (tradename and grade), and thickness categories' combinations. Each different material/ thickness combination must be tested and submitted separately for listing on the QPL. Thickness of 1/2, 1, 2 and 4 inches are preferred, but not required, for qualification testing.

4.3 LOT ACCEPTANCE TESTS

Only materials listed on or approved to be listed on the QPL are acceptable under this specification. In addition, each casting is to be tested and pass the Lot Acceptance tests specified herein. A single casting cut or split into several pieces need only pass the Lot Acceptance tests once. A notarized copy of the test results (see Form 2) shall accompany each casting shipped to the fabricator.

Table 1. Thickness Categories Based on Nominal Thickness Ranges.

Nominal Thickness Range	Thickness Category
Equal to 0.500 in.	1.
Greater than 0.500 to 1.000 in.	2.
Greater than 1.000 to 2.250 in.	3.
Greater than 2.250 to 4.250 in.	4.
Greater than 4.250 in.	5.

A-5

4.4 VISUAL INSPECTION

Each sheet or casting conforming to this specification must be inspected separately and meet the requirements of visual inspection specified herein.

4.5 TESTING RESPONSIBILITY

4.5.1 Qualification Tests. The material supplier may qualify his product by submitting data (Form 1) for QPL. For nonqualified material the procurer is responsible for doing or having done the qualification tests.

4.5.2 Lot Acceptance and Visual Inspection Tests. Lot Acceptance tests and visual inspection tests are the responsibility of the material supplier. The procurer can buy QPL listed material off-the-shelf and do or have done the lot acceptance and visual inspection tests.

4.6 RETEST

4.6.1 Rejected Material. Unless there is legitimate reason to doubt the reported values, rejected material shall not be resubmitted.

4.6.2 Periodic Qualification Checks. The procurer may ask that qualification tests be done on any lot of ordered material. Values reported on these rechecks shall take precedence over original qualification test results and passing them shall be the basis for QPL listing. These are the responsibility of the procurer. Those tests done for lot acceptance need not be rerun for qualification recheck.

SECTION 5

REQUIREMENTS

5.1 QUALIFICATION TESTING

5.1.1 Tests and Values Required. Tables 2 and 3 list the tests that must be made and the required values of qualification tests for conformance to the specification.

Table 2. Qualification Tests that Apply to all Thicknesses.

Test No.	Property	Required Value
1	Izod notched impact strength	0.3 ft-lbs/in. min
2	Refractive index	1.49 ± 0.01
3	Water absorption, 24 hours	0.25% max
4	Compressive deformation, 4000 psi, 122°F	1.0% max

6	Tensile, ultimate strength
	  elongation at break
	  modulus
		9,000 psi min
		2% min
		400.000 psi min

8	Compressive, yield strength modulus	15,000 psi min 400,000 psi min
9	Shear, ultimate strength	8,000 psi min
10	Rockwell hardness	M scale 90 min
11	Flexural, ultimate strength	14,000 psi min
12	Specific gravity	1.19 ± 0.01
14	Residual monomer, methyl methacrylate ethyl acrylate	1.5% max 0.005%
15	Ultraviolet (290-330 nm) light transmittance	5% max
16	Clarity, visually rated	Must pass readability

17	Coefficient of linear thermal expansion
	    at −40°F
	      −20°F
	      − 0°F
	      +20°F
	      +40°F
	      +60°F
	      +80°F
	      +100°F
		(in $10^{-5}/°F$)
		2.8 max
		3.0
		3.2
		3.5
		3.7
		4.0
		4.3
		4.7

18	Craze resistance (Type 3 only)	No crazing

Table 3. Qualification tests for Specific Thicknesses.

Test No.	Property	Values Required for Thicknesses of				
		1/2 in.	>1/2 in. ≤1 in.	>1 in. ≤2 in.	>2 in. ≤4.250 in.	>4.250 in.
5	Displacement factor	50 max	80 max	125 max	NR	NR
7	Deflection temp 264 psi	85°C min	88°C min	93°C min	93°C min	93°C min
13	Light transmittance	89% min	87% min	87% min	85% min	NR
13	Haze	3% max	NR	NR	NR	NR

Note: NR means not required.

5.1.2 Test Methods and Sampling for Qualification Tests. ASTM test methods are preferred and should be used where applicable. If feasible, samples shall be cut from the 18 in. X 18 in. blank used for the optical uniformity of distortion tests (5.1.2.5) after those tests have been completed. Samples are to be cut so that no surface is closer to an unfinished cast surface than the normal trim cut. Test samples shall be cut from the central portion of the original casting of a large casting cut to yield several smaller nominal size castings. Area sampled must yield some strips about 10 in. in length (flexural and tensile tests).

5.1.2.1 Izod notched impact strength. Use ASTM D-256 Method A and report average of five test specimens. Specimens are to be cut in one arbitrarily chosen direction.

5.1.2.2 Refractive index. Use ASTM D-542 Refractometric Method and test one specimen the exposed surface of which has been given the necessary polish without gross removal of material (if possible).

5.1.2.3 Water absorption. Use ASTM D-570 Procedure 6.1 (24 hours immersion) and average three test specimens cut so that the length is in one arbitrarily chosen direction. For castings greater than 1/2 in. nominal thickness machine specimens to 3 in. X 1 in. X 1/2 in. size.

5.1.2.4 Compressive deformation. Use ASTM D-621 Method A and report average of five test specimens loaded to 4,000 psi (based on original cross section) and test at 122°F. The sample size is a 1/2 in. cube. Test nominal 1/2 in. thick material so that the as-cast surfaces serve as the load-bearing surfaces and do *not* stack samples to reach 1/2 in. height, instead test a sample 1/2 in. X 1/2 in. X nominal thickness. Nominal thicknesses over 1/2 in. should yield standard test specimens. These sampling procedures override those called out in D-621.

5.1.2.5 Optical uniformity and distortion. Determine the displacement factor per ASTM D-637 on one test specimen of 18 in. X 18 in. X thickness cut with the edges at least 3 in. from the original edge of the casting. The entire casting can be used instead of the 18 in. X 18 in. coupon, provided displacement factors are measured no closer to the edge than 3 in.

5.1.2.6 Tensile properties. Five specimens shall be tested and averaged per ASTM D-638, using testing speed "B." If feasible, specimens shall have an as-cast surface (if it is smooth enough) as one of the faces. Specimens are to be cut in one arbitrary direction.

5.1.2.7 Heat resistance. Determine the average deflection temperature under flexural load per ASTM D-648 of three specimens loaded to an outer fiber stress of 264 psi. If feasible, specimens shall be prepared so that they are loaded parallel to the original surface (if it is smooth enough). Specimens are to be cut in one arbitrary direction.

5.1.2.8 Compressive properties. Use ASTM D-695 and report average of five test specimens cut with the long axis in one arbitrary direction. The specimen shall be one solid piece whose dimensions are 1 in. X 1/2 in. X thickness of casting. When the thickness exceeds 1/2 in. samples are to be 1 in. X 1/2 in. X 1/2 in. in dimension.

5.1.2.9 Shear strength. Use ASTM D-732 and test and average five specimens cut in one arbitrary direction. When the thickness of the casting exceeds 1/2 in., machine specimen down to 1/2 in. thickness.

5.1.2.10 Rockwell hardness. Use ASTM D-785 Procedure A and make five determinations on a single 1 in. X 1 in. X thickness of casting specimen. Report average. Only a smooth as-cast surface or equivalent shall be suitable for testing. If necessary the thickness may be reduced only as much as is needed to fit the test instrument.

5.1.2.11 Flexural properties. Use ASTM D-790 Method 1 and Procedure A with a 16/1 span-to-depth ratio. Average results of five test specimens cut in one arbitrary direction. If the thickness of the casting exceeds 1/2 in., machine specimens to 1/2 in. X 1/2 in. X 10 in. leaving one as-cast surface intact if feasible. Whenever a smooth as-cast surface exists, it should be tested in tension.

5.1.2.12 Specific gravity. Use ASTM D-792 Method A-1 and report average of three test specimens.

5.1.2.13 Light transmission and haze. Test per ASTM D-1003 Method A using illuminant C on one specimen. If the available test equipment will not handle the larger thickness, a calibrated photoelectric device can be substituted.

5.1.2.14 Residual monomer or degree of polymerization. A sample of suitable size shall be obtained and analyzed for unpolymerized methyl methacrylate and unpolymerized ethyl acrylate monomers by the techniques described in 2.1.3 or test methods producing equivalent results. Some acrylic plastics do not dissolve in solvents. The residual monomers of

these are measured in the material that is extractable from the plastic swollen in an appropriate chemical; e.g., a solid piece of Type 3 acrylic material, weighing 1 gram, is placed in 20 ml of methylene chloride in a glass bottle and placed on a shaker for 24 hours. The fluid portion of this is analyzed for monomeric methyl methacrylate and monomeric ethyl acrylate using the techniques mentioned above.

5.1.2.15 Presence of ultraviolet light absorber. Using a monochromator having a bandwidth of 10-nanometer (nm) or less, a photometer having reproducibility of ± 1 percent of full scale and the practices of ASTM E-308 measure the spectral transmittance in the 290- to 330-nm wavelength band. Report value of one specimen of nominal 1/2 in. thickness or adjust value to 1/2 in. thickness. Measurements can be made on the casting or on the monomer mix from which the plastic is to be cast. Solid samples shall have two polished faces through which the light passes.

5.1.2.16 Clarity, visually rated. Visually rate the clarity of one casting by ASTM D-702-68. Paragraph 6.1.15. Clear print of size 7 lines per column inch and 16 characteristics to the linear inch shall be clearly visible when viewed from a distance of 20 in. through the thickness of the casting with opposite faces polished.

5.1.2.17 Thermal expansion. Use equipment as described in ASTM D-696 or equivalent. Test and average results of two specimens at least 5 in. long and a maximum of 1/8 in. thickness. Equilibrate the samples at -50°F and transfer to and equilibrate in constant temperatures baths controlled at -30°F, -10°F, 10°F, 30°F, 50°F, 70°F, 90°F and 110°F. A well-stirred liquid bath rising at a temperature of 2°F/min or a forced-air chamber rising at 1°F/min can be substituted for the constant-temperature baths. Measure and report the values of the coefficient of linear thermal expansion at temperatures of -40°, -20°, 0°, 20°, 40°, 60°, 80° and 100°F.

5.1.2.18 Craze resistance. Measure the craze resistance of Type 3 material only by the test method referenced in 2.1.2. Disregarding edge crazing the material shall show no evidence of crazing, cracking, or other chemical degradation in the area subjected to the action of the specified lacquer thinner only. Only a smooth as-cast surface is suitable for testing. Specimens shall be nominal 1/2 in. thick or machined to 1/2 in. thickness on the compression stressed surface only.

5.2 LOT ACCEPTANCE TESTING REQUIREMENTS

5.2.1 Tests and Values Required. Refer to Tables 2 and 3. Lot acceptance tests are Tests 4, 6, 8, 14, 15 and 16 and the values required are the same as those on qualification tests. The procurer has the option to require Tests 5, 13 and 16 as supplemental lot acceptance tests but must be willing to sacrifice the additional cost of these tests and the loss of the test specimens from his normal sheet or casting size.

5.2.2 Test Methods and Sampling. Use the same test methods and sampling techniques as when these tests are used as qualification tests.

A-10

5.3 INSPECTION OF EACH SHEET OR CASTING

5.3.1 Visual Inspection Requirements. Each sheet or casting supplied to this specification shall be visually examined and shall be:

1. completely colorless
2. free of internal cracks, checks, or crazing
3. free of defects except as modified below

5.3.2 Allowable Defects

5.3.2.1 Letgoes. Letgoes shall be permitted within an isosceles triangular area 6 in. on a side in any or all of the four corners of the sheet. The apex of the triangle must be formed by the junction of the untrimmed sheet edges. *Corner letgoes* contained in an isosceles triangle greater than 6 in. on a side but less than 12 in. on a side may be reworked and resubmitted for inspection. *Side letgoes* shall be permitted within a band not greater than 2 in. from the untrimmed sheet edge. Sheets greater than 2 in. nominal thickness may have letgoes provided they do not extend more than 1/64 in. below the surface.

5.3.2.2 Chips. Maximum allowable size shall be 1/8 in. Chips approximately 1/8 in. in size shall not have a frequency greater than one chip per 4 sq ft of surface area. Chips obviously less than 1/8 in. will be permitted unless they form a concentrated pattern that would be considered objectionable. Sheets greater than 2 in. nominal thickness may have chips provided they do not extend more than 1/16 in. above the surface.

5.3.2.3 Inclusions. Maximum allowable dimension shall be 1/16 in. Inclusions less than 1/32 in. shall be disregarded. The maximum permissible frequency for dimensions ranging from 1/32 in. to 1/16 in. shall be 1 per 4 sq ft for thicknesses up to and including 0.500 in.

5.3.2.4 Minor Defects. Minor defects which can be removed by polishing shall be permitted.

5.3.2.5 Other Defects. Other defects within 1 in. of the untrimmed edge of the sheet which do not significantly reduce the mechanical strength of the sheet shall be permitted.

5.3.2.6 Flatness of Sheets. Each sheet shall be free from edge kink warpage and from edge "S" warp. Overall bow warp of 3/8 in. or less when the casting is placed concave side down on a flat surface shall be permitted.

SECTION 6

PREPARATION FOR DELIVERY

6.1 PROTECTION

6.1.1 Masking. The viewing surfaces of each casting shall be covered by a suitably adhered paper, tape or film that can be readily removed without injury to the surfaces and that will adequately protect the surfaces from scratching or damage during handling, shipping, or storage. When removed from the surface, the masking material shall leave no residue.

6.2 MARKING

6.2.1 Traceability. A material identification and accounting system shall be used so that at any time (up to and including delivery) it is possible to trace any piece of material, test samples or test results to the particular casting from which they were cut or to which they apply.

6.2.2 Individual Castings. The protective covering of each casting shall be legible and permanently marked with the following minimum information.

    a.   The specification number.

    b.   The supplier's designation for his approved product.

    c.   The nominal thickness.

    d.   Markings consistent with 6.2.1.

Markings shall appear at least once on each casting and preferably at intervals of one ft.

6.2.3 Shipping Containers. Each package and container shall be marked permanently and legibly with the following minimum information.

    a.   Material description.

    b.   Specification number.

    c.   Purchase order number.

    d.   Manufacturer, code number, batch number, and lot number.

    e.   Date of manufacture.

    f.   Results of Lot Acceptance Tests.

    g.   Markings consistent with 6.2.1.

FORM 1

QUALIFICATION TESTS RESULTS

Trade name	Grade

Manufacturer	Nominal Thickness

Identification	Type

Thickness category

Test No.	Property	Test Method & Sampling Ref.	Results Reported to	Test Results
1	Izod impact	5.1.2.1	0.1 ft-lb/in.	
2	Refractive index	5.1.2.2	0.01	
3	Water absorption	5.1.2.3	0.01%	
4	Compressive deformation	5.1.2.4	0.1%	
5	Displacement factor	5.1.2.5	1	
6	Tensile, strength	5.1.2.6	100 psi	
	elongation		0.1%	
	modulus		10,000 psi	
7	Deflection temperature	5.1.2.7	1°C	
8	Compressive, strength	5.1.2.8	1,000 psi	
	modulus		10,000 psi	
9	Shear strength	5.1.2.9	1,000 psi	
10	Rockwell hardness	5.1.2.10	1	
11	Flexural strength	5.1.2.11	1,000 psi	
12	Specific gravity	5.1.2.12	0.01	
13	Light transmittance	5.1.2.13	1%	
14	Residual methyl methacrylate	5.1.2.14	0.1%	
	Residual ethyl acrylate		0.001%	
15	Ultraviolet transmittance	5.1.2.15	0.5%	
16	Visual clarity	5.1.2.17	pass or fail	
17	Thermal expansion at:	5.1.2.18	$0.01 \times 10^{-5}/°F$	
	$-40°F$			
	$-20°F$			
	$0°F$			
	$+20°F$			
	$+40°F$			

FORM 2

LOT ACCEPTANCE TEST RESULTS

Trade name	Grade
Manufacturer	Nominal thickness
Identification	Type

Specification Reference

Test No.	Test Method & Sampling Ref.	Property	Results Report to	Test Results
4	5.1.2.4	Compressive deformation	0.1%	
5*	5.1.2.5	Displacement factor	1	*
6	5.1.2.6	Tensile, strength	100 psi	
		elongation	0.1%	
		modulus	10,000 psi	
8	5.1.2.8	Compressive, strength	1,000 psi	
		modulus	10,000 psi	
13*	5.1.2.13	Light transmittance	1%	*
14	5.1.2.14	Residual methyl methacrylate	0.1%	
		Residual ethyl acrylate	0.001%	
15	5.1.2.15	Ultraviolet transmittance	1%	
16	5.1.2.17	Visual clarity	pass or fail	
	5.3	Inspection	pass or fail	

*These tests are supplemental lot acceptance tests and will *not* normally be run unless specifically requested (see 5.2.1).

NOTES: 1. Requirements are given in Tables 2 and 3 in 5.1.1.
2. Only materials listed on the QPL are considered eligible.
3. Each casting is to be tested.

Date _____

I, _____ of _____ County, State of _____ , being duly sworn, depose and say that the above identified material was tested in the prescribed manner and that the test results are true and accurate.

Name _____

Title _____

Company _____

Subscribed and sworn to before me on thi   day of _____ , AD _____ and
hereby affix my seal.

Name _____
Notary Public

A-14

APPENDIX B
BIBLIOGRAPHY

1. Stachiw, J. D., "Critical Pressure of Conical Acrylic Windows Under Short Term Hydrostatic Loading," ASME Transactions/Journal of Engineering for Industry, Vol. 89, No. 3, 1967; also published as Technical Report R-512 by U. S. Naval Civil Engineering Laboratory, Port Hueneme, Calif., 1967.

2. Stachiw, J. D., "Critical Pressure of Flat Acrylic Windows Under Short Term Hydrostatic Loading," ASME Paper No. 67-WA/Unt-1; also published as Technical Report R-512 by U. S. Naval Civil Engineering Laboratory, Port Hueneme, Calif., 1967.

3. Stachiw, J. D., "Critical Pressure of Spherical Shell Acrylic Windows Under Short Term Pressure Loading," ASME Transactions/Journal of Engineering for Industry, Vol. 91, No. 3, 1969; also published as Technical Report R-631 by U. S. Naval Civil Engineering Laboratory, Port Hueneme, Calif., 1969.

4. Wright, C., "Development of a Large Spherical Acrylic Viewport for the PC8B Submarine," ASME Paper No. 71-WA/Unt-4.

5. Stachiw, J. D., and Gray, K. O., "Procurement of Safe Viewports for Hyperbaric Chambers," ASME Transactions/Journal of Engineering for Industry, Vol. 93, No. 4, 1971.

6. Maison, J. R., and Stachiw, J. D., "Acrylic Pressure Hull for Johnson-Sea-Link Submersible," ASME Paper No. 71-WA/Unt-6.

7. Wilson, E. L., "Structural Analysis of Axisymmetric Solids," American Institute of Aeronautics and Astronautics, Journal, Vol. 3, No. 12, December 1965.

8. Stachiw, J. D., "Spherical Acrylic Pressure Hulls for Undersea Exploration," ASME Transactions/Journal of Engineering for Industry, Vol. 93, No. 2, 1971; also published as Technical Report R-676 by the U. S. Naval Civil Engineering Laboratory, Port Hueneme, Calif., 1970.

9. Stachiw, J. D., "Acrylic Hemispheres for NUC Undersea Elevator," ASME Paper No. 72-WA/Oct-4; also published as Technical Report TP 315 by the Naval Undersea Center, San Diego, Calif., 1972.

10. Stachiw, J. D., "Conical Acrylic Windows Under Long Term Hydrostatic Pressure of 20,000 psi," ASME Transactions/Journal of Engineering for Industry, Vol. 92, Series B, No. 1, February 1970; also published as Technical Report R-645 by U. S. Naval Civil Engineering Laboratory, Port Hueneme, Calif., October 1969.

11. Stachiw, J. D., "Conical Acrylic Windows Under Long Term Hydrostatic Pressure of 10,000 psi," ASME Transactions/Journal of Engineering for Industry, Vol. 94, Series B, No. 4, November 1972; also published as Technical Report R-708 by U. S. Naval Civil Engineering Laboratory, Port Hueneme, Calif., January 1970.

12. Stachiw, J. D., "Conical Acrylic Windows Under Long Term Hydrostatic Pressure of 5000 psi," ASME Transactions/Journal of Engineering for Industry, Vol. 94, Series B, No. 3, August 1972; also published as Technical Report R-747 by U. S. Naval Civil Engineering Laboratory, Port Hueneme, Calif., November 1971.

13. Stachiw, J. D., "Effect of Temperature and Flange Support on Critical Pressure of Conical Acrylic Windows Under Short Term Pressure Loading," ASME Transactions/ Journal of Engineering for Industry, Vol. 94, Series D, No. 4, December 1972; also published as Technical Report R-773 by U. S. Naval Civil Engineering Laboratory, Port Hueneme, Calif., August 1972.

14. Stachiw, J. D., "Effect of Bubble Inclusions on the Mechanical Properties of Cast Poly-Methyl Metacrylate," ASME Transactions/Journal of Engineering for Industry, Vol. 94, Series D, No. 4, December 1972; also published as Technical Report TP-305 by the Naval Undersea Center, San Diego, Calif., August 1972.

DOCUMENT CONTROL DATA - R & D

(Security classification of title, body of abstract and indexing annotation must be entered when the overall report is classified)

1. ORIGINATING ACTIVITY (Corporate author)	2a. REPORT SECURITY CLASSIFICATION
Naval Undersea Center San Diego, California 92132	UNCLASSIFIED 2b. GROUP

3. REPORT TITLE

RECOMMENDED PRACTICES FOR THE DESIGN, FABRICATION, PROOFTESTING AND INSPECTION OF WINDOWS IN MAN-RATED HYPERBARIC CHAMBERS

4. DESCRIPTIVE NOTES (Type of report and inclusive dates)

Independent Exploratory Development   JANUARY 1972 – JUNE 1973

5. AUTHOR(S) (First name, middle initial, last name)

Jerry D. Stachiw

6. REPORT DATE	7a. TOTAL NO. OF PAGES	7b. NO. OF REFS
December 1973	59	

8a. CONTRACT OR GRANT NO.	9a. ORIGINATOR'S REPORT NUMBER(S)
b. PROJECT NO	NUC TP 378
c.	9b. OTHER REPORT NO(S) (Any other numbers that may be assigned this report)
d.	

10. DISTRIBUTION STATEMENT

Approved for public release; distribution unlimited.

11. SUPPLEMENTARY NOTES	12. SPONSORING MILITARY ACTIVITY
	Director of Navy Laboratories Washington, D. C. 20390

13. ABSTRACT

A concise recommendation is given for the design, fabrication, proof-testing and inspection in-service of acrylic plastic windows for manned hyperbaric chambers (this includes PTC's, DDC's, one atmosphere habitats, high altitude simulation chambers, recompression chambers, et cetera).

The recommendation is limited to a temperature range of -60°F to +150°F and maximum pressure of +3500 psi. The standard window shapes discussed are flat disc, conical frustum and spherical shell sector.

Detailed recommendation is also given for qualification and lot acceptance tests that the acrylic plastic material must pass in order to be accepted as fabrication stock for windows in manned hyperbaric chambers.

DD FORM 1473 (PAGE 1)
1 NOV 65
0102-014-6600

14 KEY WORDS	LINK A		LINK B		LINK C	
	ROLE	WT	ROLE	WT	ROLE	WT
hyperbaric chambers						
acrylic plastic						
window						
view ports						
decompression chambers						
personnel transfer capsules						
undersea habitats						
vacuum chambers						
pressure vessel						